Note that the integration limits are now $-\infty$ to $+\infty$, in contrast to the speed distribution in which the limits were 0 to ∞. We must include all atoms in the integral—those that are moving toward the observer as well as those that are moving away. Evaluating the integral, we find $A^{-1} = Nh\sqrt{m/2\pi kT}/2mL(2s+1)$ and thus we have the *Maxwell velocity distribution*

$$N(v_x) = N\left(\frac{m}{2\pi kT}\right)^{1/2} e^{-mv_x^2/2kT} \tag{10.25}$$

This function is plotted in Figure 10.13. The shaded strip shows the number $dN = N(v_x)dv_x$ having velocity components between v_x and $v_x + dv_x$. This is a familiar curve known as the *Gaussian distribution* or the *normal distribution* (also called the "bell-shaped curve"), which has applications in many areas of probability and statistics.

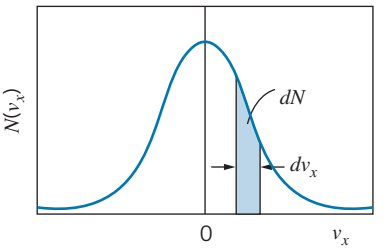

FIGURE 10.13 The Maxwell velocity distribution for gas molecules. The distribution is centered on $v_x = 0$. The shaded strip represents the number of molecules with velocity components between v_x and $v_x + dv_x$.

To complete the analysis of the Doppler broadening, we must change the distribution function so it describes frequency or wavelength. That is, let's find out how many atoms will emit frequencies in the range from f to $f + df$, which we can write as $dN = N(f)df$. The relationship between frequency and velocity is given by Eq. 2.22. We'll change notation somewhat and let f_0 represent the unshifted frequency while f represents the observed (Doppler-shifted) frequency. We then have

$$f = f_0\sqrt{\frac{1 - v_x/c}{1 + v_x/c}} = f_0\frac{1 - v_x/c}{\sqrt{1 - v_x^2/c^2}} \cong f_0(1 - v_x/c) \tag{10.26}$$

where we have replaced the square root in the denominator with 1 because $v_x \ll c$ for thermal motions. Solving for v_x, we obtain $v_x = c(1 - f/f_0)$ and taking the magnitude of the differentials we then have $|dv_x| = c\,df/f_0$. With these substitutions the number of atoms in the small interval becomes

$$dN = N(f)\,df = N(v_x)dv_x = N\left(\frac{m}{2\pi kT}\right)^{1/2} e^{-mc^2(1-f/f_0)^2/2kT}\frac{c\,df}{f_0} \tag{10.27}$$

and so the frequency distribution function is

$$N(f) = \frac{Nc}{f_0}\left(\frac{m}{2\pi kT}\right)^{1/2} e^{-mc^2(1-f/f_0)^2/2kT} \tag{10.28}$$

The frequency distribution function is shown in Figure 10.14. The broadening is usually characterized by giving the width of the spectral line Δf, defined as the range over which the intensity falls to half the maximum value on either side. (This is known as the "full width at half maximum" or FWHM.) The only factor in Eq. 10.28 that depends on frequency is the exponential, and so the width is determined by the frequencies at which the exponential (which is equal to 1 at $f = f_0$) falls by half: $e^{-mc^2(1-f/f_0)^2/2kT} = 1/2$ or, taking the logarithm of both sides,

$$-\frac{mc^2}{2kT}\left(1 - \frac{f}{f_0}\right)^2 = \ln(1/2) \tag{10.29}$$

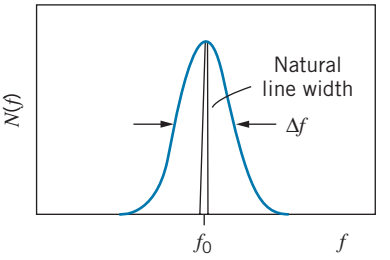

FIGURE 10.14 Doppler-broadened spectral line. The natural linewidth has been exaggerated for the drawing—typically the natural linewidth is no more than 10^{-5} to 10^{-4} of the broadened linewidth.

which can be solved to give $f = f_0(1 \pm \sqrt{(2\ln 2)kT/mc^2})$. The two solutions (corresponding to the + and − signs) give the two points at which the distribution falls to half its maximum. The interval between those two points is

$$\Delta f = 2f_0\sqrt{(2\ln 2)kT/mc^2} \tag{10.30}$$

We can write a similar expression for the wavelength broadening because $\Delta f/f_0 = \Delta\lambda/\lambda_0$. The Doppler broadening is directly related to the temperature, and so a measurement of the width of spectral lines provides a way to determine the temperature of the emitting atoms. This is a powerful means of determining the temperatures of stars from observing the widths of their spectral lines.

10.5 QUANTUM STATISTICS

As we discussed in Section 10.2, the distribution functions for the indistinguishable particles of quantum physics are different from those of classical physics. Because of the unusual behavior of quantum systems, we must have separate distribution functions for particles that obey the Pauli exclusion principle (such as electrons) and particles that do not obey the Pauli principle (such as photons). We will not derive these distribution functions, but merely state them and discuss some of their properties and their applications.

Particles that do not obey the Pauli principle are those with integral spins (0, 1, 2, ..., in units of $\hbar$). Their statistical properties are determined by the *Bose-Einstein distribution function*:

$$f_{\text{BE}}(E) = \frac{1}{A_{\text{BE}}e^{E/kT} - 1} \tag{10.31}$$

Particles described by this distribution are known collectively as *bosons*. The constant A_{BE} serves as a kind of normalization constant, in analogy with the factor A in the Maxwell-Boltzmann distribution (and the comparison shows why we included this factor as A^{-1} in Eq. 10.16).

Particles of half-integral spin ($\frac{1}{2}, \frac{3}{2}, \ldots$) that obey the Pauli principle, such as electrons or nucleons, are described by the *Fermi-Dirac distribution function*:

$$f_{\text{FD}}(E) = \frac{1}{A_{\text{FD}}e^{E/kT} + 1} \tag{10.32}$$

These particles are known collectively as *fermions*.

How the minor change in sign in the denominator between f_{BE} and f_{FD} gives such a radical change in the form of the distribution function is not immediately obvious, and to show the differences we need to know more about the normalization coefficient A_{FD}, which is not a constant but depends on T. For the Bose-Einstein distribution, in most cases of practical interest A_{BE} is either independent of T or depends so weakly on T that the exponential term $e^{E/kT}$ dominates the temperature dependence. However, for the Fermi-Dirac

distribution, A_{FD} is strongly dependent on T, and the dependence is usually approximately exponential, so A_{FD} is written as

$$A_{FD} = e^{-E_F/kT} \tag{10.33}$$

and the Fermi-Dirac distribution becomes

$$f_{FD}(E) = \frac{1}{e^{(E-E_F)/kT} + 1} \tag{10.34}$$

where E_F is called the *Fermi energy*.

Let us look qualitatively at the differences between f_{BE} and f_{FD} at low temperatures. For the Bose-Einstein distribution, assuming for the moment $A_{BE} = 1$, in the limit of small T the exponential factor becomes large for large E, and so $f_{BE} \to 0$ for states with large energies. The only energy levels that have any real chance of being populated are those with $E = 0$, for which the exponential factor approaches 1, the denominator becomes very small, and $f_{BE} \to \infty$. Thus when T is small, all of the particles in the system try to occupy the lowest energy state. This effect is known as "Bose-Einstein condensation," and we will see that it has some rather startling consequences.

This effect is not possible for fermions, such as electrons. We know that the electrons in an atom, for example, do not all occupy the lowest energy state, no matter what the temperature. Let us see how the Fermi-Dirac distribution function prevents this. The exponential factor in the denominator of f_{FD} is $e^{(E-E_F)/kT}$. For values of $E > E_F$, when T is small the exponential factor becomes large and f_{FD} goes to zero, just like f_{BE}. When $E < E_F$, however, the story is very different, for then $E - E_F$ is negative, and $e^{(E-E_F)/kT}$ goes to zero for small T, so $f_{FD} = 1$. *The occupation probability is therefore only one per quantum state,* just as required by the Pauli principle. Even at very low temperatures, fermions do not "condense" into the lowest energy level.

In Figures 10.15 to 10.17, the three distributions f_{MB}, f_{BE}, and f_{FD} are plotted as functions of the energy E. (Note the qualitative similarity with Figures 10.4 to 10.6.) You can see, by comparing these figures, that all of the distribution functions fall to zero at large values of E; when $E \gg kT$, the occupation probability is very small, as we calculated for f_{MB} in the case of the first excited state of the hydrogen atom in Example 10.3. Notice also that, even though f_{MB} becomes large for small E, it remains finite. The Bose-Einstein distribution, f_{BE}, on the other hand, becomes infinite as $E \to 0$; this is the "condensation" effect referred to earlier, in which all of the particles try to occupy the lowest quantum state.

You can see that f_{FD} never becomes larger than 1.0, just as we expect for particles that obey the Pauli principle. The function f_{FD} has the value 1.0 for states with low energy (all states are filled), and it falls quickly to zero at high energy (all states are empty). The Fermi energy E_F gives the point at which the distribution function has the value 1/2. At absolute zero, all states below E_F are filled and all states above E_F are empty.

The normalization constant ultimately depends on the number of particles in the system, determined by integrating the distribution function $f(E)$ after multiplying it by the density of states $g(E)$. Note how changing the number of particles changes the normalizations of the different distributions. For the Maxwell-Boltzmann distribution, increasing N increases the area under the curve by raising the intercept, thus raising the entire curve. For the Fermi-Dirac

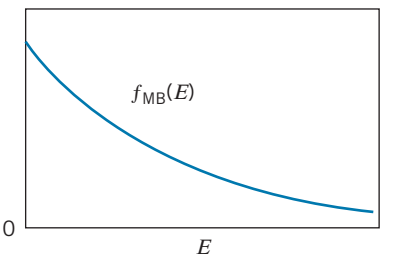

FIGURE 10.15 The Maxwell-Boltzmann distribution function.

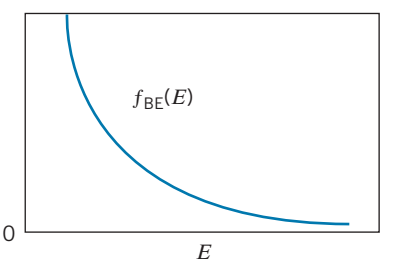

FIGURE 10.16 The Bose-Einstein distribution function.

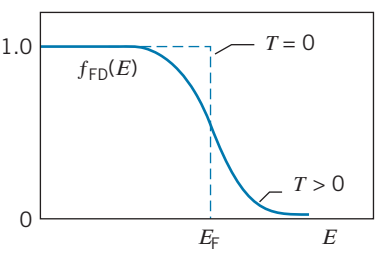

FIGURE 10.17 The Fermi-Dirac distribution function.

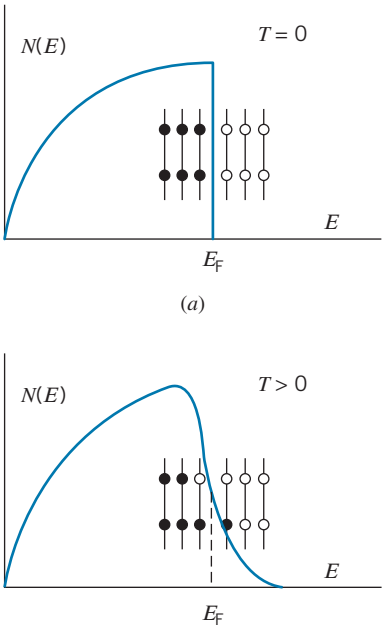

FIGURE 10.18 The occupation probability of electrons in an electron gas (*a*) at $T = 0$ and (*b*) at $T > 0$. The solid dots represent filled states and the open dots represent empty states. Each energy level can hold a maximum of 2 electrons (spin up and spin down).

distribution, on the other hand, increasing N increases the area by widening the curve to the right (increasing E_F) while keeping the intercept at 1.0.

Let's consider a gas of electrons described by the density of states function $g(E)$ given in Eq. 10.12 and thus with $N(E) = Vg(E)f_{FD}(E)$. Figure 10.18*a* shows a hypothetical set of energy levels and how they would be populated at $T = 0$ (with 2 electrons in each quantum state). As T increases, some levels above E_F are partially occupied ($f_{FD} > 0$), while some levels below E_F are partially empty ($f_{FD} < 1$). Figure 10.18*b* shows how the energy levels of a system might be populated at $T > 0$. The higher the temperature, the more the distribution spreads, but notice that only states in the vicinity of E_F are affected. The states at much lower energies remain filled, and those at much higher energies remain empty.

The Fermi energy varies only slightly with temperature for most materials, and we can regard it as constant for many applications. As we will see in Section 10.7, for electrons in a metal E_F depends on the electron density of the material, which doesn't change much with temperature. For some materials, notably semiconductors, the density of *conduction* electrons can change significantly with temperature, and thus E_F in these materials is temperature dependent.

Limit of Classical Statistics

Under what circumstances can we treat a system classically rather then according to the laws of quantum mechanics? The quantum behavior can be neglected if the de Broglie wavelength of a particle is much smaller than the physical separation between the particles. That is, no particle lies within the wave packet of its neighbors. If we take kT as a representative measure of the kinetic energy of a particle in a collection of particles at temperature T, then with $p^2/2m = kT$ we obtain the de Broglie wavelength as

$$\lambda = \frac{h}{p} = \frac{h}{\sqrt{2mkT}} = \frac{hc}{\sqrt{2mc^2kT}} \tag{10.35}$$

The density N/V gives the number of particles per unit volume, and so the average spacing d between particles is about $(N/V)^{-1/3}$. The condition for the applicability of classical physics is then $\lambda \ll d$ or $\lambda/d \ll 1$, which gives

$$\frac{\lambda}{d} = \frac{hc/\sqrt{2mc^2kT}}{(N/V)^{-1/3}} = \frac{hc(N/V)^{1/3}}{\sqrt{2mc^2kT}} \ll 1 \tag{10.36}$$

The normalization constant we found from Eq. 10.18 for the Maxwell-Boltzmann distribution can be written

$$A^{-1} = \frac{N(hc)^3}{V(2s+1)(2\pi mc^2kT)^{3/2}} = \frac{1}{(2s+1)\pi^{3/2}}\left[\frac{hc(N/V)^{1/3}}{\sqrt{2mc^2kT}}\right]^3 \tag{10.37}$$

The quantity in brackets on the right is just λ/d from Eq. 10.36. Apart from some small factors of order unity, Eq. 10.36 is equivalent to requiring that the normalization constant of the Maxwell-Boltzmann distribution is small: $A^{-1} \ll 1$, or that the number of *occupied* states in the gas is much smaller than the number of *available* states.

10.6 APPLICATIONS OF BOSE-EINSTEIN STATISTICS

Thermal Radiation

As we did in our discussion of thermal radiation in Chapter 3, we consider a cavity filled with electromagnetic radiation. For this calculation, we assume the box to be filled with a "gas" of photons. Photons have spin 1, so they are bosons and obey Bose-Einstein statistics.

The normalization parameter A_{BE} of the Bose-Einstein distribution, Eq. 10.34, depends on the total number of particles described by the distribution. Because photons are continuously created and destroyed as radiation is emitted or absorbed by the walls of the cavity, the total number of particles is not constant, and the parameter A_{BE} loses its significance. We can eliminate this factor from the Bose-Einstein distribution by setting $A_{\text{BE}} = 1$ in Eq. 10.34.

The number of photons having energy in the range E to $E + dE$ is, according to the Bose-Einstein distribution and using the density states for the photon gas from Eq. 10.15,

$$dN = N(E)\,dE = Vg(E)f_{\text{BE}}(E)\,dE = V\frac{8\pi}{(hc)^3}E^2\frac{1}{e^{E/kT}-1}\,dE \tag{10.38}$$

The radiant energy carried by photons with energy between E and $E + dE$ is $E\,dN = EN(E)dE$, and the contribution to the energy density (energy per unit volume) of photons with energy E is

$$u(E)\,dE = \frac{EN(E)\,dE}{V} = \frac{8\pi E^3}{(hc)^3}\frac{1}{e^{E/kT}-1}\,dE \tag{10.39}$$

The total energy density over all photon energies is

$$U = \int_0^\infty u(E)\,dE = \frac{8\pi}{(hc)^3}\int_0^\infty \frac{E^3\,dE}{e^{E/kT}-1} = \frac{8\pi(kT)^4}{(hc)^3}\int_0^\infty \frac{x^3\,dx}{e^x-1} \tag{10.40}$$

where $x = E/kT$. The integral is a standard form and has the value $\pi^4/15$, so

$$U = \frac{8\pi^5 k^4}{15(hc)^3}T^4 \tag{10.41}$$

This is identical with Stefan's law (Eq. 3.26) using the Stefan-Boltzmann constant from Eq. 3.42 and accounting for the factor $c/4$ that takes us from energy density of the radiation to radiant intensity I.

We can show that our expression for the energy density leads to Planck's equation for the intensity of cavity radiation by changing variables from E to λ. Substituting $E = hc/\lambda$ and $|dE| = (hc/\lambda^2)d\lambda$, we find

$$u(\lambda)\,d\lambda = u(E)\,dE = \frac{8\pi hc}{\lambda^5}\frac{1}{e^{hc/\lambda kT}-1}\,d\lambda \tag{10.42}$$

Multiplying by $c/4$ to convert from the energy density of the radiation to the intensity, we obtain the result that was given in Eq. 3.41.

Thus the Planck theory of blackbody radiation, which was so successful in accounting for experimental results, can be derived from the Bose-Einstein distribution for photons (but Planck's original work was done two decades before the development of Bose-Einstein statistics).

Liquid Helium

One of the most remarkable substances we can study in the laboratory is liquid helium. Here are some of its properties:

1. Helium gas is the most inert of the inert gases. Under normal conditions, it forms no compounds, and it has the lowest boiling point, 4.18 K, of any material.
2. Just below its boiling point of 4.18 K, helium behaves much like an ordinary liquid. As the helium boils, the escaping gas forms bubbles, like a boiling pot of water. As the liquid is cooled further, a sudden transition occurs at a temperature of 2.17 K: the violent boiling stops, and the liquid becomes absolutely still. (Evaporation continues, but only from the surface.)
3. As the liquid is cooled below 2.17 K, the specific heat and the thermal conductivity both increase suddenly and discontinuously. Figure 10.19 shows the specific heat as a function of temperature. The form of the figure looks rather like the Greek letter λ, and so the transition point at 2.17 K has become known as the *lambda point*. The thermal conductivity rises at the λ point by a factor of perhaps 10^6.
4. Above 2.17 K, liquid helium can be held in a vessel with a porous plug in the bottom. As soon as the liquid is cooled below 2.17 K, the liquid begins to flow easily through the plug.
5. Below the lambda point, liquid helium has the power to seemingly defy gravity, flowing up and over the walls of its container. The helium forms a thin film, which lines the walls of the container; the remaining liquid is then drawn up by the film like a siphon, and the helium can be seen dripping from the bottom of the container, as in the photograph of Figure 10.20.

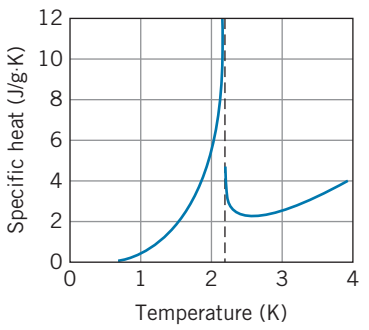

FIGURE 10.19 The specific heat of liquid helium. The discontinuity at 2.17 K is called the lambda point.

All of these strange properties occur because liquid helium obeys Bose-Einstein statistics. Ordinary helium has two electrons filling the 1*s* shell, so the total angular momentum of the electrons is zero. It happens that the helium nucleus (alpha particle) also has a spin of zero. Therefore the total spin of the atom (electron spin + nuclear spin) is zero, and a helium atom behaves like a boson. At 2.17 K, a *change of phase* occurs in the helium liquid. Above the lambda point, helium behaves like an ordinary liquid; below the lambda point, liquid helium begins to become a *superfluid*. As the temperature is decreased from the lambda point toward absolute zero, the relative concentration of the normal fluid decreases and that of the superfluid increases. The unusual properties of liquid helium are all caused by the superfluid component, which is also known as a *quantum liquid*. Because the helium atoms obey Bose-Einstein statistics, the Pauli principle does not prevent all of the atoms from being in the same quantum state. This begins to happen at the lambda point. We can think of the superfluid as being a single quantum state made up of a very large number of atoms; the atoms behave in a cooperative way, giving the superfluid its unusual properties.

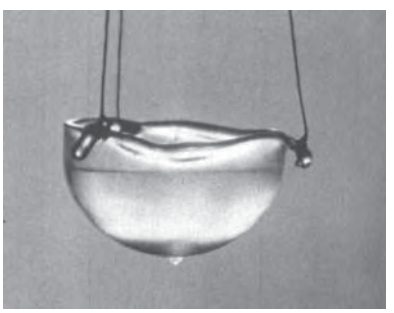

FIGURE 10.20 Liquid helium can be seen dripping from the bottom of this container, as a result of a thin film flowing up and over the walls from the liquid inside the container.

By way of comparison, if we try the same kinds of experiments with the rarer isotope of helium, ^{3}He, the behavior is very different. Although ^{3}He has zero electronic spin, just like ^{4}He, it has only three particles rather than four in its nucleus, and its *nuclear* spin is ½. The total atomic (electronic + nuclear)

spin is therefore ½, and ^{3}He behaves like a fermion and obeys the Fermi-Dirac distribution. Because the Pauli principle prevents more than one fermion from occupying any quantum state, no superfluidity is expected for ^{3}He, and indeed none is observed until ^{3}He is cooled to about 0.002 K. At this point the weak coupling of two ^{3}He to form a boson occurs, and the ^{3}He pairs can display the effects of Bose-Einstein statistics. (A related effect involving the pairing of electrons is responsible for superconductivity; see Section 11.5.)

Bose-Einstein Condensation

Let's consider the expression for the total number of particles of a system of bosons in a volume V. We can treat the bosons as a quantum system similar to the electron gas—particles with wave functions that vanish at the boundaries of the volume. The density of states is then given by Eq. 10.12 and the total number of particles in the volume V is then

$$N = \int dN = \int_0^\infty N(E)\,dE = \int_0^\infty Vg(E)f_{\text{BE}}(E)\,dE$$
$$= \frac{(2s+1)4\pi\sqrt{2}Vm^{3/2}}{h^3}\int_0^\infty \frac{E^{1/2}}{A_{\text{BE}}e^{E/kT}-1}\,dE \qquad (10.43)$$

Previously our approach to an equation of this type was to evaluate the integral and solve the resulting equation for the constant A, which provides the normalization to make the total number of particles equal to N. That procedure poses some difficulties for this integral, so we'll try a different approach: we'll see what Eq. 10.43 tells us about the *maximum* number of particles that can be accommodated in the volume V. Because A_{BE} is a pure number that is always $\geq +1$ (otherwise the denominator of f_{BE} could become negative, which makes no sense for a distribution function), we can find this maximum value by making the denominator in the integral as small as possible, that is, by putting $A_{\text{BE}} = 1$. The resulting integral has the value $1.306\pi^{1/2}(kT)^{3/2}$, and the maximum number of particles is then

$$N = 2.612V(2s+1)\left(\frac{2\pi mkT}{h^2}\right)^{3/2} \qquad (10.44)$$

It appears that we can violate this maximum limit by either (1) putting more particles into the volume V than Eq. 10.44 permits, or (2) lowering the temperature (and thus reducing the maximum N) so that the actual number of particles in the system becomes greater than the maximum limit given by Eq. 10.44 for that temperature. How can we still refer to a "maximum" number of particles in these cases?

To resolve this apparent difficulty, we must look more carefully at what happens for $E = 0$. Clearly the Bose-Einstein distribution function $f_{\text{BE}}(E)$ becomes infinite for $E = 0$ when $A_{\text{BE}} = 1$. The integral in Eq. 10.43 doesn't blow up at $E = 0$ because the numerator $E^{1/2}$ is zero at $E = 0$. But there is something very wrong with that restriction, which requires that the density of states (Eq. 10.12) be zero at $E = 0$. Our system must have a ground state, so there is at least one state at $E = 0$. This contradicts the calculation which puts $g(0) = 0$.

If we try to put more particles into the system than the maximum given by Eq. 10.44 (or equivalently if we try to reduce the temperature below its limit for a given N), the additional particles all can go into the $E = 0$ ground state, which is not subject to the restriction on the maximum value of N. This is Bose-Einstein condensation—all excess particles are "condensing" into the ground state. Note

that the use of the word "condensation" to describe this effect does *not* refer to a gas condensing into a liquid. The particles are "condensed" into the same quantum state, where they are all described by the same wave function, but they are all still in the gaseous state.

What we are thus actually calculating in Eq. 10.44 is the number of particles in all states *except* the ground state, that is, the number in all the excited states. Let's call that value N_{ex}. It is this value that is limited by the restriction on the maximum number of particles that can be accommodated by the Bose-Einstein distribution. The number of particles in the ground state, N_0, has no restriction. The total number of particles is $N_{total} = N_0 + N_{ex}$.

Let's solve Eq. 10.44 for the critical temperature at which we expect this condensation to occur:

$$T_{BEC} = \left(\frac{N_{total}/V}{2.612(2s+1)}\right)^{2/3} \frac{h^2}{2\pi mk} \tag{10.45}$$

Above this temperature, all of the particles can be in excited states of the system without restriction. When the temperature is reduced to T_{BEC}, the excited states are all fully populated, and any further reduction of the temperature below this value means that particles must be transforming from excited states into the ground state. With N_{ex} as the number of particles calculated in Eq. 10.44, we can combine that equation with Eq. 10.45 to give $N_{ex}/N_{total} = (T/T_{BEC})^{3/2}$, or

$$\frac{N_0}{N_{total}} = 1 - \left(\frac{T}{T_{BEC}}\right)^{3/2} \tag{10.46}$$

This applies only to temperatures at or below T_{BEC}. At $T = T_{BEC}, N_0 = 0$—all of the particles are in the excited states. As T is reduced below T_{BEC}, the fraction N_0/N_{total} increases, approaching 1 (all particles in the ground state) as $T \to 0$. This is the Bose-Einstein condensation.

Einstein first predicted this effect in dilute gases in 1925, but it took 70 years until the first experiments were done in 1995. The reason for this is apparent from considering the temperature necessary to observe the condensation. If we start with an ordinary gas at room temperature (with a density of around 2.4×10^{25} molecules/m^3), then Eq. 10.45 gives a temperature of around 0.001 K = 1 mK. This is the temperature at which the condensate begins to form, and to have a significant number of particles in the condensate we must be well below this temperature. It is clear that *very* low temperatures are required to observe the condensate. However, even if the gas molecules were only weakly interacting, a gas at ordinary densities would become a liquid at these temperatures. It is therefore necessary to work with gases at extremely low densities, and from Eq. 10.45 you can see that as we reduce the density, the temperature necessary to observe the Bose-Einstein condensation becomes even smaller.

To avoid the gas condensing into a liquid, we want to molecules to be very far apart (corresponding to a very low density). How far apart must they be? In an ordinary gas, the mean free path (average distance between collisions) is the order of 100 molecular diameters. To avoid molecules from colliding and therefore sticking together (which might trigger the formation of the liquid), let's assume the spacing between molecules must be the order of 100 times larger than it is in an ordinary gas, which means the density must be smaller by a factor of $(10^{-2})^3 = 10^{-6}$. From Eq. 10.45 we see that if the density is smaller by 10^{-6}, then T_{BEC} will be smaller by a factor of $(10^{-6})^{2/3} = 10^{-4}$. Thus instead of a

temperature of 1 mK, the observation of a Bose-Einstein condensation requires temperatures of the order of 100 nK.

Such incredibly low temperatures require extraordinary means to produce, and that is why it took 70 years to observe the first Bose-Einstein condensate. Several successful experiments have been done since 1995, and the experiments generally use a combination of *laser cooling* and *magnetic cooling* to achieve these temperatures. In laser cooling, a collection of gas atoms is illuminated with a laser beam that is tuned to one of the atomic absorption frequencies. A gas atom that happens to be moving toward the laser will absorb a photon and slow down. However, a gas atom that is moving away from the laser will absorb a photon and speed up. How can this result in an overall slowing of the gas atoms?

The trick in laser cooling is to take advantage of the Doppler broadening of the absorption due to the distribution in the velocities of the gas atoms. The laser beam is tuned so that its frequency is a bit below the central frequency of the broadened peak. Frequencies smaller than the central frequency correspond to atoms moving toward the laser beam; such atoms can absorb at the frequency of the laser and thus slow down. Atoms moving in the opposite direction cannot absorb at that frequency (because their Doppler shifts are opposite) and so are not affected. If a second laser beam, also tuned below the central frequency, illuminates the atoms from the opposite side, then atoms moving in either direction will be slowed and therefore cooled. In practice, the gas is illuminated by lasers in all six directions to achieve cooling by slowing the atoms in three dimensions. The excited state formed by absorbing the photon will decay back to the ground state by emitting a photon, but the emission occurs in random directions and so doesn't change the velocity distribution of the atoms.

Laser cooling by itself is insufficient to achieve the temperatures necessary for Bose-Einstein condensation. It is also necessary to use some form of magnetic cooling. For example, suppose we confine the atoms in a region in which there is a magnetic field that is produced by a set of coils. The atoms are moving very slowly and do not have enough energy to escape the potential energy barrier that is established by the magnetic field. If the magnetic field strength is then reduced slightly, the more energetic atoms can escape. The remaining atoms still confined by the (weaker) magnetic field are the ones with smaller kinetic energies, and thus they have a lower temperature. With each lowering of the field strength, the more energetic atoms escape and the remaining gas cools. This is similar to evaporative cooling of a cup of hot coffee—the faster-moving atoms are the most likely to leave the liquid, and the remaining atoms have a smaller average kinetic energy and thus a lower temperature.

The first observations of a Bose-Einstein condensation were reported in 1995 by Eric Cornell and Carl Wieman using Rb vapor and by Wolfgang Ketterle using Na vapor. Figure 10.21 shows the velocity distribution illustrating the formation of the condensate in Rb vapor from the original work of Cornell and Wieman. At a temperature of 400 nK, the distribution shows a broad peak corresponding to a Maxwell velocity distribution centered at $v = 0$. At 200 nK, a narrow peak is superimposed on top of the Maxwell distribution at $v = 0$. This represents the atoms all moving with the same speed, as would be expected for a condensate with a large number of atoms in the same state of motion. At still lower temperatures (50 nK), the Maxwell distribution has disappeared, so that nearly all of the atoms are in the condensed ground state, consistent with Eq. 10.45.

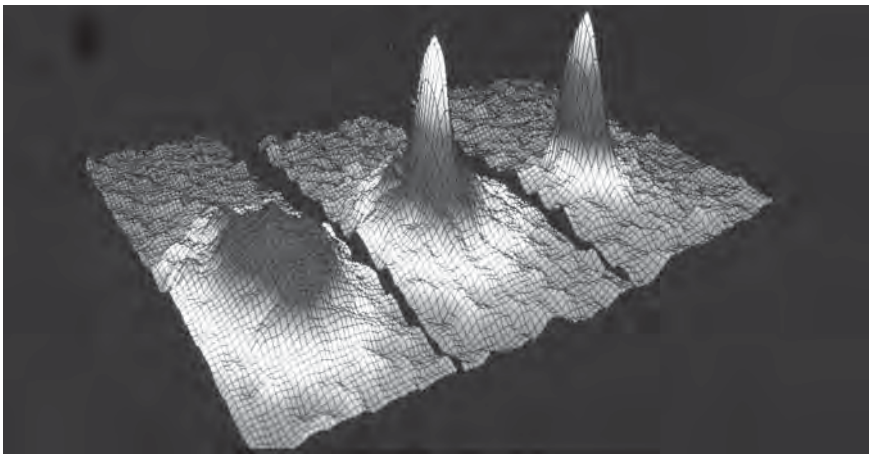

FIGURE 10.21 Bose-Einstein condensation in Rb atoms. The graphs show a representation of the velocity distribution at 400 nK (left), 200 nK (center), and 50 nK (right). At 400 nK, there is a broad Maxwellian distribution, but as the temperature is reduced, the molecules condense into a single quantum state characterized by a much narrower velocity profile.

For the experimental observations of the Bose-Einstein condensation, Cornell, Wieman, and Ketterle shared the 2001 Nobel Prize in physics.

10.7 APPLICATIONS OF FERMI-DIRAC STATISTICS

Now let's consider some applications of Fermi-Dirac statistics. We'll discuss several different systems consisting of spin-½ particles: electrons in metals, electrons and neutrons in stars, and ^{3}He in liquid ^{4}He.

The Free Electron Model of Metals

In a metal, the valence electrons are not very strongly bound to individual atoms, and consequently they travel rather freely throughout the volume of the metal. We can treat these electrons as a "gas" that obeys the Fermi-Dirac distribution, with a density of states given by Eq. 10.12. The number of electrons with energies between E and $E + dE$ is then

$$dN = N(E)\,dE = Vg(E)f_{\text{FD}}(E)\,dE = V\frac{8\pi\sqrt{2}m^{3/2}}{h^3}E^{1/2}\frac{1}{e^{(E-E_{\text{F}})/kT}+1}\,dE \tag{10.47}$$

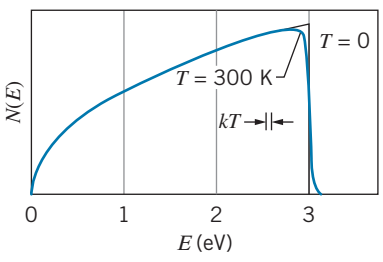

FIGURE 10.22 The number of occupied energy levels for electrons at $T = 0$ and $T = 300$ K, according to the Fermi-Dirac distribution. The Fermi energy E_{F} is chosen to be 3.0 eV.

Figure 10.22 shows a graph of $N(E)$. Note that the energy kT is only a small interval compared with the range of occupied energy states. When the temperature of the metal is increased from 0 K to 300 K (room temperature), only a very small fraction of the electrons is affected—a small number move from filled states just below E_{F} to formerly empty states just above E_{F}.

We can find a numerical value for E_{F} at $T = 0$ by normalizing Eq. 10.47 so that the sample contains a total number N of these free electrons:

$$N = \int dN = \int_0^\infty N(E)\,dE = \frac{8\pi V\sqrt{2}m^{3/2}}{h^3}\int_0^\infty \frac{E^{1/2}}{e^{(E-E_{\text{F}})/kT}+1}\,dE \tag{10.48}$$

At $T = 0$, the Fermi-Dirac distribution function has the value 1 for $E < E_F$ and 0 for $E > E_F$, so the integral reduces to

$$N = \frac{8\pi V\sqrt{2}m^{3/2}}{h^3}\int_0^{E_F} E^{1/2}\,dE = \frac{8\pi V\sqrt{2}m^{3/2}}{h^3}\frac{2}{3}E_F^{3/2} \tag{10.49}$$

Solving for E_F, we obtain

$$E_F = \frac{h^2}{2m}\left(\frac{3N}{8\pi V}\right)^{2/3} \tag{10.50}$$

We can also find the mean or average energy of the electrons

$$E_m = \frac{1}{N}\int_0^{\infty} EN(E)\,dE \tag{10.51}$$

and it is left as an exercise to show that

$$E_m = \tfrac{3}{5}E_F \tag{10.52}$$

Example 10.8

Compute the Fermi energy E_F for sodium.

Solution

Each sodium atom contributes one valence electron to the metal, and so the number of electrons per unit volume, N/V, is equal to the number of sodium atoms per unit volume. This in turn can be found from the density ρ and the molar mass M of sodium:

$$\frac{N}{V} = \frac{\rho N_A}{M} = \frac{(0.971 \times 10^3\ \text{kg/m}^3)(6.02 \times 10^{23}\ \text{atoms/mole})}{0.023\ \text{kg/mole}}$$
$$= 2.54 \times 10^{28}\ \text{m}^{-3}$$

The Fermi energy now can be found from Eq. 10.50:

$$E_F = \frac{h^2}{2m}\left(\frac{3}{8\pi}\frac{N}{V}\right)^{2/3} = \frac{h^2c^2}{2mc^2}\left(\frac{3}{8\pi}\frac{N}{V}\right)^{2/3}$$
$$= \frac{(1240\ \text{eV}\cdot\text{nm})^2}{2(0.511 \times 10^6\ \text{eV})}\left(\frac{3}{8\pi}2.54 \times 10^{28}\ \text{m}^{-3}\right)^{2/3}$$
$$= 3.15\ \text{eV}$$

The average energy of the valence electrons is $\frac{3}{5}E_F$ or 1.89 eV. *Even at the absolute zero of temperature*, the electrons still have quite a large average energy.

From Figure 10.22 we see that the change in $N(E)$ between $T = 0$ and $T = 300$ K (room temperature) is relatively small, and so these values for E_F and E_m are approximately correct at room temperature.

The meaning of these numbers is as follows. Instead of isolated atoms with individual energy levels, we consider the metal to be a single system with a very large number of energy levels (at least as far as the valence electrons are concerned). Electrons fill these energy levels, in accordance with the Pauli principle, beginning at $E = 0$. By the time we add 2.54×10^{22} valence electrons to 1 cm^3 of sodium, we have filled energy levels up to $E_F = 3.15$ eV; all levels below E_F are filled and all levels above E_F are empty. Electrons have an almost continuous energy distribution (the levels are discrete, but they are very close together) from $E = 0$ to $E = E_F$, with an average energy of 1.89 eV. At $T = 300$ K, a relatively small number of electrons is excited from below E_F to above E_F;

the range over which electrons are excited is of order $kT \cong 0.025$ eV, so that only electrons within about 0.025 eV of E_F are affected by the change from $T = 0$ to $T = 300$ K.

In a similar fashion, if we apply a modest electric field to a metal, the only effect is to change the state of motion of a relatively small number of electrons near the Fermi energy. Most of the electrons can't be affected by the electric field, because all of the nearby states are already filled. In Chapter 11, we'll discuss the heat capacity and the electrical conductivity of metals based on the Fermi-Dirac distribution of the electrons.

White Dwarf Stars

A star like the Sun has a constant radius because the outward pressure due to the radiation traveling from the center (where the fusion reactions take place) balances the inward gravitational force that tends toward collapse. Eventually the hydrogen fuel will be converted to helium, the rate of fusion reactions will decrease, and gravity will take over. The Sun will collapse to a smaller and smaller radius, until further contraction is stopped by the Pauli principle. This is the *white dwarf* stage of stellar evolution.

Let's consider a star of mass M to be composed originally of hydrogen, with equal numbers of protons (hydrogen nuclei) and electrons. (The star is too hot for atomic hydrogen to form, so we consider the star to be a "gas" of protons and a "gas" of electrons occupying the same spherical volume.) After the hydrogen has been converted into helium, the star will contain N electrons and $N/2$ helium nuclei (alpha particles). The helium nuclei are bosons, so the Pauli principle does not apply to them during the collapse. The collapse ends when the electrons cannot be forced closer together because the Pauli principle would be violated. At that point, all of the electron energy levels are filled from 0 to the Fermi energy. The average energy E_m of the electrons is $\frac{3}{5}E_F$, as given by Eq. 10.52, and so the total energy of N electrons is

$$E_{elec} = NE_m = \frac{3}{5}NE_F = \frac{3}{5}N\frac{h^2}{2m_e}\left(\frac{3N}{8\pi V}\right)^{2/3} = \frac{3Nh^2}{10m_e}\frac{1}{R^2}\left(\frac{9N}{32\pi^2}\right)^{2/3} \tag{10.53}$$

assuming the electrons to be distributed uniformly throughout a sphere of radius R and volume $V = \frac{4}{3}\pi R^3$.

The total gravitational energy of the star can be found from the mass distribution of the helium (the electron mass is negligible in comparison with the helium mass). For simplicity, we assume the star to be of uniform density. The result (see Problem 38) is

$$E_{grav} = -\frac{3}{5}\frac{GM^2}{R} = -\frac{3}{5}\frac{GN^2m_\alpha^2}{4R} \tag{10.54}$$

with $M = (N/2)m_\alpha$. The total energy is

$$E = E_{elec} + E_{grav} = \frac{3Nh^2}{10m_e}\frac{1}{R^2}\left(\frac{9N}{32\pi^2}\right)^{2/3} - \frac{3GN^2m_\alpha^2}{20R} \tag{10.55}$$

The star collapses until its energy reaches a minimum value, at which point we can find its radius by setting dE/dR equal to 0 and solving the resulting equation,

which gives

$$R = \frac{h^2}{GN^{1/3}m_e m_\alpha^2}\left(\frac{9}{4\pi^2}\right)^{2/3} \tag{10.56}$$

Let's consider the white dwarf star Sirius B, which has a mass of 2.09×10^{30} kg (about 5% greater than the mass of the Sun). Equation 10.56 gives a radius of 7.2×10^6 m for Sirius B. The measured radius is about 5.6×10^6 m. The difference between the calculated and observed values is probably due mostly to the relativistic motion of the electrons. Our calculation of the Fermi energy assumed the electrons to move nonrelativistically. The Fermi energy of Sirius B is about 200 keV, which means that the kinetic energy of electrons near the Fermi energy is not small compared with the rest energy (511 keV). We also oversimplified the structure of the star by assuming it to be of uniform density (which was necessary to obtain Eq. 10.54 for the gravitational energy). Nevertheless, even this very rough calculation gives us a good approximation to the properties of white dwarf stars and demonstrates another system in which Fermi-Dirac statistics can be applied.

Note that the radius of the white dwarf is comparable to the radius of the Earth; that is, the white dwarf has the mass of the Sun but the radius of the Earth. The average density of Sirius B is about 10^9 kg/m^3, which is about one million times the average density of objects on Earth. The white dwarf is indeed an extreme state of matter!

If we treat the electrons relativistically, we can obtain an estimate for the mass of the star at which the Pauli principle applied to the electrons is not able to prevent gravitational collapse. This value, which is called the *Chandrasekhar limit*, is about 1.4 solar masses. For stars with greater masses, the extreme density forces the protons and electrons to combine into neutrons until the star collapses into a *neutron star*, composed entirely of neutrons. Because neutrons obey the Pauli principle, we can apply Fermi-Dirac statistics to analyze the properties of neutron stars (see Problem 27). From a calculation similar to that for the white dwarf, we can find the radius at which the energy of a neutron star is at a minimum:

$$R = \frac{h^2}{GN^{1/3}m_n^3}\left(\frac{9}{32\pi^2}\right)^{2/3} \tag{10.57}$$

In this equation, N refers to the number of neutrons in the star. For a star of 1.5 solar masses, the radius would be about 11 km with a density of about 5×10^{17} kg/m^3.

Neutron stars are commonly observed as *pulsars* in which the magnetic field of the neutrons traps electrons outside the neutron star, and the rapid rotation of the neutron star causes a beam of electromagnetic radiation from the accelerated electrons to sweep past the Earth somewhat like the rotating light in a lighthouse. For stars heavier than about 6 solar masses, not even the Pauli principle applied to the neutrons can prevent further gravitational collapse, and the star will either explode as a supernova or collapse to a black hole.

The Heat Capacity of Dilute Solutions of ^{3}He in ^{4}He

Helium has two stable isotopes, ^{3}He and ^{4}He. The isotope ^{3}He is very rare (about 10^{-6} in abundance relative to ^{4}He) in natural He gas. The two isotopes are chemically identical and have the same electronic structure, but differ in their

atomic masses (^{3}He has a mass of about 3 u and ^{4}He is about 4 u). The difference comes about as a result of their nuclei: the nucleus of ^{3}He contains 2 protons and 1 neutron, while the nucleus of ^{4}He contains 2 protons and 2 neutrons. Protons, neutrons, and electrons all have a spin of ½. In ^{4}He, the 2 electrons combine to a total spin of 0, as do the 2 protons and the 2 neutrons. The total spin of ^{4}He is therefore 0. In ^{3}He, the 2 electrons combine to give a spin of 0 as do the 2 protons, but with only 1 neutron the total spin of ^{3}He is ½. As a result, ^{4}He behaves like a boson and ^{3}He like a fermion.

As discussed above, ^{4}He becomes a superfluid at temperatures below 2.17 K, while ^{3}He does not. In a dilute mixture of liquid ^{3}He and ^{4}He below 2.17 K, the ^{4}He serves as a mostly inert background medium for the ^{3}He, and so we can treat the ^{3}He as a dilute "gas" of fermions, just as we treated the electron gas in analyzing metals.

The heat capacity of a dilute mixture of ^{3}He in ^{4}He is relatively straightforward to measure, so let's try to calculate the heat capacity using the Fermi-Dirac distribution to describe the ^{3}He. Starting with fermions at $T = 0$, we add energy until the collection is at temperature T. Because all of the energy states below E_F are filled at $T = 0$, most of the particles are not able to absorb any additional energy. A particle with energy far below E_F cannot absorb energy of the order of kT and move to an empty state, because there are no empty states nearby. The only particles that can change their state are those within a small energy range of about kT at E_F, as shown in Figure 10.22. In going from temperature 0 to temperature T, only a relatively small number of particles moves from just below E_F to just above E_F, with the rest of the particles remaining in their same energy states.

Figure 10.23 shows a greatly magnified view of the region around E_F. As the temperature is raised from 0 to T, the particles in the region just below E_F move to fill states just above E_F. In particular, consider the small number of particles dN in the narrow region of width dE located a small energy $-\varepsilon = E - E_F$ below E_F. The particles fill states in that region at $T = 0$, but when the temperature is raised to T they move to fill states in the corresponding region at an energy ε above E_F. Each particle in that narrow interval thus gains an energy of 2ε, and the total energy gained by all the particles in that narrow strip is $dE_{ex} = 2\varepsilon dN$. The strip has height N_{ex} given by the difference between $N(E)$ at $T = 0$ and $N(E)$ at temperature T:

$$N_{ex} = N(E, T = 0) - N(E, T) = Vg(E)[1 - f_{FD}(E)] \tag{10.58}$$

where we have used $N(E) = Vg(E)f_{FD}(E)$ and $f_{FD} = 1$ for $T = 0$. The width of the strip is dE, so the number of particles in the strip is $dN = N_{ex}dE$. With $-\varepsilon = E - E_F$ and $|d\varepsilon| = |dE|$, we obtain the energy gained by the particles in the narrow strip:

$$dE_{ex} = 2\varepsilon\, dN = 2\varepsilon N_{ex}\, d\varepsilon = 2\varepsilon Vg(E_F - \varepsilon)\left(1 - \frac{1}{e^{-\varepsilon/kT} + 1}\right) d\varepsilon \tag{10.59}$$

The energy difference ε, which we defined as the energy of the strip below E_F, runs from E_F (where $E = 0$) to 0 (where $E = E_F$). The total excitation energy of all of the particles that are excited from below E_F to above E_F is

$$E_{ex} = \int dE_{ex} = 2V \int_{E_F}^{0} \varepsilon g(E_F - \varepsilon)\left(1 - \frac{1}{e^{-\varepsilon/kT} + 1}\right) d\varepsilon \tag{10.60}$$

We can simplify the calculation by noting that $g(E)$ is a very slowly varying function compared with f_{FD} in the region near E_F, and even though we are

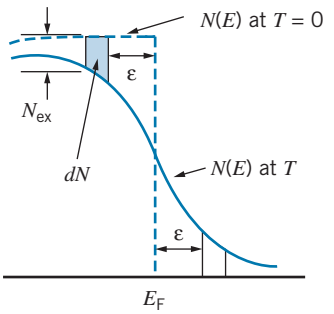

FIGURE 10.23 The region near E_F, showing $N(E)$ at $T = 0$ and at temperature T. When the temperature is raised from 0 to T, the dN particles in the shaded region move to the corresponding region above E_F, increasing their energy by 2ε in the process.

integrating from E_F to 0 the integral is nonzero only in a region very close to E_F. We can therefore take $g(E_F - \varepsilon) \cong g(E_F)$ and bring it out of the integral. Again because the integrand is nonzero only in a very small region, we can replace the lower limit on the integral by ∞.

$$E_{ex} = 2Vg(E_F) \int_{\infty}^{0} \varepsilon \left(1 - \frac{1}{e^{-\varepsilon/kT} + 1}\right) d\varepsilon \tag{10.61}$$

The heat capacity is defined as $C = dE_{ex}/dT$. The derivative with respect to T can be moved inside the integral, and so

$$C = \frac{dE_{ex}}{dT} = 2Vg(E_F) \int_{\infty}^{0} \varepsilon \left[\frac{-e^{-\varepsilon/kT}}{(e^{-\varepsilon/kT} + 1)^2} \left(\frac{\varepsilon}{kT^2}\right)\right] d\varepsilon$$

$$= \frac{2Vg(E_F)}{kT^2} (kT)^3 \int_{0}^{\infty} \frac{x^2 e^x}{(e^x + 1)^2} dx \tag{10.62}$$

where $x = \varepsilon/kT$. The integral is a standard form that has the value $\pi^2/6$. Putting in the value for $g(E_F)$ from Eqs. 10.12 and 10.50, we finally obtain

$$C = \frac{\pi^2 k^2 NT}{2E_F} \tag{10.63}$$

This equation predicts that the heat capacity of a dilute gas of fermions at low temperature should be proportional to T. Figure 10.24 shows the low-temperature heat capacity of a dilute mixture of 5% ^{3}He in ^{4}He, and you can see how well the data agree with the prediction. The relationship is indeed linear in T at low temperature. This same behavior also describes the low-temperature heat capacity of metals, in which the electrons can also be treated as a dilute gas of fermions, but as we will see in the next chapter the contribution of the atoms to the heat capacity can often be much larger than the contribution of the electrons.

Equation 10.63 predicts that the slope of the plot of C against T should be $\pi^2 k^2 N/2E_F$, which works out to be 1.24 J/K^2 for the experiment that obtained the results shown in Figure 10.24 (a 5% mixture of ^{3}He in ^{4}He and a total of 0.5 mole of liquid). The measured slope is 3.11 J/K^2, which differs from the expected slope by a factor of 2.5. The discrepancy comes about because we treated the ^{3}He atoms like those of a gas, in which the particles move freely. However, when ^{3}He moves through ^{4}He, there are viscous and other forces that act on the atoms. We can account for the difference by assigning the ^{3}He an "effective mass," which is greater than its actual mass; the greater mass simulates the sluggish behavior of the ^{3}He atoms as they move through ^{4}He. This same factor of about 2.5 appears in experiments with very different concentrations of ^{3}He, so it is not related to any interaction of ^{3}He atoms with other ^{3}He atoms. It also arises in other experiments, such as the study of heat conduction in ^{3}He-^{4}He mixtures, so it does indeed seem to describe the properties of the mixture itself rather than any particular experiment.

The success of the Fermi-Dirac distribution function in accounting for the properties of such a diverse array of systems—metals, white dwarf stars, and dilute mixtures of ^{3}He in ^{4}He—is truly impressive. In the next chapter, we shall explore in more detail how both Bose-Einstein and Fermi-Dirac statistics can be used to help us understand various properties of solids.

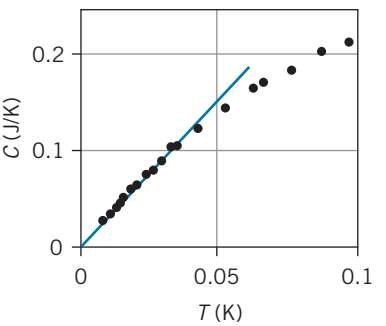

FIGURE 10.24 The heat capacity of 0.5 mole of a dilute (5%) mixture of ^{3}He in ^{4}He. The straight line is a fit to the linear portion of the plot below about 40 mK.

Chapter Summary

		Section
Probability of energy observation	$p(E) = \dfrac{\sum N_i W_i}{N \sum W_i}$	10.2
Number of particles with discrete energy	$N_n = d_n f(E_n)$	10.3
Density of states in gas of particles	$g(E) = \dfrac{4\pi(2s+1)\sqrt{2}(mc^2)^{3/2}}{(hc)^3} E^{1/2}$	10.3
Density of states in gas of photons	$g(E) = \dfrac{1}{\pi^2(\hbar c)^3} E^2 = \dfrac{8\pi}{(hc)^3} E^2$	10.3
Maxwell-Boltzmann energy distribution	$N(E) = \dfrac{2N}{\sqrt{\pi}(kT)^{3/2}} E^{1/2} e^{-E/kT}$	10.4
Maxwell speed distribution	$N(v) = N\sqrt{\dfrac{2}{\pi}} \left(\dfrac{m}{kT}\right)^{3/2} v^2 e^{-mv^2/2kT}$	10.4
Maxwell velocity distribution	$N(v_x) = N \left(\dfrac{m}{2\pi kT}\right)^{1/2} e^{-mv_x^2/2kT}$	10.4
Doppler broadening of spectral line	$\Delta f = 2 f_0 \sqrt{(2 \ln 2) kT/mc^2}$	10.4
Bose-Einstein distribution function	$f_{\text{BE}}(E) = \dfrac{1}{A_{\text{BE}} e^{E/kT} - 1}$	10.5
Fermi-Dirac distribution function	$f_{\text{FD}}(E) = \dfrac{1}{e^{(E-E_{\text{F}})/kT} + 1}$	10.5
Fermi energy	$E_{\text{F}} = \dfrac{h^2}{2m} \left(\dfrac{3N}{8\pi V}\right)^{2/3}$	10.7
Radius of white dwarf star	$R = \dfrac{h^2}{GN^{1/3} m_e m_\alpha^2} \left(\dfrac{9}{4\pi^2}\right)^{2/3}$	10.7

Questions

1. Suppose a container filled with a gas moves with constant velocity v. How is the Maxwell velocity distribution different for such a gas, compared with the same container of gas at rest?
2. The population inversion necessary for the operation of a laser is sometimes called a "negative temperature." What is the meaning of a negative temperature? Does it have a physical interpretation?
3. Figure 10.25 shows two different experimental arrangements used to measure the distribution of molecular speeds. Based on the figures, explain how each apparatus might operate, and try to guess how the observed distribution of molecules might appear. Where do the fastest molecules land? The slowest?
4. How would Figure 10.13 change if the temperature of the gas were increased?
5. How is the speed distribution of a gas at temperature T different from that at temperature $2T$? The energy distribution? Sketch the speed and energy distributions at the two temperatures.

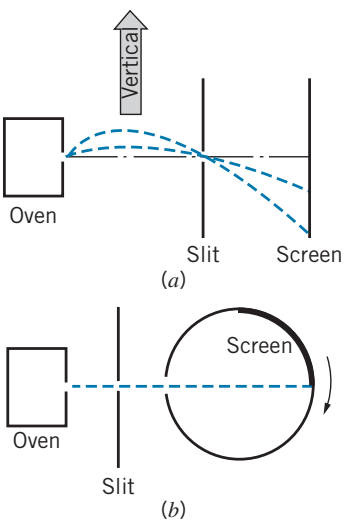

FIGURE 10.25 Question 3.

6. Consider a mixture of two gases of molecular masses m_1 and $m_2 = 2m_1$ in thermal equilibrium at temperature T. How do their speed distributions differ? How do their energy distributions differ?
7. It is generally more convenient, wherever possible, to use Maxwell-Boltzmann statistics rather than quantum statistics. Under what circumstances can a quantum system be described by Maxwell-Boltzmann statistics?
8. Suppose we had a gas of hydrogen *atoms* at relatively high density. Do the atoms behave as fermions or as bosons? Would a gas of deuterium (heavy hydrogen) atoms behave any differently? (*Hint:* The nuclear spin is $\frac{1}{2}$ for hydrogen and 1 for deuterium.)
9. The early universe contained a large density of neutrinos (massless spin-$\frac{1}{2}$ particles that travel at the speed of light). Which statistical distribution would be needed to describe the properties of the neutrinos?
10. Would you expect the photoelectric effect to depend on the temperature of the surface of the metal? Explain.
11. Estimate the mean kinetic energy of the "free" electrons in a metal if they obeyed Maxwell-Boltzmann statistics. How does this compare with the result of applying Fermi-Dirac statistics? Why is there such a difference?

Problems

10.1 Statistical Analysis

1. A collection of three noninteracting particles shares 3 units of energy. Each particle is restricted to having an integral number of units of energy. (*a*) How many macrostates are there? (*b*) How many microstates are there in each of the macrostates? (*c*) What is the probability of finding one of the particles with 2 units of energy? With 0 units of energy?
2. (*a*) Considering the numbers of heads and tails, how many macrostates are there when 5 coins are tossed? (*b*) What is the total number of possible microstates in tossing 5 coins? (*c*) Find the number of microstates for each macrostate, and be sure the total agrees with your answer to part (*b*).
3. Consider a system consisting of two particles, one with spin $s = 1$ and another with spin $s = \frac{1}{2}$. (*a*) Considering a microstate to be an assignment of the z component of the spins of each of the particles, what is the total number of microstates of the two-particle system? (*b*) How many macrostates are there for the total spin of the two-particle system? (*c*) Find the number of microstates for each macrostate, and be sure the total number agrees with your answer to part (*a*).

10.2 Classical and Quantum Statistics

4. Calculate the probabilities for $E = 0, 3$ and 5 listed in Table 10.2.
5. Calculate the probabilities given in Table 10.3 for $E = 0$ and $E = 3$ for (*a*) integral spin and (*b*) spin 1/2.
6. A system of four oscillator-like particles shares 8 units of energy. (That is, the particles can accept energy only in equal units, in which the oscillator spacing is 1 unit.) (*a*) List the macrostates, and for each macrostate give the number of microstates for distinguishable classical particles, indistinguishable quantum particles with integral spin, and indistinguishable quantum particles with half-integral spin. (*b*) Calculate the probability to find a particle with exactly 2 units of energy for each of the three different types of particles.
7. A system consists of two particles, each of which has a spin of $\frac{3}{2}$. (*a*) Assuming the particles to be distinguishable, what are the macrostates of the z component of the total spin, and what is the multiplicity of each? (*b*) What are the possible values of the total spin S and what is the multiplicity of each value? Verify that the total multiplicity matches that of part (*a*). (*c*) Now suppose the particles behave like indistinguishable quantum particles. What is the multiplicity of each of the macrostates of the z component of the total spin? (*d*) Show that for these quantum particles it is possible to have only combinations with total spin $S = 3$ or 1.

10.3 The Density of States

8. The universe is filled with photons left over from the Big Bang that today have an average energy of about 2×10^{-4} eV (corresponding to a temperature of 2.7 K). What is the number of available energy states per unit volume for these photons in an interval of 10^{-5} eV?
9. In certain semiconductors, the conducting regions are grown in very thin layers, which can be regarded as two-dimensional regions holding an electron gas. Calculate the density of states (per unit area) for a gas of particles of mass m and spin s confined to move in two dimensions in a square region of length L on each side.
10. Calculate the density of states (per unit area) for a collection of photons confined to a two-dimensional region in the shape of a square a length L on each side.
11. In a conductor like copper, each atom provides one electron that is available to conduct electric currents. If we assume that the electrons behave like a gas of particles at room temperature with a most probable energy of 0.0252 eV, what is the density of states in an interval of 1% about the most probable energy?

10.4 The Maxwell-Boltzmann Distribution

12. A system consists of N particles that can occupy two energy levels: a nondegenerate ground state and a three-fold

degenerate excited state, which is at an energy of 0.25 eV above the ground state. At a temperature of 960 K, find the number of particles in the ground state and in the excited state.

13. A system with nondegenerate energy levels has three energy states: a ground state at $E = 0$ and excited states at energies of 0.045 eV and 0.135 eV. At a temperature of 650 K, find the relative numbers of particles in the three states.
14. Show that the most probable speed v_p of the Maxwell speed distribution is $(2kT/m)^{1/2}$.
15. A container holds one mole of helium gas at a temperature of 293 K. (*a*) Show that the mean energy E_m of the molecules is 0.0379 eV. (*b*) How many molecules have energies in an interval of width $0.01E_m$ centered on E_m?
16. A cubic container holds one mole of argon gas at a temperature of 293 K. (*a*) How many molecules have speeds between 500 and 510 m/s? (*b*) How many molecules have velocities between 500 and 510 m/s in one particular direction? Explain any differences between the answers to (*a*) and (*b*).
17. The photosphere of the Sun has a temperature of 5800 K. (*a*) Calculate the energy linewidth of the first transition in the Lyman series of hydrogen in the Sun's photosphere. (*b*) For comparison, calculate the natural linewidth, assuming a lifetime of 10^{-8} s.

10.5 Quantum Statistics

18. Do we expect to be able to use Maxwell-Boltzmann statistics to analyze (*a*) nitrogen gas at standard conditions (room temperature, 1 atmosphere pressure); (*b*) liquid water at room temperature; (*c*) liquid helium at 4 K; (*d*) conduction electrons in copper at room temperature?
19. (*a*) What pressure must be applied to nitrogen gas at room temperature before Maxwell-Boltzmann statistics begins to fail? (*b*) To what temperature must we cool nitrogen gas at 1 atmosphere before Maxwell-Boltzmann statistics begins to fail?

10.6 Applications of Bose-Einstein Statistics

20. (*a*) Show that the total number of photons per unit volume at temperature T is $N/V = 8\pi(kT/hc)^3 \int_0^\infty x^2 dx/(e^x - 1)$. (*b*) The value of the integral is about 2.404. How many photons per cubic centimeter are there in a cavity filled with radiation at $T = 300$ K? At $T = 3$ K?
21. A blackbody is radiating at a temperature of 2.50×10^3 K. (*a*) What is the total energy density of the radiation? (*b*) What fraction of the energy is emitted in the interval between 1.00 and 1.05 eV? (*c*) What fraction is emitted between 10.00 and 10.05 eV?
22. Find the photon energy at which the blackbody energy spectrum $u(E)$ is a maximum. Compare this result with Wien's displacement law (see Chapter 3) and account for any differences.

10.7 Applications of Fermi-Dirac Statistics

23. Compute the Fermi energy and the average electron energy for copper.
24. Calculate the Fermi energy for magnesium, assuming two free electrons per atom.
25. A certain metal has a Fermi energy of 3.00 eV. Find the number of electrons per unit volume with energy between 5.00 eV and 5.10 eV for (*a*) $T = 295$ K; (*b*) $T = 2500$ K.
26. Derive Eq. 10.52 from Eq. 10.51.
27. Assume a neutron star consists of N neutrons (fermions with spin $1/2$) in a sphere of radius R and uniform density. The star is in equilibrium because the inward gravitational force, which tends to collapse the star, is opposed by a repulsion due to the Pauli principle, which prevents the neutrons from moving closer together. (*a*) Find an expression for the radius of a neutron star. (*b*) Evaluate the radius for a star of mass equal to 3 solar masses. (*c*) What is the density of the star?
28. Consider a neutron star of mass equal to twice the mass of the Sun. (*a*) Evaluate the Fermi energy and determine whether classical or relativistic kinematics should be used in the analysis. (*b*) Find the de Broglie wavelength of a neutron at the Fermi energy and compare with the average distance between neutrons.
29. For a 5.0% mixture of ^{3}He in 0.50 mole of ^{4}He, calculate the heat capacity in J/K at a temperature of 0.025 mK and compare with the data shown in Figure 10.24. The density of liquid ^{4}He at this temperature is 2.2×10^{28} atoms/m^3. Assume an effective mass of ^{3}He that is 2.5 times its ordinary mass.

General Problems

30. Show that a system of 2 indistinguishable quantum particles with spin 2 can combine only to a total spin of 0, 2, or 4.
31. Consider a collection of N noninteracting atoms with a single excited state at energy E. Assume the atoms obey Maxwell-Boltzmann statistics, and take both the ground state and the excited state to be nondegenerate. (*a*) At temperature T, what is the ratio of the number of atoms in the excited state to the number in the ground state? (*b*) What is the average energy of an atom in this system? (*c*) What is the total energy of the system? (*d*) What is the heat capacity of this system?
32. Suppose we have a gas in thermal equilibrium at temperature T. Each molecule of the gas has mass m. (*a*) What is the ratio of the number of molecules at the Earth's surface to the number at height h (with potential energy mgh)? (*b*) What is the ratio of the density of the gas at height h to the density ρ_0 at the surface? (*c*) Would you expect this simple model to give an adequate description of the Earth's atmosphere?
33. A collection of noninteracting hydrogen atoms is maintained in the $2p$ state in a magnetic field of strength 5.0 T. (*a*) At room temperature (293 K), find the fraction of the atoms in the $m_l = +1, 0$, and -1 states. (*b*) If the $2p$ state made a

transition to the 1*s* state, what would be the relative intensites of the three normal Zeeman components? Ignore any effects of electron spin.

34. The following method is used to measure the molecular weight of very heavy molecules. A liquid containing the molecules is spun rapidly in a centrifuge, which establishes a variation in the density of the liquid. The density is measured, such as by absorption of light, to determine the molecular weight. Assign a fictitious "centrifugal" force to act on the molecules and show that the density varies as $\rho = \rho_0 e^{m\omega^2 x^2/2kT}$ where ω is the angular velocity of the centrifuge and x measures the distance along the centrifuge tube.
35. In sodium metal at room temperature, compute the energy difference between the points at which the Fermi-Dirac distribution function has the values 0.1 and 0.9. What do you conclude about the "sharpness" of the distribution?
36. In sodium metal (see Example 10.8), calculate the number of electrons per unit volume at room temperature in an interval of width $0.01E_F$ at the mean energy E_m.
37. Protons and neutrons are spin-$\frac{1}{2}$ particles in the nucleus. Find the average energy of the protons and neutrons in the nucleus of a uranium atom, which contains 92 protons and 143 neutrons and has the shape of a sphere of radius of 7.4×10^{-15} m.
38. Consider a uniform spherical distribution of matter of radius r and density ρ. (*a*) Imagine that a small increment of mass dm is brought from infinity to radius r. What is the change in the gravitational potential energy of the system consisting of the sphere and this mass increment? (*b*) Suppose we bring in from infinity a series of small mass increments that eventually form a thin spherical shell of radius r and thickness dr about the central sphere. What is the change in the potential energy of the system? (*c*) What is the total change in potential energy involved with creating a sphere of mass M and radius R?
39. (*a*) For a white dwarf star of mass equal to the mass of the Sun, find the de Broglie wavelength for electrons at the Fermi energy. Use nonrelativistic kinematics and assume the star to be composed of helium nuclei (alpha particles) and of uniform density. (*b*) Estimate the average distance between the electrons and compare with their de Broglie wavelength. What can you conclude from this comparison?
40. Measuring the relative population of magnetic substates of nuclei provides a direct way of determining the temperature for very cold systems, using a thermometer that is absolute and needs no calibration. The nucleus ^{60}Co behaves as if it has a spin of 5 and a magnetic moment of $\vec{\boldsymbol{\mu}} = \gamma \vec{\mathbf{S}}$, where $\vec{\mathbf{S}}$ represents the nuclear spin and γ is a constant equal to $3.64 \times 10^7\ \mathrm{T^{-1}s^{-1}}$. When Co atoms are imbedded in a piece of magnetized iron, the Co nuclei experience a magnetic field of $\vec{\mathbf{B}} = -B\hat{\mathbf{k}}$, where $B = 29.0$ T and $\hat{\mathbf{k}}$ is the unit vector in the z direction. (*a*) In a certain experiment using a Co in Fe thermometer, the ratio r of the population of the second lowest substate to that population of the lowest substate was observed to be $r = 0.419$. What is the corresponding temperature? (*b*) At that temperature, what is the ratio of the population of the $m = 0$ substate to that of the lowest substate?
41. The molecule cyanogen (CN), which is commonly found in interstellar gas clouds, has rotational excited states that can absorb visible light. These rotational states are populated by the warming effect of the cosmic background radiation that is a remnant of the creation of the universe. The energy of the first excited rotational state ($L = 1$) is 4.71×10^{-4} eV above the ground state. (*a*) The ratio of the intensity of the radiation absorbed in the first excited rotational state to the intensity of the radiation absorbed in the rotational ground state is 0.421 ± 0.017. Assuming this factor represents the relative populations of the two states, calculate the temperature of the cyanogen molecules and its uncertainty. (*b*) Based on your deduced temperature, calculate the expected ratio of the absorption intensity from the *second* rotational state to that of the ground state and compare with the observed relative intensity (0.0121 ± 0.0014). Direct observation of this background radiation shows it to have the expected thermal radiation spectrum at this temperature (see Chapter 15).

Chapter 11

SOLID-STATE PHYSICS

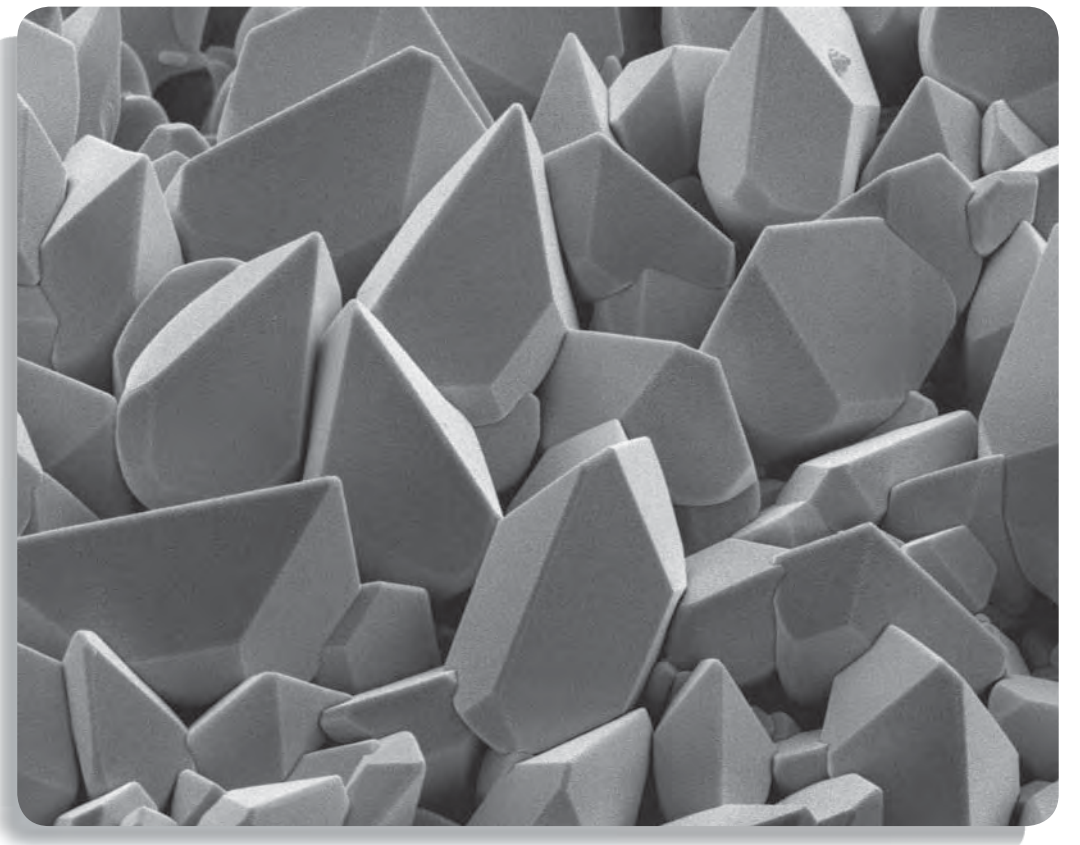

This scanning electron microscope image shows crystals of the metallic element tungsten. The shape of the crystal is determined by the geometrical arrangement of tungsten atoms, which are bound together in the body-centered cubic structure.

In this chapter we study the way atoms or molecules combine to make solids. In particular, we discuss how the principles of quantum mechanics are essential in understanding the properties of solids.

At first thought, there seem to be so many different solids that to classify them and form some general rules for their properties would appear to be a hopeless task. The book you are reading is made of paper and cloth, held together by a glue made from resins, once liquid and now solid. Your desk might be made of wood, metal, or plastic; your chair might be made of similar materials, and might perhaps be covered with cloth, leather, or plastic fabric and contain fiber or synthetic foam padding. Around you, there might be many books and papers, pencils made of wood and metal and graphite, rubber erasers, pens of metal and plastic. A plastic body and a liquid crystal display surround the semiconductors that lie at the heart of your calculator or computer, your cell phone, and your portable multimedia player. Looking out through a glass window, you see structures made of wood, bricks, concrete, or metal, selected for strength, utility, or attractiveness. Each of these solids has a characteristic color, texture, strength, hardness, or ductility; it has a certain measurable electrical conductivity, heat capacity, thermal conductivity, magnetic susceptibility, and melting point; it has certain characteristic emission or absorption spectra in the visible, infrared, ultraviolet, or other regions of the electromagnetic spectrum.

It is a fair generalization to say that all of these properties depend on two features of the structure of the material: the type of atoms or molecules of which the substance is made, and the way those atoms or molecules are joined or stacked together to make the solid. It is the formidable task of the *solid-state* (or *condensed-matter*) *physicist* or *physical chemist* to try to relate the structure of materials to their observed physical or chemical properties.

Quantum mechanics plays a fundamental role in determining properties of the solid: mechanical, electrical, thermal, magnetic, optical, and so forth. In this chapter we illustrate the application of quantum mechanics to the study of solids by studying some of their thermal, electrical, and magnetic properties.

11.1 CRYSTAL STRUCTURES

Our discussion will concentrate on materials in which the atoms or molecules occupy regular or periodic sites; this structure is called a *lattice,* and materials with this structure are called *crystals.* Crystalline materials include many metals, chemical salts, and semiconductors. One property that distinguishes crystals is their *long-range order*—once we begin constructing the lattice in one location, we determine the placement of atoms that are quite far away. In this respect, the crystal is like a brick wall, in which the bricks are stacked in a periodic array and the placement of a brick is predetermined by the original arrangement of bricks far away compared with the size of a brick. (By contrast, *amorphous* materials such as glass or paper have no long-range order, and their structure is more similar to a pile of bricks than to a brick wall.)

Solid crystals can be classified by the cohesive forces that are responsible for holding the lattice together, as well as by the shape of the arrangement of the atoms in the lattice. We'll look at a few different ways that atoms can be bound together in solids.

Ionic Solids

As we learned in Chapter 9, the cohesive forces in ionic molecules originate from the electrostatic attraction between a closed-shell ion, such as Na^+, and another closed-shell ion, such as Cl^-. Ionic materials can also form solids readily, because a Na^+ ion can simultaneously attract many Cl^- ions to itself, thereby building up a solid structure. The ions are held together by electrostatic forces, so we might suppose that the more negative ions there are around a positive ion, the more stable and strong the solid will be. (Covalent bonds, on the other hand, involve specific electron wave functions and so are limited in the number of near neighbors that can participate in the bonding.)

Ionic solids are crystalline, rather than amorphous, because we can pack ions together more efficiently in a regular array than in a random arrangement. (The same is true for bricks: In a regular array, there are more bricks per unit volume than in a random pile, and their average separation is smaller.)

The simplest type of crystal lattice is the *cubic* lattice, in which we imagine the atoms to be placed at the corners of a succession of cubes that cover the volume of the crystal. Figure 11.1 shows the basic cubic structure. This type of stacking is not the most efficient, because there are large gaps at the center of each face of the cube, and also in the middle of the cube itself. We get a better stacking arrangement, which has more atoms per unit volume, if we place another atom either at the center of each face of the cube or at the center of the body of the cube. These two lattices are known as *face-centered cubic* (fcc) and *body-centered cubic* (bcc) and are illustrated in Figures 11.2 and 11.3.

The fcc lattice gives a slightly more efficient packing (more atoms per unit volume) and so it is usually the most stable structure. However, atoms do not stack like hard spheres, and often the bcc structure is preferred. These two crystal types, fcc and bcc, also occur for materials other than ionic solids, such as certain metals.

A common material that has the fcc lattice structure is NaCl, and for that reason the fcc lattice is often called the *NaCl structure*. In order to have the atoms attract one another, we must alternate Na^+ and Cl^- ions, as is shown in Figure 11.4.

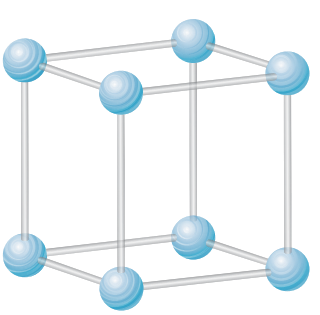

FIGURE 11.1 The simple cubic crystal. The atoms are shown as small spheres for clarity; in an actual solid, the atoms should be imagined as spheres in contact in this cubic geometry.

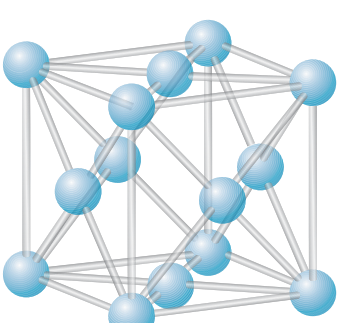

FIGURE 11.2 The face-centered cubic structure.

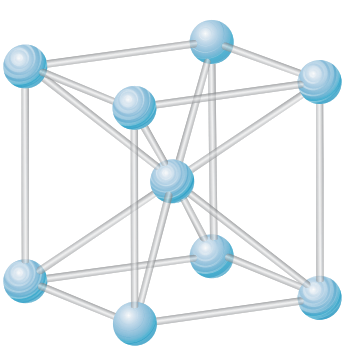

FIGURE 11.3 The body-centered cubic structure.

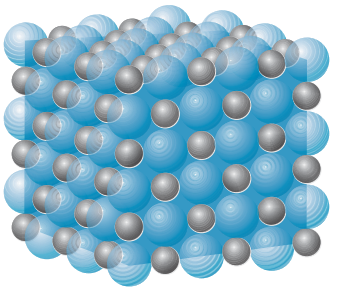

FIGURE 11.4 Packing of Na (small spheres) and Cl (large spheres) in a fcc crystal of NaCl.

In this illustration you can see how the atoms pack together just like hard spheres in contact. Notice that a given Na^+ ion is attracted by 6 close Cl^- neighbors, and does not "belong to" any single Cl^- ion. *It is therefore wrong to consider ionic solids as being composed of molecules.*

A typical bcc structure is CsCl, as shown in Figure 11.5, and so the bcc lattice is often known as the *CsCl structure*. In this case each ion is surrounded by 8 neighbors of the opposite charge.

Each Na^+ ion in the NaCl structure is surrounded at a distance R by 6 Cl^- ions exerting attractive electrostatic forces. At the slightly larger distance of $R\sqrt{2}$ from each Na^+ ion are 12 Na^+ ions exerting repulsive forces, and at the still greater distance of $R\sqrt{3}$ there are 8 Cl^- ions exerting attractive forces. To find the total Coulomb potential energy U_C, we can continue in this way to add the alternating attractive and repulsive contributions:

$$\begin{aligned} U_C &= \sum \frac{q_1 q_2}{4\pi\varepsilon_0 r} = \frac{e^2}{4\pi\varepsilon_0}\left(-6\frac{1}{R} + 12\frac{1}{R\sqrt{2}} - 8\frac{1}{R\sqrt{3}} + \cdots\right) \\ &= -\frac{e^2}{4\pi\varepsilon_0}\frac{1}{R}\left(6 - \frac{12}{\sqrt{2}} + \frac{8}{\sqrt{3}} - \cdots\right) = -\alpha\frac{e^2}{4\pi\varepsilon_0}\frac{1}{R} \end{aligned} \tag{11.1}$$

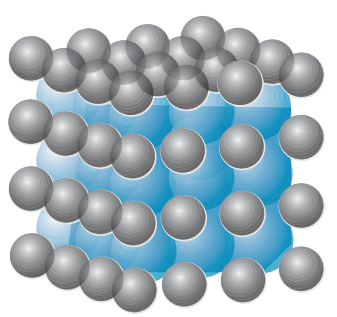

FIGURE 11.5 Packing of Cs (large spheres) and Cl (small spheres) in a bcc crystal of CsCl.

where α, called the *Madelung constant*, is the factor in parentheses in Eq. 11.1:

$$\alpha = 6 - \frac{12}{\sqrt{2}} + \frac{8}{\sqrt{3}} - \cdots \tag{11.2}$$

This quantity depends only on the geometry of the lattice and is evaluated by summing the slowly converging series of alternating positive and negative terms. The result is

$$\alpha = 1.7476 \qquad \text{(fcc or NaCl lattice)}$$

For the bcc lattice, a similar calculation gives

$$\alpha = 1.7627 \qquad \text{(bcc or CsCl lattice)}$$

As in the case of ionic molecules, the net attractive electrostatic force is opposed by a repulsive force due to the Pauli principle, which keeps the filled subshells from overlapping. The repulsive potential energy can be approximated as

$$U_R = AR^{-n} \tag{11.3}$$

where A gives the strength of the potential energy and n determines how rapidly it increases at small R. For most ionic crystals, n is in the 8–10 range. The total potential energy of an ion in the lattice is the sum of the Coulomb and repulsive potential energies:

$$U = U_C + U_R = -\alpha\frac{e^2}{4\pi\varepsilon_0}\frac{1}{R} + \frac{A}{R^n} \tag{11.4}$$

The energies are illustrated in Figure 11.6. There is a stable minimum in the energy, that determines both the equilibrium separation R_0 and the binding energy. To find this minimum, we set dU/dR to zero, which gives

$$A = \frac{\alpha e^2 R_0^{n-1}}{4\pi\varepsilon_0 n} \tag{11.5}$$

TABLE 11.1 Properties of Ionic Crystals

	Nearest-Neighbor Separation	Cohesive Energy (kJ/mol)	n	Structure
LiF	0.201	1030	6	fcc
LiCl	0.257	834	7	fcc
NaCl	0.281	769	9	fcc
NaI	0.324	682	9.5	fcc
KCl	0.315	701	9	fcc
KBr	0.330	671	9.5	fcc
RbF	0.282	774	8.5	fcc
RbCl	0.329	680	9.5	fcc
CsCl	0.356	657	10.5	bcc
CsI	0.395	600	12	bcc
MgO	0.210	3795	7	fcc
BaO	0.275	3029	9.5	fcc

The binding energy B of an ion in the crystal is the depth of the energy well at $R = R_0$, the equilibrium separation between nearest-neighbor ions. Substituting Eq. 11.5 into Eq. 11.4 and evaluating the resulting equation at $R = R_0$, we obtain

$$B = -U(R_0) = \frac{\alpha e^2}{4\pi\varepsilon_0 R_0}\left(1 - \frac{1}{n}\right) \tag{11.6}$$

From thermodynamic measurements, it is possible to determine the bulk *cohesive energy* of a solid. In effect, the cohesive energy of an ionic solid is defined as the energy necessary to dismantle the solid into individual ions. Some measured values of the cohesive energies and nearest-neighbor spacings are given in Table 11.1. The value of the exponent n is determined from compressibility data.

The cohesive energy of a bulk sample can be calculated by multiplying the binding energy for a single ion, determined from Eq. 11.6, by the number of ions in the sample, except that such a calculation would count each ion twice.* In one mole of an ionic solid, there are Avogadro's number N_A of positive ions and also N_A negative ions, for a total of $2N_A$ ions per mole. The relationship between the molar cohesive energy E_{coh} and the ionic binding energy B is then

$$E_{coh} = \tfrac{1}{2}(B)(2N_A) = BN_A \tag{11.7}$$

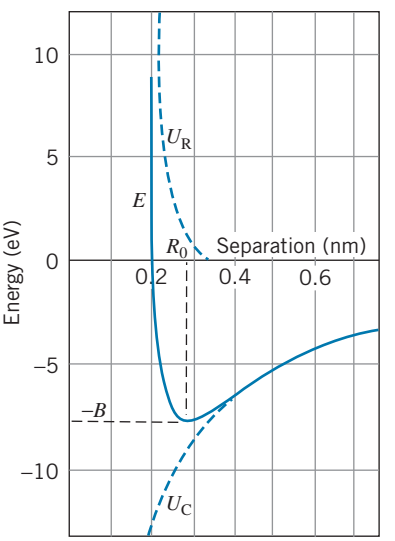

FIGURE 11.6 Contributions to the energy of an ionic crystal. Numerical values are for NaCl.

*Consider ions A and B. If we use Eq. 11.6 to compute the binding energy of ion A, the result includes the interaction of ion A with *all* the ions of the solid, including ion B. Similarly, the binding energy of ion B calculated from Eq. 11.6 includes the interaction of B with A. If we calculated the total binding energy of the solid by adding together the binding energies of all ions A and B, we would be including the interaction between A and B twice.

where the factor of 1/2 corrects for the problem of double counting of the ions.

The following examples illustrate the relationship between cohesive energy of the bulk solid and the binding energy per ion pair.

Example 11.1

(*a*) Determine the experimental value of the binding energy of an ion pair in the NaCl lattice from the cohesive energy. (*b*) Find the expected value of the binding energy based on the lattice parameters.

Solution

(*a*) From Eq. 11.7, we have

$$B = \frac{E_{\text{coh}}}{N_{\text{A}}} = \frac{769 \times 10^3 \text{ J/mol}}{(6.02 \times 10^{23} \text{ ions/mol})(1.60 \times 10^{-19} \text{ J/eV})}$$

$$= 7.98 \text{ eV}$$

(*b*) The calculated value of the ionic binding energy is obtained from Eq. 11.6:

$$B = \frac{\alpha e^2}{4\pi\varepsilon_0 R_0}\left(1 - \frac{1}{n}\right)$$

$$= \frac{(1.7476)(1.44 \text{ eV} \cdot \text{nm})}{0.281 \text{ nm}}(0.889) = 7.96 \text{ eV}$$

The agreement between the experimental and calculated values is very good.

Example 11.2

How much energy *per neutral atom* would be needed to take apart a crystal of NaCl?

Solution

If we supply an energy of E_{coh} to a mole of NaCl, we obtain N_{A} Na^+ ions and N_{A} Cl^- ions. To convert these to neutral atoms, we must remove an electron from each Cl^-, which costs us the electron affinity of Cl (3.61 eV), and then we must attach that electron to the Na^+, which returns the ionization energy of Na (5.14 eV). The net cost per pair of Na and Cl atoms is

$$7.98 \text{ eV} + 3.61 \text{ eV} - 5.14 \text{ eV} = 6.45 \text{ eV}$$

Expending this much energy gives two neutral atoms (Na and Cl), so the net cost per atom is half that amount, or 3.23 eV.

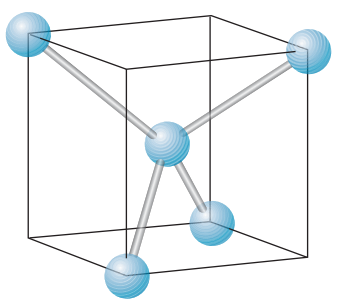

FIGURE 11.7 The tetrahedral structure of carbon.

The large cohesive energies of ionic solids such as NaCl gives them a common set of properties: They are hard, with high melting and vaporization temperatures (because it takes a lot of thermal energy to break the bonds). They are soluble in polar liquids such as water, in which the dipole moment of the water molecule can supply the electrostatic force necessary to break the ionic bonds. There are no free or valence electrons, so they are poor electrical conductors and not strongly magnetic. They are transparent to visible light (because light rays have too little energy to excite electrons from the filled shells), but absorb strongly in the infrared (corresponding to the vibrational frequencies of the atoms in their lattice sites).

Covalent Solids

As we discussed in Chapter 9, carbon forms molecules by covalent bonding of its four outer electrons in sp^3 hybrid orbits. Such bonds are highly *directional*, and we have seen how it is possible to calculate the angle between the bonds based on the symmetry of the bonding configuration. Solid carbon, in the form of diamond, is an example of a solid in which the interatomic forces are also of a covalent nature. As in a molecule, the four equivalent sp^3 hybrid states participate in covalent bonds, and because they are equivalent they must make equal angles with one another. The manner in which this is done is shown in Figure 11.7. A central carbon atom is covalently bound to four other carbons that occupy four

TABLE 11.2 Some Covalent Solids

Crystal	Nearest-Neighbor Distance (nm)	Cohesive Energy (kJ/mol)
ZnS	0.235	609
C (diamond)	0.154	710
Si	0.234	447
Ge	0.244	372
Sn	0.280	303
CuCl	0.236	921
GaSb	0.265	580
InAs	0.262	549
SiC	0.189	1185

corners of a cube as shown. The angle between the bonds is 109.5°, as it was in the covalently bonded molecules.

Figure 11.8 illustrates how the solid structure characteristic of diamond is constructed of such bonds. Each carbon has four close neighbors with which it shares electrons in covalent bonds. The basic structure is known as *tetrahedral*, and many compounds have a similar structure as a result of covalent bonding. Table 11.2 shows some of these compounds. The cohesive energy is the energy required to dismantle the solid into individual atoms. The structure is also known as the *zinc sulfide* or *zinc blende* structure.

Some of the covalent solids listed in Table 11.2 have bond energies larger than those of ionic solids. Substances such as diamond and silicon carbide are particularly hard. Other covalent solids with structures similar to carbon are silicon and germanium; the structure of these solids is responsible for their behavior as semiconductors.

The covalent solids do not have the same similarity of characteristics that ionic solids do, and so we cannot make the same generalizations. Carbon, in the diamond structure, has a large bond energy and is therefore very hard and transparent to visible light; germanium and tin have similar structures, but are metallic in appearance and highly reflective. Carbon (as diamond) has an extremely high melting point (4000 K); germanium and tin melt at much lower temperatures more characteristic of ordinary metals. Some (like diamond) are extremely poor electrical conductors, while others (like Si, Ge, and Sn) can conduct electricity but not nearly as well as most metals. Of course, these differences depend on the actual bond energy in the solid, which in turn depends on the type of atoms of which the solid is made. Those solids with large bond energies are hard, have high melting points, are poor electrical and thermal conductors, and are transparent to visible light. Those solids with small bond energies may have very different properties.

Metallic Bonds

The valence electrons in a metal are usually rather loosely bound, and frequently the electronic shells are only partially filled, so that metals tend not to form covalent bonds. The basic structure of metals is a "sea" or "gas" of approximately free electrons surrounding a lattice of positive ions. The metal is held together by the attractive force between each individual metal ion and the electron gas.

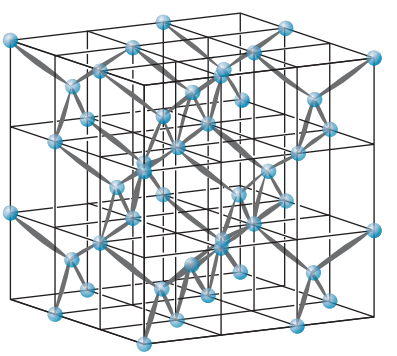

FIGURE 11.8 The lattice structure of diamond.

TABLE 11.3 Structure of Metallic Crystals

Metal	Crystal Type	Nearest-Neighbor Distance (nm)	Cohesive Energy (kJ/mol)
Fe	bcc	0.248	418
Li	bcc	0.304	158
Na	bcc	0.372	107
Cu	fcc	0.256	337
Ag	fcc	0.289	285
Pb	fcc	0.350	196
Co	hcp	0.251	424
Zn	hcp	0.266	130
Cd	hcp	0.298	112

The most common crystal structures of metallic solids are fcc, bcc, or a third type known as *hexagonal close-packed (hcp)*. The hcp structure is shown in Figure 11.9; like the fcc structure, it is a particularly efficient way of packing atoms together. Some metals and their characteristics are shown in Table 11.3. The cohesive energy of metal bonds tends to fall in the range 100–400 kJ/mol (1–4 eV/atom), making the metals less strongly bound than ionic or covalent solids. As a result, many metals have relatively low melting points (some below a few hundred °C). The relatively free electrons in the metal interact readily with photons of visible light, so metals are not transparent. The free electrons are responsible for the high electrical and thermal conductivity of metals. Because metallic bonds don't depend on any particular sharing or exchange of electrons between specific atoms, the exact nature of the atoms of the metal is not as important as it is in the case of ionic or covalent solids; as a result we can make many kinds of metallic alloys by mixing together different metals in varying proportions.

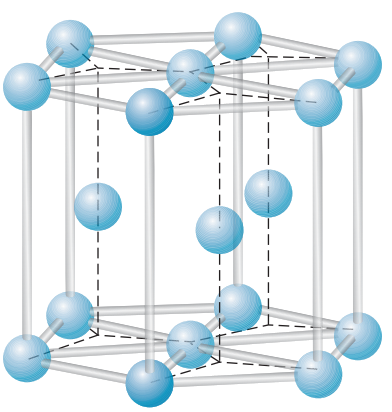

FIGURE 11.9 Arrangement of atoms in a hexagonal close-packed crystal.

Molecular Solids

None of the solids we have discussed so far can be considered as composed of individual molecules. It is, however, possible for molecules to exert forces on one another and to bind together in solids. The electrons in a molecule are already shared in *molecular* bonds, so there are no available electrons to participate in ionic, covalent, or metallic bonds with other molecules. Moreover, molecules are electrically neutral, so there are no Coulomb forces involved. Molecular solids are held together by much weaker forces, which generally depend on the *electric dipole moments* of the molecules. Because these forces are much weaker than the internal forces that hold a molecule together, a molecule *can* retain its identity in a molecular solid.

The electric dipole moment of one molecule can exert an attractive force on the dipole moment of another. The dipole cohesive force (which is proportional to $1/R^3$) in molecular solids is generally weaker than the $1/R^2$ Coulomb force that is responsible for the cohesive energies of other solids. Molecular solids are therefore more weakly bound and have lower melting points than ionic, covalent, or metallic solids, because it takes less thermal energy to break the bonds of a molecular solid.

Some molecules (called *polar molecules*) have permanent electric dipole moments consisting of a positive charge on one end of the molecule and an equal negative charge on the opposite end. For example, in a water molecule, the oxygen atom tends to attract all of the electrons of the molecule and so looks like the negative end of the dipole; the two "bare" protons are the positive ends of the dipole. The dipole forces between water molecules are responsible for the beautiful hexagonal patterns of snowflakes. When bonding of this sort involves hydrogen atoms, as it does in water, it is known as *hydrogen bonding*.

It is also possible to have dipole forces exerted between atoms or molecules that have no permanent dipole moments. Quantum mechanical fluctuations* can produce an instantaneous electric dipole moment in one atom, which then induces a dipole moment by polarizing a neighboring atom. The result is an attractive dipole-dipole force known as the *van der Waals force*, which is responsible for the bonding in certain molecular solids (as well as for such physical effects as surface tension and friction). Examples of solids that are bound by the van der Waals force include those composed of the inert gases (Ne, Ar, Kr, and Xe), symmetric molecules such as CH_4 and $GeCl_4$, halogens, and other gases such as H_2, N_2, and O_2.

The van der Waals force is extremely weak; it falls off with separation distance like R^{-7}. In inert gas crystals, the nearest neighbor distance is 0.3–0.4 nm, but the cohesive energies are typically only 10 kJ/mol or 0.1 eV/atom. Solids bound by these weak forces have low melting points, because little thermal energy is required to break the bonds. In fact, because the induced dipole moment of an atom or molecule should be approximately proportional to its *total number* of electrons, we might expect that the melting points of nonpolar molecular solids should be roughly proportional to the number of electrons in each molecule. Figure 11.10 shows this relationship; although the properties of the individual solids cause

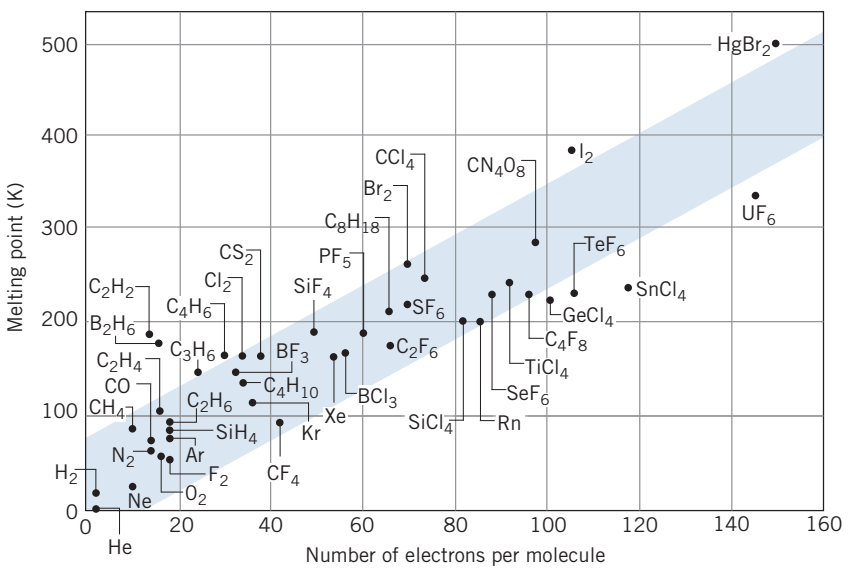

FIGURE 11.10 The melting points of molecular solids depend approximately on the number of electrons per molecule.

*These fluctuations are too rapid to be observed in the laboratory. Measurements give only the *average* value of this fluctuating dipole moment, which is zero.

considerable scatter of the points, the relationship is roughly as we expect it should be.

11.2 THE HEAT CAPACITY OF SOLIDS

Just as we discussed in Chapter 1 for the heat capacity of gases, the heat capacity of solids provides another example of the breakdown of classical statistical mechanics and the need for a more detailed theory based on quantum mechanics. (You might find it helpful to review the classical calculation of the heat capacity for gases in Section 1.3.)

Let's first consider what classical thermodynamics predicts for the heat capacity of a solid. In contrast to a gas, an atom in a solid occupies a specific position in the lattice, so no translational motion is possible. Thus there are no degrees of freedom corresponding to the translational motion. The atom can move only by vibrating about its equilibrium position in the lattice. We can imagine the atom to behave as if it were connected to all of its closest neighbors by springs. It can vibrate in any of the three coordinate directions independently of the other two—the initial displacements of the springs in the x, y, and z directions can be chosen independently, and the initial velocities in each direction can be set independently of one another. Consequently there are 6 degrees of freedom in this situation—2 degrees of freedom (corresponding to the vibrational potential and kinetic energies) for each of the three directions. According to the equipartition theorem, the average energy for each degree of freedom is $\frac{1}{2}kT$, so the average energy per atom is $6 \times \frac{1}{2}kT = 3kT$. The total internal energy of one mole (N_A atoms) would then be $E_{int} = 3N_A kT = 3RT$ (where $R = N_A k$ is the universal gas constant), and the corresponding molar heat capacity is

$$C = \frac{\Delta E_{int}}{\Delta T} = 3R = 24.9 \text{ J/mol} \cdot \text{K} \tag{11.8}$$

This is the expected value of the molar heat capacity of solids based on classical statistical mechanics and is known as the *law of Dulong and Petit*.

How well does this prediction compare with experiment? Table 11.4 shows some values of the molar heat capacities at room temperature (approximately 300 K) and at 100 K and 25 K for some metallic elements. There is good agreement with the Dulong and Petit prediction at room temperature, but poor agreement as the temperature is reduced. (Note that the classical value is independent of temperature.)

Figure 11.11 shows the temperature dependence of the heat capacities of Pb, Cu, and Cr at temperatures between 1 K and 100 K. It appears that the heat capacity approaches 0 at the lowest temperatures. As the temperature is increased, the heat capacity rises, eventually reaching the Dulong and Petit value at high enough temperature. However, the rate of increase is very different for these metals: Pb rises quickly (approaching the Dulong and Petit value by 100 K), Cu rises more slowly, and Cr rises even more slowly.

Clearly the classical calculation fails to account for the heat capacities of these solids. One possible resolution of this problem would be to consider the application of quantum statistics to the electrons in these metals. In Chapter 10, we discussed the heat capacity of a gas of fermions. We applied the model to a dilute solution of ^{3}He in ^{4}He, but the result can apply equally as well to any system of particles governed by Fermi-Dirac statistics.

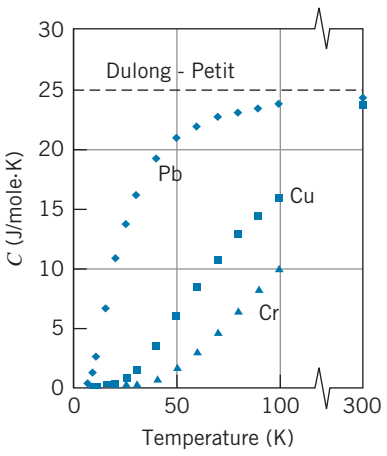

FIGURE 11.11 Molar heat capacity of Pb (diamonds), Cu (squares), and Cr (triangles) at temperatures below 100 K. The room temperature values are shown at the right.

TABLE 11.4 Heat Capacities of Common Metals*

Metal	$T = 300$ K		$T = 100$ K	$T = 25$ K
	J/kg · K	J/mole · K	J/mole · K	J/mole · K
Al	0.904	23.4	12.8	0.420
Ag	0.235	24.3	20.0	3.05
Au	0.129	23.4	21.1	5.11
Cr	0.461	23.8	10.0	0.199
Cu	0.387	23.9	16.0	0.971
Fe	0.450	24.6	12.0	0.398
Pb	0.128	24.7	23.8	14.0
Sn	0.222	23.8	22.0	6.80

*The value of the heat capacity depends on the circumstances under which it is determined. Usually measured values are observed at constant pressure (C_P), while calculated values are more easily obtained for constant volume (C_V). The first data column in this table is the experimental specific heat (heat capacity per unit mass) at constant pressure, and the remaining columns all give the molar heat capacity at constant volume. In most cases C_P is just a few percent larger than C_V.

We can treat the electrons in a metal as a Fermi gas. In deriving Eq. 10.63 for the heat capacity, the only assumption we made was that $kT \ll E_F$. For most metals, E_F is a few eV and even at room temperature kT is only 0.025 eV, so the approximation should be pretty good. Let's rewrite Eq. 10.63 for one mole of a substance ($N = N_A$) as follows:

$$C = \frac{\pi^2 k^2 N_A T}{2E_F} = \frac{\pi^2}{2}\frac{RkT}{E_F} \tag{11.9}$$

where $R = 8.31$ J/mole · K. Equation 11.9 is written as if each atom of the lattice contributes one electron to the electron gas, so that N (the number of electrons) is equal to N_A (for one mole of atoms). If, for example, the metal had a valence of 2, then we would have $N = 2N_A$.

For copper $E_F = 7.03$ eV and Eq. 11.9 gives $C = 0.146$ J/mole · K at room temperature. This value is far smaller than the experimental value, indicating that the electrons provide only a small contribution to the heat capacity, at least at room temperature. So the correct explanation for the behavior of the heat capacity must lie elsewhere than the electrons.

Einstein Theory of Heat Capacity

In an ordinary solid, most of the physical properties originate either with the valence electrons or with the latticework of atoms. Electrical conductivity, for example, originates with the valence electrons, while the propagation of mechanical waves is due to the lattice of atoms. The heat capacities of solids have contributions from both lattice and conduction electrons; at all but the lowest temperatures, the lattice contribution is dominant.

The explanation for the failure of classical physics to account for the heat capacity of solids was first given by Einstein, who assumed that the *oscillations* (not the atoms) of the solid obeyed Bose-Einstein statistics. Just as electromagnetic

waves are analyzed as "particles" (quanta of electromagnetic energy, or photons) that obey Bose-Einstein statistics, so are mechanical or acoustic waves analyzed as "particles" (quanta of vibrational energy, called *phonons*) that also obey Bose-Einstein statistics. Einstein made the simplifying assumption that all of the phonons (oscillations) have the same frequency.

We have seen in Chapter 5 that a quantized oscillator has an energy of $\hbar\omega(n + \frac{1}{2})$. Each additional value of n represents an additional phonon; to go from a vibrational energy of $\frac{5}{2}\hbar\omega$ to $\frac{7}{2}\hbar\omega$ we must "create" a phonon of energy $\hbar\omega$. One mole of the solid contains N_A atoms and thus $3N_A$ oscillators. The density of states (number of states per unit volume) is thus $3N_A/V$, and the integral of Eq. 10.7 is evaluated only at the single energy $E = \hbar\omega$ (because all phonons have energy $\hbar\omega$). Using the Bose-Einstein distribution, the number of phonons is then $N = 3N_A/(e^{\hbar\omega/kT} - 1)$, and the total internal energy of the solid is the number of phonons times the energy of each phonon:

$$E_{\text{int}} = N\hbar\omega = 3N_A\hbar\omega\frac{1}{e^{\hbar\omega/kT} - 1} \tag{11.10}$$

The heat capacity can be found from dE_{int}/dT:

$$C = \frac{dE_{\text{int}}}{dT} = 3N_A\hbar\omega\frac{(e^{\hbar\omega/kT})(\hbar\omega/kT^2)}{(e^{\hbar\omega/kT} - 1)^2}$$

$$= 3R\left(\frac{\hbar\omega}{kT}\right)^2\frac{e^{\hbar\omega/kT}}{(e^{\hbar\omega/kT} - 1)^2} = 3R\left(\frac{T_E}{T}\right)^2\frac{e^{T_E/T}}{(e^{T_E/T} - 1)^2} \tag{11.11}$$

where we have replaced $\hbar\omega/k$ with the parameter T_E, called the *Einstein temperature*. The vibrational energy $\hbar\omega$ (or the Einstein temperature T_E) is an adjustable parameter of the theory and takes different values for different materials. Typically, T_E is of the order of several hundred kelvins.

When T is small, the exponential term in the denominator dominates, and $C \propto e^{-T_E/T}$, so indeed C approaches 0 for small T, in agreement with experiment. Figure 11.12 shows the molar heat capacity of Cu compared with the behavior predicted by Eq. 11.11, with $T_E = 225$ K giving the best fit to the data. As you can see, the agreement is reasonably good. However, even though the shape of the theoretical curve matches the overall trend of the data, it fails to do a good job at accounting for the behavior at the lowest temperatures (the data approach zero more slowly than the theory predicts).

In this calculation we have oversimplified by assuming all of the oscillations to have the same frequency. A better calculation, which was first done in 1912 by Peter Debye*, assumes a distribution of frequencies with a density of states given by an expression of the same form as that for the "photon gas" of blackbody radiation; the predicted low temperature behavior is then

$$C = \frac{12\pi^4}{5}R\left(\frac{T}{T_D}\right)^3 \tag{11.12}$$

where T_D is a parameter of the theory known as the *Debye temperature,* which is different for different materials.

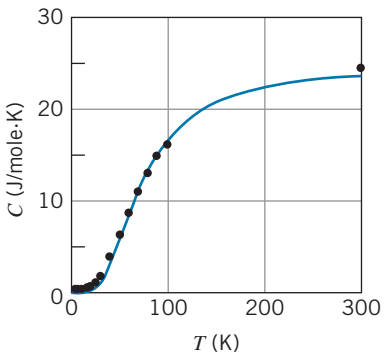

FIGURE 11.12 Molar heat capacity of Cu. The solid curve gives the temperature dependence expected according to the Einstein theory (Eq. 11.11).

*Peter Debye (1884–1966) was born in the Netherlands but spent most of his academic career in German universities (where at one point he served as Schrödinger's professor) and finally moved to the U.S. in 1940. He is perhaps best known for his analysis of X-ray diffraction patterns (such as Figure 3.8), for which he received the 1936 Nobel Prize in chemistry.

At the lowest temperatures, we therefore can identify two terms in the heat capacity: a term due to the electrons, which is linear in the temperature (Eq. 11.9), and another term due to the lattice vibrations of the atoms, which is proportional to T^3. Combining these two terms, we then expect the low-temperature heat capacity to be of the form $C = aT + bT^3$, where a is the coefficient of T in Eq. 11.9 and b is the coefficient of T^3 in Eq. 11.12. As T approaches 0, the T^3 term drops off more rapidly than the linear term, so at the very lowest temperatures we expect the electrons to have a more significant contribution. We can turn this equation into a linear graph and identify both contributions by writing $C/T = a + bT^2$ and plotting C/T as a function of T^2, which should give a straight line of slope b and y-intercept a. Figure 11.13 shows the results for copper. The data do indeed fall on a straight line, in excellent agreement with the Debye theory. If the electronic part if the heat capacity were not present (that is, if there were only the lattice contribution from Eq. 11.12), then the line would go through the origin and the intercept would be zero. So the intercept tells us about the electronic contribution to the heat capacity. The slope of the line tells us about the lattice contribution and depends on the Debye temperature.

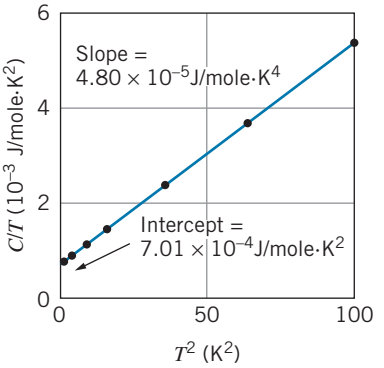

FIGURE 11.13 Molar heat capacity for Cu, plotted as C/T against T^2. The slope gives the lattice contribution and the intercept gives the contribution of the electrons.

Example 11.3

(*a*) From the slope of the line in Figure 11.13, determine the Debye temperature of copper. (*b*) Using the Fermi energy of copper (7.03 eV), determine the expected value of the intercept.

Solution

(*a*) The slope b is equal to the coefficient of T^3 in Eq. 11.12, so $b = 12\pi^4 R/5T_D^3$ and

$$T_D = \left(\frac{12\pi^4 R}{5b}\right)^{1/3} = \left[\frac{12\pi^4(8.31\ \text{J/mole}\cdot\text{K})}{5(4.80\times10^{-5}\ \text{J/mole}\cdot\text{K}^4)}\right]^{1/3}$$
$$= 343\ \text{K}$$

(*b*) The intercept a is the coefficient of T in the electronic contribution to the heat capacity (Eq. 11.9):

$$a = \frac{\pi^2 kR}{2E_F}$$
$$= \frac{\pi^2(8.617\times10^{-5}\ \text{eV/K})(8.31\ \text{J/mole}\cdot\text{K})}{2(7.03\ \text{eV})}$$
$$= 5.03\times10^{-4}\ \text{J/mole}\cdot\text{K}^2$$

The expected value of the intercept based on the free-electron model doesn't quite agree with the experimental value from Figure 11.13 for exactly the same reason that our analysis of the ^{3}He data in Chapter 10 didn't agree with the predictions: an electron moving through a copper lattice doesn't behave as a free electron would in an electron gas. We can account for the forces exerted by the lattice on the electrons by assigning the electrons an "effective mass" that is larger than the mass of a free electron. The additional mass accounts for the "sluggish" behavior of the electrons in moving through the lattice. The mass enters the calculation through the Fermi energy (Eq. 10.50); making the mass larger results in a smaller value of E_F and thus a larger value of the intercept a. For copper, the effective mass of the electrons is about 1.4 times their free mass.

The Debye theory also gives good agreement with the experimental data at higher temperatures. Except at room temperature, the data of Table 11.4 seem to have little in common. At 100 K the heat capacities vary by more than a factor of 2, and they vary by two orders of magnitude at 25 K. In the Debye theory, the heat capacity for any substance can be written as a function of T/T_D. If we plot the heat

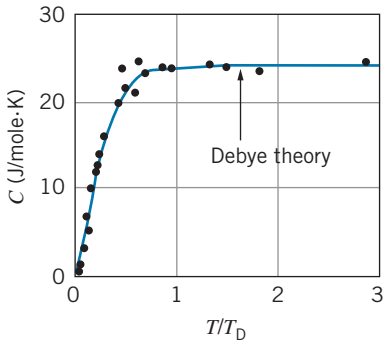

FIGURE 11.14 The heat capacity for eight different metals plotted against T/T_D. All values fall along the same curve calculated from the Debye theory.

capacities of the eight metals listed in Table 11.4 against T/T_D, the large variation among the values for different metals disappears, as shown in Figure 11.14. The data for all substances fall along the same curve calculated from the Debye theory. Understanding these widely different materials in a common basis is a great triumph for the quantum theory and for the application of Bose-Einstein statistics.

11.3 ELECTRONS IN METALS

In metals, each atom contributes one or more loosely bound electrons to an "electron gas" of nearly free electrons that can easily move throughout the metal. In analogy with an ordinary molecular gas, these electrons move freely and experience forces only when they scatter from the ion cores in the lattice. For now, we'll assume the distribution of occupied electron states is determined by the density of states for the electron gas and the Fermi-Dirac distribution function. In the next section, we will see that a more detailed analysis of the properties of the interaction of the electrons with the atoms of the lattice forbids certain ranges of energy values, but we'll ignore that effect for this discussion. With these assumptions, we can use the electron gas model to study many of the properties of metals, such as electrical conduction, heat capacity, and heat conduction.

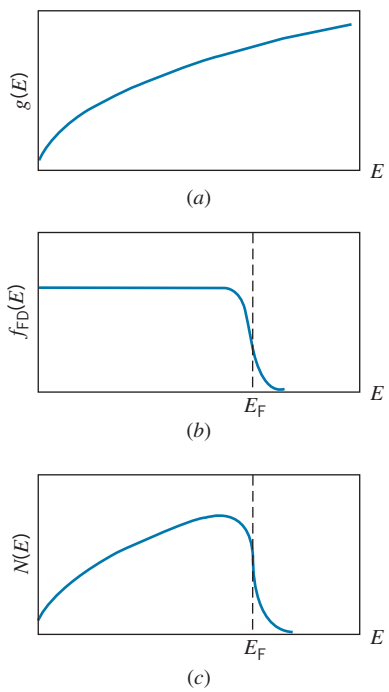

FIGURE 11.15 (*a*) The density of states factor for electrons (Eq. 10.12). (*b*) The Fermi-Dirac distribution function (Eq. 10.34). (*c*) The number of occupied states per unit energy interval, determined from the product of (*a*) and (*b*).

Figure 11.15 reviews the main details of the Fermi-Dirac energy distribution, which we discussed in Chapter 10, as it might be applied to electrons in metals. The distribution of occupied electron states is determined by the product of the density of states factor, Eq. 10.12, and the Fermi-Dirac distribution function, Eq. 10.34. At $T = 0$, all states above the Fermi energy E_F are empty and all states below E_F are occupied. For temperatures greater than 0, E_F identifies the point at which the Fermi-Dirac factor has the value $\frac{1}{2}$. The difference between $N(E)$ at $T = 0$ and at room temperature was illustrated in Figure 10.22; only a small number of electrons near E_F are affected by the temperature change.

We calculated the Fermi energy at $T = 0$ by using Eq. 10.49, in which the integral of $N(E)$ over all energies gives the total number of electrons N. The same procedure can be used to find E_F at any temperature:

$$N = \int_0^\infty N(E)\,dE = \frac{8\sqrt{2}\pi V m^{3/2}}{h^3} \int_0^\infty \frac{E^{1/2}\,dE}{e^{(E-E_F)/kT} + 1} \tag{11.13}$$

In principle, we can evaluate the integral and solve for E_F, as we did to obtain Eq. 10.50. However, the integral cannot be evaluated in closed form. The solution can be approximated as

$$E_F(T) \approx E_F(0)\left[1 - \frac{\pi^2}{12}\left(\frac{kT}{E_F(0)}\right)^2\right] \tag{11.14}$$

Here $E_F(T)$ represents the Fermi energy at temperature T and $E_F(0)$ represents the Fermi energy at $T = 0$ (Eq. 10.50). At room temperature, $kT = 0.025$ eV, and for most metals the Fermi energy is a few eV, so the change in the Fermi energy between 0 K and room temperature is only about 1 part in 10^4. We can therefore

regard the Fermi energy as a constant for our applications, and we will represent it simply as E_F. Table 11.5 shows the Fermi energies of some metals.

TABLE 11.5 Fermi Energies of Some Metals

Metal	E_F (eV)
Ag	5.50
Au	5.53
Ba	3.65
Ca	4.72
Cs	1.52
Cu	7.03
Li	4.70
Mg	7.11
Na	3.15

Electrical Conduction

When an electric field $\vec{\mathbf{E}}$ is applied to a metal, a current flows in the direction of the field. The flow of charges is described in terms of a *current density* $\vec{\mathbf{j}}$, the current per unit cross-sectional area. In an ordinary metal, the current density is proportional to the applied electric field:

$$\vec{\mathbf{j}} = \sigma \vec{\mathbf{E}} \tag{11.15}$$

where the proportionality constant σ is the *electrical conductivity* of the material. We would like to understand the conductivity in terms of the properties of the metal.

The free electrons in our electron gas experience a force $\vec{\mathbf{F}} = -e\vec{\mathbf{E}}$ and a corresponding acceleration $-e\vec{\mathbf{E}}/m$. We observe that in a conductor the current is constant in time, so the increase in velocity from the electric field must be opposed, in this case by collisions with the lattice. This model of conduction in metals views the electrons as accelerated by the field only for short intervals, following which they are slowed by collisions. The net result is that the electrons acquire on the average a steady *drift velocity* $\vec{\mathbf{v}}_d$, given by the acceleration times the average time τ between collisions:

$$\vec{\mathbf{v}}_d = \frac{-e\vec{\mathbf{E}}}{m}\tau \tag{11.16}$$

The magnitude of the current density is determined by the number of charge carriers and their average speed:

$$\vec{\mathbf{j}} = -ne\vec{\mathbf{v}}_d \tag{11.17}$$

where n is the density of electrons available for conduction. Substituting for the drift velocity, we obtain

$$\vec{\mathbf{j}} = \frac{ne^2\tau}{m}\vec{\mathbf{E}} \tag{11.18}$$

and the conductivity is therefore

$$\sigma = \frac{ne^2\tau}{m} \tag{11.19}$$

The unknown factor in Eq. 11.19 is the time between collisions, which we can express as

$$\tau = \frac{l}{v_{av}} \tag{11.20}$$

where l is the *mean free path* of the electrons, the average distance the electrons travel between collisions, and v_{av} is their average speed through the lattice. (Note that this speed is *not* the same as the drift speed, which is the small increment of speed that comes about from applying the electric field.)

Let's see how this theory compares with experimentally observed conductivities.

Example 11.4

Assuming the average distance traveled between collisions is roughly the distance between atoms, estimate the electrical conductivity of copper at room temperature.

Solution

The nearest neighbor spacing between atoms in a copper lattice is 0.256 nm. If we treat the electron gas semiclassically, the average kinetic energy of an electron is $\frac{3}{2}kT$, and so the average speed of an electron at room temperature ($kT = 0.0252$ eV) is

$$v_{av} = \sqrt{\frac{3kT}{m}} = \sqrt{\frac{3(0.0252\text{ eV})}{0.511 \times 10^6\text{ eV}/c^2}} = 1.15 \times 10^5\text{ m/s}$$

The average time between collisions is then

$$\tau = l/v_{av} = (0.256 \times 10^{-9}\text{ m})/(1.15 \times 10^5\text{ m/s}) = 2.22 \times 10^{-15}\text{ s}$$

The density of copper atoms is

$$n = \frac{\rho N_A}{M} = \frac{(8.96 \times 10^3\text{ kg/m}^3)(6.02 \times 10^{23}\text{ atoms/mole})}{0.0635\text{ kg/mole}} = 8.49 \times 10^{28}\text{ atoms/m}^3$$

and the conductivity is

$$\sigma = \frac{ne^2\tau}{m} = \frac{(8.49 \times 10^{28}\text{ m}^{-3})(1.60 \times 10^{-19}\text{ C})^2(2.22 \times 10^{-15}\text{ s})}{9.11 \times 10^{-31}\text{ kg}} = 5.30 \times 10^6\,\Omega^{-1}\text{ m}^{-1}$$

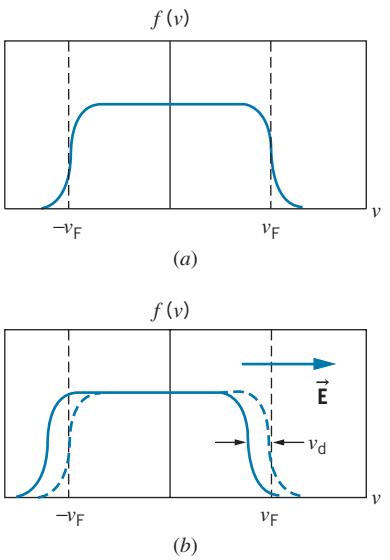

FIGURE 11.16 (*a*) The Fermi-Dirac velocity distribution function. (*b*) When an electric field is applied, the distribution shifts as the electrons are accelerated in a direction opposite to the field.

The measured conductivity of copper at room temperature is $5.96 \times 10^7\ \Omega^{-1}\text{m}^{-1}$, so our calculation is off by more than an order of magnitude. Moreover, the temperature dependence is wrong: this calculation predicts that the conductivity should decrease as $T^{-1/2}$ in this temperature region, while the measured conductivity decreases like T^{-1}.

We have actually made a couple of errors in this calculation, both of which have to do with ignoring the effects of quantum mechanics in the conduction process. Let's see how we can remedy these defects.

Quantum Theory of Electrical Conduction

Figure 11.16*a* represents the Fermi distribution of electron velocities in the metal. Like the Fermi energy distribution, it is flat at $v = 0$ and it falls to zero near the Fermi velocity v_F, but (unlike the energy distribution) it has positive and negative branches because the electrons can move in either direction. When an electric field is applied, all electrons acquire on the average an additional velocity component equal to the drift velocity v_d, which shifts the entire velocity distribution to the left (opposite the field direction), as shown in Figure 11.16*b*. Even though the entire distribution shifts, the net effect of applying the electric field is centered on a small number of electrons in the vicinity of v_F. The electric field causes some electron states near v_F in the direction of $\vec{\mathbf{E}}$ to become unoccupied, while an equal number of states near v_F in a direction opposite to $\vec{\mathbf{E}}$ become occupied.

The only electrons affected by the field are those in a narrow interval near the Fermi energy. These electrons are moving with a speed $v_F = \sqrt{2E_F/m}$, which for copper with $E_F = 7.03$ eV works out to be 1.57×10^6 m/s. This speed is

about an order of magnitude larger than the speed we found in Example 11.4, which would give us a shorter average time between collisions and hence a *smaller* conductivity. This seems to make the disagreement between theory and experiment even worse! Moreover, the Fermi energy is nearly independent of temperature, so the speed of electrons near the Fermi energy should likewise not change with temperature, nor should the conductivity.

That leaves the mean free path l as our last resort in fixing the calculation. However, in a perfectly arranged lattice, the mean free path should be infinite! Because atoms are mostly empty space, an electron should have a clear path through the material without scattering from the lattice ions. A perfect lattice should have an infinite conductivity! In practice, we find that the mean free path of an electron may be many hundreds of times the spacing between atoms, so that an encounter of an electron with a lattice ion is not very common.

In a real metallic lattice, two effects contribute to the scattering of electrons: (1) the atoms are in random thermal motion (oscillating about their equilibrium positions) and therefore do not occupy exactly the positions of a perfectly arranged lattice, and (2) lattice imperfections and impurities cause deviations from the ideal lattice. The first effect is temperature dependent and dominates at high temperatures; the second effect is independent of temperature and dominates at the lowest temperatures. In fact, because the average vibrational potential energy (which depends on the square of the vibrational amplitude) is proportional to the temperature, the average area that a vibrating atom presents to an electron moving through the lattice is also proportional to T. Therefore the conductivity decreases like T^{-1}, in agreement with observations.

Figure 11.17 shows the resistivity (the inverse of conductivity) of sodium metal as a function of the temperature. You can see the temperature-independent part at low temperature and the temperature-dependent part at higher temperatures (which increases linearly with T).

The same principles that govern electrical conductivity in a metal also govern *thermal conductivity*. Heat entering the material causes electrons in a small interval (of width kT) near the Fermi energy to move more rapidly, and those electrons can transfer their energy to the lattice in collisions with the ions. Assuming the mean free paths for electrical conduction and thermal conduction are the same, the ratio of the thermal conductivity to the electrical conductivity should be independent of the material but should depend only on the temperature (because the interval kT determines the number of electrons available for thermal conduction).

The ratio $K/\sigma T$ (where K is the thermal conductivity) should be the same for all materials and all temperatures. The proportionality of the thermal and electrical conductivities is known as the *Wiedemann-Franz law*. The ratio $K/\sigma T$ can be calculated from the parameters of the electron gas model to be

$$L = \pi^2 k^2 / 3e^2 = 2.44 \times 10^{-8}\ \mathrm{W \cdot \Omega / K^2} \tag{11.21}$$

which is called the *Lorenz number*. Figure 11.18 shows the ratio $K/\sigma T$ for a variety of metals at room temperature. In this region the thermal and electrical conductivities vary by nearly two orders of magnitude, but the ratio remains fairly constant and agrees with the Lorenz value. This agreement is another successful application of Fermi-Dirac statistics to the properties of electrons in solids.

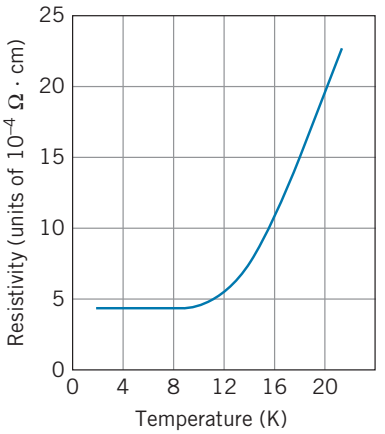

FIGURE 11.17 The electrical resistivity of sodium metal as a function of the temperature.

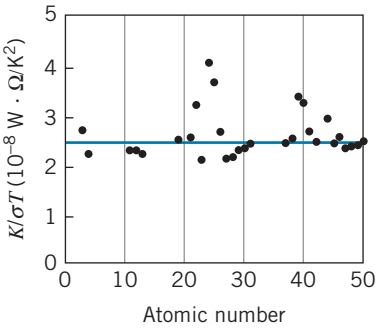

FIGURE 11.18 The Wiedemann-Franz ratio $K/\sigma T$ for various metals at room temperature. The solid line is the Lorenz number.

11.4 BAND THEORY OF SOLIDS

The model of treating a conductor as a gas of free electrons has taken us a long way toward understanding the properties of materials, but to gain a deeper understanding we must consider the interaction of the electrons with the atoms of the lattice. We'll see that this interaction leads to a profound difference between the electron energies of the free electron gas (continuous from zero up to the Fermi energy) and the electron energies in an interacting system (an alternating series of allowed and forbidden energy regions).

When two identical atoms, such as sodium, are very far apart, the electronic levels in one are not affected by the presence of the other. The 3*s* electron of each atom has a single energy with respect to its nucleus. As we bring the atoms closer together, the electron wave functions begin to overlap, and two different 3*s* levels form, depending on whether the two wave functions add or subtract. This effect is responsible for molecular binding, as discussed in Section 9.2. Figure 11.19 shows a representation of the energy levels.

As we bring together more atoms, the same sort of effect occurs. When the sodium atoms are far apart, all 3*s* electrons have the same energy, and as we begin to move them together, the energy levels begin to "split." The situation for five atoms is shown in Figure 11.20. There are now five energy levels that result from the five overlapping electron wave functions. As the number of atoms is increased to the very large numbers that characterize an ordinary piece of metal (perhaps 10^{22} atoms), the levels become so numerous and so close together that we can no longer distinguish the individual levels, as shown in Figure 11.21. We can regard the N atoms as forming an almost continuous *band* of energy levels. Because those levels were identified with the 3*s* atomic levels of sodium, we refer to the 3*s band*.

Each energy band in a solid with N atoms has a total of N individual levels. Each level can hold $2(2l + 1)$ electrons (corresponding to the two different orientations of the electron spin and the $2l+1$ orientations of the electron orbital angular momentum) so that the capacity of each band is $2(2l + 1)N$ electrons.

Figure 11.22 shows a more complete representation of the energy bands in sodium metal. The 1*s*, 2*s*, and 2*p* bands are each full; the 1*s* and 2*s* bands each contain $2N$ electrons and the 2*p* band contains $6N$ electrons. The 3*s* band *could*

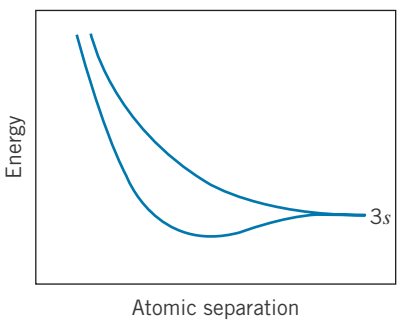

FIGURE 11.19 Splitting of 3*s* level when two atoms are brought together.

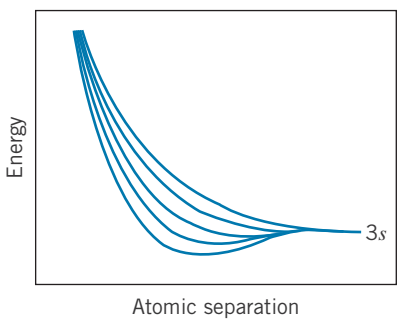

FIGURE 11.20 Splitting of 3*s* level when five atoms are brought together.

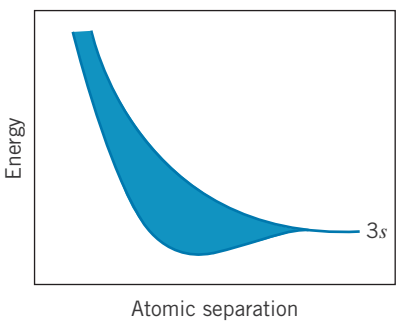

FIGURE 11.21 Formation of 3*s* band by a large number of atoms.

accommodate $2N$ electrons as well; however, each of the N atoms contributes only one $3s$ electron to the solid, and so there is a total of only N $3s$ electrons available. The $3s$ band is therefore half full. Above the $3s$ band is a $3p$ band, which could hold $6N$ electrons, but which is completely empty.

The situation we have described is the ground state of sodium metal. When we add energy to the system (thermal or electrical energy, for example), the electrons can move from the filled states to any of the empty states. In this case, electrons from the partially full $3s$ band can absorb a small amount of energy and move to empty $3s$ states within the $3s$ band, or they can absorb a larger amount of energy and move to the $3p$ band.

We can describe this situation in a more correct way using the Fermi-Dirac distribution. At a temperature of $T = 0\,\text{K}$, all electron levels below the Fermi energy E_F are filled and all levels above the Fermi energy are empty. In the case of sodium, the Fermi energy is in the middle of the $3s$ band, because all electron levels below that energy are occupied (Figure 11.23). At higher temperatures the Fermi energy gives the level at which the occupation probability is 0.5; the Fermi energy does not change significantly as we increase the temperature, but the occupation probability of the levels above E_F is no longer zero. Figure 11.24 shows a situation in which the thermal excitation of electrons leads to a small population of the $3p$ band and some vacant states in the $2p$ band.

Sodium is an example of a substance that is a good electrical conductor. When we apply a very modest potential difference, of the order of 1 V, electrons can easily absorb energy because there are N unoccupied states within the $3s$ band, all within an energy of about 1 eV. Electrons absorb energy as they are accelerated by the applied voltage, and they are therefore free to move as long as there are many unoccupied states within the accessible energy range. In sodium there are N relatively free electrons that can easily move to N unoccupied energy states, and sodium is therefore a good conductor.

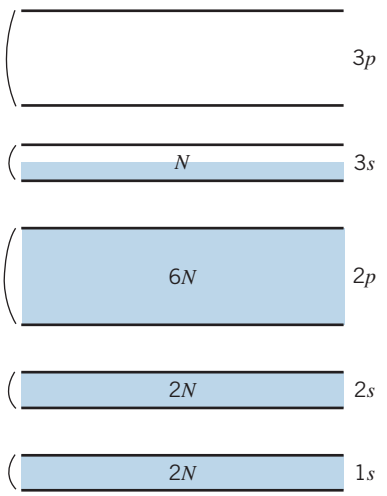

FIGURE 11.22 Energy bands in sodium metal.

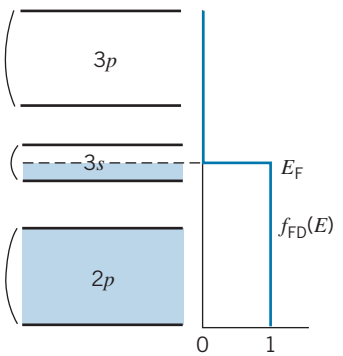

FIGURE 11.23 Energy bands in sodium at $T = 0$ (the filled $1s$ and $2s$ bands are not shown). The Fermi energy is at the center of the half-filled $3s$ band. Note that the Fermi-Dirac distribution function is drawn with the energy axis vertical.

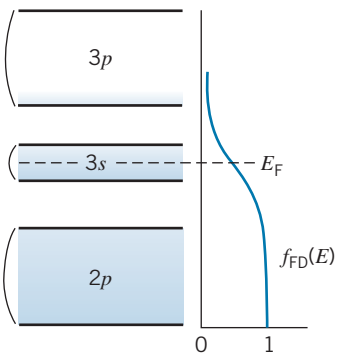

FIGURE 11.24 Energy bands in sodium at $T > 0$. The $2p$ band is no longer completely full (there are a few vacant states near the top), and the $3p$ band is no longer completely empty.

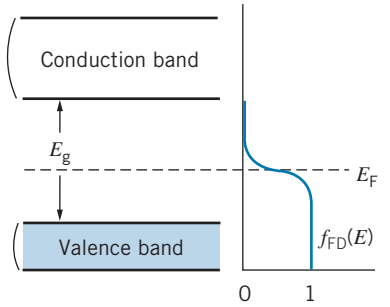

FIGURE 11.25 When $E_g \gg kT$, there are no electrons in the conduction band. This situation characterizes an insulator.

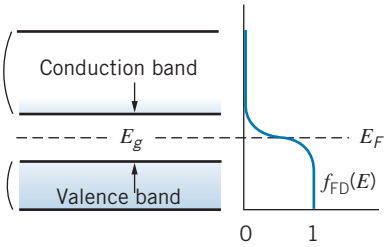

FIGURE 11.26 Band structure of a semiconductor. The gap is much smaller than in an insulator, so there is now a small population of the conduction band.

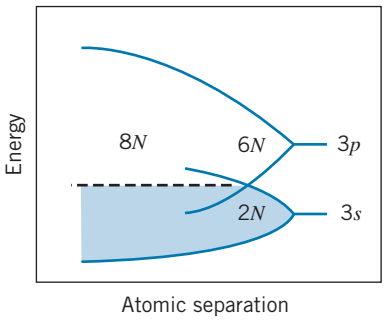

FIGURE 11.27 Band structure in magnesium. The filled 3*s* and empty 3*p* bands overlap, forming a single partially filled band.

The band structure of sodium, in which the Fermi level lies in the middle of a band, is characteristic of many good electrical conductors. A completely different situation occurs when the Fermi level lies in the gap between two bands, so that the band below E_F is completely full and the band above is completely empty. If the gap energy E_g is large compared with kT, then even though the Fermi-Dirac distribution spreads as the temperature is raised, it doesn't spread enough to result in a significant population of states in the upper band (called the *conduction band*) or a significant number of empty states in the lower band, called the *valence band*. This situation is shown in Figure 11.25. There are many electrons in the valence band available for electrical conduction, but there are few empty states for them to move through, so they do not contribute to the electrical conductivity. There are many empty states in the conduction band, but at ordinary temperatures there are so few electrons in that band that their contribution to the electrical conductivity is also very small. These substances are classified as *insulators* and in general they have two properties: a large energy gap (a few electron-volts) between the valence and conduction bands, and a Fermi level that is in the gap between the bands (i.e., a filled valence band and an empty conduction band).

A material with the same basic structure but a much smaller energy gap (1 eV or less) shows quite a different behavior. These materials are known as *semiconductors*. Figure 11.26 shows a representation of such a substance at ordinary temperatures. There are now many electrons in the conduction band, and of course many empty states accessible to them, so that they can conduct relatively easily. There are also many empty states in the valence band, so that some of the electrons in the valence band can also contribute to the electrical conductivity by moving about through those states. We consider these two mechanisms of electrical conduction in detail in Section 11.6. For now we note two characteristic properties of semiconductors that relate directly to the band structure as shown in Figure 11.26. (1) Because thermal excitation across the gap is relatively probable, the electrical conductivity of semiconductors depends more strongly on temperature than the electrical conductivity of insulators or conductors. (2) It is possible to alter the structure of these materials, by adding impurities in very low concentration, in such a way that the Fermi energy changes and may move up toward the conduction band or down toward the valence band. This process, known as *doping*, can have a great effect on the conductivity of a semiconductor.

In the examples we have discussed so far, it is not apparent why the band theory is so useful in understanding the properties of a solid. Sodium, for example, is expected to be a good conductor based on its atomic properties alone (a relatively loosely bound 3*s* electron); on the other hand, solid xenon has only filled atomic shells and should be a poor conductor. These conclusions follow either from simple atomic theory or from band theory. However, there are many cases in which atomic theory leads to wrong predictions while band theory gives correct results. We consider two examples. (1) Magnesium has a filled 3*s* shell, and on the basis of atomic theory alone we expect it to be a poor electrical conductor. It is, however, a very good electrical conductor. (2) The 2*p* shell of carbon has only two electrons of the maximum number of six. Carbon should therefore be a relatively good conductor; instead it is an extremely poor conductor.

We can understand both of these materials based on the unusual way the bands of these solids behave when the atoms are close enough so that the band gap disappears and the bands overlap. In magnesium (Figure 11.27), for example, the (filled) 3*s* and (empty) 3*p* bands overlap, and the result is a single band with a capacity of $2N + 6N = 8N$ levels. Only $2N$ of those are filled, and so magnesium

behaves like a material with a single band filled only to one-fourth its capacity. Magnesium is therefore a very good conductor.

In carbon, the overlap of the electronic wave functions at close range first causes mixing of the 2*s* and 2*p* bands, in a way similar to magnesium; a single band is created with a capacity of 8*N* electrons (Figure 11.28). The 2*s* states contribute 2*N* electrons, and the 2*p* states contribute another 2*N* (out of a maximum capacity of 6*N*). As the atoms approach still closer, the band divides into two separate bands, each with a capacity of 4*N* electrons. Because carbon has four valence electrons (two 2*s* and two 2*p*), the lower 4*N* states are completely filled and the upper 4*N* states of the conduction band are completely empty. Carbon is therefore an insulator. Germanium and silicon have the same type of structure as carbon, but their equilibrium separation is greater, so the gap between the valence and conduction bands is smaller, about 1 eV; it is this feature that causes Ge and Si to be semiconductors.

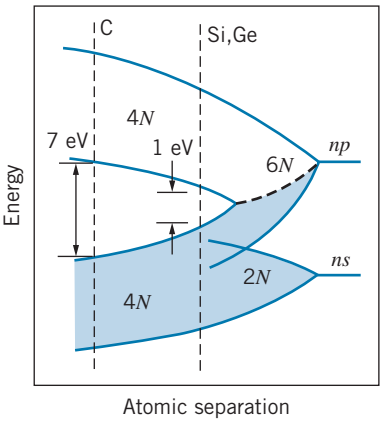

FIGURE 11.28 Band structure of carbon ($n = 2$), silicon ($n = 3$), and germanium ($n = 4$). The combined $ns + np$ band splits into two bands, each of which can hold $4N$ electrons. The atomic separation of carbon gives it a gap of about 7 eV and makes it an insulator, while the larger separation of silicon and germanium results in a smaller gap of about 1 eV and makes them semiconductors.

*Justification of Band Theory

The band theory of solids has had great success in accounting for the properties of metals, insulators, and semiconductors. In this section we consider a different approach to band theory that is based on the quantum mechanics of an electron moving through a lattice of ions. In analogy with solutions to the Schrödinger equation discussed in Chapter 5, in which an electron in a potential energy well shows discrete energy levels, we will see that an electron in a periodic potential energy provided by a lattice of ions can show energy bands.

To simplify the problem we consider only a one-dimensional lattice of ions (Figure 11.29). The electron is represented by a de Broglie wave traveling through the lattice. The interaction between the electron and the lattice can be represented as a scattering problem, similar to Bragg scattering (Section 3.1). The Bragg condition for scattering is

$$2d \sin\theta = n\lambda \qquad (n = 1, 2, 3, \ldots) \tag{11.22}$$

where d is the atomic spacing and θ is the angle of incidence measured from the plane of atoms (*not* from the normal). In a two-dimensional lattice, the incident wave can be scattered in many different directions, depending on the plane where we imagine the reflection to occur (recall Figure 3.6); in one dimension, however, only one possible reflection can occur—the incident wave can be reflected back in the opposite direction. We can use the Bragg condition for this case, with $d = a$ (the spacing between the ions or atoms of the lattice) and $\theta = 90^\circ$ (the angle between the "reflecting plane" and the incident wave). With $2a \sin 90^\circ = n\lambda$ and $\lambda = 2\pi/k$ (where k is the wave number), we find

$$k = n\frac{\pi}{a} \tag{11.23}$$

For wave numbers that do not satisfy this condition, the electron propagates freely through the lattice and behaves like a free particle whose energy is only kinetic:

$$E = \frac{p^2}{2m} = \frac{\hbar^2 k^2}{2m} \tag{11.24}$$

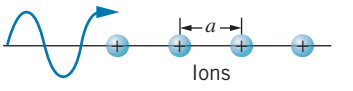

FIGURE 11.29 One-dimensional Bragg scattering. The only possible scattering is a reflection back in the opposite direction.

*This is an optional section that may be skipped without loss of continuity.

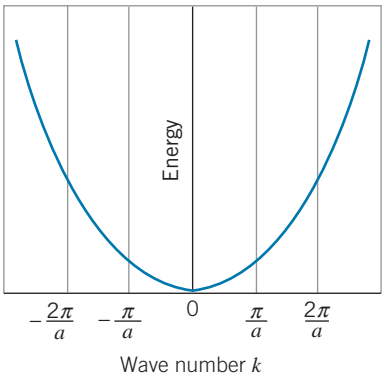

FIGURE 11.30 The parabolic relationship between energy and wave number for a free particle.

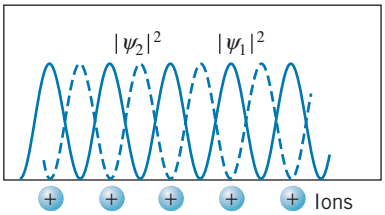

FIGURE 11.31 Probability densities for two different standing waves in the one-dimensional lattice.

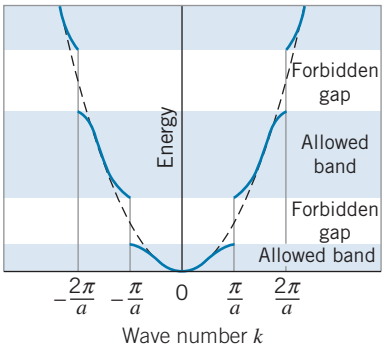

FIGURE 11.32 The relationship between energy and wave number for a one-dimensional lattice. The dashed curve is the parabola that represents the free particles. The solid curves represent waves scattered by the lattice.

There are no restrictions on k, so all values of E are allowed. This relationship between E and k for free electrons defines a parabola, as shown in Figure 11.30.

For wave numbers that satisfy the Bragg condition, the reflected and incident waves add to produce standing waves, which always result when we superpose two waves of equal wavelengths traveling in opposite directions. Depending on the phase difference between the waves, their amplitudes can add or subtract, so two different possible standing waves can result. Their probability densities are shown in Figure 11.31. For one of the waves (ψ_1), the electrons are more likely to be found close to the positive ions; these electrons are more tightly bound to the lattice—the energy of the electron is a bit lower than that of the free electron, due to the negative potential energy between the electron and the ions. Electrons represented by the other wave (ψ_2) are most likely to be found in the region between the ions; they are less tightly bound, so their energies are a bit above those of the unscattered electrons (for which the probability density is flat, so they are equally likely to be found at any location).

The resulting dependence of the energy of the electrons on the wave number k is illustrated by the S-shaped curve segments in Figure 11.32. For wave numbers that are far from satisfying the Bragg condition (that is, values of k that are not close to $n\pi/a$), the curve segments overlap the dashed parabola representing the free particle. Close to the wave numbers that satisfy the Bragg condition, however, the energy deviates from that of the free particle, a bit below the parabola for the more tightly bound electrons that spend more time near the ions and a bit above the parabola for the less tightly bound electrons that are more likely found between the ions.

Notice from Figure 11.32 that, even though all values of k are permitted, there are certain allowed bands of energy values separated by forbidden gaps. An electron traveling in this lattice is permitted to have energies only in the regions corresponding to the allowed bands. This indicates how a periodic array of atoms results in energy bands.

A more detailed calculation in three dimensions gives a better representation of the allowed and forbidden bands, but you can see that even this basic one-dimensional model shows how the bands can arise from the interactions of the electrons with a periodic lattice.

11.5 SUPERCONDUCTIVITY

At low temperatures, the resistivity of a metal (the inverse of its conductivity) is nearly constant. As the temperature of a material is lowered, the lattice contribution to the resistivity decreases while the impurity contribution remains approximately constant, and as we approach $T = 0\,\text{K}$ the resistivity should approach a constant value. Many metals, known as *normal* metals, behave in this way, as illustrated in Figure 11.17.

The behavior of another class of metals is quite different. These metals behave normally as the temperature is decreased, but at some critical temperature T_c (which depends on the properties of the metal), the resistivity drops suddenly to zero, as shown in Figure 11.33. These materials are known as *superconductors*. The resistivity of a superconductor is not merely very small at temperatures below T_c; it vanishes! Such materials can conduct electric currents even in the absence of an applied voltage, and the conduction occurs with no i^2R (joule heating) losses.

Superconductivity has been observed in 28 elements at ordinary pressures, in several additional elements at high pressure, and in hundreds of compounds and alloys. Since the original discovery of superconductivity in Hg in 1911, the focus of research has been to search for materials with the highest possible critical temperature, because many possible large-scale applications of superconductivity are presently impractical owing to the high cost of keeping materials below their critical temperatures. Table 11.6 summarizes some superconducting materials and their critical temperatures. You can see that before 1986, progress in raising the critical temperature was very slow, but since 1986 dramatic and rapid increases in T_c have been achieved.

Conspicuously absent from the list of superconductors are the best metallic conductors (Cu, Ag, Au), which suggests that superconductivity is *not* caused by a good conductor getting better but instead must involve some fundamental change in the material. In fact, superconductivity results from a kind of paradox: ordinary materials can be good conductors if the electrons have a relatively weak interaction with the lattice, but superconductivity results from a *strong* interaction between the electrons and the lattice.

Consider an electron moving through the lattice. As it moves, it attracts the positive ions and disturbs the lattice, much as a boat moving through water creates a wake. These disturbances propagate as lattice vibrations, which can then interact with another electron. In effect, two electrons interact with one another through the intermediary of the lattice; the electrons move in correlated pairs that do not lose energy by interacting with the lattice. (These pairs are not necessarily traveling together through the lattice; they may be separated by a large distance.) In the absence of a net current, the members of a pair have opposite momenta; when a net current is established, both members of the pair acquire a slight increase in momentum in the same direction, and this motion is responsible for the current.

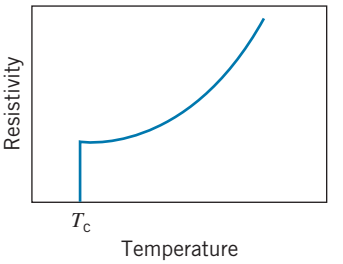

FIGURE 11.33 Resistivity of a superconductor.

TABLE 11.6 Some Superconducting Materials

Material	T_c (K)	Gap (meV)	Year
Zn	0.85	0.24	1933
Al	1.18	0.34	1937
Sn	3.72	1.15	1913
Hg	4.15	1.65	1911
Pb	7.19	2.73	1913
Nb	9.25	3.05	1930
Nb_3Sn	18.1		1954
Nb_3Ge	23.2		1973
$La_xBa_{2-x}CuO_4$	36		1986
$La_xSr_{2-x}CuO_5$	40		1986
$YBa_2Cu_3O_7$	93		1987
$Tl_2Ba_2Ca_2Cu_3O_{10}$	125		1988
$Hg_{12}Tl_3Ba_{30}Ca_{30}Cu_{45}O_{127}$	138		1994

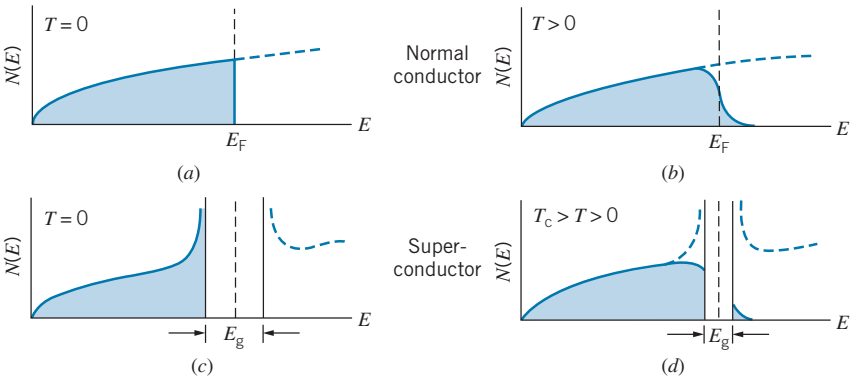

FIGURE 11.34 The number of filled electron states in (*a*) a normal conductor at $T = 0$; (*b*) a normal conductor at $T > 0$; (*c*) a superconductor at $T = 0$; (*d*) a superconductor at $T > 0$ but less than T_c. In (*c*), there is an energy gap of width E_g, and states displaced from within the gap pile up on either side of the gap. At higher temperatures, as in (*d*), the gap is narrower and there are empty states below the gap and filled states above the gap. As the temperature is increased to T_c, the gap width becomes 0 and the distribution of occupied states of the superconductor approaches that of the normal conductor. The gap width is exaggerated in the figure; generally, $E_g \sim 10^{-3}$ eV.

According to the successful BCS theory of superconductivity,* below the critical temperature there is a small energy gap E_g in the occupation probability of electrons in a superconductor (Figure 11.34). Below the gap, the electrons form pairs, which are known as *Cooper pairs*. Once a single Cooper pair forms, it is energetically favorable for other pairs to form, so the change from the normal state above T_c to the superconducting state below T_c is quite sudden. (As shown in Figure 11.34*c*, the population can *exceed* the limits imposed by the Fermi-Dirac distribution of at most one electron per quantum state. When the electrons are paired, they no longer behave like fermions and so it is possible to have more than one in each quantum state.)

When a superconductor is cooled below T_c, the gap opens and Cooper pairs begin to form. As the material is cooled further, the gap widens. Values of the energy gap listed in Table 11.6 correspond to the limiting case as $T \to 0$. The energy gaps, which can be regarded as representing the binding energy of a Cooper pair, are very small, of the order of 10^{-3} eV. At $T = 0$, all states below the gap are occupied. When $0 < T < T_c$, there are some unoccupied states below the gap, and some states above the gap are occupied by normal (unpaired) electrons.

It seems reasonable that there should be a direct relationship between the critical temperature and the energy gap: the larger the energy gap, the more thermal energy is required to break the Cooper pairs to destroy the superconductivity. The BCS theory gives this relationship:

$$E_g = 3.53kT_c \tag{11.25}$$

*The theory of superconductivity was developed in 1957 by John Bardeen, Leon N. Cooper, and J. Robert Schrieffer, who were awarded the 1972 Nobel Prize in physics for their work. Bardeen also shared the 1956 Nobel Prize for his research on semiconductors and his development of the transistor.

As the temperature is raised to T_c, the gap width decreases, and the superconductivity disappears above T_c where the gap width becomes zero.

Beginning in 1986, a new class of superconductors was discovered with unusually high values of T_c. In the 75 years from the discovery of superconductivity in 1911 until 1986, the highest T_c had gone from 4 K to about 23 K. In 1986, several materials were discovered with T_c in the range 30–40 K. By 1987 it was up to 93 K, and it rose to 138 K in 1994. Crossing the boundary at 77 K is important, because it means that cooling can be accomplished with liquid nitrogen instead of liquid helium, which costs nearly an order of magnitude more than liquid nitrogen. The rapid increase in T_c has led to the hope that it might be possible to develop materials that are superconductors at room temperature. Such materials could enable the transmission of electric power over long distances without resistive losses.

The high-T_c superconductors are oxides of copper in combination with other elements. They are ceramics, which means that they are rather brittle and not easily formed into wires to carry current. The crystal structure is characterized by planes of copper and oxygen between planes of the other elements. It seems likely that the superconductivity occurs in the copper oxide planes, but it is not yet clear that the complete explanation for these new superconductors is given by the BCS theory.

Superconducting materials have many applications that take advantage of their abilities to carry electrical currents without resistive losses. Electromagnets can be constructed that carry large currents and therefore produce large magnetic fields (of order 5 to 10 T). Currents as large as 100 A can be carried by very fine superconducting wires, of order 0.1 mm diameter, and thus such magnets can be constructed in a smaller space, using less material, than would be possible with ordinary conductors. Once started, a current in a superconducting loop of wire can circulate for years with no external source to drive it. Superconducting wires are also used to produce magnetic fields in magnetically levitated trains and in magnetic resonance imaging, and also to bend beams of particles in high-energy accelerators, such as the Large Hadron Collider, which began operation in 2008.

Josephson Effect

Imagine a thin layer of insulating material sandwiched between two identical superconductors. The insulating layer is thin enough that the electron pairs can tunnel through from one superconductor to another. This is a typical case of one-dimensional barrier penetration, such as we discussed in Chapter 5.

Figure 11.35 represents the arrangement. In the superconductors (regions 1 and 3), the electron pairs move freely, so the wave functions are of the form of the free particle: $\psi_1(x) = Ae^{i(kx+\alpha_1)}$ and $\psi_3(x) = Ae^{i(kx+\alpha_3)}$, where α_1 and α_3 are arbitrary phase angles (the amplitude A is taken to be real). At the two boundaries on either side of the barrier, the waves are $\psi_1 = Ae^{i\phi_1}$ and $\psi_3 = Ae^{i\phi_3}$, where ϕ_1 and ϕ_3 represent the values of the exponents at the boundaries. Inside the barrier of height U_0, the wave function is of the form $\psi_2(x) = Be^{k'x} + Ce^{-k'x}$, where $k' = \sqrt{2mU_0/\hbar^2}$. Applying the two boundary conditions on ψ, we ultimately obtain a current of the form

$$i = i_0 \sin(\phi_1 - \phi_3) \tag{11.26}$$

The existence of this "supercurrent" through the junction was first predicted by British physicist Brian Josephson in 1969, and it is now known as the *Josephson effect*. Josephson shared the 1973 Nobel Prize in physics for this discovery.

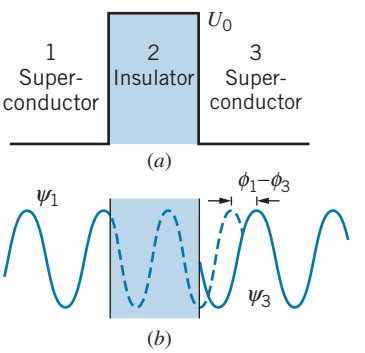

FIGURE 11.35 (*a*) A thin insulator sandwiched between two superconductors provides a potential energy barrier of height U_0 to the flow of current. (*b*) There is a phase difference of $\phi_1 - \phi_3$ between the wave functions ψ_1 and ψ_3 in the superconductors.

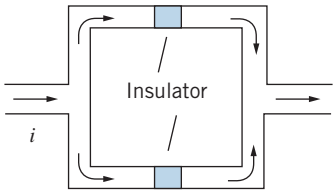

FIGURE 11.36 Two Josephson junctions can be combined to form a quantum interference device.

One important application of the Josephson effect is in the measurement of very weak magnetic fields. Consider a device with two Josephson junctions, as shown in Figure 11.36. Under ordinary circumstances the current divides equally in the two branches, and the phase difference is the same across both junctions. Now suppose a magnetic field is applied perpendicular to the plane of the loop. An additional current is induced around the loop. This additional current, either clockwise or counterclockwise depending on the direction of the magnetic field, will add to the current in one of the Josephson junctions and subtract from the current in the other, causing a relative change in the phase differences across the two junctions. When the currents combine, this phase difference causes maxima and minima in the net current leaving the loop in a manner that is very similar to the maxima and minima in double-slit interference. Observing the maxima and minima serves as a sensitive measurement of the magnetic field in the loop. This device is called a SQUID (Superconducting QUantum Interference Device) and allows measurements of magnetic fields of less than 10^{-17} T. Such sensitive devices allow precise mapping of the magnetic fields inside the brain and also find use in other medical procedures including magnetic resonance imaging (MRI).

In another application, a DC voltage ΔV is applied across a single Josephson junction. This voltage changes the energy of an electron pair on one side of the junction by $2e\Delta V$. For example, if region 1 is made more positive than region 3, the wave function at the boundary in region 1 would become $\psi_1 = Ae^{i(\varphi_1 + 2e\Delta Vt/\hbar)}$ using the usual procedure (see Eq. 5.6) for including the time dependence of the wave function (the factor $e^{-i\omega t}$ with $\omega = E/\hbar = -2e\Delta V/\hbar$). The current through the junction then becomes

$$i = i_0 \sin\left(\phi_1 - \phi_3 + \frac{2e\Delta V}{\hbar}t\right) \tag{11.27}$$

Applying a DC voltage to the junction produces an AC current! Because frequencies can be measured very precisely, a measurement of the frequency of this AC current can be used to determine ΔV. As a result, since 1990 the AC Josephson effect has been accepted by the General Conference on Weights and Measures as the international standard for the volt.

11.6 INTRINSIC AND IMPURITY SEMICONDUCTORS

A semiconductor is a material with an energy gap E_g of order 1 eV between the valence band and the conduction band. At $T = 0$, all states in the valence band are full and all states in the conduction band are empty; recall that the Fermi-Dirac distribution is a step function at $T = 0$ and gives an occupation probability of exactly 1 for all states below E_F and exactly 0 for all states above E_F. As the temperature is raised, however, some states above E_F are occupied and some states below E_F are empty. At room temperature, the relationship between the Fermi energy, the valence and conduction bands, and the electron energy distribution might be as shown in Figure 11.26.

Although the value of the room-temperature Fermi-Dirac distribution function is nearly zero in the conduction band, it is not *exactly* zero; Figure 11.37 shows a greatly magnified view of $f_{FD}(E)$ near the bottom of the conduction band. The value of $E - E_F$ is about 0.5 eV if E_F lies near the middle of the 1 eV energy

gap, and therefore $E - E_F \gg kT$, because at room temperature $kT \sim 0.025\,\text{eV}$. The 1 in the denominator of the Fermi-Dirac distribution is therefore negligible, and $f_{FD}(E)$ is approximately exponential, as shown in Figure 11.37.

Assuming the Fermi energy to lie near the middle of the gap, the occupation probability near the bottom of the conduction band is of order $e^{-E_g/2kT} \cong 10^{-9}$. Thus one atom in 10^9 contributes an electron to the electrical conductivity; compare this with a metal in which essentially *every* atom contributes an electron to the conductivity. (On the other hand, consider an insulator, which has a band structure very similar to that of a semiconductor, except the energy gap is perhaps 5 eV instead of 1 eV. This small difference in the size of the energy gap has an enormous effect on the occupation probability of the conduction band at room temperature: $e^{-E_g/2kT} \cong 10^{-44}$. Thus in a sample containing of order 10^{20} atoms, there may be 10^{11} conduction electrons in a semiconductor, 10^{20} in a conductor, and none in an insulator.)

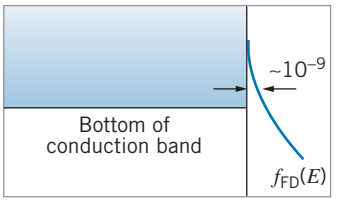

FIGURE 11.37 The tail of the Fermi-Dirac distribution function near the bottom of the conduction band. On the scale of this greatly magnified drawing, the 1 of $f_{FD}(E)$ would be about 1000 km off to the right, and E_F is about 1 m below the edge of this page.

Figure 11.38 shows the corresponding region near the top of the valence band. If there are a few filled states in the conduction band, there must be a few *empty* states in the valence band, and the Fermi-Dirac distribution is just a tiny bit smaller than 1; in fact it is approximately $1 - e^{(E-E_F)/kT}$. This number is about $1 - 10^{-9}$, based on our discussion for the electrons in the conduction band. (Because all the electrons in the conduction band came originally from the valence band, the number of electrons in the conduction band is *exactly* equal to the number of vacancies in the valence band. The Fermi-Dirac distribution is therefore symmetric in the conduction and valence bands, so the Fermi energy must lie at the center of the gap.)

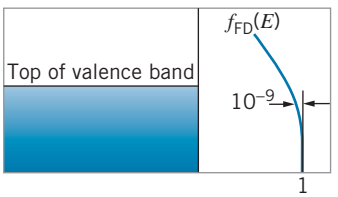

FIGURE 11.38 The Fermi-Dirac distribution function near the top of the valence band, showing the small fraction of empty states.

In practice it is much easier to analyze the behavior of a relatively small number of vacancies in the valence band rather than the large number of electrons in that band. When we apply an electric field to the semiconductor, the electrons in the *conduction* band can move easily, because there are many empty states to move into. There are few vacancies in the *valence* band, however. Under the influence of the electric field, an electron in the valence band can move only if there is a vacancy nearby for it to move into. When that electron moves into the vacancy, it creates another vacancy, which can in turn be filled by another electron. In this way, electrons moving in one direction cause an apparent motion of the vacancy in the opposite direction. The situation is similar to the motion of cars in a parking lot with one vacancy (Figure 11.39).

These vacancies in the valence band are known as *holes*, and they behave as if they have positive charges. In an electric field, electrons in the conduction band acquire a drift velocity in a direction opposite to the field (see Eq. 11.16) but (because electrons carry negative charge) they give a current opposite to the velocity and thus in the same direction as the field (see Eq. 11.17). The holes in the valence band acquire a velocity in the same direction as the field and give a current in the same direction as their velocity (that is, in the direction of the field). The current due to the electrons in the conduction band is therefore in the same direction as the current due to the holes in the valence band.

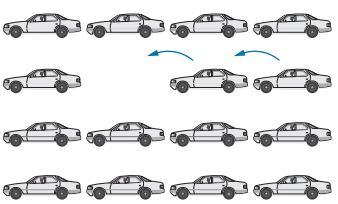

FIGURE 11.39 One car moves to the left, filling the vacancy but creating a new vacancy, which is then filled by the next car moving to the left. The motion of cars to the left, each filling a vacant space, is equivalent to the motion of the vacant space to the right.

The current in a semiconductor therefore consists of two parts: the negatively charged electrons in the conduction band and the positively charged holes in the valence band. Although the number of electrons in the conduction band is equal to the number of holes in the valence band, the two contributions to the current are in general not equal, because the electrons in the conduction band move more easily than the electrons in the valence band. Typically, the contribution of the electrons to the current at room temperature is about two to four times the contribution of the holes.

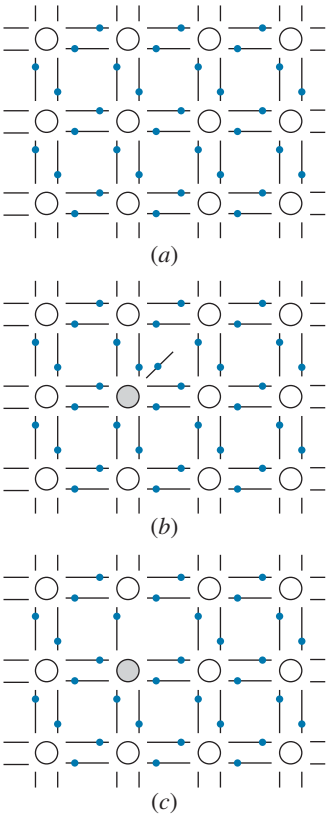

FIGURE 11.40 (*a*) Covalent bonding in Si or Ge. Each atom provides four electrons for covalent bonds with its neighbors. (*b*) When a Si or Ge atom is replaced with a valence-5 atom (shaded), there is an extra electron that does not participate in covalent bonds. (*c*) If a Si or Ge atom is replaced by a valence-3 atom (shaded), one electron from a neighboring atom is not paired in a covalent bond.

The material we have been describing thus far is an *intrinsic* semiconductor and is characterized by several features: (1) the number of electrons in the conduction band is equal to the number of holes in the valence band; (2) the Fermi energy lies at the middle of the gap; (3) the electrons contribute most to the current, but the holes are important also; (4) about 1 electron in 10^9 contributes to the conduction.

Because only 1 electron in 10^9 contributes to the conductivity of an intrinsic semiconductor, the presence of impurities can significantly alter the conductivity of the semiconductor in a way that might not be easily controllable. However, if impurities with known properties are *deliberately* introduced into the semiconductor in carefully controlled amounts, their contribution to the conductivity can be precisely determined. At impurity levels of only 1 part in 10^6 or 10^7, the impurity contribution to the conductivity dominates the intrinsic contribution.

Such materials are known as *impurity* semiconductors, and the process of introducing the impurity is known as *doping*. Impurity semiconductors can be of two varieties: those in which the impurity contributes additional electrons to the conduction band and those in which the impurity contributes additional holes to the valence band.

Let us consider a material such as silicon or germanium, in which there are four valence electrons in hybrid orbitals. In the band theory view, these fill the $4N$ states of the valence band; in the atomic view the lattice is constructed so that each Ge or Si atom has four neighbors with which it shares an electron, and so all electrons participate in covalent bonding (Figure 11.40*a*). Now suppose we replace one of the Si or Ge atoms with an atom that has five valence electrons, such as phosphorus, arsenic, or antimony. Four of the five electrons form covalent bonds with the neighboring Si or Ge atoms, but the fifth electron is relatively weakly bound to the impurity atom and can be easily detached to contribute to the conductivity (Figure 11.40*b*). Alternatively, we could replace one of the Si or Ge atoms with an atom that has three valence electrons, such as boron, aluminum, gallium, or indium. Its three valence electrons form covalent bonds with the neighboring Si or Ge (Figure 11.40*c*), but one of the surrounding atoms has an unpaired electron. Completing the four pairs of covalent bonds is energetically very favorable, so an electron is easily captured to complete the symmetry of the lattice. This creates a hole in the valence band and therefore contributes to the conductivity.

On an energy-level diagram, the electron energies of these impurity atoms appear as discrete levels in the energy gap, either just below the conduction band (as in Figure 11.41*a*), or just above the valence band (as in Figure 11.41*b*). The energy needed for these electrons to enter the conduction band, or for electrons from the valence band to fill the low-lying empty states, is relatively small, about 0.01 eV in Ge and 0.05 eV in Si. As a result, even at room temperature ($kT \sim 0.025$ eV) these excitations can occur easily.

The energy levels formed by valence-5 impurities are known as *donor states* and the impurity is known as a *donor*, because electrons are "donated" to the conduction band. A semiconductor that has been doped with donor impurities is known as an *n-type* semiconductor, because the conductivity is due mostly to the negative electrons.

The energy levels formed by valence-3 impurities are known as *acceptor states*, because they can "accept" electrons from the valence band. A material that has been doped with acceptor impurities is known as a *p-type* semiconductor, because the conductivity is due mostly to the positively charged holes. (Remember that *n*-type and *p*-type materials are both *electrically neutral* because they are made from neutral atoms. The designations *n* and *p* refer only to the charge carriers, not

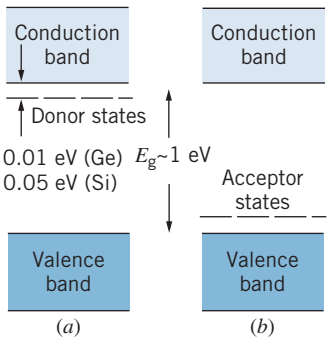

FIGURE 11.41 (*a*) Energy levels of donor states. (*b*) Energy levels of acceptor states.

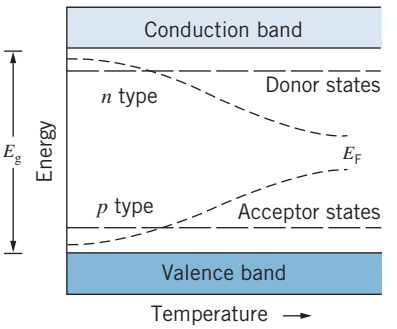

FIGURE 11.42 In a semiconductor, the Fermi energy moves toward the middle of the gap as the temperature increases.

to the material itself. Depending on whether we add or remove electrons, *n*-type and *p*-type materials can become either negatively or positively charged).

At $T = 0$ the Fermi energy in *n*-type semiconductors lies between the donor states and the conduction band (remember, all states below E_F are full and all above E_F are empty; at $T = 0$ the donor states are all occupied). In *p*-type semiconductors, the Fermi energy at $T = 0$ lies between the valence band and the acceptor states. As the temperature is raised, the thermal excitation of electrons from the valence band to the conduction band (as in an intrinsic semiconductor) causes the Fermi energy to move toward the center of the energy gap, as shown in Figure 11.42. For low doping levels and at a high enough temperature, the material may behave like an intrinsic semiconductor.

11.7 SEMICONDUCTOR DEVICES

The *p-n* Junction

When a *p*-type semiconductor is placed in contact with an *n*-type semiconductor (Figure 11.43) electrons flow from the *n*-type material into the *p*-type material, until equilibrium is established. This equilibrium occurs when the Fermi energies in the two substances become identical.

The resulting energy level diagram is shown in Figure 11.44. The region between the two materials is known as the *depletion* region, because it has been somewhat depleted of charge carriers. Electrons from the donor states of the *n*-type material fill the holes of the acceptor states of the *p*-type material. In this region the donor states *do not* provide electrons for the conduction band and the acceptor states *do not* provide holes in the valence band.

Actually, these devices are not made by bringing two different materials into contact, but rather by doping one side of a material so that it becomes *n* type and the other side so that it becomes *p* type. The doping is carefully controlled, and typically depletion layers have a thickness of the order of 1 μm.

The excess electrons that have entered the *p*-type material give that side of the depletion region a negative charge, which tends to repel additional electrons from the *n* region. There is a corresponding positive charge in the *n* region (because it has lost electrons to the *p* region). These charges are associated with the fixed

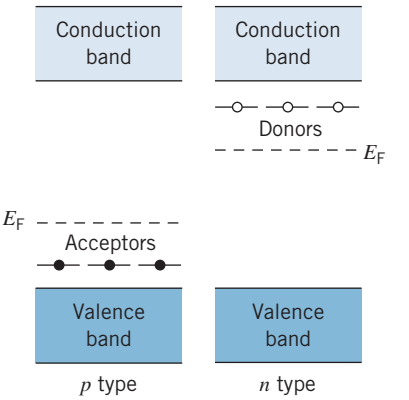

FIGURE 11.43 *n*-type and *p*-type semiconductors before contact.

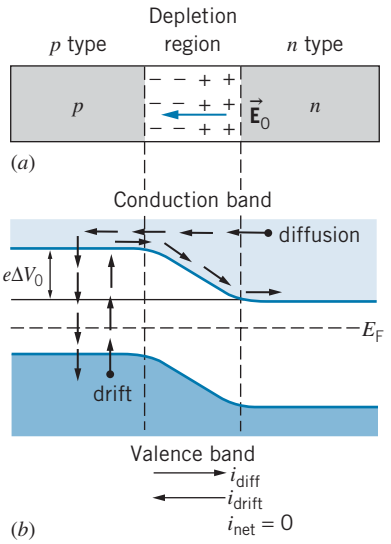

FIGURE 11.44 (*a*) A *p*-*n* junction. The electric field in the depletion region inhibits the additional flow of electrons. (*b*) Energy levels in *p*-*n* junction. Energetic electrons in the tail of the Fermi-Dirac distribution contribute to the diffusion current, while thermal excitation gives an equal and opposite drift current.

ions in those regions; the acceptor atoms in the *p* region acquire an electron and become fixed sites of negative charge, while the donor atoms in the *n* region lose an electron and become fixed sites of positive charge.

In equilibrium, enough negative charge builds up to stop the flow of electrons completely. There is a net electric field $\vec{\mathbf{E}}_0$ in the depletion region that results in a force (in the opposite direction) on the electrons, preventing any further flow of charge. Equivalently, there is a potential difference ΔV_0 between the *n*-type and *p*-type regions; for electrons to flow from the *n* region to the *p* region, they must climb the energy barrier of height $e\Delta V_0$.

In the tail of the Fermi distribution of electrons in the conduction band of the *n* region, there will be a small number of electrons with enough energy to climb the energy barrier and enter the *p* region, where they recombine with holes (that is, they "fall" from the conduction band of the *p* region into the valence band). This gives the *diffusion* or *recombination* contribution to the current, which is directed from the *p* region to the *n* region (the current direction always being opposite to the direction of electron flow).

Even though holes provide the dominant contribution to the conduction in the *p* region, there are also electrons that provide a smaller contribution to the current. Electrons are thermally excited from the valence band in the *p* region to the conduction band, where they are accelerated by the electric field and travel into the *n* region. This gives the *drift* or *thermal* contribution to the current. At equilibrium, the two contributions to the current cancel one another, so that the net current is zero, as shown in Figure 11.44.

Let us now apply an external voltage ΔV_{ext} across the junction so that the *p*-type material is made more positive than the *n* material; that is, we connect the + terminal of a battery to the *p* side of the junction and the – terminal of the battery to the *n* side (Figure 11.45). The effect of the battery is to *lower* the energy hill by an amount $e\Delta V_{ext}$. (The vertical axis shows electron energy, and a potential difference of ΔV_{ext} gives an electron energy of $-e\Delta V_{ext}$.) This situation is called a *forward voltage* or *forward biasing*. The forward bias causes the depletion region to become narrower, because the battery pulls electrons out of the *p* region and injects them back into the *n* region. Because the energy hill is lower, more electrons can diffuse from the *n* region into the *p* region, so the diffusion current is considerably increased. (That is, there are more electrons in the *n* region in the tail of the Fermi distribution with energies above the bottom of the conduction band of the *p* region.) The drift current, however, is unaffected by the presence of the battery or the height of the hill. There is now a net current through the junction in the forward direction.

Now we reverse the battery connections (Figure 11.46), a situation known as *reverse voltage* or *reverse biasing*. This *raises* the hill by the amount $e\Delta V_{ext}$, *widens* the depletion region (because the battery pulls more electrons from the *n* region and injects them into the *p* region), and *decreases* the diffusion current. The drift current is again unchanged, so now there is a relatively small net current in the reverse direction.

Figure 11.47 shows the upper tail of the Fermi-Dirac distribution of the electrons extending into the conduction band of the *n*-type region. Only those electrons in the portion of the tail above the energy E_c of the bottom of the conduction band of the *p*-type region can flow back across into the *p*-type region and it is these electrons that produce the diffusion current. The number of electrons in that tail above the energy E_c is approximately

$$N_1 = ne^{-(E_c - E_F)/kT} \tag{11.28}$$

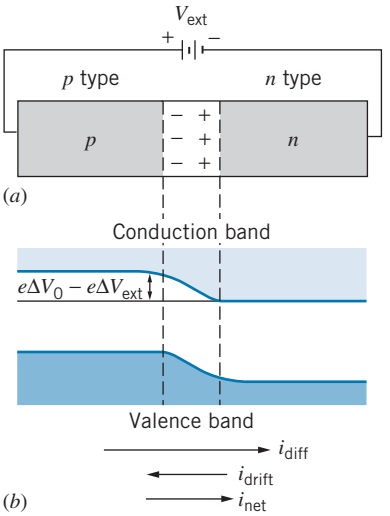

FIGURE 11.45 (*a*) A forward-biased *p-n* junction. (*b*) The energy level diagram. The potential energy hill is smaller, the diffusion current is larger, and there is a net forward current.

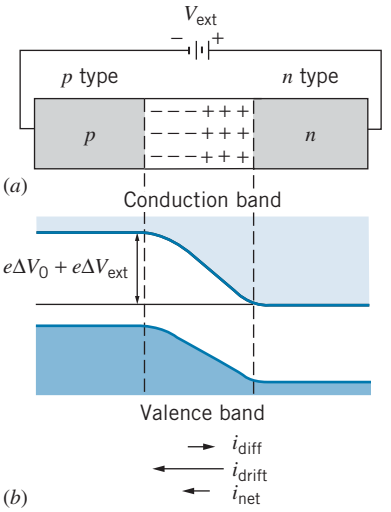

FIGURE 11.46 (*a*) A reversed-biased *p-n* junction. (*b*) The energy level diagram. The potential energy hill is larger, the diffusion current is smaller, and there is a small reverse current.

where n is some proportionality factor, and where we have approximated the Fermi-Dirac function as an exponential by neglecting the 1 in the denominator. (Because $E_c - E_F \geqslant 1\text{eV}$ and $kT = 0.025$ eV, this is an excellent approximation.) The diffusion current is proportional to N_1, and because the drift and diffusion currents are equal, the drift current is also proportional to N_1. Applying ΔV_{ext} changes the level E_c to $E_c - e\Delta V_{ext}$, and the number of electrons in the tail above $E_c - e\Delta V_{ext}$ is

$$N_2 = ne^{-(E_c - e\Delta V_{ext} - E_F)/kT} \tag{11.29}$$

The diffusion current is now proportional to N_2; applying the bias did not change the drift current, so it is still proportional to N_1. The net current is given by the difference:

$$i \propto N_2 - N_1 = ne^{-(E_c - E_F)/kT}(e^{e\Delta V_{ext}/kT} - 1) \tag{11.30}$$

We can rewrite this expression as

$$i = i_0(e^{e\Delta V_{ext}/kT} - 1) \tag{11.31}$$

This function is plotted in Figure 11.48, and it is immediately obvious why such *p-n* junctions, also known as *diodes*, have the property of *rectifying* varying currents. When the applied voltage is such that the junction is forward biased, a large forward current can flow. (When $\Delta V_{ext} = 1\text{V}$, $i = 2 \times 10^{17} i_0$.) When the applied voltage is such that the junction is reverse biased, only a very small current can flow. (When $\Delta V_{ext} = -1\text{V}$, $i \cong -i_0$.) Even very small forward voltages can produce large forward currents; even very large reverse voltages can produce only small reverse currents.

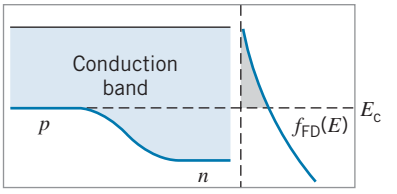

FIGURE 11.47 The diffusion current depends on the number of electron states in the tail of the Fermi-Dirac distribution above the energy E_c of the bottom of the conduction band in the *p*-type material.

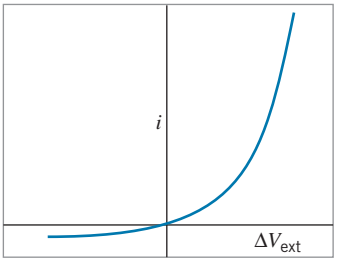

FIGURE 11.48 Current-voltage characteristics of an ideal *p-n* junction.

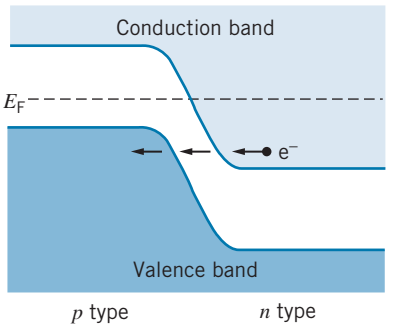

FIGURE 11.49 Energy level diagram of a *p*-*n* junction under heavy doping. Electrons can tunnel across the narrow gap.

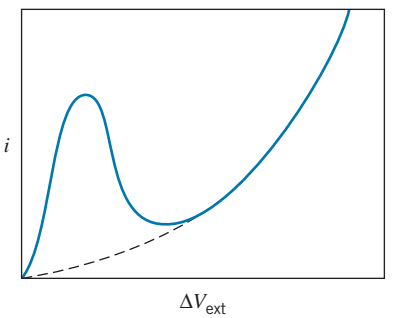

FIGURE 11.50 Current-voltage characteristics of a tunnel diode. The dashed curve shows the characteristics of an ordinary *p*-*n* junction diode.

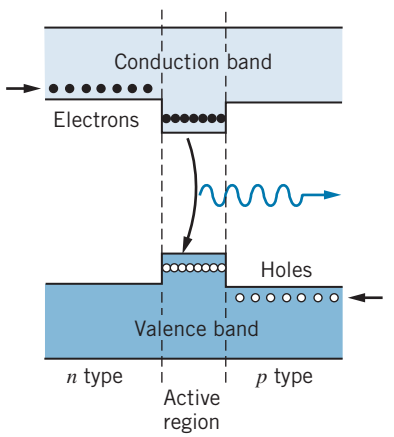

FIGURE 11.51 Energy bands in a diode laser. The active region has a smaller gap than the *n*-type and *p*-type regions on either side.

The Tunnel Diode

When the *p* and *n* regions are very heavily doped, the depletion layer becomes much narrower, perhaps 10 nm, and the energy diagram might look like Figure 11.49. When a small forward bias is applied, there is now a third contribution to the current—an electron from the conduction band of the *n* region can "tunnel" through the forbidden region directly into the valence band of the *p* region. This process of course depends on the wave nature of the electron and is an example of the type of barrier penetration we have discussed previously, in Section 5.6. The narrow depletion layer makes the process possible. The wavelength of an electron near the Fermi surface is about 1 nm, and if the thickness of the depletion layer were many orders of magnitude larger than this, tunneling would be unlikely to occur.

As the forward voltage is increased, the potential hill is lowered, and soon it no longer becomes possible for an electron to tunnel directly through the forbidden region. For a voltage of a few tenths of a volt, the tunneling current becomes zero. At this point the tunnel diode behaves like an ordinary diode. Figure 11.50 illustrates the characteristic current-voltage relationship for a tunnel diode.

Tunnel diodes are useful in electric circuits as high-speed elements, because the characteristics of the device can change as rapidly as the bias voltage can be changed. They can also be used as switches. If we were to pass current through the tunnel diode so that we were on the peak of the characteristic curve, a small increase in the current would cause the voltage to jump suddenly to a much larger value.

Photodiodes

A photodiode is a *p*-*n* junction whose operation involves the emission or absorption of light. These devices operate on principles similar to ordinary atoms. An electron in the valence band can absorb a photon and make a transition to the conduction band. Photons of visible light have energies of order 2 to 3 eV, so a semiconductor with its gap of order 1 eV is just right for such a transition. Conversely, an excited electron from the conduction band can drop back down to the valence band, emitting a photon in the process.

A common device that emits visible light is the LED, or light-emitting diode. An external current supplies the energy necessary to excite electrons to the conduction band, and when the electrons fall back down to recombine with holes, a photon is emitted. The energy is of course equal to the difference in energy of the electronic states. By varying the chemical composition, it is possible to produce LEDs emitting any color of visible light. LEDs find wide use as indicator lights and in video displays, including televisions and computer monitors. Broad-spectrum LEDs emitting white light are used in environmental lighting.

It is possible for photodiodes to operate in reverse, in which an incoming photon is absorbed in the depletion region and produces an electron-hole pair. An electric field sweeps up the electron-hole pairs and produces an electric signal. Such devices are used to produce electric current (as in a silicon solar cell) or to count photons (as in light meters for cameras or detectors of X rays or gamma rays in space probes).

Figure 11.51 shows another application of the emission of light by a semiconductor, in this case a *diode laser* or *semiconductor laser*. A thin layer of semiconducting material is sandwiched between *n*-type and *p*-type regions having a slightly larger energy gap. Electrons are injected from an external circuit into the *n*-type material, from which they diffuse into the middle layer. The electrons are prevented from diffusing into the *p*-type layer by a potential barrier, so they tend to concentrate in the middle layer. In a similar fashion, holes are injected into the

p-type layer and again concentrate in the middle layer. This creates a population inversion similar to that described in our discussion of the laser in Section 8.7. An electron drops into the valence band accompanied by the emission of a photon; that photon then induces other transitions leading to the avalanche of photons that gives the lasing action.

The physical construction of a typical diode laser is illustrated in Figure 11.52. The lasing material is a narrow (0.2 μm) layer of GaAs, and the *p*-type and *n*-type layers are GaAlAs a few μm in thickness. The ends of the material are cleaved to create mirrorlike surfaces that reflect a portion of the light wave, enhancing stimulated emission in the active region. This device emits at a wavelength of 840 nm, in the near infrared region. Diode lasers at this wavelength are commonly used in communication to send signals along optical fibers. By varying the materials of the laser, it is possible to obtain visible radiation in almost any color. Diode lasers find common use in bar-code scanners and in players for CDs and DVDs. There are also many medical uses, for example in laser surgery.

Diode lasers are of small size, and they consume very little power (typically 10 mW, compared with the standard HeNe laser that may consume several watts). As a result, diode lasers can be powered by ordinary batteries. The light signal can be turned on or off in switching times that are characteristic of semiconductors (< 100 ps), and thus we have a device that can rapidly modulate the beam. Even though conventional lasers are capable of performing many of the same functions as diode lasers, the small size, low cost, low power consumption, and rapid switching times make diode lasers the superior choice for most low-power applications.

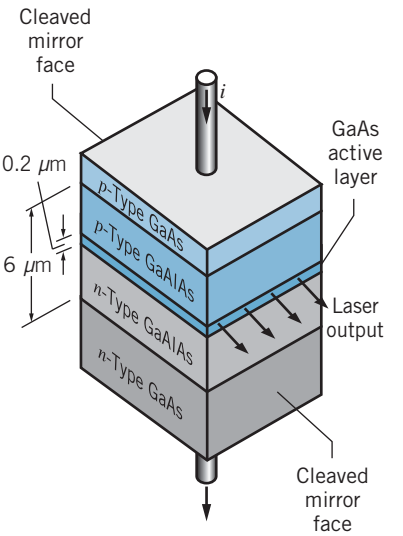

FIGURE 11.52 A diode laser. The lasing action occurs in the thin GaAs layer.

11.8 MAGNETIC MATERIALS

Our final example of the application of quantum physics to solids concerns the magnetic behavior of materials. The magnetic susceptibility of atoms was discussed briefly in Section 8.4 (see Figure 8.10). Most atoms have permanent magnetic dipole moments, due either to the spin or orbital angular momentum of the electrons (or both). Ordinarily, these magnetic moments point in random directions, so the net total magnetic dipole moment of a sample of the material is zero. However, when a magnetic field is applied, the magnetic moments rotate into partial or full alignment with the applied field, and the vector sum of the dipole moments gives the material a net magnetization. Specifically, the total magnetization $\vec{\mathbf{M}}$ is defined as the sum of all the individual atomic magnetic dipole moments $\vec{\boldsymbol{\mu}}_i$ per unit volume:

$$\vec{\mathbf{M}} = \frac{\sum_{i=1}^{N} \vec{\boldsymbol{\mu}}_i}{V} \tag{11.32}$$

where the sum is carried out over all the N individual particles (atoms, for example) in the material.

Over a fairly wide range of applied magnetic fields, in many materials we find that the net magnetization is directly proportional to the applied field $\vec{\mathbf{B}}_{\text{app}}$. That is, the stronger the applied field, the more the individual magnetic moments rotate into alignment with the field. (Clearly this proportionality cannot continue indefinitely as the field strength increases, because eventually all dipoles will be aligned with the field and further increases in the field will have little or no effect.)

The proportionality constant between the magnetization and the applied field is called the *magnetic susceptibility* χ:

$$\mu_0 \vec{\mathbf{M}} = \chi \vec{\mathbf{B}}_{\text{app}} \tag{11.33}$$

For many materials, χ is small (10^{-5} to 10^{-1}) and positive. These materials are called *paramagnetic*. In other materials, χ is observed to be negative (that is, the direction of the net magnetization is opposite to the direction of the applied field). These materials, which are called *diamagnetic*, usually have no permanent atomic magnetic moments, often because they have only paired electrons (as for example the inert gases); their magnetic behavior is due to a slight change in the orbital motion of the atomic electrons in response to the applied field. Diamagnetism is ordinarily a very weak effect, with susceptibilities in the range of -10^{-5} to -10^{-4}. (The effect responsible for diamagnetism, the alteration of the orbital motion of the electrons, can also occur in paramagnetic materials, but it is generally much weaker than the paramagnetism. However in some materials, such as copper, the paramagnetism is so weak that the diamagnetism is dominant.) In yet other materials, the magnetization remains after the applied field is removed. These include the *ferromagnetic* substances, and the susceptibility is undefined for ferromagnets.

Magnetic effects are often strongly temperature dependent. In fact materials can change from ferromagnetic to paramagnetic as the temperature is increased.

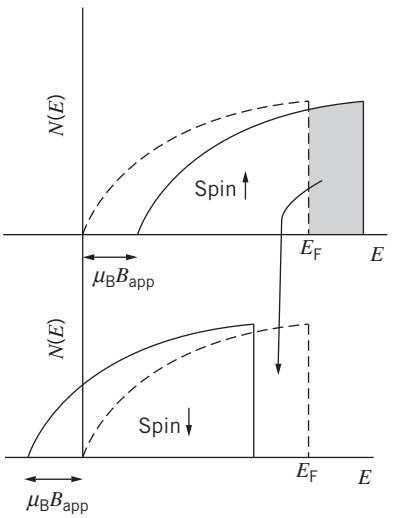

FIGURE 11.53 The dashed lines show the number of electrons in the Fermi-Dirac distribution drawn separately for spin up (top) and spin down (bottom). In an applied magnetic field, the energies of the spin-up electrons increase and the energies of the spin-down electrons decrease. To maintain the same Fermi energy with the field on, the spin-up electrons in the shaded strip flip their spins and move into the equivalent area with spin down.

Paramagnetism of Electron Gas

Let's begin by investigating the magnetic behavior of an electron gas. When we apply a magnetic field to an electron gas, the energy of an electron in the field is $E = -\vec{\boldsymbol{\mu}}_s \cdot \vec{\mathbf{B}}_{\text{app}}$, where $\vec{\boldsymbol{\mu}}_s = -(e/m)\vec{\mathbf{s}}$ is the spin magnetic moment of the electron. The energy of the interaction of an electron with the field is then (assuming the field is in the z direction)

$$E = -\vec{\boldsymbol{\mu}}_s \cdot \vec{\mathbf{B}}_{\text{app}} = \frac{e}{m}\,\vec{\mathbf{s}} \cdot \vec{\mathbf{B}}_{\text{app}} = \frac{e}{m}\,s_z B_{\text{app}} = \frac{e}{m}\,m_s \hbar B_{\text{app}} = \pm \mu_B B_{\text{app}} \tag{11.34}$$

with $m_s = \pm 1/2$. The symbol μ_B represents the Bohr magneton $e\hbar/2m$ (see Eq. 7.23). The electrons with $m_s = +1/2$ gain energy $\mu_B B_{\text{app}}$ and those with $m_s = -1/2$ lose an equal amount of energy.

Figure 11.53 shows the Fermi-Dirac distribution of populated electron states separately for the spin-up and spin-down electrons (half of the electrons are in each group). All of the spin-up electrons move up in energy by $\mu_B B_{\text{app}}$ and all of the spin-down electrons move down. Because the two groups of electrons are in contact, the higher-energy electrons in the shaded region with spin up flip their spins and fill the vacant energy states in the spin-down group until the two groups equalize their Fermi energies. As a result, there is an excess of electrons with spin down in a strip of width $\Delta E = 2\mu_B B_{\text{app}}$. The number of electrons in the strip is $\Delta N = \frac{1}{2} V g(E) f_{\text{FD}}(E) \Delta E$, where the factor of $1/2$ comes from the fact that the spin-up and spin-down distributions each have $1/2$ of the total number of electrons. The drawing of Figure 11.53 has been exaggerated; the strips are very narrow compared with E_F, and we assume that we are at a reasonably low temperature in which the Fermi-Dirac distribution is fairly sharp, so we can evaluate the density of states at $E = E_F$ and take $f_{\text{FD}} = 1$:

$$\Delta N = N(\downarrow) - N(\uparrow) = V g(E_F) \mu_B B_{\text{app}} \tag{11.35}$$

From Eq. 11.32, the z component of the magnetization is $V^{-1}\sum \mu_{iz} = V^{-1}\mu_B \Delta N$, so

$$\chi = \frac{\mu_0 M}{B_{app}} = \mu_0 \mu_B^2\, g(E_F) = \frac{3\mu_0 \mu_B^2}{2E_F}\frac{N}{V} \tag{11.36}$$

using $g(E_F) = 3N/2VE_F$. This calculation was first done by Wolfgang Pauli, and the result is often called the *Pauli paramagnetic susceptibility*. Note that N/V in this equation is the number of free electrons per unit volume, which might differ from the number of atoms per unit volume in materials in which there is more than one valence electron per atom.

Equation 11.36 can be used to calculate values for the susceptibility of materials in which the electrons behave like a gas of fermions. However, comparing calculated susceptibility values with experimental values can often be challenging because of the many different units that are used. On the surface, it appears that the susceptibility is a dimensionless quantity, but in fact it can be calculated in many different ways: susceptibility per unit volume (as in Eq. 11.36) or per unit mass or per mole. Furthermore, it can be expressed in either cgs units or SI units (our choice). The tabulated values in the literature are often given as the molar susceptibility in cgs units. The conversion procedure is $\chi^{SI}_{volume} = 4\pi\chi^{cgs}_{volume} = 4\pi(\rho/M)\chi^{cgs}_{molar}$, where ρ is the density of the solid and M is its molar mass (don't confuse this with the magnetization!). With the conversion written in this way, ρ and M must be in cgs units.

With that warning in mind, let's look at how Eq. 11.36 compares with experiment. Table 11.7 shows a few calculated and measured values. The agreement is surprisingly good, particularly in view of our omitting a number of important effects from the calculation, including a diamagnetic correction. For many metals, the diamagnetic contribution is larger than the Pauli paramagnetism, and as a result their susceptibility is negative (copper and gold are examples). The diamagnetic contribution is important because the Pauli susceptibility is so small (only a small fraction of the electrons near the Fermi energy contribute). Metal ions in salts typically have paramagnetic susceptibilities that can be several orders of magnitude larger, as we discuss next.

It is also interesting to note that Eq. 11.36 predicts that the susceptibility of these substances should be independent of temperature. Raising the temperature should broaden the distribution of both the spin-up and spin-down distributions (Figure 11.53) by about the same amount, making a negligible contribution to the susceptibility. Indeed, the susceptibility of these metals has only a very weak dependence on temperature. In sodium, for example, the susceptibility changes by only a few percent between room temperature (300 K) and liquid helium temperature (4 K).

TABLE 11.7 Pauli Magnetic Susceptibility of Some Solids

Element	Experimental susceptibility ($\times 10^{-6}$)		Calculated susceptibility ($\times 10^{-6}$)
	cgs, per mole	SI, per volume	
Al	16.5	20.7	15.7
K	20.8	5.8	6.2
Mg	13.1	11.8	12.2
Na	16	8.5	8.2

Example 11.5

(*a*) Compute the Pauli paramagnetic susceptibility of Mg. (*b*) The experimental value of the molar susceptibility is 13.1×10^{-6} in cgs units. What is the value of the volume susceptibility in SI units?

Solution

(*a*) For Mg (which has valence 2),

$$\begin{aligned}\frac{N}{V} &= \frac{2\rho N_A}{M} \\ &= \frac{2(1.74 \times 10^3 \text{ kg/m}^3)(6.02 \times 10^{23} \text{ atoms/mole})}{0.0243 \text{ kg/mole}} \\ &= 8.62 \times 10^{28} \text{ m}^{-3}\end{aligned}$$

The susceptibility is

$$\begin{aligned}\chi &= \frac{3\mu_0\mu_B^2}{2E_F}\frac{N}{V} \\ &= \frac{3(4\pi \times 10^{-7} \text{ T} \cdot \text{m/A})(9.27 \times 10^{-24} \text{ J/T})^2(8.62 \times 10^{28} \text{ m}^{-3})}{2(7.13 \text{ eV})(1.602 \times 10^{-19} \text{ J/eV})} \\ &= 12.2 \times 10^{-6}\end{aligned}$$

To see how the units cancel, it is helpful to realize that the magnetic moment has units of either J/T or $\text{A} \cdot \text{m}^2$ (the latter coming from the definition $\mu = iA$ for the magnetic moment of a current i in a loop of area A).

(*b*)

$$\begin{aligned}\chi_{\text{volume}}^{\text{SI}} &= 4\pi\frac{\rho}{M}\chi_{\text{molar}}^{\text{cgs}} \\ &= 4\pi\frac{1.74 \text{ g/cm}^3}{24.3 \text{ g/mole}}(13.1 \times 10^{-6}) \\ &= 11.8 \times 10^{-6}\end{aligned}$$

Note that the density and molar mass are in cgs units for the conversion.

Paramagnetism of Atoms and Ions

Instead of the free electrons, let's consider the contribution of the atoms or ions to the paramagnetism. We'll represent the effective electronic spin of each atom by J, which might represent the total intrinsic spin S of the electrons in the atom, their total orbital angular momentum L, or a combination of both (the nuclear spin is excluded, because nuclear magnetic effects are negligible compared with electronic magnetic effects). Depending on the number of electrons in the atom, J might be integral or half-integral.

The angular momentum J has all of the usual properties of quantum angular momentum. It has z component $J_z = m_J\hbar$, where m_J runs from $-J$ to $+J$ in integer steps. For any J, there are $2J + 1$ possible values of m_J. For example, if $J = {}^3/_2$, then $m_J = -{}^3/_2, -{}^1/_2, +{}^1/_2, +{}^3/_2$. Associated with this angular momentum there is an effective magnetic moment $\vec{\boldsymbol{\mu}} = -g_J\mu_B\vec{\mathbf{J}}$, where g_J is a dimensionless factor of order unity that describes how the spin and orbital angular momenta combine to give J. (The minus sign is present because electrons have negative charge.) Assuming the magnetic field defines the z direction, the energy of interaction of this magnetic moment with the applied field is $E = -\vec{\boldsymbol{\mu}} \cdot \vec{\mathbf{B}}_{\text{app}} = g_J\mu_B m_J B_{\text{app}}$.

We'll treat the atoms or ions as if they are independent of one another, so that they can be described by Maxwell-Boltzmann statistics. Because the magnetic substates m_J are nondegenerate, we can write the number of atoms in each magnetic substate in the form of Eq. 10.4: $N_{m_J} = A^{-1}e^{-E/kT} = A^{-1}e^{-g_J\mu_B m_J B_{\text{app}}/kT}$, where A^{-1} is the normalization constant for the Maxwell-Boltzmann distribution.

The normalization condition requires that N be the total number of atoms in all substates: $N = \sum_{m_J=-J}^{+J} N_{m_J} = A^{-1} \sum_{m_J=-J}^{+J} e^{-g_J \mu_B m_J B_{app}/kT}$. We therefore have:

$$N_{m_J} = \frac{N e^{-g_J \mu_B m_J B_{app}/kT}}{\sum_{m_J=-J}^{+J} e^{-g_J \mu_B m_J B_{app}/kT}} \tag{11.37}$$

The z component of the magnetization is then

$$\begin{aligned} M = V^{-1} \sum_{\text{all atoms}} \mu_z &= -V^{-1} \sum_{m_J=-J}^{+J} N_{m_J} g_J \mu_B m_J \\ &= -\frac{N V^{-1} g_J \mu_B \sum_{m_J=-J}^{+J} m_J e^{-g_J \mu_B m_J B_{app}/kT}}{\sum_{m_J=-J}^{+J} e^{-g_J \mu_B m_J B_{app}/kT}} \end{aligned} \tag{11.38}$$

The magnetic susceptibility is

$$\chi = \frac{\mu_0 M}{B_{app}} = -\frac{\mu_0 N V^{-1} g_J \mu_B \sum_{m_J=-J}^{+J} m_J e^{-g_J \mu_B m_J B_{app}/kT}}{B_{app} \sum_{m_J=-J}^{+J} e^{-g_J \mu_B m_J B_{app}/kT}} \tag{11.39}$$

Let's examine the form of χ for the simplest case in which $J = 1/2$, so that we have only two terms in the sums ($m_J = -1/2$ and $+1/2$). Equation 11.39 becomes

$$\begin{aligned} \chi &= \frac{-\mu_0 N g_J \mu_B [(-1/2) e^{g_J \mu_B B_{app}/2kT} + (+1/2) e^{-g_J \mu_B B_{app}/2kT}]}{V B_{app} (e^{g_J \mu_B B_{app}/2kT} + e^{-g_J \mu_B B_{app}/2kT})} \\ &= \frac{\mu_0 N g_J \mu_B}{2 V B_{app}} \tanh(g_J \mu_B B_{app}/kT) \end{aligned} \tag{11.40}$$

Figure 11.54 shows the susceptibility of a spin-1/2 atom as a function of $1/T$, so the high-temperature region is on the left side of the graph and the low-temperature region is on the right side. In the low-temperature region, the magnetic moments become fully aligned, and neither additional cooling nor an increase in the applied field can change the magnetization. In the high-temperature region, the graph is nearly a straight line, indicating that the susceptibility is linear in $1/T$. (How high must the temperature be to observe this linear behavior? For a fairly large field of 1 T the quantity $\mu_B B_{app}$ is about 0.060 meV. When T is 10 K, kT is 0.862 meV. Thus even with moderately large fields, "high temperature" for this discussion means anything above about 10 K. At low fields the "high temperature region" might reach all the way down to 1 K.)

In the high-temperature region, the exponents in Eq. 11.39 are small and we can use the approximation $e^x \cong 1 + x$ for small x (with $x = g_J \mu_B m_J B_{app}/kT$):

$$\chi = -\frac{\mu_0 N V^{-1} g_J \mu_B \sum_{m_J=-J}^{+J} m_J (1 - g_J \mu_B m_J B_{app}/kT)}{B_{app} \sum_{m_J=-J}^{+J} (1 - g_J \mu_B m_J B_{app}/kT)} \tag{11.41}$$

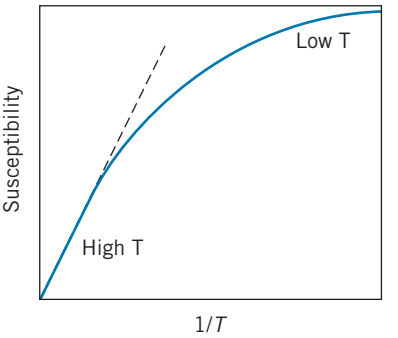

FIGURE 11.54 Magnetic susceptibility as a function of inverse temperature for a spin-1/2 material. Note the linear behavior at high temperature.

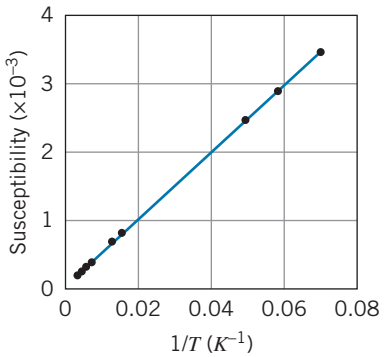

FIGURE 11.55 Susceptibility of paramagnetic copper sulfate ($CuSO_4 \cdot 5H_2O$) between room temperature and 14 K.

All quantities other than m_J come out of the sums, leaving us three summations to evaluate:

$$\sum_{m_J=-J}^{+J} 1 = 2J+1 \qquad \sum_{m_J=-J}^{+J} m_J = 0 \qquad \sum_{m_J=-J}^{+J} m_J^2 = \tfrac{1}{3}J(J+1)(2J+1) \quad (11.42)$$

After making these substitutions and clearing terms, the result is

$$\chi = \frac{\mu_0 N g_J^2 \mu_B^2 J(J+1)}{3VkT} \quad (11.43)$$

This shows the linear dependence of the susceptibility on $1/T$, as we observed in the high-temperature region of Figure 11.54. This result is known as *Curie's law**, which is often expressed in the form $\chi = C/T$ where C (the combination of factors in Eq. 11.43) is called the *Curie constant*. (It is not a true constant, as it takes different values for different substances, but it is constant for any single substance.) Figure 11.55 shows the susceptibility of the paramagnetic salt copper sulfate, which clearly shows the expected linear behavior down to a temperature of about 14 K.

Example 11.6

The slope of the graph in Figure 11.55 is 0.0499 K. Assuming the paramagnetism resides with the copper ions, find the value of the quantity $g_J^2 J(J+1)$ for copper sulfate.

Solution

We first need the value of N/V, which requires the density (2.28×10^3 kg/m^3) and molar mass (0.250 kg/mole) of copper sulfate:

$$\frac{N}{V} = \frac{\rho N_A}{M} = \frac{(2.28 \times 10^3 \text{ kg/m}^3)(6.02 \times 10^{23} \text{ atoms/mole})}{0.250 \text{ kg/mole}} = 5.49 \times 10^{27} \text{ atoms/m}^3$$

Because each molecule of copper sulfate has only one Cu ion, this number also gives us the density of Cu ions. We then have

$$\begin{aligned} C &= \frac{\mu_0 N \mu_B^2}{3Vk} g_J^2 J(J+1) \\ &= (4\pi \times 10^{-7} \text{ T} \cdot \text{m/A})(5.49 \times 10^{27} \text{ m}^{-3}) \\ &\quad \times (9.27 \times 10^{-24} \text{ J/T})^2 g_J^2 J(J+1) \\ &\quad \times [3(1.38 \times 10^{-23} \text{ J/K})]^{-1} \\ &= (0.0143 \text{ K})\, g_J^2 J(J+1) = 0.0499 \text{ K} \end{aligned}$$

As a result, $g_J^2 J(J+1) = 3.49$. Such experiments give us important information about the behavior of ions in crystals that is otherwise difficult to obtain. In this case we can learn about the value of the effective spin J that describes the copper ion.

In copper sulfate, the divalent copper ion Cu^{++} has the outer electronic configuration $3d^9$ (recall that neutral Cu atoms have the configuration $3d^{10}4s^1$). According to the rules for finding the total S and L for atoms (see Section 8.6), the nine $3d$ electrons in Cu^{++} have $S = 1/2$ (the maximum possible value of the total M_S) and $L = 2$ (the maximum possible resulting value of the total M_L). However, the measured value of $g_J^2 J(J+1)$ of 3.49 from Example 11.6 is more consistent with the configuration $S = 1/2, L = 0$ (for which its value would be 3.00), than

*Physicist Pierre Curie (1859–1906) was the husband of Marie Curie. Together they shared the 1903 Nobel Prize in physics for their research on radioactivity. Pierre Curie also contributed to the study of magnetism.

it is with any configuration involving $S = 1/2$ and $L = 2$ (which give values of either 2.40 or 12.60).

This is a common observation for paramagnetic crystals involving the transition metals (those in which the $3d$ shell is filling). In a magnetic field, which has a single preferred direction (usually taken to be the z direction), the component of the orbital angular momentum L_z along that direction is fixed, while the other components (L_x and L_y) average to zero. In a crystal, however, there is a strong electric field that may have three equivalent directions, and all three components of $\vec{\mathbf{L}}$ might average to zero. As a result, the ion behaves as if it has $L = 0$ (we say that the orbital angular momentum is "quenched"), and so only the total S contributes to the magnetic moment. In contrast, the rare earth elements also form many paramagnetic crystals, but both L and S contribute to J. In the rare earths, the electrons in the unfilled $4f$ shell are shielded by the filled $5s$ and $5p$ shells, which have the strongest interactions with the electric field of the crystal (because the average radii of their orbits are larger). The "inner" $4f$ electrons are not much affected by the electric field of the crystal and so they contribute their large orbital angular momentum to the total J of the ion.

Ferromagnetism

In some materials, the individual magnetic dipoles of the ions can align with one another even in the absence of an external magnetic field. In this case a net magnetization M is present when B_{app} is zero, so clearly the susceptibility is undefined for these materials. The most familiar example of this behavior is *ferromagnetism*, in which the neighboring dipoles all align in the same direction. (It is also possible to have *antiferromagnetic* materials, in which the neighboring dipoles orient in opposite directions.)

It is perhaps tempting at first to think of the interaction responsible for ferromagnetism as a result of the magnetic field due to one dipole exerting a magnetic force to align the neighboring dipole. However, this dipole-dipole interaction is far too weak to account for the strong coupling between neighbors that produces ferromagnetic alignment. Instead, the effect results from the overlap of the wave functions of the electrons in neighboring atoms, in a manner similar to covalent bonding but depending on the spins of the electrons. This effect is very sensitive to the interaction between the spins and also to the distance between the neighboring ions.

In Fe, Co, and Ni the value of the atomic spacing results in an energy minimum for the parallel orientation of neighboring spins, and so these materials are ferromagnetic at room temperature (but they become paramagnetic at a sufficiently high temperature, where the thermal energy kT exceeds the interaction energy). In other materials (such as some of the rare earth elements) the interaction is weaker, so they may not exhibit their ferromagnetic behavior until they are cooled to a point where the thermal energy kT is smaller than the interaction energy. In still other cases, the atomic spacing of the pure element may not permit ferromagnetism, but a different atomic spacing in certain compounds containing that element may allow the overlap interaction that causes the spins to align. For example, Cr is weakly paramagnetic at room temperature, but CrO_2 (which is used to make magnetic recording tape) is ferromagnetic.

The band theory provides a framework for understanding ferromagnetic behavior. Consider iron, which has the electronic configuration $3d^6 4s^2$. The partially filled $3d$ band can be split into two subbands, one with spin up and one with spin down. In the absence of the overlap interaction, the bands are at the same

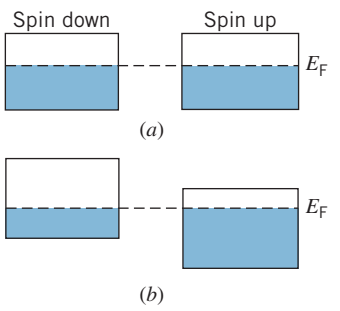

FIGURE 11.56 The $3d$ band in Fe. (*a*) In the absence of the interaction, there are 3 electrons per atom in the spin-up and spin-down subbands. (*b*) The interaction lowers the relative energy of the spin-up band, so there are now 4 electrons per atom with spin up and 2 with spin down.

energy and each band has 3 electrons per atom (out of its maximum capacity of 5) as in Figure 11.56*a*. The effect of the overlap interaction is to raise the energy of one band relative to the Fermi energy and lower the energy of the other (as in Figure 11.56*b*). Now there are roughly 4 electrons per atom in the spin-up subband and 2 in the spin-down subband, and this difference of approximately 2 electrons per atom in the 3*d* band is responsible for the net magnetization of iron.

Chapter Summary

		Section
Binding energy of ion in crystal	$B = \dfrac{\alpha e^2}{4\pi\varepsilon_0 R_0}\left(1 - \dfrac{1}{n}\right)$	11.1
Cohesive energy of crystal	$E_{\text{coh}} = BN_{\text{A}}$	11.1
Electron contribution to heat capacity	$C = \dfrac{\pi^2 k^2 N_{\text{A}} T}{2E_{\text{F}}} = \dfrac{\pi^2}{2}\dfrac{RkT}{E_{\text{F}}}$	11.2
Einstein heat capacity	$C = 3R\left(\dfrac{T_{\text{E}}}{T}\right)^2 \dfrac{e^{T_{\text{E}}/T}}{(e^{T_{\text{E}}/T} - 1)^2}$	11.2
Debye heat capacity	$C = \dfrac{12\pi^4}{5} R\left(\dfrac{T}{T_{\text{D}}}\right)^3$	11.2
Conductivity of free electron gas	$\sigma = ne^2\tau/m$	11.3
Lorenz number	$L = \pi^2 k^2/3e^2 = 2.44 \times 10^{-8}\ \text{W}\cdot\Omega/\text{K}^2$	11.3
BCS gap energy in superconductor	$E_{\text{g}} = 3.53kT_{\text{c}}$	11.5
Current in *p-n* junction diode	$i = i_0(e^{e\Delta V_{\text{ext}}/kT} - 1)$	11.7
Pauli paramagnetic susceptibility	$\chi = \dfrac{3\mu_0\mu_{\text{B}}^2}{2E_{\text{F}}}\dfrac{N}{V}$	11.8
Paramagnetic susceptibility of atoms	$\chi = -\mu_0 NV^{-1} g_J \mu_{\text{B}} \times \sum_{m_J=-J}^{+J} m_J e^{-g_J\mu_{\text{B}} m_J B_{\text{app}}/kT} \times \left(B_{\text{app}} \sum_{m_J=-J}^{+J} e^{-g_J\mu_{\text{B}} m_J B_{\text{app}} kT}\right)^{-1}$	11.8
Curie's law	$\chi = \dfrac{\mu_0 N g_J^2 \mu_{\text{B}}^2 J(J+1)}{3VkT} = \dfrac{C}{T}$	11.8

Questions

1. Compare the equilibrium separations and binding energies of ionic *solids* (Table 11.1) with those of the corresponding ionic *molecules* (Table 9.5). Account for any systematic differences.
2. How should Eq. 11.7 be modified to be valid for MgO and BaO?
3. From Figure 11.11, estimate the Einstein temperature for lead. (*Hint:* Consider Eq. 11.11 when $T = T_{\text{E}}$.)
4. A graph of C/T vs. T^2 for solid argon (similar to Figure 11.13) goes through the origin; that is, its y-intercept is zero. Explain.
5. Assuming that its other properties don't also change with temperature, at what temperature would you expect carbon to begin to behave like a semiconductor?
6. Would you expect the Wiedemann-Franz law to apply to semiconductors? To insulators?
7. (*a*) Why does the electrical conductivity of a metal decrease as the temperature is increased? (*b*) How would you expect the conductivity of a semiconductor to change with temperature?
8. Why is it that only the electrons near E_{F} contribute to the electrical conductivity?
9. Would you expect silicon to behave like an insulator at a low enough temperature? Would it behave like a conductor at a high enough temperature?
10. What determines the drift speed of an electron in a metal? What determines the Fermi speed?
11. Do the superconducting elements have any particular electronic structure or configuration in common?
12. Three different materials have filled valence bands and empty conduction bands, and the Fermi energy lies in the middle of the gap. The gap energies are 10 eV, 1 eV, and 0.01 eV. Classify the electrical properties of these materials at room temperature and at 3 K.
13. In what way does a *p-n* junction behave as a capacitor?

14. Semiconductors are sometimes called "nonohmic" materials. Why?
15. If a semiconductor is doped at a level of one impurity atom per 10^9 host atoms, what is the average spacing between the impurity atoms?
16. Explain the processes that contribute to the current in a forward-biased *p-n* junction. Do the same for a reverse-biased junction.
17. What limits the response time of a *p-n* junction when the external voltage is varied? Why does a tunnel diode not have the same limits?
18. The energy gap E_g is 0.72 eV for Ge and 1.10 eV for Si. At what wavelengths will Ge and Si be transparent to radiation? At what wavelengths will they begin to absorb significantly?
19. Why is a semiconductor better than a conductor for applications as a solar cell or photon detector? Would an insulator be even better?
20. Why is the magnetic susceptibility of an electron gas almost independent of temperature?
21. Would a sample of paramagnetic material be attracted or repelled by the N pole of a magnet? By the S pole? How would a sample of diamagnetic material behave? How would ferromagnetic material behave?
22. Is it possible for a material that has a positive magnetic susceptibility at room temperature to have a negative susceptibility at higher temperature?

Problems

11.1 Crystal Structures

1. Consider the packing of hard spheres in the simple cubic geometry of Figure 11.1. Imagine eight spheres in contact with their nearest neighbors, with their centers at the corners of the basic cube. (*a*) What fraction of the volume of each sphere is inside the volume of the basic cube? (*b*) Let r be the radius of each sphere and let a be the length of a side of the cube. Express a in terms of r. (*c*) What fraction of the volume of the cube is taken up by the portions of the spheres? This fraction is called the *packing fraction*.
2. Compute the packing fractions (see Problem 1) of (*a*) the fcc structure (Figure 11.2) and (*b*) the bcc structure (Figure 11.3). Which structure fills the space most efficiently?
3. Derive Eqs. 11.5 and 11.6.
4. Calculate the first three contributions to the electrostatic potential energy of an ion in the CsCl lattice.
5. (*a*) Find the binding energy per ion pair in CsCl from the cohesive energy. (*b*) Find the binding energy per ion pair in CsCl from Eq. 11.7. (*c*) Find the binding energy per atom for CsCl. The ionization energy of Cs is 3.89 eV.
6. (*a*) Find the binding energy per ion pair in LiF from the cohesive energy. (*b*) Find the binding energy per ion pair in LiF from Eq. 11.7. (*c*) Find the binding energy per atom for LiF. The ionization energy of Li is 5.39 eV, and the electron affinity of F is 3.45 eV.
7. Calculate the Coulomb energy and the repulsion energy for NaCl at its equilibrium separation.
8. The density of sodium is 0.971 g/cm^3 and its molar mass is 23.0 g. In the bcc structure, what is the distance between sodium atoms?
9. Copper has a density of 8.96 g/cm^3 and molar mass of 63.5 g. Calculate the center-to-center distance between copper atoms in the fcc structure.
10. Calculate the binding energy per atom for metallic Na and Cu.

11.2 The Heat Capacity of Solids

11. At what temperature do the lattice and electronic heat capacities of copper become equal to each other? Take $T_D = 343$ K and $E_F = 7.03$ eV. Which contribution is larger above this temperature? Below this temperature?
12. (*a*) The heat capacity of solid argon at a temperature of 2.00 K is 2.00×10^{-2} J/mole·K. What is the Debye temperature of solid argon? (See Question 4.) (*b*) What value do you expect for the heat capacity at a temperature of 3.00 K?
13. When C/T is plotted against T^2 for potassium, the graph gives a straight line with a slope of 2.57×10^{-3} J/mole·K^4. What is the Debye temperature for potassium?
14. At a temperature of 4 K, the heat capacity of silver is 0.0134 J/mole·K. The Debye temperature of silver is 225 K. (*a*) What is the electronic contribution to the heat capacity at 4 K? (*b*) What are the lattice and electronic contributions and the total heat capacity at 2 K?

11.3 Electrons in Metals

15. (*a*) In copper at room temperature, what is the electron energy at which the Fermi-Dirac distribution function has the value 0.1? (*b*) Over what energy range does the Fermi-Dirac distribution function for copper drop from 0.9 to 0.1?
16. Calculate the de Broglie wavelength of an electron with energy E_F in copper, and compare the value with the atomic separation in copper.
17. What is the number of occupied energy states per unit volume in sodium for electrons with energies between 0.10

and 0.11 eV above the Fermi energy at room temperature (293 K)?

18. The electrical conductivity of copper at room temperature is $5.96 \times 10^7\ \Omega^{-1}\text{m}^{-1}$. Evaluate the average distance between electron scatterings. How many lattice spacings does this amount to?
19. At what temperature would the Fermi energy of Au be reduced by 1%? Compare this temperature with the melting point of Au (1337 K). Is it reasonable to assume the Fermi energy is a constant, independent of temperature?
20. A copper wire of diameter 0.50 mm carries a current of 2.5 mA. What fraction of the copper electrons contributes to the electrical conduction?
21. Use the Wiedemann-Franz ratio to calculate the thermal conductivity of copper at room temperature. The electrical conductivity is $5.96 \times 10^7\ \Omega^{-1} \cdot \text{m}^{-1}$.

11.4 Band Theory of Solids

22. Estimate the ratio of the concentration of electrons in the conduction band of carbon (an insulator) and silicon (a semiconductor) at room temperature (293 K). The energy gaps are 5.5 eV for carbon and 1.1 eV for silicon. Assume the Fermi energy lies at the center of the gap.
23. Estimate the ratio of the number of electrons in the conduction bands of germanium ($E_g = 0.66$ eV) and silicon ($E_g = 1.12$ eV) at a temperature of 400 K. Assume the Fermi energy is at the center of the gap.
24. The valence band in Si has a width of 12 eV. In a cube of Si that measures 1.0 mm on each side, calculate (*a*) the total number of states in the valence band, and (*b*) the average spacing between the states. The density of sodium is $2.33\ \text{g/cm}^3$.

11.5 Superconductivity

25. (*a*) Zirconium metal has a superconducting transition temperature of 0.61 K. Assuming the validity of the BCS theory, what is the energy gap for Zr? (*b*) If a beam of photons were incident on superconducting Zr, what wavelength of photons would be sufficient to break up the Cooper pairs? In what region of the electromagnetic spectrum are these photons?
26. When superconducting tantalum metal is illuminated with a beam of photons, it is found that photon wavelengths of up to 0.91 mm are sufficient to destroy the superconducting state. According to the BCS theory, find the energy gap and critical temperature for Ta.
27. Find the frequency of the current that results when a voltage difference of 1.25 μV is applied across a Josephson junction.

11.6 Intrinsic and Impurity Semiconductors

28. The temperature of a sample of intrinsic silicon is increased by 100 K over room temperature (293 K). Estimate the increase in conductivity that we would expect from this increase in temperature. The gap energy in silicon is 1.1 eV.
29. (*a*) Estimate the fraction of the electrons in the valence band of intrinsic silicon that can be excited to the conduction band at a temperature of 100 K and at room temperature. Take the energy gap in silicon to be 1.1 eV. (*b*) By what factor would the conductivity of a metal change over this same temperature interval?
30. Estimate the temperature at which the density of conduction electrons in intrinsic germanium equals that of intrinsic silicon at room temperature (293 K). The gap energies are 1.12 eV for Si and 0.66 eV for Ge.
31. (*a*) When we replace an atom of silicon with an atom of phosphorus, the outer electron of phosphorus is screened so that the atom behaves like a single-electron atom with $Z_{\text{eff}} \cong 1$. Compute the energy of the electron, assuming that silicon has a dielectric constant of 12 that effectively reduces the electric field experienced by the electron. (*b*) The additional electron in Si has an effective mass that is 0.43 times the free electron mass. How does this correction factor change the electron energy?
32. Assuming the energy gap in intrinsic silicon is 1.1 eV and that the Fermi energy lies at the middle of the gap, calculate the occupation probability at 293 K of (*a*) a state at the bottom of the conduction band and (*b*) a state at the top of the valence band.
33. In a sample of germanium at room temperature (293 K), what fraction of the Ge atoms must be replaced with donor atoms in order to increase the population of the conduction band by a factor of 3? Assume all donor atoms are ionized, and take the energy gap in Ge to be 0.66 eV.

11.7 Semiconductor Devices

34. (*a*) In a *p-n* junction at room temperature, what is the ratio between the current with a forward bias of 2.00 V to the current with a forward bias of 1.00 V? (*b*) Evaluate the same ratio at a temperature of 400 K.
35. Under certain conditions, the current in a *p-n* junction at room temperature is observed to be 1.5 mA when a forward bias of 0.25 V is applied. If the same voltage were used to reverse bias the junction, what would be the current?
36. Gallium phosphide ($E_g = 2.26$ eV) and zinc selenide ($E_g = 2.87$ eV) are commonly used to make LEDs. What is the most prominent emission wavelength of these devices, and what color is the corresponding light?
37. LEDs of varying colors can be made by mixing GaN ($E_g = 3.4$ eV) and InN ($E_g = 0.7$ eV) in different proportions. Calculate the relative amounts of GaN and InN needed to produce an LED that emits (*a*) green light (550 nm) and (*b*) violet light (400 nm).

11.8 Magnetic Materials

38. Estimate the fraction of spin-up electrons in sodium that flip their spins (as in Figure 11.53) and thus contribute to the Pauli paramagnetism. Assume a magnetic field of 1 T.

39. In copper sulfate, the Cu^{++} ions behave as if they have $J = 1/2$, for which $g_J = 2$. In a magnetic field of 0.25 T, calculate the relative numbers of copper ions in the $m_J = +1/2$ and $m_J = -1/2$ states at (*a*) 300 K and (*b*) 4.2 K.
40. Compute the Pauli paramagnetic susceptibilities for (*a*) Li and (*b*) Ba. Compare with the experimental values, which are respectively 14.2×10^{-6} and 20.6×10^{-6} (in cgs units per mole).
41. (*a*) Calculate the expected paramagnetic susceptibility for gold, assuming it to behave like a free electron gas. (*b*) The observed cgs molar susceptibility at room temperature is -28.0×10^{-6}. Assuming the susceptibility consists only of the diamagnetic and paramagnetic parts, find the diamagnetic contribution to the susceptibility of gold.
42. (*a*) The experimental paramagnetic susceptibility of $MnCl_2$ at room temperature (293 K) in cgs units per mole is 14350×10^{-6}. What is the value of $g_J^2 J(J+1)$ for the Mn^{++} ion? (*b*) What is the electronic configuration expected for the Mn^{++} ion? For this configuration, and assuming that the electronic S corresponds to maximizing the total M_S, what is the value of S for Mn^{++}? For the arrangement with that S, what is the corresponding total L? (*c*) With $J = L + S$, what is the value of g_J that follows from the experimental susceptibility?

General Problems

43. By summing the contributions for the attractive and repulsive Coulomb potential energies, show that the Madelung constant has the value 2 ln 2 for a one-dimensional "lattice" of alternating positive and negative ions.
44. Plot the cohesive energies of ionic crystals (see Table 11.1 and other data that you may find) against their melting points (see, for example, the *Handbook of Chemistry and Physics*). Is there a correlation between cohesive energies and melting points?
45. Plot the cohesive energies of metallic crystals (see Table 11.3 and other data that you may find) against their melting points (see, for example, the *Handbook of Chemistry and Physics*). Is there a correlation between cohesive energies and melting points?
46. (*a*) By taking the derivative of the total potential energy of an ion in a lattice, find an expression for the force on the ion. (*b*) Suppose an ion is displaced from its equilibrium position by a small distance x, so that $R = R_0 + x$. Show that for small values of x, the force can be written as $F = -kx$. Express k in terms of the other parameters of the crystal. (*c*) Find the value of k for NaCl and evaluate the oscillation frequency for a sodium ion. (*d*) Suppose a sodium ion in the lattice absorbed a photon of this frequency and began to oscillate. Find the wavelength of the photon. In what region of the electromagnetic spectrum is this photon?
47. The electric field of a dipole is proportional to $1/r^3$. Assuming that the induced dipole moment of molecule B is proportional to the electric dipole field of molecule A, show that the van der Waals force is proportional to r^{-7}. (*Hint:* Show that the potential energy of dipole B in the electric field caused by dipole A is proportional to r^{-6}.)
48. (*a*) Obtain the data for the heat capacity of aluminum between 1 K and 100 K (see, for example, the *Handbook of Chemistry and Physics*). Plot the data, and by trial and error find the value of the Einstein temperature that gives the best fit to the data. (*b*) Plot the data for temperatures below 10 K as C/T vs. T^2, determine the slope and intercept, and deduce the Debye temperature and effective mass for Al (using $E_F = 11.7$ eV).
49. (*a*) Obtain the data for the heat capacity of gold between 1 K and 100 K (see, for example, the *Handbook of Chemistry and Physics*). Plot the data, and by trial and error find the value of the Einstein temperature that gives the best fit to the data. (*b*) Plot the data for temperatures below 10 K as C/T vs. T^2, determine the slope and intercept, and deduce the Debye temperature and effective mass for Au (using $E_F = 5.53$ eV).
50. (*a*) A Cooper pair in a superconductor can be considered to be a bound state with an energy uncertainty that is of the order of the gap energy E_g. Assuming these pairs exist close to the Fermi energy, find the uncertainty in the location of a Cooper pair, which is a good estimate of its size. (*b*) Estimate the size of a Cooper pair for aluminum ($E_F = 11.7$ eV) and compare with the lattice spacing in aluminum (0.286 nm).
51. When a material such as germanium is used as a photon detector, an incoming photon makes many interactions and excites many electrons across the gap between the valence and the conduction band. (*a*) ^{137}Cs emits a 662-keV gamma ray. How many electrons are excited across the 0.66-eV gap of germanium by the absorption of this gamma ray? (*b*) The number N calculated in part (*a*) is subject to statistical fluctuations of $\sqrt{N}$. Compute the variation in N and the fractional variation in N. (*c*) What is the corresponding variation in the measured energy of the gamma ray? This result is the experimental resolution of the detector.
52. On a single graph, sketch the atomic paramagnetic susceptibility as a function of inverse temperature for $J = 1/2, 1$, and $3/2$. Assume all other coefficients $(N/V, g_J, B_{app})$ to be the same for these three cases. Plot the ratio of the susceptibility to its maximum for that spin, so you can compare the variation in the approach to saturation for these three spins.
53. The magnetic field at a distance r from a magnetic dipole μ is $B = \mu_0 \mu / 2\pi r^3$. Show that the dipole-dipole interaction energy is too small to account for the ferromagnetism of iron at all but the lowest temperatures. Assume an effective magnetic dipole moment of 2.2 μ_B per atom.
54. (*a*) Oxygen gas is observed to be paramagnetic at room temperature, but nitrogen gas is diamagnetic. Explain this based on the filling of the bonding and antibonding $2p$ orbitals in O_2 and N_2. (*Hint:* See Example 9.1.) (*b*) Would you expect NO gas to be paramagnetic or diamagnetic?

Chapter 12

NUCLEAR STRUCTURE AND RADIOACTIVITY

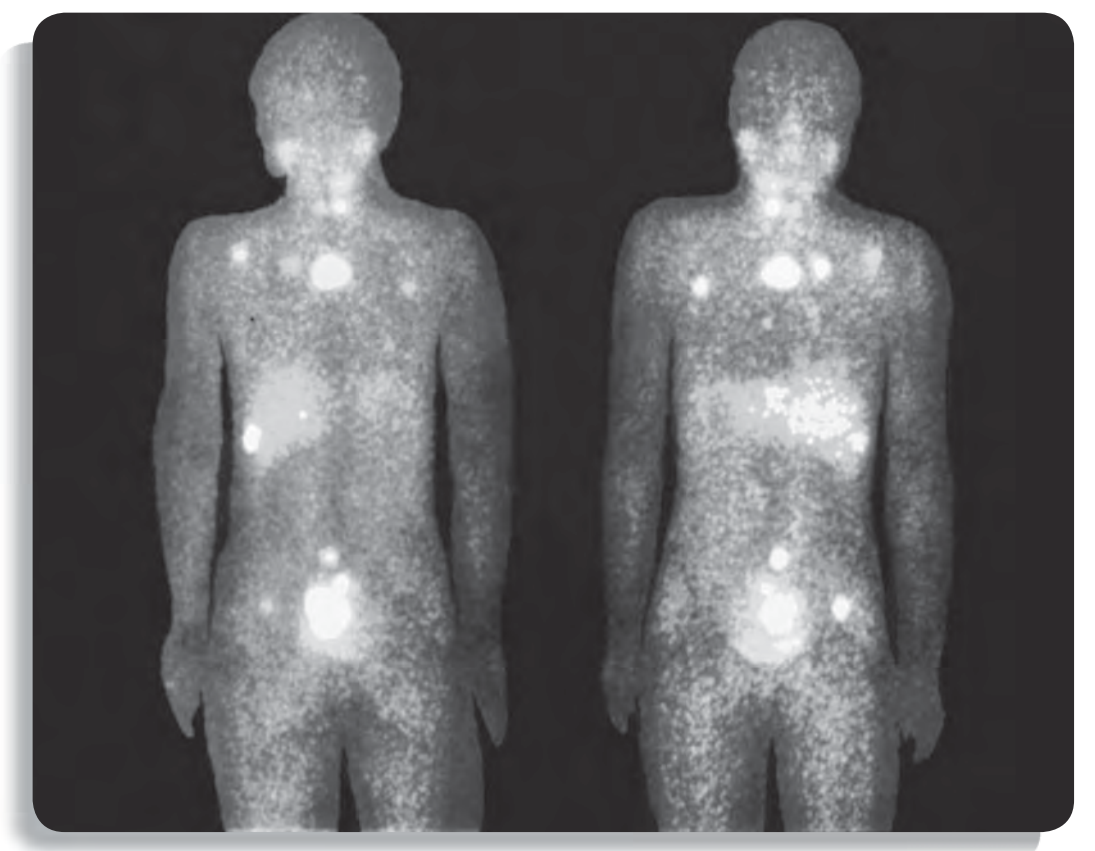

Radioactive isotopes have proven to be valuable tools for medical diagnosis. The photo shows gamma-ray emission from a man who has been treated with a radioactive element. The radioactivity concentrates in locations where there are active cancer tumors, which show as bright areas in the gamma-ray scan. This patient's cancer has spread from his prostate gland to several other locations in his body.

The nucleus lies at the center of the atom, occupying only 10^{-15} of its volume but providing the electrical force that holds the atom together. Within the nucleus there are Z positive charges. To keep these charges from flying apart, the nuclear force must supply an attraction that overcomes their electrical repulsion. This nuclear force is the strongest of the known forces; it provides nuclear binding energies that are millions of times stronger than atomic binding energies.

There are many similarities between atomic structure and nuclear structure, which will make our study of the properties of the nucleus somewhat easier. Nuclei are subject to the laws of quantum physics. They have ground and excited states and emit photons in transitions between the excited states. Just like atomic states, nuclear states can be labeled by their angular momentum.

There are, however, two major differences between the study of atomic and nuclear properties. In atomic physics, the electrons experience the force provided by an external agent, the nucleus; in nuclear physics, there is no such external agent. In contrast to atomic physics, in which we can often consider the interactions among the electrons as a perturbation to the primary interaction between electrons and nucleus, in nuclear physics the mutual interaction of the nuclear constituents is just what provides the nuclear force, so we cannot treat this complicated many-body problem as a correction to a single-body problem. We therefore cannot avoid the mathematical difficulties in the nuclear case, as we did in the atomic case.

The second difference between atomic and nuclear physics is that we cannot write the nuclear force in a simple form like the Coulomb force. There is no closed-form analytical expression that can be written to describe the mutual forces of the nuclear constituents.

In spite of these difficulties, we can learn a great deal about the properties of the nucleus by studying the interactions between different nuclei, the radioactive decay of nuclei, and the properties of some nuclear constituents. In this chapter and the next we describe these studies and how we learn about the nucleus from them.

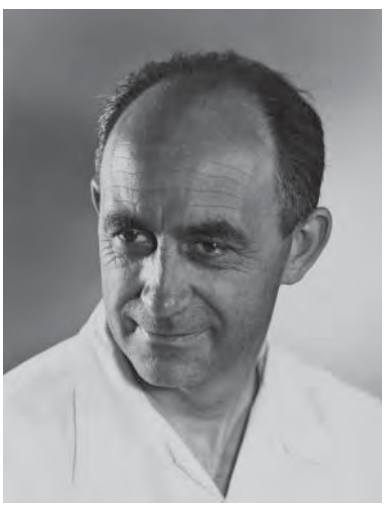

Enrico Fermi (1901–1954, Italy-United States). There is hardly a field of modern physics to which he did not make contributions in theory or experiment. He developed the statistical laws for spin-$\frac{1}{2}$ particles, and in the 1930s he proposed a theory of beta decay that is still used today. He was the first to demonstrate the transmutation of elements by neutron bombardment (for which he received the 1938 Nobel Prize), and he directed the construction of the first nuclear reactor.

12.1 NUCLEAR CONSTITUENTS

The work of Rutherford, Bohr, and their contemporaries in the years between 1911 and 1920 showed that the positive charge of the atom is confined in a very small nuclear region at the center of the atom, that the nucleus in an atom of atomic number Z has a charge of $+Ze$, and that the nucleus provides most (99.9%) of the atomic mass. It was also known that the masses of the atoms (measured in atomic mass units) were very nearly integers; a glance at Appendix D confirms this observation, usually to within about 0.1%. We call this integer A the *mass number*. It was therefore reasonable to suppose that nuclei are composed of a number A of more fundamental units whose mass is very close to 1 u. Because the only particle known at that time with a mass close to 1 u was the proton (the nucleus of hydrogen, with a mass of 1.0073 u and a charge of $+e$), it was postulated (incorrectly, as we shall see) that the nucleus of an atom of mass number A contained A protons.

Such a nucleus would have a nuclear charge of Ae rather than Ze; because $A > Z$ for all atoms heavier than hydrogen, this model gives too much positive charge to the nucleus. This difficulty was removed by the *proton-electron model,* in which it was postulated (again incorrectly) that the nucleus also contained $(A - Z)$ electrons. Under these assumptions, the nuclear mass would be about

A times the mass of the proton (because the mass of the electrons is negligible) and the nuclear electric charge would be $A(+e) + (A - Z)(-e) = Ze$, in agreement with experiment. However, this model leads to several difficulties. First, as we discovered in Chapter 4 (see Example 4.7), the presence of electrons in the nucleus is not consistent with the uncertainty principle, which would require those electrons to have unreasonably large ($\sim$ 19 MeV) kinetic energies.

A more serious problem concerns the total *intrinsic spin* of the nucleus. From measurements of the *very* small effect of the nuclear magnetic moment on the atomic transitions (called the *hyperfine splitting*), we know that the proton has an intrinsic spin of $^1/_2$, just like the electron. Consider an atom of deuterium, sometimes known as "heavy hydrogen." It has a nuclear charge of $+e$, just like ordinary hydrogen, but a mass of two units, twice that of ordinary hydrogen. The proton-electron nuclear model would then require that the deuterium *nucleus* contain two protons and one electron, giving a net mass of two units and a net charge of one. Each of these three particles has a spin of $^1/_2$, and the rules for adding angular momenta in quantum mechanics would lead to a spin of deuterium of either $^1/_2$ or $^3/_2$. However, the measured total spin of deuterium is 1. For these and other reasons, the hypothesis that electrons are a nuclear constituent must be discarded.

The resolution of this dilemma came in 1932 with the discovery of the *neutron*, a particle of roughly the same mass as the proton (actually about 0.1% more massive) but having no electric charge. According to the *proton-neutron* model, a nucleus consists of Z protons and $(A - Z)$ neutrons, giving a total charge of Ze and a total mass of roughly A times the mass of the proton, because the proton and neutron masses are roughly the same.

The proton and neutron are, except for their electric charges, very similar to one another, and so they are classified together as *nucleons.* Some properties of the two nucleons are listed in Table 12.1.

The chemical properties of any element depend on its atomic number Z, but not on its mass number A. It is possible to have two different nuclei with the same Z but with different A (that is, with the same number of protons but different numbers of neutrons). Atoms of these nuclei are identical in all their chemical properties, differing only in mass and in those properties that depend on mass. Nuclei with the same Z but different A are called *isotopes.* Hydrogen, for example, has three isotopes: ordinary hydrogen ($Z = 1, A = 1$), deuterium ($Z = 1, A = 2$), and tritium ($Z = 1, A = 3$). All of these are indicated by the chemical symbol H. When we discuss nuclear properties it is important to distinguish among the different isotopes. We do this by indicating, along with the chemical symbol, the atomic number Z, the mass number A, and the *neutron number* $N = A - Z$ in the following format:

$$^A_Z X_N$$

where X is any chemical symbol. The chemical symbol and the atomic number Z give the same information, so it is not necessary to include both of them in the isotope label. Also, if we specify Z then we don't need to specify *both* N and

TABLE 12.1 Properties of the Nucleons

Name	Symbol	Charge	Mass	Rest Energy	Spin
Proton	p	$+e$	1.007276 u	938.28 MeV	$^1/_2$
Neutron	n	0	1.008665 u	939.57 MeV	$^1/_2$

A. It is sufficient to give only the chemical symbol and A. The three isotopes of hydrogen would be indicated as ${}_1^1H_0$, ${}_1^2H_1$, and ${}_1^3H_2$, or more compactly as ${}^1H$, ${}^2H$, and ${}^3H$. In Appendix D you will find a list of isotopes and some of their properties.

Example 12.1

Give the symbol for the following: (*a*) the isotope of helium with mass number 4; (*b*) the isotope of tin with 66 neutrons; (*c*) an isotope with mass number 235 that contains 143 neutrons.

Solution

(*a*) From the periodic table, we find that helium has $Z = 2$. With $A = 4$, we have $N = A - Z = 2$. Thus the symbol would be ${}_2^4He_2$ or ${}^4He$.

(*b*) Again from the periodic table, we know that for tin (Sn), $Z = 50$. We are given $N = 66$, so $A = Z + N = 116$. The symbol is ${}_{50}^{116}Sn_{66}$ or ${}^{116}Sn$.

(*c*) Given that $A = 235$ and $N = 143$, we know that $Z = A - N = 92$. From the periodic table, we find that this element is uranium, and so the proper symbol for this isotope is ${}_{92}^{235}U_{143}$ or ${}^{235}U$.

12.2 NUCLEAR SIZES AND SHAPES

Like atoms, nuclei lack a hard surface or an easily definable radius. In fact, different types of experiments can often reveal different values of the radius for the same nucleus.

From a variety of experiments, we know some general features of the nuclear density. Its variation with the nuclear radius is shown in Figure 12.1. Because the nuclear force is the strongest of the forces, we might expect that this strong force would cause the protons and neutrons to congregate at the center of the nucleus, giving an increasing density in the central region. However, Figure 12.1 shows that this is not the case—the density remains quite uniform. This gives some important clues about the short range of the nuclear force, as we discuss in Section 12.4.

Another interesting feature of Figure 12.1 is that the density of a nucleus seems not to depend on the mass number A; very light nuclei, such as ${}^{12}C$, have roughly the same central density as very heavy nuclei, such as ${}^{209}Bi$. Stated another way, the number of protons and neutrons per unit volume is approximately constant over the entire range of nuclei:

$$\frac{\text{number of neutrons and protons}}{\text{volume of nucleus}} = \frac{A}{\frac{4}{3}\pi R^3} \cong \text{constant}$$

assuming the nucleus to be a sphere of radius R. Thus $A \propto R^3$, which suggests a proportionality between the nuclear radius R and the cube root of the mass number: $R \propto A^{1/3}$or, defining a constant of proportionality R_0,

$$R = R_0 A^{1/3} \tag{12.1}$$

The constant R_0 must be determined by experiment, and a typical experiment might be to scatter charged particles (alpha particles or electrons, for example) from the nucleus and to infer the radius of the nucleus from the distribution of scattered particles. From such experiments, we know the value of R_0 is

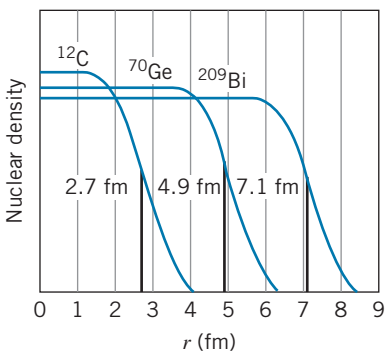

FIGURE 12.1 The radial dependence of the nuclear charge density.

approximately 1.2×10^{-15} m. (The exact value depends, as in the case of atomic physics, on exactly how we define the radius, and values of R_0 usually range from 1.0×10^{-15} m to 1.5×10^{-15} m.) The length 10^{-15} m is 1 femtometer (fm), but physicists often refer to this length as one fermi, in honor of the Italian-American physicist Enrico Fermi.

Example 12.2

Compute the approximate nuclear radius of carbon ($A = 12$), germanium ($A = 70$), and bismuth ($A = 209$).

Solution

Using Eq. 12.1, we obtain:

Carbon: $R = R_0 A^{1/3} = (1.2 \text{ fm})(12)^{1/3} = 2.7 \text{ fm}$

Germanium: $R = R_0 A^{1/3} = (1.2 \text{ fm})(70)^{1/3} = 4.9 \text{ fm}$

Bismuth: $R = R_0 A^{1/3} = (1.2 \text{ fm})(209)^{1/3} = 7.1 \text{ fm}$

As you can see from Figure 12.1, these values define the mean radius, the point at which the density falls to half the central value.

Example 12.3

Compute the density of a typical nucleus, and find the resultant mass if we could produce a nucleus with a radius of 1 cm.

Solution

Making a rough estimate of the nuclear mass m as A times the proton mass, we have

$$\rho = \frac{m}{V} = \frac{Am_p}{\frac{4}{3}\pi R^3} = \frac{Am_p}{\frac{4}{3}\pi R_0^3 A}$$

$$= \frac{1.67 \times 10^{-27} \text{ kg}}{\frac{4}{3}\pi (1.2 \times 10^{-15} \text{ m})^3} = 2 \times 10^{17} \text{ kg/m}^3$$

The mass of a hypothetical nucleus with a 1-cm radius would be

$$m = \rho V = \rho(\tfrac{4}{3}\pi R^3)$$
$$= (2 \times 10^{17} \text{ kg/m}^3)(\tfrac{4}{3}\pi)(0.01 \text{ m})^3$$
$$= 8 \times 10^{11} \text{ kg}$$

about the mass of a 1-km sphere of ordinary matter!

The result of Example 12.3 shows the great density of what physicists call *nuclear matter*. Although examples of such nuclear matter in bulk are not found on Earth (a sample of nuclear matter the size of a large building would have a mass as great as that of the entire Earth), they are found in certain massive stars, in which the gravitational force causes protons and electrons to merge into neutrons, creating a neutron star (see Section 10.7) that is in effect a giant atomic nucleus!

One way of measuring the size of a nucleus is to scatter charged particles, such as alpha particles, as in Rutherford scattering experiments. As long as the alpha particle is outside the nucleus, the Rutherford scattering formula holds, but when the distance of closest approach is less than the nuclear radius, deviations from the Rutherford formula occur. Figure 12.2 shows the results of a Rutherford scattering experiment in which such deviations are observed. (Problem 33 suggests how a value for the nuclear radius can be inferred from these data.)

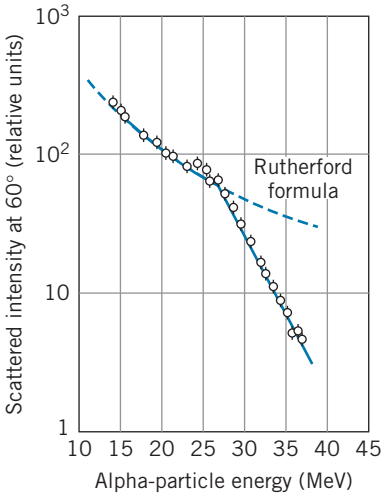

FIGURE 12.2 Deviations from the Rutherford formula in scattering from ^{208}Pb are observed for alpha-particle energies above 27 MeV.

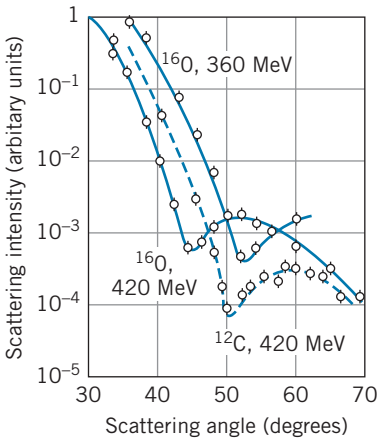

FIGURE 12.3 Diffraction of 360-MeV and 420-MeV electrons by ^{12}C and ^{16}O nuclei.

Other scattering experiments can also be used to measure the nuclear radius. Figure 12.3 shows a sort of "diffraction pattern" that results from the scattering of energetic electrons by a nucleus. In each case the first diffraction minimum is clearly visible. (The intensity at the minimum doesn't fall to zero because the nuclear density doesn't have a sharp edge, as illustrated in Figure 12.1.) For scattering of radiation of wavelength λ by a circular disc of diameter D, the first diffraction minimum should appear at an angle of $\theta = \sin^{-1}(1.22\lambda/D)$. (Review Example 4.2 for another example of this calculation.) At an electron energy of 420 MeV, the observed minima for ^{16}O and ^{12}C give a radius of 2.6 fm for ^{16}O and 2.3 fm for ^{12}C (see Problem 34), in agreement with the values 3.0 fm and 2.7 fm computed from Equation 12.1.

12.3 NUCLEAR MASSES AND BINDING ENERGIES

Suppose we have a proton and an electron at rest separated by a large distance. The total energy of this system is the total rest energy of the two particles, $m_p c^2 + m_e c^2$. Now we let the two particles come together to form a hydrogen atom in its ground state. In the process, several photons are emitted, the *total* energy of which is 13.6 eV. The total energy of this system is the rest energy of the hydrogen atom, $m(\mathrm{H})c^2$, plus the total photon energy, 13.6 eV. Conservation of energy demands that the total energy of the system of isolated particles must equal the total energy of atom plus photons: $m_e c^2 + m_p c^2 = m(\mathrm{H})c^2 + 13.6\,\mathrm{eV}$, which we write as

$$m_e c^2 + m_p c^2 - m(\mathrm{H})c^2 = 13.6\,\mathrm{eV}$$

That is, the rest energy of the combined system (the hydrogen atom) is less than the rest energy of its constituents (an electron and a proton) by 13.6 eV. This energy difference is the *binding energy* of the atom. We can regard the binding energy as either the "extra" energy we obtain when we assemble an atom from its components or else the energy we must supply to disassemble the atom into its components.

Nuclear binding energies are calculated in a similar way. Consider, for example, the nucleus of deuterium, ${}_1^2\mathrm{H}_1$, which is composed of one proton and one neutron. The nuclear binding energy of deuterium is the difference between the total rest energy of the constituents and the rest energy of their combination:

$$B = m_\mathrm{n}c^2 + m_\mathrm{p}c^2 - m_\mathrm{D}c^2 \tag{12.2}$$

where m_D is the mass of the deuterium nucleus. To finish the calculation, we replace the nuclear masses m_p and m_D with the corresponding *atomic* masses: $m({}^1\mathrm{H})c^2 = m_\mathrm{p}c^2 + m_\mathrm{e}c^2 - 13.6\,\mathrm{eV}$ and $m({}^2\mathrm{H})c^2 = m_\mathrm{D}c^2 + m_\mathrm{e}c^2 - 13.6\,\mathrm{eV}$. Substituting into Eq. 12.2, we obtain

$$\begin{aligned} B &= m_\mathrm{n}c^2 + [m({}^1\mathrm{H})c^2 - m_\mathrm{e}c^2 + 13.6\,\mathrm{eV}] - [m({}^2\mathrm{H})c^2 - m_\mathrm{e}c^2 + 13.6\,\mathrm{eV}] \\ &= [m_\mathrm{n} + m({}^1\mathrm{H}) - m({}^2\mathrm{H})]c^2 \end{aligned}$$

Notice that the electron mass cancels in this calculation. For deuterium, we then have

$$B = (1.008665\ \mathrm{u} + 1.007825\ \mathrm{u} - 2.014102\ \mathrm{u})(931.5\,\mathrm{MeV/u}) = 2.224\,\mathrm{MeV}$$

Here we use $c^2 = 931.5\,\mathrm{MeV/u}$ to convert mass units to energy units.

Let's generalize this process to calculate the binding energy of a nucleus X of mass number A with Z protons and N neutrons. Let m_X represent the mass of this nucleus. Then the binding energy of the nucleus is, by analogy with Eq. 12.2, the difference between the nuclear rest energy and the total rest energy of its constituents (N neutrons and Z protons):

$$B = Nm_\mathrm{n}c^2 + Zm_\mathrm{p}c^2 - m_\mathrm{X}c^2 \tag{12.3}$$

In order to use tabulated atomic masses to do this calculation, we must replace the nuclear mass m_X with its corresponding atomic mass: $m({}_Z^A\mathrm{X}_N)c^2 = m_\mathrm{X}c^2 + Zm_\mathrm{e}c^2 - B_\mathrm{e}$, where B_e represents the total binding energy of all the electrons in this atom. Nuclear rest energies are of the order of 10^9 to 10^{11} eV, total electron rest energies are of the order of 10^6 to 10^8 eV, and electron binding energies are of the order of 1 to 10^5 eV. Thus B_e is very small compared with the other two terms, and we can safely neglect it to the accuracy we need for these calculations.

Substituting atomic masses for the nuclear masses m_p and m_X, we obtain an expression for the total binding energy of any nucleus ${}_Z^A\mathrm{X}_N$:

$$B = [Nm_\mathrm{n} + Zm({}_1^1\mathrm{H}_0) - m({}_Z^A\mathrm{X}_N)]c^2 \tag{12.4}$$

The electron masses cancel in this equation, because on the right side we have the difference between the mass of Z hydrogen atoms (with a total of Z electrons) and the atom of atomic number Z (also with Z electrons). The masses that appear in Eq. 12.4 are *atomic* masses.

Example 12.4

Find the total binding energy B and also the average binding energy per nucleon B/A for $^{56}_{26}\mathrm{Fe}_{30}$ and $^{238}_{92}\mathrm{U}_{146}$.

Solution

From Eq. 12.4, for $^{56}_{26}\mathrm{Fe}_{30}$ with $N = 30$ and $Z = 26$,

$$B = [30(1.008665\,\mathrm{u}) + 26(1.007825\,\mathrm{u}) - 55.934937\,\mathrm{u}](931.5\,\mathrm{MeV/u})$$
$$= 492.3\,\mathrm{MeV}$$
$$\frac{B}{A} = \frac{492.3\,\mathrm{MeV}}{56} = 8.790\,\mathrm{MeV\ per\ nucleon}$$

For $^{238}_{92}\mathrm{U}_{146}$,

$$B = [146(1.008665\,\mathrm{u}) + 92(1.007825\,\mathrm{u}) - 238.050788\,\mathrm{u}](931.5\,\mathrm{MeV/u})$$
$$= 1802\,\mathrm{MeV}$$
$$\frac{B}{A} = \frac{1802\,\mathrm{MeV}}{238} = 7.570\,\mathrm{MeV\ per\ nucleon}$$

Example 12.4 gives us insight into an important aspect of nuclear structure. The values of B/A show that the nucleus ^{56}Fe is *relatively* more tightly bound than the nucleus ^{238}U; the average binding energy *per nucleon* is greater for ^{56}Fe than for ^{238}U. Alternatively, this calculation shows that, given a large supply of protons and neutrons, we would release more energy by assembling those nucleons into nuclei of ^{56}Fe than we would by assembling them into nuclei of ^{238}U.

Repeating this calculation for the entire range of nuclei, we obtain the results shown in Figure 12.4. The binding energy per nucleon starts at small values

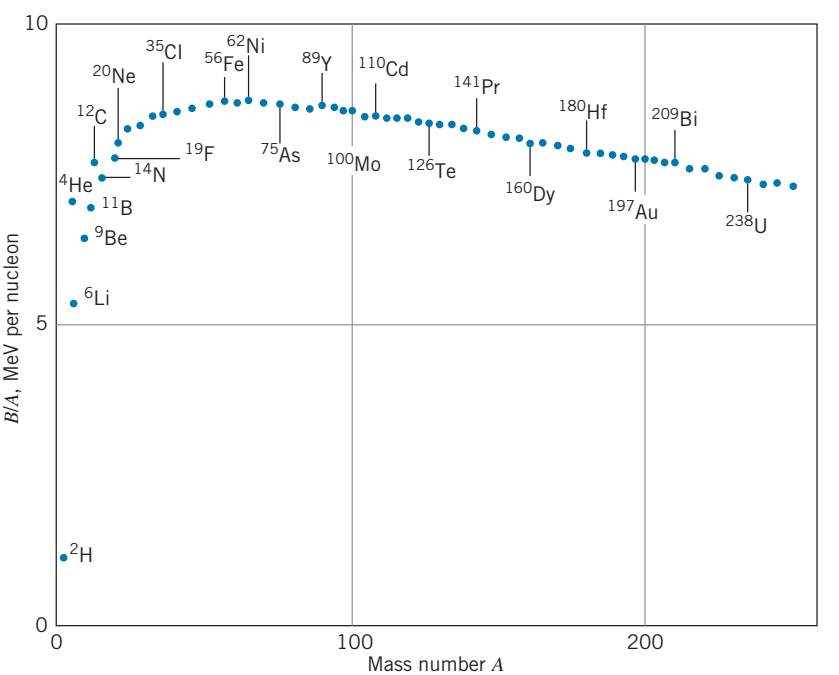

FIGURE 12.4 The binding energy per nucleon.

(0 for the proton and neutron, 1.11 MeV for deuterium), rises to a maximum of 8.795 MeV for ^{62}Ni, and then falls to values of around 7.5 MeV for the heavy nuclei.

The binding energy per nucleon is roughly constant over a fairly wide range of nuclei. From the region around $A = 60$ there is a sharp decrease for light nuclei, which is caused by their having an increasing relative fraction of loosely bound protons and neutrons on the surface. There is a gradual decrease for the more massive nuclei, due to the increasing Coulomb repulsion of the protons.

Figure 12.4 suggests that we can liberate energy from the nucleus in two different ways. If we split a massive nucleus (say, $A > 200$) into two lighter nuclei, energy is released, because the binding energy per nucleon is greater for the two lighter fragments than it is for the original nucleus. This process is known as *nuclear fission.* Alternatively, we could combine two light nuclei ($A < 10$, for example) into a more massive nucleus; again, energy is released when the binding energy per nucleon is greater in the final nucleus than it is in the two original nuclei. This process is known as *nuclear fusion*. We consider fission and fusion in greater detail in Chapter 13.

Proton and Neutron Separation Energies

If we add the ionization energy E_i (13.6 eV) to a hydrogen atom, we obtain a hydrogen ion H^+ and a free electron. In terms of the rest energies of the particles, we can write this process as $E_i + m(H)c^2 = m(H^+)c^2 + m_e c^2$. If we generalize to an arbitrary element X, this becomes $E_i + m(X)c^2 = m(X^+)c^2 + m_e c^2$, or

$$X \rightarrow X^+ + e^-: \quad E_i = m(X^+)c^2 + m_e c^2 - m(X)c^2 = [m(X^+) + m_e - m(X)]c^2$$

In the case of element X, the ionization energy gives the smallest amount of energy necessary to remove an electron from an atom, and we saw in Figure 8.8 how the ionization energy provides important information about the properties of atoms.

For nuclei, a process similar to ionization consists of removing the least tightly bound proton or neutron from the nucleus. The energy required to remove the least tightly bound proton is called the *proton separation energy* S_p. If we add energy S_p to a nucleus ${}^A_Z X_N$, we obtain the nucleus ${}^{A-1}_{Z-1}X'_N$ and a free proton. In analogy with the atomic case, we can write the separation energy as

$$ {}^A_Z X_N \rightarrow {}^{A-1}_{Z-1}X'_N + p: \qquad S_p = [m({}^{A-1}_{Z-1}X'_N) + m({}^1H) - m({}^A_Z X_N)]c^2 \tag{12.5}$$

using atomic masses. Similarly, if we add the *neutron separation energy* S_n to nucleus ${}^A_Z X_N$, we obtain the nucleus ${}^{A-1}_{Z}X_{N-1}$ and a free neutron:

$$ {}^A_Z X_N \rightarrow {}^{A-1}_{Z}X_{N-1} + n: \qquad S_n = [m({}^{A-1}_{Z}X_{N-1}) + m_n - m({}^A_Z X_N)]c^2 \tag{12.6}$$

Proton and neutron separation energies are typically in the range of 5–10 MeV. It is no coincidence that this energy is about the same as the average binding energy per nucleon. The total binding energy B of a nucleus is the energy needed to take it apart into Z free protons and N free neutrons. This energy is the sum of A proton and neutron separation energies.

Example 12.5

Find the proton separation energy and the neutron separation energy of ^{125}Te.

Solution

To separate a proton, $^{125}\text{Te} \rightarrow {}^{124}\text{Sb} + \text{p}$. Using Eq. 12.5, the proton separation energy is

$$\begin{aligned} S_p &= [m(^{124}\text{Sb}) + m(^{1}\text{H}) - m(^{125}\text{Te})]c^2 \\ &= (123.905936\ \text{u} + 1.007825\ \text{u} \\ &\qquad -124.904431\ \text{u})(931.50\ \text{MeV/u}) \\ &= 8.691\ \text{MeV} \end{aligned}$$

For neutron separation, $^{125}\text{Te} \rightarrow {}^{124}\text{Te} + \text{n}$. The neutron separation energy is (from Eq. 12.6)

$$\begin{aligned} S_n &= [m(^{124}\text{Te}) + m_n - m(^{125}\text{Te})]c^2 \\ &= (123.902818\ \text{u} + 1.008665\ \text{u} \\ &\qquad -124.904431\ \text{u})(931.50\ \text{MeV/u}) \\ &= 6.569\ \text{MeV} \end{aligned}$$

The proton and neutron separation energies play a role in nuclei similar to that of the ionization energy in atoms. Figure 12.5 shows a plot of the neutron separation energies of nuclei with a "valence" neutron (and no valence proton) from $Z = 36$ to $Z = 62$. As we add neutrons, the neutron separation energy decreases smoothly except near $N = 50$ and $N = 82$, where there are more sudden decreases in the separation energy. In analogy with atomic physics (see Figure 8.8), these sudden decreases are associated with the filling of shells. The motions of neutrons and protons in the nucleus are described in terms of a shell structure that is similar to that of atomic shells, and when a neutron or proton is placed into a new shell it is less tightly bound and its separation energy decreases. The neutron separation data indicate that there are closed neutron shells at $N = 50$ and $N = 82$. Relationships such as Figure 12.5 provide important information about the shell structure of nuclei.

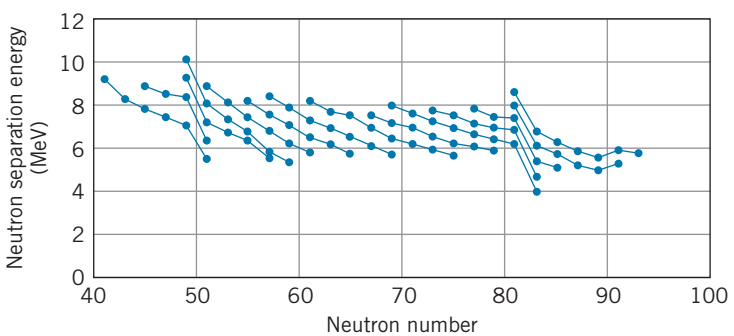

FIGURE 12.5 The neutron separation energy. The lines connect isotopes of the same element that have an odd neutron, starting on the left at $Z = 36$ and ending on the right at $Z = 62$.

12.4 THE NUCLEAR FORCE

Our successful experience with using the simplest atom, hydrogen, to gain insights into atomic structure suggests that we should begin our study of the nuclear force by looking at the simplest system in which that force operates—the deuterium

nucleus, which consists of one proton and one neutron. For example, we might hope to learn something about the nuclear force from the photons emitted in transitions between the excited states of this nucleus. Unfortunately, this strategy does not work—deuterium has *no nuclear excited states.* When we bring a proton and an electron together to form a hydrogen atom, many photons may be emitted as the electron drops into its ground state; from this spectrum we learn the energies of the excited states. When we bring a proton and a neutron together to form a deuterium nucleus, only one photon (of energy 2.224 MeV) is emitted as the system drops directly into its ground state.

Even though we can't use the excited states of deuterium, we can learn about the nuclear force in the proton-neutron system by scattering neutrons from protons as well as by doing a variety of different experiments with heavier nuclei. From these experiments we have learned the following characteristics of the nuclear force:

1. The nuclear force is the strongest of the known forces, and so it is sometimes called the *strong* force. For two adjacent protons in a nucleus, the nuclear interaction is 10–100 times stronger than the electromagnetic interaction.
2. The strong nuclear force has a very short range—the distance over which the force acts is limited to about 10^{-15} m. This conclusion follows from the constant central density of nuclear matter (Figure 12.1). As we add nucleons to a nucleus, each added nucleon feels a force only from its nearest neighbors, and *not* from all the other nucleons in the nucleus. In this respect, a nucleus behaves somewhat like a crystal, in which each atom interacts primarily with its nearest neighbors, and additional atoms make the crystal larger but don't change its density. Another piece of evidence for the short range comes from Figure 12.4. Because the binding energy per nucleon is roughly constant, total nuclear binding energies are roughly proportional to A. For a force with long range (such as the gravitational and electrostatic forces, which have infinite range) the binding energy is roughly proportional to the square of the number of interacting particles. (For example, because each of the Z protons in a nucleus feels the repulsion of the other $Z - 1$ protons, the total electrostatic energy of the nucleus is proportional to $Z(Z - 1)$, which is roughly Z^2 for large Z.)

   Figure 12.6 illustrates the dependence of the nuclear binding energy on the separation distance between the nucleons. The binding energy is relatively constant for separation distances less than about 1 fm, and it is zero for separation distances much greater than 1 fm.
3. The nuclear force between any two nucleons does not depend on whether the nucleons are protons or neutron—the n-p nuclear force is the same as the n-n nuclear force, which is in turn the same as the nuclear portion of the p-p force.

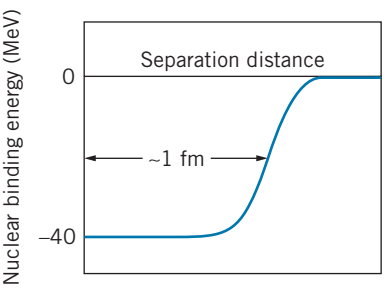

FIGURE 12.6 Dependence of nuclear binding energy on the separation distance of nucleons.

A successful model for the origin of this short-range force is the *exchange force.* Suppose we have a neutron and a proton next to one another in the nucleus. The neutron emits a particle, on which it exerts a strong attractive force. The proton also exerts a strong force on the particle, perhaps strong enough to absorb the particle. The proton then emits a particle that can be absorbed by the neutron. The proton and neutron each exert a strong force on the exchanged particle, and thus they appear to exert a strong force on each other. The situation is similar to that shown in Figure 12.7, in which two people play catch with a ball to which each is attached by a spring. Each player exerts a force on the ball, and the effect is as if each exerted a force on the other.

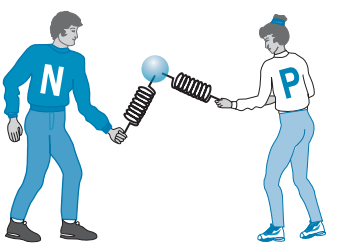

FIGURE 12.7 An attractive exchange force.

How can a neutron of rest energy $m_n c^2$ emit a particle of rest energy mc^2 and still remain a neutron, without violating conservation of energy? The answer to this question can be found from the uncertainty principle, $\Delta E \Delta t \sim \hbar$.

We don't know that energy has been conserved unless we measure it, and we can't measure it more accurately than the uncertainty ΔE in a time interval Δt. We can therefore "violate" energy conservation by an amount ΔE for a time interval of at most $\Delta t = \hbar/\Delta E$. The amount by which energy conservation is violated in our exchange force model is mc^2, the rest energy of the exchanged particle. This particle can thus exist only for a time interval (in the laboratory frame) of at most

$$\Delta t = \frac{\hbar}{mc^2} \tag{12.7}$$

The longest distance this particle can possibly travel in the time Δt is $x = c\Delta t$, since it can't move faster than the speed of light. With $x = c\Delta t = c\hbar/mc^2$, we then have a relationship between the maximum range of the exchange force and the rest energy of the exchanged particle:

$$mc^2 = \frac{\hbar c}{x} \tag{12.8}$$

Inserting into this expression an estimate for the range of the nuclear force of 10^{-15} m or 1 fm, we can estimate the rest energy of the exchanged particle:

$$mc^2 = \frac{\hbar c}{x} = \frac{200\,\text{MeV} \cdot \text{fm}}{1\,\text{fm}} = 200\,\text{MeV}$$

The exchanged particle cannot be observed in the laboratory during the exchange, for to do so would violate energy conservation. However, if we provide energy to the nucleons from an external source (for example, by causing a nucleus to absorb a photon), the "borrowed" energy can be repaid and the particle can be observed. When we carry out this experiment, the nucleus is found to emit pi mesons (pions), which have a rest energy of 140 MeV, remarkably close to our estimate of 200 MeV. Many observable properties of the nuclear force have been successfully explained by a model based on the exchange of pions. We discuss the properties of pions in Chapter 14. Other exchanged particles contribute to different aspects of the nuclear force. For example, an exchanged particle is responsible for the repulsive part of the force at very short range, which keeps the nucleons from all collapsing toward the center of the nucleus (see Problem 10).

12.5 QUANTUM STATES IN NUCLEI

Ideally we would like to solve the Schrödinger equation using the nuclear potential energy. This process, if it were possible, would give us a set of energy levels for the protons and neutrons that we could then compare with experiment (just as we did for the energy levels of electrons in atoms). Unfortunately, we cannot carry through with this program for several reasons: the nuclear potential energy cannot be expressed in a convenient analytical form, and it is not possible to solve the nuclear many-body problem except by approximation.

Nevertheless, we can make some simplifications that allow us to analyze the structure and properties of nuclei by using techniques already introduced in this

book. We'll represent the nuclear potential energy as a finite potential well of radius R equal to the nuclear radius. That confines the nucleons to a nucleus-sized region and allows them to move freely inside that region.

Let's consider ^{125}Te (a nucleus very close to the center of the range of nuclei), which we analyzed in Example 12.5. The width of the potential energy well is equal to the nuclear radius, which we find from Eq. 12.1: $R = (1.2\text{ fm})(125)^{1/3} = 6.0\text{ fm}$. The second quantity we need to know is the depth of the potential energy well. We'll consider the neutrons and protons separately. The 73 neutrons in ^{125}Te will fill a series of energy levels in the potential energy well. The top of the well is at $E = 0$ (above which the neutrons would become free). The bottom of the well is at a negative energy $-U_0$. The neutrons fill the levels in the well starting at $-U_0$ and ending *not* at energy zero but at energy -6.6 MeV, as we found in Example 12.5. That is, we must add a minimum of 6.6 MeV to raise the least tightly bound neutron out of the well and turn it into a free neutron.

To find the energy difference between the bottom of the well and the highest filled state, we can consider the nucleus to be a "gas" of neutrons and protons whose energies are described by the Fermi-Dirac distribution (Chapter 10). A statistical distribution is intended to describe systems with large numbers of particles, but it should be a reasonable rough approximation for our "gas" of 73 neutrons. To find the energy of the highest filled state, we need the Fermi energy of the neutrons (using Eq. 10.50 with $V = \frac{4}{3}\pi R^3 = 900\text{ fm}^3$ as the volume of the ^{125}Te nucleus):

$$E_F = \frac{h^2}{2m}\left(\frac{3N}{8\pi V}\right)^{2/3} = \frac{h^2c^2}{2mc^2}\left(\frac{3N}{8\pi V}\right)^{2/3}$$
$$= \frac{(1240\text{ MeV}\cdot\text{ fm})^2}{2(940\text{ MeV})}\left[\frac{3(73)}{8\pi(900\text{ fm}^3)}\right]^{2/3} = 37.0\text{ MeV}$$

Figure 12.8 shows the resulting potential energy well for neutrons. The depth of the well is the sum of the neutron separation energy S_n and the Fermi energy: $U_0 = S_n + E_F = 6.6\text{ MeV} + 37.0\text{ MeV} = 43.6\text{ MeV}$.

A similar calculation for the 52 protons in ^{125}Te gives $E_F = 29.5\text{ MeV}$. For the protons, $S_p + E_F = 8.7\text{ MeV} + 29.5\text{ MeV} = 38.2\text{ MeV}$, much less than the depth we determined for the neutron well. The difference between the depths of the neutron and proton wells is due to the Coulomb repulsion energy of the protons, which makes the protons less tightly bound than the neutrons. Figure 12.9 gives a representation of the proton states in their potential energy well.

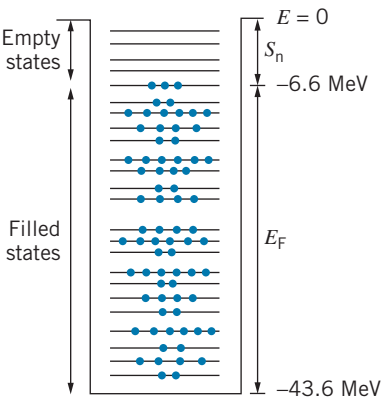

FIGURE 12.8 Neutron states in a potential energy well for the 73 neutrons of ^{125}Te.

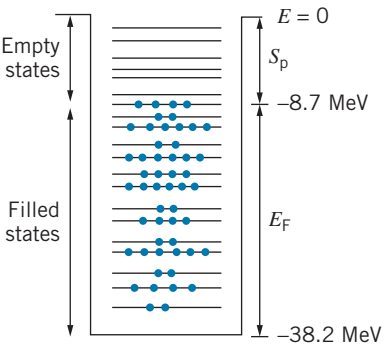

FIGURE 12.9 Proton states in a potential energy well for the 52 protons of ^{125}Te.

Quantum States and Radioactive Decay

Figure 12.10 shows the protons and neutrons near the top of their potential energy wells. Note that we can add energy to the nucleus that is less than the proton or neutron separation energies. In the region between $E = -S_n$ or $-S_p$ and $E = 0$ are the nuclear excited states in which a proton or a neutron can absorb energy and move from its ground state to one of the unoccupied higher states. As was the case with atoms, the nucleus can make transitions from excited states to lower excited states or to the ground state by photon emission. In the case of nuclei, those photons are called *gamma rays* and have typical energies of 0.1 MeV to a few MeV.

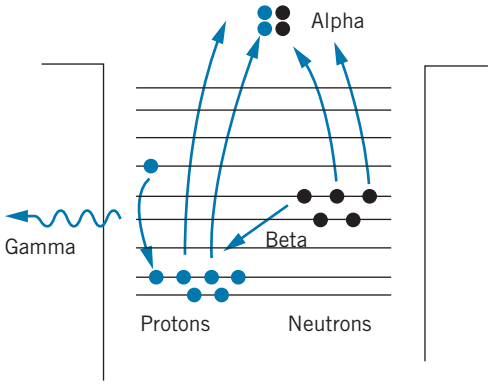

FIGURE 12.10 Proton and neutron states near the top of the well for ^{125}Te. Alpha decay is represented by two protons and two neutrons being boosted from negative energy bound states to positive energy free states and forming an alpha particle. Beta decay is represented by a neutron transforming into a proton. Gamma decay can occur among the empty states above the highest occupied proton and neutron states.

It is also possible to have other nuclear transformations that can be represented in Figure 12.10. It is clearly not possible for this nucleus spontaneously to emit a proton or a neutron—we have seen that it takes many MeV to boost a bound proton or neutron to a free state. However, it is possible simultaneously to boost *two* protons and *two* neutrons and form them into an alpha particle ($^4_2\text{He}_2$). If the energy gained in the formation of the alpha particle (its binding energy, 28.3 MeV) is greater than the sum of the four separation energies, there will be a net energy gain in the process; this energy can appear as the kinetic energy of the alpha particle that is emitted by the nucleus. This process is called *nuclear alpha decay*. You can see from the neutron and proton separation energies that this process does not occur for ^{125}Te.

Another type of transformation occurs under certain circumstances when a neutron changes into a proton and drops into one of the empty proton states at lower energy. Under other circumstances, in which the proton levels are higher and the neutron levels are lower, a proton can transform into a neutron and drop into one of the empty neutron states. This process is called *nuclear beta decay*. It is not always obvious from diagrams such as Figure 12.10 whether this type of transformation will occur, because changing a neutron to a proton increases the net Coulomb energy of the nucleus and thus increases the energy of all of the proton states. Neither the neutron-to-proton nor the proton-to-neutron transformation can occur for ^{125}Te.

12.6 RADIOACTIVE DECAY

Figure 12.11 shows a plot of all the known nuclei, with stable nuclei indicated by dark shading. For the lighter stable nuclei, the neutron and proton numbers are roughly equal. However, for the heavy stable nuclei, the factor $Z(Z-1)$ in the Coulomb repulsion energy grows rapidly, so extra neutrons are required to supply the additional binding energy needed for stability. For this reason, all heavy stable nuclei have $N > Z$.

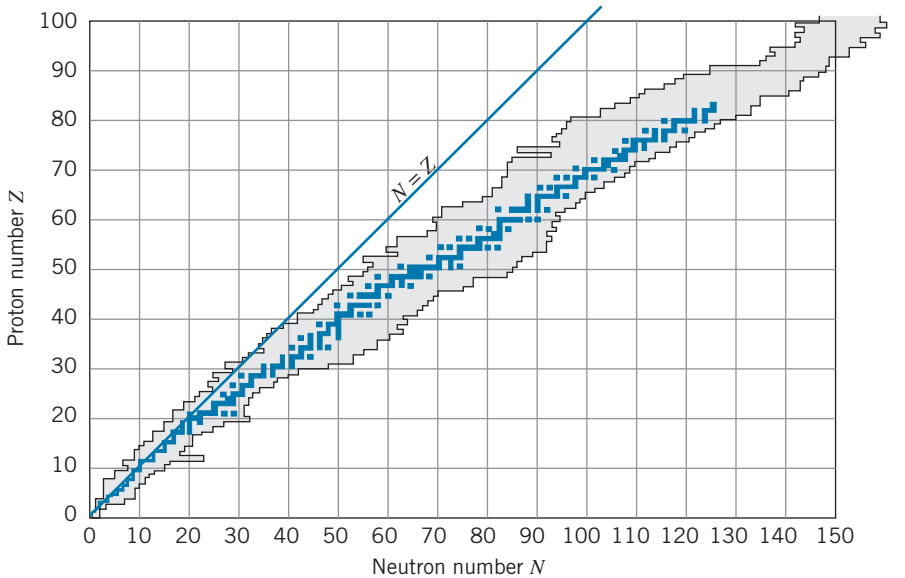

FIGURE 12.11 Stable nuclei are shown in color; known radioactive nuclei are in light shading.

Most of the nuclei represented in Figure 12.11 are unstable, which means that they transform themselves into more stable nuclei by changing their Z and N through *alpha decay* (emission of ^{4}He) or *beta decay* (changing a neutron to a proton or a proton to a neutron). Nuclei are unstable in excited states, which can transition to ground states through *gamma decay* (emission of photons). The three decay processes (alpha, beta, and gamma decay) are examples of the general subject of *radioactive decay.* In the remainder of this section, we establish some of the basic properties of radioactive decay, and in the following sections we treat alpha, beta, and gamma decay separately.

The rate at which unstable radioactive nuclei decay in a sample of material is called the *activity* of the sample. The greater the activity, the more nuclear decays per second. (The activity has nothing to do with the *kind* of decays or of radiations emitted by the sample, or with the *energy* of the emitted radiations. The activity is determined only by the *number* of decays per second.)

The basic unit for measuring activity is the *curie*.* Originally, the curie was defined as the activity of one gram of radium; that definition has since been replaced by a more convenient one:

$$1 \text{ curie (Ci)} = 3.7 \times 10^{10} \text{ decays/s}$$

One curie is quite a large activity, and so we work more often with units of millicurie (mCi), equal to 10^{-3} Ci, and microcurie (μCi), equal to 10^{-6} Ci.

*The SI unit of activity is the becquerel (Bq), named for Henri Becquerel, the French scientist who discovered radioactivity in 1896. One becquerel equals one decay/s, so 1 Ci = 3.7×10^{10}Bq.

Marie Curie (1867–1934, Poland-France). Her pioneering studies of the natural radioactivity of radium and other elements earned her two Nobel Prizes, the physics prize in 1903 for the discovery of radioactivity (shared with Henri Becquerel and with her husband, Pierre) and the unshared chemistry prize in 1911 for the isolation of pure radium. She established the Institute of Radium at the University of Paris, where she continued to pursue research in the medical applications of radioactive materials. Her daughter Irene was awarded the 1935 Nobel Prize in chemistry for the discovery of artificial radioactivity.

Consider a sample with a mass of a few grams, containing the order of 10^{23} atoms. If the activity were as large as 1 Ci, about 10^{10} of the nuclei in the sample would decay every second. We could also say that for any one nucleus, the probability of decaying during each second is about $10^{10}/10^{23}$ or 10^{-13}. This quantity, the decay probability per nucleus per second, is called the *decay constant* (represented by the symbol λ). We assume that λ is a small number, and that it is constant in time for any particular material—the probability of any one nucleus decaying doesn't depend on the age of the sample. The activity a depends on the number N of radioactive nuclei in the sample and also on the probability λ for each nucleus to decay:

$$a = \lambda N \tag{12.9}$$

which is equivalent to decays/s = decays/s per nucleus $\times$ number of nuclei.

Both a and N are functions of the time t. As our sample decays, N certainly decreases—there are fewer radioactive nuclei left. If N decreases and λ is constant, then a must also decrease with time, and so the number of decays per second becomes smaller with increasing time.

We can regard a as the change in the number of radioactive nuclei per unit time—the more nuclei decay per second, the larger is a.

$$a = -\frac{dN}{dt} \tag{12.10}$$

A minus sign must be present because dN/dt is negative (N is decreasing with time), and we want a to be a positive number.) Combining Eqs. 12.9 and 12.10 we have $dN/dt = -\lambda N$, or

$$\frac{dN}{N} = -\lambda\, dt \tag{12.11}$$

This equation can be integrated directly to yield

$$N = N_0 e^{-\lambda t} \tag{12.12}$$

where N_0 represents the number of radioactive nuclei originally present at $t = 0$. Equation 12.12 is the *exponential law of radioactive decay*, which tells us how the number of radioactive nuclei in a sample decreases with time. We can't easily measure N, but we can put this equation in a more useful form by multiplying on both sides by λ, which gives

$$a = a_0 e^{-\lambda t} \tag{12.13}$$

where a_0 is the original activity ($a_0 = \lambda N_0$).

Suppose we count the number of decays of our sample in one second (by counting for one second the radiations resulting from the decays). Repeating the measurement, we could then plot the activity a as a function of time, as shown in Figure 12.12. This plot shows the exponential dependence expected on the basis of Eq. 12.13.

It is often more useful to plot a as a function of t on a semilogarithmic scale, as shown in Figure 12.13. On this kind of plot, Eq. 12.13 gives a straight line of slope $-\lambda$.

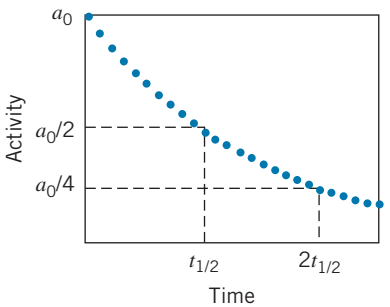

FIGURE 12.12 Activity of a radioactive sample as a function of time.

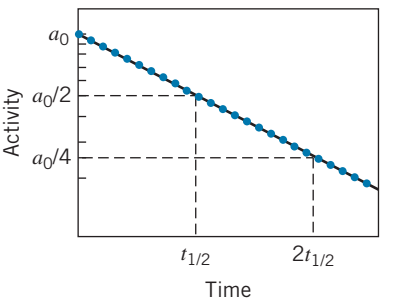

FIGURE 12.13 Semilog plot of activity versus time.

The *half-life*, $t_{1/2}$, of the decay is the time that it takes for the activity to be reduced by half, as shown in Figure 12.12. That is, when $t = t_{1/2}, a = \frac{1}{2}a_0 = a_0 e^{-\lambda t_{1/2}}$, from which we find

$$t_{1/2} = \frac{1}{\lambda} \ln 2 = \frac{0.693}{\lambda} \tag{12.14}$$

Another useful parameter is the *mean lifetime* τ (see Problem 37):

$$\tau = \frac{1}{\lambda} \tag{12.15}$$

When $t = \tau, a = a_0 e^{-1} = 0.37 a_0$.

Example 12.6

The half-life of ^{198}Au is 2.70 days. (*a*) What is the decay constant of ^{198}Au? (*b*) What is the probability that any ^{198}Au nucleus will decay in one second? (*c*) Suppose we had a 1.00-μg sample of ^{198}Au. What is its activity? (*d*) How many decays per second occur when the sample is one week old?

Solution

(*a*)

$$\lambda = \frac{0.693}{t_{1/2}} = \frac{0.693}{2.70 \text{ d}} \frac{1 \text{ d}}{24 \text{ h}} \frac{1 \text{ h}}{3600 \text{ s}}$$

$$= 2.97 \times 10^{-6} \text{ s}^{-1}$$

(*b*) The decay probability per second is just the decay constant, so the probability of any ^{198}Au nucleus decaying in one second is 2.97×10^{-6}.

(*c*) The number of atoms in the sample is determined from the Avogadro constant N_A and the molar mass M:

$$N = \frac{mN_A}{M}$$

$$= \frac{(1.00 \times 10^{-6} \text{ g})(6.02 \times 10^{23} \text{ atoms/mole})}{198 \text{ g/mole}}$$

$$= 3.04 \times 10^{15} \text{ atoms}$$

$$a = \lambda N = (2.97 \times 10^{-6} \text{ s}^{-1})(3.04 \times 10^{15})$$

$$= 9.03 \times 10^{9} \text{ Bq} = 0.244 \text{ Ci}$$

(*d*) The activity decays according to Eq. 12.13:

$$a = a_0 e^{-\lambda t}$$

$$= (9.03 \times 10^{9} \text{ Bq}) e^{-(2.97 \times 10^{-6} \text{ s}^{-1})(7 \text{ d})(3600 \text{ s/d})}$$

$$= 1.50 \times 10^{9} \text{ Bq}$$

Example 12.7

The half-life of ^{235}U is 7.04×10^8 y. A sample of rock, which solidified with the Earth 4.55×10^9 years ago, contains N atoms of ^{235}U. How many ^{235}U atoms did the same rock have at the time it solidified?

Solution

The age of the rock corresponds to

$$\frac{4.55 \times 10^9 \text{ y}}{7.04 \times 10^8 \text{ y}} = 6.46 \text{ half-lives}$$

Each half-life reduces N by a factor of 2, so the overall reduction in N has been $2^{6.46} = 88.2$. The original rock therefore contained $88.2N$ atoms of ^{235}U.

Conservation Laws in Radioactive Decays

Our study of radioactive decays and nuclear reactions reveals that nature is not arbitrary in selecting the outcome of decays or reactions, but rather that certain laws limit the possible outcomes. We call these laws *conservation laws*, and we believe these laws give us important insight into the fundamental workings of nature. Several of these conservation laws are applied to radioactive decay processes.

1. Conservation of Energy Perhaps the most important of the conservation laws, conservation of energy tells us which decays are energetically possible and enables us to calculate rest energies or kinetic energies of decay products. A nucleus X will decay into a lighter nucleus X′, with the emission of one or more particles we call collectively x only if the rest energy of X is greater than the total rest energy of X′ + x The excess rest energy is known as the *Q value* of the decay $X \rightarrow X' + x$:

$$Q = [m_X - (m_{X'} + m_x)]c^2 \tag{12.16}$$

where the m's represent the *nuclear masses.* The decay is possible only if this Q value is positive. The excess energy Q appears as kinetic energy of the decay products (assuming X is initially at rest):

$$Q = K_{X'} + K_x \tag{12.17}$$

2. Conservation of Linear Momentum If the initially decaying nucleus is at rest, then the total linear momentum of all of the decay products must sum to zero:

$$\vec{\mathbf{p}}_{X'} + \vec{\mathbf{p}}_x = 0 \tag{12.18}$$

Usually the emitted particle or particles x are much less massive than the residual nucleus X′, and the *recoil momentum* $p_{X'}$ yields a very small kinetic energy $K_{X'}$.

If there is only one emitted particle x, Eqs. 12.17 and 12.18 can be solved simultaneously for $K_{X'}$ and K_x. If x represents two or more particles, we have more unknowns than we have equations, and no unique solution is possible. In this case, a range of values from some minimum to some maximum is permitted for the decay products.

3. Conservation of Angular Momentum The total spin angular momentum of the initial particle before the decay must equal the total angular momentum (spin plus orbital) of all of the product particles after the decay. For example, the decay of a neutron (spin angular momentum = $\frac{1}{2}$) into a proton plus an electron is forbidden by conservation of angular momentum, because the spins of the proton and electron, each equal to $\frac{1}{2}$, can be combined to give a total of either 0 or 1, neither of which is equal to the initial angular momentum of the neutron. Adding integer units of orbital angular momentum to the electron does not restore angular momentum conservation in this decay process.

4. Conservation of Electric Charge This is such a fundamental part of all decay and reaction processes that it hardly needs elaborating. The total net electric charge before the decay must equal the net electric charge after the decay.

5. Conservation of Nucleon Number In some decay processes, we can create particles (photons or electrons, for example) which did not exist before the decay occurred. (This of course must be done out of the available energy—that is, it takes 0.511 MeV of energy to create an electron.) However, nature does *not* permit us to create or destroy protons and neutrons, although in certain decay processes we can convert neutrons into protons or protons into neutrons. *The total nucleon number A does not change in decay or reaction processes.* In some decay processes, A remains constant because both Z and N remain unchanged; in other processes Z and N both change in such a way as to keep their sum constant.

12.7 ALPHA DECAY

In alpha decay, an unstable nucleus disintegrates into a lighter nucleus and an alpha particle (a nucleus of ^{4}He), according to

$$ {}^{A}_{Z}\mathrm{X}_{N} \rightarrow {}^{A-4}_{Z-2}\mathrm{X}'_{N-2} + {}^{4}_{2}\mathrm{He}_{2} \tag{12.19} $$

where X and X′ represent different nuclei. For example, ${}^{226}_{88}\mathrm{Ra}_{138} \rightarrow {}^{222}_{86}\mathrm{Rn}_{136} + {}^{4}_{2}\mathrm{He}_{2}$.

Decay processes release energy, because the decay products are more tightly bound than the initial nucleus. The energy released, which appears as the kinetic

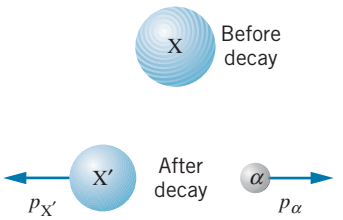

FIGURE 12.14 A nucleus X alpha decays, resulting in a nucleus X′ and an alpha particle.

energy of the alpha particle and the "daughter" nucleus X′, can be found from the masses of the nuclei involved according to Eq. 12.16:

$$Q = [m(\mathrm{X}) - m(\mathrm{X}') - m(^4\mathrm{He})]c^2 \tag{12.20}$$

As we did in our calculations of binding energy, we can show that the electron masses cancel in Eq. 12.20, and so we can use *atomic masses*. This energy Q appears as kinetic energy of the decay products:

$$Q = K_{X'} + K_\alpha \tag{12.21}$$

assuming we choose a reference frame in which the original atom X is at rest. Linear momentum is also conserved in the decay process, as shown in Figure 12.14, so that

$$p_\alpha = p_{X'} \tag{12.22}$$

From Eqs. 12.21 and 12.22 we eliminate $p_{X'}$ and $K_{X'}$, because we normally don't observe the daughter nucleus in the laboratory. Typical alpha decay energies are a few MeV; thus the kinetic energies of the alpha particle and the nucleus are much smaller than their corresponding rest energies, and so we can use nonrelativistic mechanics to find

$$K_\alpha \cong \frac{A-4}{A} Q \tag{12.23}$$

Example 12.8

Find the kinetic energy of the alpha particle emitted in the alpha decay process $^{226}\mathrm{Ra} \rightarrow {}^{222}\mathrm{Rn} + {}^4\mathrm{He}$.

Solution

From Eq. 12.20 the Q value is

$$\begin{aligned} Q &= [m(^{226}\mathrm{Ra}) - m(^{222}\mathrm{Rn}) - m(^4\mathrm{He})]c^2 \\ &= (226.025410\ \mathrm{u} - 222.017578\ \mathrm{u} \\ &\qquad -4.002603\ \mathrm{u})(931.5\ \mathrm{MeV/u}) \\ &= 4.871\ \mathrm{MeV} \end{aligned}$$

The kinetic energy is given by Eq. 12.23:

$$\begin{aligned} K_\alpha &= \frac{A-4}{4} Q = \left(\frac{222}{226}\right)(4.871\ \mathrm{MeV}) \\ &= 4.785\ \mathrm{MeV} \end{aligned}$$

Table 12.2 shows some sample alpha decays and their half-lives. You can see from the table that small changes in the decay energy (about a factor of 2) result in enormous changes in the half-life (24 orders of magnitude)! For example, for the isotopes ^{232}Th and ^{230}Th (which have the same Z and therefore the same Coulomb interaction between the alpha particle and the product nucleus) the kinetic energy changes by only 0.68 MeV (about 15%), while the half-life changes by about five orders of magnitude. Any successful calculation of the alpha decay probabilities must account for this sensitivity to the decay energy.

TABLE 12.2 Some Alpha Decay Energies and Half-Lives

Isotope	K_α (MeV)	$t_{1/2}$	λ (s^{-1})
^{232}Th	4.01	1.4×10^{10} y	1.6×10^{-18}
^{238}U	4.19	4.5×10^{9} y	4.9×10^{-18}
^{230}Th	4.69	7.5×10^{4} y	2.9×10^{-13}
^{241}Am	5.64	432 y	5.1×10^{-11}
^{230}U	5.89	20.8 d	3.9×10^{-7}
^{210}Rn	6.16	2.4 h	8.0×10^{-5}
^{220}Rn	6.29	56 s	1.2×10^{-2}
^{222}Ac	7.01	5 s	0.14
^{215}Po	7.53	1.8 ms	3.9×10^{2}
^{218}Th	9.85	0.11 μs	6.3×10^{6}

Quantum Theory of Alpha Decay

Alpha decay is an example of quantum-mechanical barrier penetration, as we discussed in Chapter 5. Suppose it is energetically possible for two neutrons and two protons to form an alpha particle, as represented in Figure 12.10. The alpha particle is trapped inside the nucleus by a barrier due to the Coulomb energy. The height of this barrier U_B is the Coulomb potential energy of the alpha particle and daughter nucleus at the radius R:

$$U_B = \frac{1}{4\pi\varepsilon_0}\frac{q_1 q_2}{r} = \frac{2(Z-2)e^2}{4\pi\varepsilon_0 R} \tag{12.24}$$

which gives 30 to 40 MeV for a typical heavy nucleus. Here $q_1 = 2e$ is the electric charge of the alpha particle, and $q_2 = (Z-2)e$ is the electric charge of the nucleus after the decay, which is responsible for the Coulomb force.

Figure 12.15 shows the potential energy barrier encountered by the alpha particle as it tries to leave the interior of the nucleus ($r < R$). The energy of the alpha particle is typically in the range of 4–8 MeV, and so it is impossible for the alpha particle to surmount the barrier; the only way the alpha particle can escape is to "tunnel" through the barrier. A representation of the alpha particle wave function as it tunnels through the barrier is shown in Figure 12.15*b*.

The probability per unit time λ for the alpha particle to appear in the laboratory is the probability of its penetrating the barrier multiplied by the number of times per second the alpha particle strikes the barrier in its attempt to escape. If the alpha particle is moving at speed v inside a nucleus of radius R, it will strike the barrier as it bounces back and forth inside the nucleus at time intervals of $2R/v$. In a heavy nucleus with $R \sim$ 6 fm, the α particle strikes the "wall" of the nucleus about 10^{22} times per second!

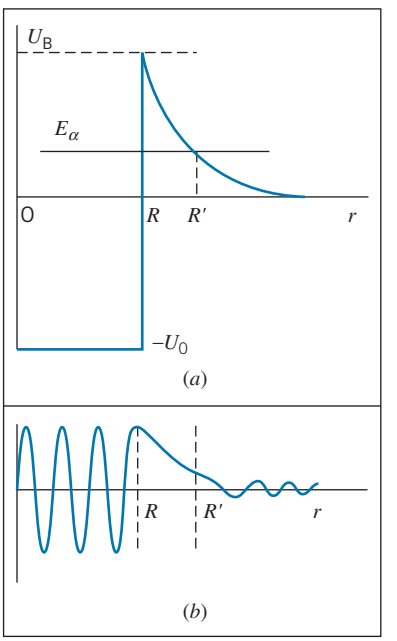

FIGURE 12.15 (*a*) The potential energy barrier for an alpha particle. (*b*) A representation of the wave function of the alpha particle.

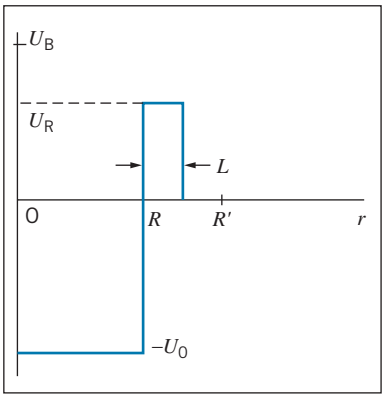

FIGURE 12.16 Replacing the Coulomb barrier for alpha decay with a flat barrier of height U_R.

The probability for the alpha particle to penetrate the barrier can be found by solving the Schrödinger equation for the potential energy shown in Figure 12.15. To simplify this calculation, we can replace the Coulomb barrier with a "flat" barrier, as shown in Figure 12.16. As we discussed in Chapter 5, the probability to penetrate a potential energy barrier is determined by the exponential factor e^{-2kL}, where L is the thickness of the barrier and where $k = \sqrt{(2m/\hbar^2)(U_0 - E)}$ for a barrier of height U_0 and a particle of energy E. The decay probability can then be estimated as

$$\lambda = \frac{v}{2R} e^{-2kL} \tag{12.25}$$

which includes both the rate at which the particle strikes the barrier and its probability to penetrate it. By making suitable rough estimates for the thickness and height of the barrier (see Problem 41), you should be able roughly to reproduce the range of values for the decay probabilities given in Table 12.2.

An exact calculation of the decay probability can be done by replacing the Coulomb barrier with a series of thin, flat barriers that are chosen to fit the Coulomb barrier as closely as possible. This calculation was first done in 1928 by George Gamow and was one of the first successful applications of the quantum theory.

Some nuclei can be unstable to the emission of other particles or collections of particles. Nuclei that have a large abundance of protons (those at the left-hand boundary of the light shaded region of Figure 12.11) may emit protons in a rare process similar to alpha decay. In this way they reduce their proton excess and move closer to stability. An example of this process is ${}^{151}_{71}\mathrm{Lu}_{80} \rightarrow {}^{150}_{70}\mathrm{Yb}_{80} + \mathrm{p}$.

Other nuclei have recently been shown to emit clusters of particles such as ${}^{12}\mathrm{C}$, ${}^{14}\mathrm{C}$, or ${}^{20}\mathrm{Ne}$. The following example illustrates this process.

Example 12.9

The nucleus ${}^{226}\mathrm{Ra}$ decays by alpha emission with a half-life of 1600 y. It also decays by emitting ${}^{14}\mathrm{C}$. Find the Q value for ${}^{14}\mathrm{C}$ emission and compare with that for alpha emission (see Example 12.8).

Solution

If ${}^{226}\mathrm{Ra}$ emits ${}^{14}\mathrm{C}$, which contains 6 protons and 8 neutrons, the resulting nucleus is ${}^{212}\mathrm{Pb}$, so the decay process is ${}^{226}\mathrm{Ra} \rightarrow {}^{212}\mathrm{Pb} + {}^{14}\mathrm{C}$. The Q value can be found from Eq. 12.16, where we can again use atomic masses because the electron masses cancel.

$$\begin{aligned} Q &= [m({}^{226}\mathrm{Ra}) - m({}^{212}\mathrm{Pb}) - m({}^{14}\mathrm{C})]c^2 \\ &= (226.025410\ \mathrm{u} - 211.991898\ \mathrm{u} \\ &\qquad -14.003242\ \mathrm{u})(931.5\ \mathrm{MeV/u}) \\ &= 28.197\ \mathrm{MeV} \end{aligned}$$

Even though the Q value far exceeds the Q value for alpha decay (4.871 MeV), the Coulomb barrier for ${}^{14}\mathrm{C}$ decay is roughly 3 times higher and thicker than it is for alpha decay [change $q_1 q_2$ to $6(Z-6)e^2$ in Eq. 12.24]. As a result, the probability for ${}^{14}\mathrm{C}$ decay turns out to be only about 10^{-9} of the probability for alpha decay; that is, ${}^{226}\mathrm{Ra}$ emits one ${}^{14}\mathrm{C}$ for every 10^9 alpha particles. See Problem 42 for a calculation of the relative decay probabilities.

12.8 BETA DECAY

In beta decay a neutron in the nucleus changes into a proton (or a proton into a neutron); Z and N each change by one unit, but A doesn't change. The emitted particles, which were called beta particles when first observed in 1898, were soon identified as electrons. In the most basic beta decay process, a free neutron decays into a proton and an electron: $n \rightarrow p + e$ (plus a third particle, as we discuss later).

The emitted electron is *not* one of the orbital electrons of the atom. It also is not an electron that was previously present within the nucleus, for as we have seen (Example 4.7) the uncertainty principle forbids electrons of the observed energies to exist inside the nucleus. The electron is "manufactured" by the nucleus out of the available energy. If the rest energy *difference* between the nuclei is at least $m_e c^2$, this will be possible.

In the 1910s and 1920s, beta decay experiments revealed two difficulties. First, the decay $n \rightarrow p + e^-$ appears to violate the law of conservation of angular momentum, as we discussed in Section 12.6. Second, measurements of the energy of the emitted electrons showed that the energy spectrum of the electrons is continuous, from zero up to some maximum value K_{max}, as shown in Figure 12.17. This implies an apparent violation of conservation of energy, because all electrons should emerge from the decay $n \rightarrow p + e^-$ with precisely the same energy. Instead, all electrons emerge with less energy, but in varying amounts.

For example, in the decay $n \rightarrow p + e^-$, the Q value is

$$Q = (m_n - m_p - m_e)c^2 = 0.782\,\text{MeV} \tag{12.26}$$

Except for a very small correction, which accounts for the recoil energy of the proton, all of this energy should appear as kinetic energy of the electron, and all emitted electrons should have *exactly* this energy. However, experiments in the 1920s showed that all the emitted electrons have less than this energy—they have a continuous range of energies from 0 to 0.782 MeV.

The problem of this "missing" energy was very puzzling until 1930 when Wolfgang Pauli found the ingenious solution to *both* the apparent violations of conservation of angular momentum and energy—he suggested that there is a *third* particle emitted in beta decay. Electric charge is already conserved by the proton and electron, so this new particle cannot have electric charge. If it has spin $^1/_2$, it will satisfy conservation of angular momentum, because we can combine the spins of the three decay particles to give $^1/_2$, which matches the spin of the original decaying neutron. The "missing" energy is the energy carried away by this third particle, and the observed fact that the energy spectrum extends all the way to the value 0.782 MeV suggests that this particle has a very small mass.

This new particle is called the *neutrino* ("little neutral one" in Italian) and has the symbol ν. As we discuss in Chapter 14, every particle has an *antiparticle,* and the antiparticle of the neutrino is the *antineutrino* $\overline{\nu}$. It is, in fact, the antineutrino that is emitted in neutron beta decay. The complete decay process is thus

$$n \rightarrow p + e^- + \overline{\nu} \tag{12.27}$$

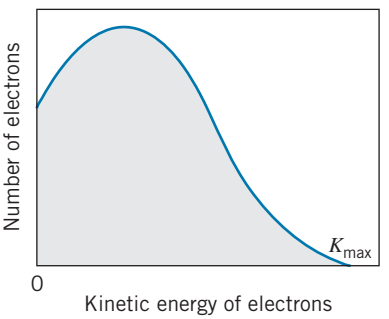

FIGURE 12.17 Spectrum of electrons emitted in beta decay.

Neutron decay can also occur in a nucleus, in which a nucleus with Z protons and N neutrons decays to a nucleus with $Z + 1$ protons and $N - 1$ neutrons:

$$ {}^{A}_{Z}\mathrm{X}_{N} \rightarrow {}^{A}_{Z+1}\mathrm{X}'_{N-1} + \mathrm{e}^{-} + \overline{\nu} \tag{12.28} $$

The Q value for this decay is

$$ Q = [m({}^{A}\mathrm{X}) - m({}^{A}\mathrm{X}')]c^2 \tag{12.29} $$

It can be shown (Problem 23) that the electron masses cancel in calculating Q, so it is *atomic masses* that appear in Eq. 12.29. The antineutrino does not appear in the calculation of the Q value because its mass is negligibly small (of the order of eV/c^2, compared with the atomic masses measured in units of $10^3\ \mathrm{MeV}/c^2$).

The energy released in the decay (the Q value) appears as the energy E_ν of the antineutrino, the kinetic energy K_e of the electron, and a small (usually negligible) recoil kinetic energy of the nucleus X′:

$$ Q = E_\nu + K_\mathrm{e} + K_{\mathrm{X}'} \cong E_\nu + K_\mathrm{e} \tag{12.30} $$

The electron (which must be treated relativistically, because its kinetic energy is *not* small compared with its rest energy) has its maximum kinetic energy when the antineutrino has a negligibly small energy. Figure 12.17 shows the energy distribution of electrons emitted in a typical negative beta decay. The electron and neutrino share the decay energy Q; the kinetic energy of the electron (equal to $Q - K_\mathrm{e}$) ranges from 0 (when the neutrino has its maximum energy, $E_\nu = Q$) to Q (when $E_\nu = 0$).

Another beta decay process is

$$ \mathrm{p} \rightarrow \mathrm{n} + \mathrm{e}^{+} + \nu \tag{12.31} $$

in which a *positive electron,* or *positron*, is emitted. The positron is the antiparticle of the electron; it has the same mass as the electron but the opposite electric charge. The neutrino emitted in this process is similarly the antiparticle of the antineutrino that is emitted in neutron beta decay.

Proton beta decay has a negative Q value, and so it is never observed in nature for free protons. (This is indeed fortunate—if the free proton were unstable to beta decay, stable hydrogen atoms, the basic material of the universe, could not exist!) However, protons in some nuclei can undergo this decay process:

$$ {}^{A}_{Z}\mathrm{X}_{N} \rightarrow {}^{A}_{Z-1}\mathrm{X}'_{N+1} + \mathrm{e}^{+} + \nu \tag{12.32} $$

The Q value for this process is (Problem 23)

$$ Q = [m({}^{A}\mathrm{X}) - m({}^{A}\mathrm{X}') - 2m_\mathrm{e}]c^2 \tag{12.33} $$

in which the masses are *atomic masses.* In this case, the positron and neutrino share the decay energy Q (again neglecting the small recoil energy of the nucleus X′). Figure 12.18 shows the energy distribution of positrons emitted in a typical positive beta decay.

A nuclear decay process that competes with positron emission is *electron capture*; the basic electron capture process is

$$\mathrm{p} + \mathrm{e}^- \rightarrow \mathrm{n} + \nu \tag{12.34}$$

in which a proton captures an atomic electron from its orbit and converts into a neutron plus a neutrino. The electron necessary for this process is one of the inner orbital electrons in an atom, and we identify the capture process by the shell from which the captured electron comes: K-shell capture, L-shell capture, and so forth. (The electronic orbits that come closest to, or even penetrate, the nucleus have the higher probability to be captured.) In nuclei the process is

$$^{A}_{Z}\mathrm{X}_N + \mathrm{e}^- \rightarrow {}^{A}_{Z-1}\mathrm{X}'_{N+1} + \nu \tag{12.35}$$

and the Q value, using atomic masses, is

$$Q = [m(^{A}\mathrm{X}) - m(^{A}\mathrm{X}')]c^2 \tag{12.36}$$

In this case, neglecting the small initial kinetic energy of the electron and the recoil energy of the nucleus, the neutrino takes all of the available final energy:

$$E_\nu = Q \tag{12.37}$$

In contrast to other beta-decay processes, a *monoenergetic* neutrino is emitted in electron capture.

Table 12.3 gives some typical beta decay processes, along with their Q values and half-lives.

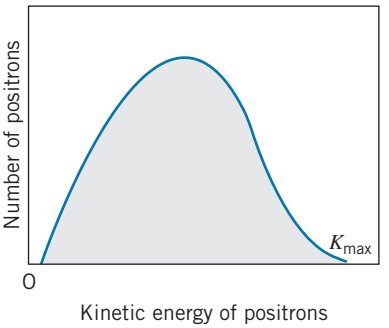

FIGURE 12.18 Spectrum of positrons emitted in beta decay.

TABLE 12.3 Typical Beta Decay Processes

Decay	Type	Q (MeV)	$t_{1/2}$
$^{19}\mathrm{O} \rightarrow {}^{19}\mathrm{F} + \mathrm{e}^- + \bar{\nu}$	β^-	4.82	27 s
$^{176}\mathrm{Lu} \rightarrow {}^{176}\mathrm{Hf} + \mathrm{e}^- + \bar{\nu}$	β^-	1.19	3.6×10^{10} y
$^{25}\mathrm{Al} \rightarrow {}^{25}\mathrm{Mg} + \mathrm{e}^+ + \nu$	β^+	3.26	7.2 s
$^{124}\mathrm{I} \rightarrow {}^{124}\mathrm{Te} + \mathrm{e}^+ + \nu$	β^+	2.14	4.2 d
$^{15}\mathrm{O} + \mathrm{e}^- \rightarrow {}^{15}\mathrm{N} + \nu$	EC	2.75	122 s
$^{170}\mathrm{Tm} + \mathrm{e}^- \rightarrow {}^{170}\mathrm{Er} + \nu$	EC	0.31	129 d

Example 12.10

^{23}Ne decays to ^{23}Na by negative beta emission. What is the maximum kinetic energy of the emitted electrons?

Solution

This decay is of the form given by Eq. 12.28, $^{23}\text{Ne} \rightarrow {}^{23}\text{Na} + e^- + \bar{\nu}$, and the Q value is found from Eq. 12.29, using *atomic* masses:

$$\begin{aligned} Q &= [m(^{23}\text{Ne}) - m(^{23}\text{Na})]c^2 \\ &= (22.994467\ \text{u} - 22.989769\ \text{u})(931.5\ \text{MeV/u}) \\ &= 4.376\ \text{MeV} \end{aligned}$$

Neglecting the small correction for the kinetic energy of the recoiling nucleus, the maximum kinetic energy of the electrons is equal to this value (which occurs when the neutrino has a negligible energy).

Example 12.11

^{40}K is an unusual isotope, in that it decays by negative beta emission, positive beta emission, and electron capture. Find the Q values for these decays.

Solution

The process for negative beta decay is given by Eq. 12.28, $^{40}\text{K} \rightarrow {}^{40}\text{Ca} + e^- + \bar{\nu}$, and the Q value is found from Eq. 12.29 using atomic masses:

$$\begin{aligned} Q_{\beta^-} &= [m(^{40}\text{K}) - m(^{40}\text{Ca})]c^2 \\ &= (39.963998\ \text{u} - 39.962591\ \text{u})(931.5\ \text{MeV/u}) \\ &= 1.311\ \text{MeV} \end{aligned}$$

Equation 12.32 gives the decay process for positive beta emission, $^{40}\text{K} \rightarrow {}^{40}\text{Ar} + e^+ + \nu$, and the Q value is given by Eq. 12.33:

$$\begin{aligned} Q_{\beta^+} &= [m(^{40}\text{K}) - m(^{40}\text{Ar}) - 2m_e]c^2 \\ &= [39.963998\ \text{u} - 39.962383\ \text{u} - 2(0.000549\ \text{u})] \\ &\qquad \times (931.5\ \text{MeV/u}) \\ &= 0.482\ \text{MeV} \end{aligned}$$

For electron capture, $^{40}\text{K} + e^- \rightarrow {}^{40}\text{Ar} + \nu$, and from Eq. 12.36:

$$\begin{aligned} Q_{\text{ec}} &= [m(^{40}\text{K}) - m(^{40}\text{Ar})]c^2 \\ &= (39.963998\ \text{u} - 39.962383\ \text{u})(931.5\ \text{MeV/u}) \\ &= 1.504\ \text{MeV} \end{aligned}$$

12.9 GAMMA DECAY AND NUCLEAR EXCITED STATES

Following alpha or beta decay, the final nucleus may be left in an excited state. Just as an atom does, the nucleus will reach its ground state after emitting one or more photons, known as nuclear gamma rays. The energy of each photon is the energy difference between the initial and final nuclear states, less a negligibly small correction for the recoil kinetic energy of the nucleus. The energies of emitted gamma rays are typically in the range of 100 keV to a few MeV. Nuclei can likewise be excited from the ground state to an excited state by absorbing a photon of the appropriate energy, in a process similar to the resonant absorption by atomic states.

Figure 12.19 shows a typical energy-level diagram of excited nuclear states and some of the gamma-ray transitions that can be emitted. Typical values for the half-lives of the excited states are 10^{-9} to 10^{-12} s, although there are occasional cases of excited states with half-lives of hours, days, or even years.

When a gamma-ray photon is emitted, the nucleus must recoil to conserve momentum. The photon has energy E_γ and momentum $p_\gamma = E_\gamma/c$. The nucleus recoils with momentum p_R. If the nucleus is initially at rest, then momentum conservation requires that $p_R = p_\gamma$ in magnitude (and that the nucleus recoil in a direction opposite to that of the gamma ray). The recoil kinetic energy K_R is small, so that nonrelativistic equations can be used for the nucleus (of mass M):

$$K_R = \frac{p_R^2}{2M} = \frac{p_\gamma^2}{2M} = \frac{E_\gamma^2}{2Mc^2} \tag{12.38}$$

For a medium-mass nucleus of $A = 100$ and a large gamma-ray energy of 1 MeV, the recoil kinetic energy is only 5 eV. Suppose the gamma ray is emitted when the nucleus jumps from an initial state with energy E_i to a final state with energy E_f. Conservation of energy then gives $E_i = E_f + E_\gamma + K_R$, so the energy of the emitted gamma ray is

$$E_\gamma = E_i - E_f - K_R \cong E_i - E_f \tag{12.39}$$

The gamma-ray energy is equal to the difference between the initial and final energy states, because the recoil kinetic energy of the nucleus is negligibly small.

In calculating the energies of alpha and beta particles emitted in radioactive decays, we have assumed that no gamma rays are emitted. If there are gamma rays emitted, the available energy (Q value) must be shared between the other particles and the gamma ray, as the following example shows.

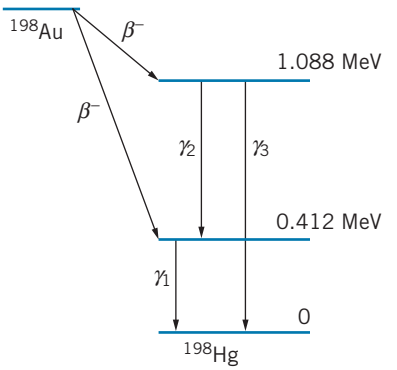

FIGURE 12.19 Some gamma rays emitted following beta decay.

Example 12.12

^{12}N beta decays to an excited state of ^{12}C, which subsequently decays to the ground state with the emission of a 4.43-MeV gamma ray. What is the maximum kinetic energy of the emitted beta particle?

Solution

To determine the Q value for this decay, we first need to find the mass of the product nucleus ^{12}C *in its excited state*. In the ground state, ^{12}C has a mass of 12.000000 u, so its mass in the excited state (indicated by ^{12}C*) is

$$\begin{aligned} m(^{12}\text{C}^*) &= 12.000000\ \text{u} + \frac{4.43\ \text{MeV}}{931.5\ \text{MeV/u}} \\ &= 12.004756\ \text{u} \end{aligned}$$

In this decay, a proton is converted to a neutron, so it must be an example of positron decay. The Q value is, according to Eq. 12.33,

$$\begin{aligned} Q &= [m(^{12}\text{N}) - m(^{12}\text{C}^*) - 2m_e]c^2 \\ &= [12.018613\ \text{u} - 12.004756\ \text{u} - 2(0.000549\ \text{u})] \\ &\qquad \times (931.5\ \text{MeV/u}) \\ &= 11.89\ \text{MeV} \end{aligned}$$

(Notice that we could have just as easily found the Q value by first finding the Q value for decay to the *ground state*, 16.32 MeV, and then subtracting the excitation energy of 4.43 MeV, because the decay to the excited state has that much less available energy.)

Neglecting the small correction for the recoil kinetic energy of the ^{12}C nucleus, the maximum electron kinetic energy is 11.89 MeV.

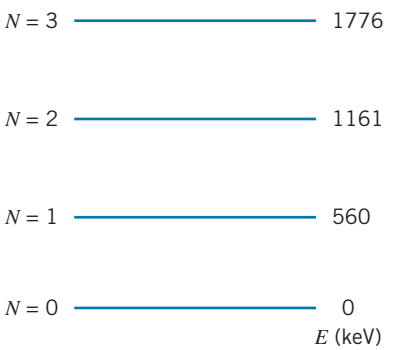

FIGURE 12.20 Nuclear vibrational states in the nucleus ^{120}Te. The states are labeled with the vibrational quantum number N. Note that the states are nearly equally spaced, as is expected for vibrations.

Nuclear Excited States

The study of nuclear gamma emission is an important tool of the nuclear physicist; the energies of the gamma rays can be measured with great precision, and they provide a powerful means of deducing the energies of the excited states of nuclei. This type of *nuclear spectroscopy* is very similar to the methods of molecular spectroscopy discussed in Chapter 9. In fact, the nuclear excited states can be formed in ways that are similar to molecular excited states:

1. Proton or Neutron Excitation Nuclear excited states can be formed when a proton or a neutron is excited from a filled state to one of the empty states shown in Figure 12.8 or 12.9, just as in molecules we can form an excited state by promoting an electron from a lower state to one of the empty molecular orbitals. When a proton or neutron drops from an excited state to a lower state, a gamma-ray photon is emitted. The energy of the photon is equal to the energy difference between the states (neglecting the small recoil kinetic energy of the nucleus). To estimate the average energy for this type of excitation, we note from Figure 12.8 that 73 neutrons occupy an energy of 37.0 MeV, so the average spacing of the filled levels is (37.0 MeV)/73 = 0.5 MeV. The spacing between the empty states, among which gamma rays are emitted, should be about the same.

2. Nuclear Vibrations The nucleus can vibrate like a jiggling water droplet. The vibrational excited states are equally spaced, just like the molecular vibrational states shown in Figure 9.22. Unlike a molecule, a nucleus vibrates like an incompressible fluid—for example, if the "equator" bulges outward, the "poles" must move inward to keep the density constant. The separation of the equally spaced vibrational states is about 0.5–1 MeV. Figure 12.20 shows an example of some vibrational nuclear excited states. Although the selection rules for photon emission in nuclei are not as strongly restrictive as they are in molecules, nuclei in higher vibrating states usually jump to lower vibrating states by changing the vibrational quantum number by one unit and emitting a gamma-ray photon in the process.

3. Nuclear Rotations The nucleus can rotate, showing the same $L(L+1)$ spacing as a molecule (see Figure 9.25). Figure 12.21 shows an example of rotational nuclear excited states. The spacing between the rotational ground state and the first rotational excited state is typically 0.05–0.1 MeV. (Note that in nuclei, as in molecules, the rotational spacing is generally much smaller than the vibrational spacing.) Nuclei in higher rotational states can jump to lower rotational states by emitting gamma-ray photons; in the case of nuclei, the selection rule restricting the change in the rotational quantum number to one unit, which was strongly followed by molecules, does not strongly apply to nuclei. In nuclei, the rotational quantum number generally changes by one or two units when gamma-ray photons are emitted in transitions between the nuclear rotational states.

*Nuclear Resonance

One way of studying atomic systems is to do *resonance* experiments. In such experiments, radiation from a collection of atoms in an excited state is incident

*This is an optional section that may be skipped without loss of continuity.

on a collection of identical atoms in their ground state. The ground-state atoms can absorb the photons and jump to the corresponding excited state. However, as we have seen, the emitted photon energy is less than the transition energy by the recoil kinetic energy K_R; moreover, it is less than the photon energy required for resonance by $2K_R$, because the *absorbing* atom must recoil also. The absorption experiment is still possible, because the excited states don't have "exact" energies—a state with a mean lifetime τ has an energy uncertainty ΔE that is given by the uncertainty relationship: $\Delta E\tau \sim \hbar$. That is, the state lives on the average for a time τ, and during that time we can't determine its energy to an accuracy less than ΔE. For typical atomic states, $\tau \sim 10^{-8}$ s, so $\Delta E \sim 10^{-7}$ eV. Because K_R, which is of the order of 10^{-10} eV, is much less than the width ΔE, the "shift" caused by the recoil is not large, and the widths of the emitting and absorbing atomic states cause sufficient overlap for the absorption process to occur. Figure 12.22 illustrates this case.

The situation is different for nuclear gamma rays. A typical lifetime might be 10^{-10} s, and so the widths are the order of $\Delta E \sim 10^{-5}$ eV. The photon energies are typically 100 keV = 10^5 eV, and so K_R is of order 1 eV. This situation is depicted in Figure 12.23, and you can immediately see that because K_R is so much larger than the width ΔE, no overlap of emitter and absorber is possible, so resonance absorption cannot occur.

In 1958, it was discovered that the overlap of the emitter and absorber can be restored by placing the radioactive nuclei and the absorbing nuclei in crystals. The crystalline binding energies are large compared with K_R, so the individual atoms are held tightly to their positions in the crystal lattice and are not free to recoil; if any recoil is to occur, it must be the whole crystal that recoils. This effect is to make the mass M that appears in Eq. 12.38 not the mass of an atom, but the mass of the entire crystal, perhaps 10^{20} times larger than an atomic mass. (As an analogy, imagine the difference between striking a brick with a baseball bat, and striking a brick wall!) Once again the recoil kinetic energy is made small, and resonant absorption can occur (Figure 12.24). For this discovery, Rudolf Mössbauer was awarded the 1961 Nobel Prize in physics, and the process of achieving nuclear resonance by embedding the emitting and absorbing nuclei in crystal lattices is now known as the *Mössbauer effect.*

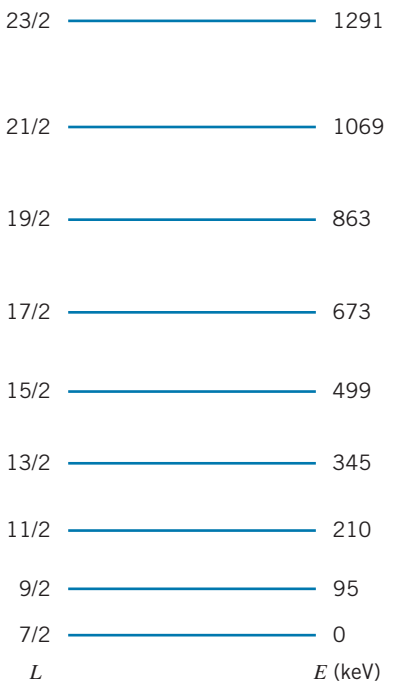

FIGURE 12.21 An example of nuclear rotational states in the nucleus ^{165}Ho. The states are labeled with the rotational quantum number L. The energies closely follow the expected $L(L+1)$ spacing.

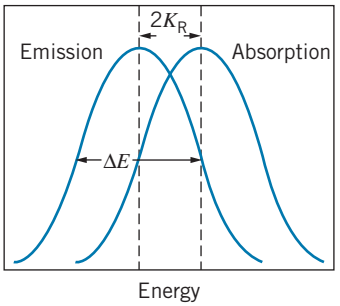

FIGURE 12.22 Representative emission and absorption energies in an atomic system.

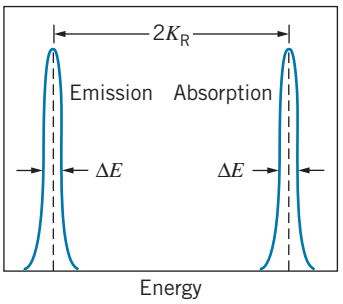

FIGURE 12.23 Representative emission and absorption energies in a nuclear system.

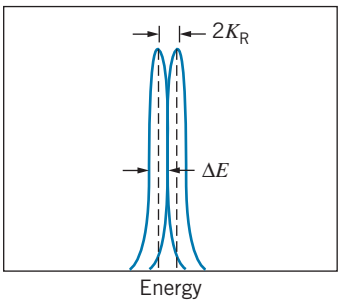

FIGURE 12.24 Emission and absorption energies for nuclei bound in a crystal lattice.

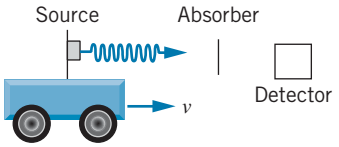

FIGURE 12.25 Mössbauer effect apparatus. A source of gamma rays is made movable, in order to Doppler-shift the photon energies. The intensity of radiations transmitted through the absorber is measured as a function of the speed of the source.

The small remaining difference between the emission and absorption energies can be eliminated to obtain complete overlap by Doppler-shifting either the emission or absorption energies. The Doppler-shifted frequency when a source moves toward the observer at speed v is given by Eq. 2.22, $f' = f(1 + v/c)$, where we ignore the $\sqrt{1 - v^2/c^2}$ term because $v \ll c$. Using $E = hf$ for the photon energy, we have

$$E' = E(1 + v/c) \tag{12.40}$$

If we take the width ΔE as a representative estimate of how far we would like to Doppler-shift the photon energy, then $E' \cong E + \Delta E$, and so $E + \Delta E \cong E + E(v/c)$. Solving for v, we find

$$v \cong c\frac{\Delta E}{E} \tag{12.41}$$

Estimating $\Delta E \sim 10^{-5}$ eV (the width of the state) and $E \sim 100$ keV (the energy of the photon), we have

$$v \cong (3 \times 10^8 \text{ m/s})\frac{10^{-5} \text{ eV}}{10^5 \text{ eV}} = 3 \text{ cm/s}$$

Such low speeds can be easily and accurately produced in the laboratory.

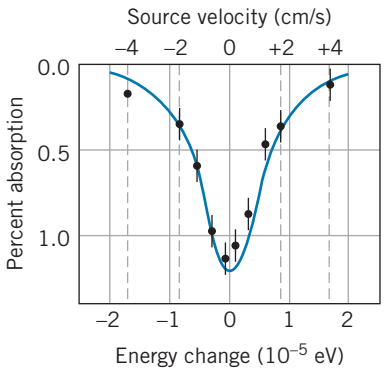

FIGURE 12.26 Typical results in a Mössbauer effect experiment. A velocity of 2 cm/s Doppler shifts the gamma rays enough to move the emission and absorption energies off resonance.

Figure 12.25 shows a diagram of the apparatus to measure the Mössbauer effect. The resonant absorption is observed by looking for decreases in the number of gamma rays that are transmitted through the absorber. At resonance, more gamma rays are absorbed and so the transmitted intensity decreases. Typical results are shown in Figure 12.26.

The Mössbauer effect is an extremely precise method for measuring small changes in the energies of photons. In one particular application, the Zeeman splitting of *nuclear* (not atomic) states can be observed. When a nucleus is placed in a magnetic field, the Zeeman effect causes an energy splitting of the nuclear m states, similar to the atomic case. However, nuclear magnetic moments are about 2000 times smaller than atomic magnetic moments, and a typical energy splitting would be about 10^{-6} eV. To observe such an effect directly we would need to measure photon energies to 1 part in 10^{11} (a photon energy of 10^5 eV is shifted by 10^{-6} eV), but using the Mössbauer effect, this is not difficult.

In Chapter 15 we discuss another application of this extremely precise technique, in which the energy gained when a photon "falls" through several meters of the Earth's gravitational field is measured in order to test one prediction of Einstein's general theory of relativity.

12.10 NATURAL RADIOACTIVITY

All of the elements beyond the very lightest (hydrogen and helium) were produced by nuclear reactions in the interiors of stars. These reactions produce not only stable elements, but radioactive ones as well. Most radioactive elements have half-lives that are much smaller than the age of the Earth (about 4.5×10^9 y), so those radioactive elements that may have been present when the Earth was formed have decayed to stable elements. However, a few of the radioactive elements

created long ago have half-lives that are as large as or even greater than the age of the Earth. These elements can still be observed to undergo radioactive decay and account for part of the background of *natural radioactivity* that surrounds us.

Radioactive decay processes either change the mass number A of a nucleus by four units (alpha decay) or don't change A at all (beta or gamma decay). A radioactive decay process can be part of a sequence or series of decays if a *radioactive* element of mass number A decays to another *radioactive* element of mass number A or $A - 4$. Such a series of processes will continue until a stable element is reached. A hypothetical such series is illustrated in Figure 12.27. Because gamma decays don't change Z or A, they are not shown; however, most of the alpha and beta decays are accompanied by gamma-ray emissions.

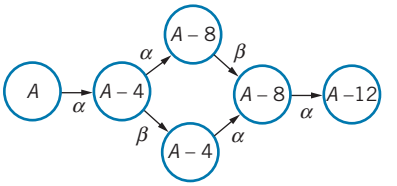

FIGURE 12.27 An example of a hypothetical radioactive decay chain.

The A values of the members of such decay chains differ by a multiple of 4 (including zero as a possible multiple) and so we expect four possible decay chains, with A values that can be expressed as $4n, 4n + 1, 4n + 2$, and $4n + 3$, where n is an integer. One of the four naturally occurring radioactive series is illustrated in Figure 12.28. Each series begins with a relatively long-lived member, proceeds through many α and β decays, which may have very short half-lives, and finally ends with a stable isotope. Three of these series begin with isotopes having half-lives comparable to the age of the Earth, and so are still observed today. The neptunium series $(4n + 1)$ begins with ^{237}Np, which has a half-life of "only" 2.1×10^6 y, much less than the 4.5×10^9 y since the formation of the Earth. Thus all of the ^{237}Np that was originally present has long since decayed to ^{209}Bi.

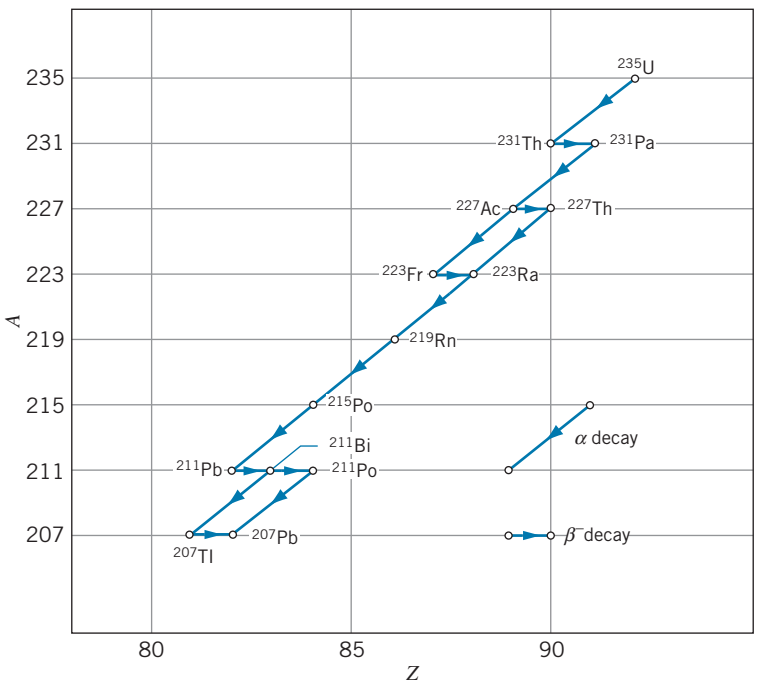

FIGURE 12.28 The ^{235}U decay chain. The diagonal lines represent α decays, and the horizontal lines show β decays.

Example 12.13

Compute the Q value for the $^{238}\text{U} \rightarrow {}^{206}\text{Pb}$ decay chain, and find the rate of energy production per gram of uranium.

Solution

Because A changes by 32, there must be 8 alpha decays in the chain. These 8 alpha decays would decrease Z by 16 units, from 92 to 76. However, the final Z must be 82, so there must also be 6 beta decays in the chain. We recall that for β^- decays, the electron masses combine with the nuclear masses in the computation of the Q value and we can therefore use atomic masses. Thus for the entire decay chain,

$$\begin{aligned} Q &= [m(^{238}\text{U}) - m(^{206}\text{Pb}) - 8m(^4\text{He})]c^2 \\ &= [238.050788\ \text{u} - 205.974465\ \text{u} — 8(4.002603\ \text{u})] \\ &\qquad \times (931.5\ \text{MeV/u}) \\ &= 51.7\ \text{MeV} \end{aligned}$$

The half-life of the decay is 4.5×10^9 y, so λ, the decay probability per atom, is

$$\begin{aligned} \lambda &= \frac{\ln 2}{t_{1/2}} = \frac{0.693}{(4.5 \times 10^9\ \text{y})(3.16 \times 10^7\ \text{s/y})} \\ &= 4.9 \times 10^{-18}\ \text{s}^{-1} \end{aligned}$$

One gram of ^{238}U is $\frac{1}{238}$ mole and therefore contains $\frac{1}{238} \times 6 \times 10^{23}$ atoms. The decay rate (activity) of the ^{238}U is given by the decay probability per atom per unit time multiplied by the number of atoms:

$$\begin{aligned} a &= \lambda N \\ &= \left(4.9 \times 10^{-18}\ \frac{\text{decays}}{\text{atom} \cdot \text{s}}\right)\left(\frac{1}{238} \times 6 \times 10^{23}\ \text{atoms}\right) \\ &= 12{,}000\ \text{decays/s} \end{aligned}$$

Each decay releases 51.7 MeV, and so the rate of energy production is

$$\begin{aligned} &12{,}000 \frac{\text{decays}}{\text{s}} \times 51.7 \frac{\text{MeV}}{\text{decay}} \times 10^6 \frac{\text{eV}}{\text{MeV}} \times 1.6 \times 10^{-19} \frac{\text{J}}{\text{eV}} \\ &= 1.0 \times 10^{-7}\ \text{W} \end{aligned}$$

This may seem like a very small rate of energy release, but if the energy were to appear as thermal energy and were not dissipated by some means (radiation or conduction to other matter, for example), the 1-g sample of ^{238}U would increase in temperature by 25°C per year and would be melted and vaporized in the order of one century! This calculation suggests that we can perhaps account for some of the internal heat of planets through natural radioactive processes.

If we examine a sample of uranium-bearing rock, we can find the ratio of ^{238}U atoms to ^{206}Pb atoms. If we assume that all of the ^{206}Pb was produced by the uranium decay and that none was present when the rock was originally formed (assumptions that must be examined with care both theoretically and experimentally), then this ratio can be used to find the age of the sample, as shown in the following example.

Example 12.14

Three different rock samples have ratios of numbers of ^{238}U atoms to ^{206}Pb atoms of 0.5, 1.0, and 2.0. Compute the ages of the three rocks.

Solution

Because all of the other members of the uranium series have half-lives that are much shorter than the half-life of ^{238}U (4.5×10^9 y), we ignore the intervening decays and consider only the ^{238}U decay. Let N_0 be the original number of ^{238}U atoms, so that $N_0 e^{-\lambda t}$ is the number that are still present today, and $N_0 - N_0 e^{-\lambda t}$ is the number that have decayed and are presently observed as ^{206}Pb. The ratio R of ^{238}U to ^{206}Pb is thus

$$\begin{aligned} R &= \frac{\text{number of } {}^{238}\text{U}}{\text{number of } {}^{206}\text{Pb}} \\ &= \frac{N_0 e^{-\lambda t}}{N_0 - N_0 e^{-\lambda t}} \\ &= \frac{1}{e^{\lambda t} - 1} \end{aligned}$$

Solving for t and recalling that $\lambda = 0.693/t_{1/2}$, we find:

$$t = \frac{t_{1/2}}{0.693} \ln\left(\frac{1}{R} + 1\right) \qquad (12.42)$$

We can then obtain the values of t corresponding to the three values of R,

$$R = 0.5 \qquad t = 7.1 \times 10^9 \text{ y}$$
$$R = 1.0 \qquad t = 4.5 \times 10^9 \text{ y}$$
$$R = 2.0 \qquad t = 2.6 \times 10^9 \text{ y}$$

The oldest rocks on Earth, dated by similar means, have ages of about 4.5×10^9 y. The age of the first rock analyzed above, 7.1×10^9 y, suggests either that the rock had an extraterrestrial origin, or else that our assumption of no initial ^{206}Pb was incorrect. The age of the third rock suggests that it solidified only 2.6×10^9 y ago; previous to that time it was molten and the decay product ^{206}Pb may have "boiled away" from the ^{238}U.

There are a number of other naturally occurring radioactive isotopes that are not part of the decay chain of the heavy elements. A partial list is given in Table 12.4; some of these can also be used for radioactive dating.

Other radioactive elements are being produced continuously in the Earth's atmosphere as a result of nuclear reactions between air molecules and the high-energy particles known as "cosmic rays." The most notable and useful of these is ^{14}C, which beta decays with a half-life of 5730 y. When a living plant absorbs CO_2 from the atmosphere, a small fraction (about 1 in 10^{12}) of the carbon atoms is ^{14}C, and the remainder is stable ^{12}C (99%), and ^{13}C (1%). When the plant dies, its intake of ^{14}C stops, and the ^{14}C decays. If we assume that the composition of the Earth's atmosphere and the flux of cosmic rays have not changed significantly in the last few thousand years, we can find the age of specimens of organic material by comparing their ^{14}C/^{12}C ratios to those of living plants. The following example shows how this *radiocarbon dating* technique is used.

TABLE 12.4 Some Naturally Occurring Radioactive Isotopes

Isotope	$t_{1/2}$
^{40}K	1.25×10^9 y
^{87}Rb	4.8×10^{10} y
^{92}Nb	3.2×10^7 y
^{113}Cd	9×10^{15} y
^{115}In	5.1×10^{14} y
^{138}La	1.1×10^{11} y
^{176}Lu	3.6×10^{10} y
^{187}Re	4×10^{10} y
^{232}Th	1.41×10^{10} y

Example 12.15

(*a*) A sample of carbon dioxide gas from the atmosphere fills a vessel of volume 200.0 cm^3 to a pressure of 2.00×10^4 Pa (1 Pa = 1 N/m^2, about 10^{-5} atm) at a temperature of 295 K. Assuming that all of the ^{14}C beta decays were counted, how many counts would be accumulated in one week? (*b*) An old sample of wood is burned, and the resulting carbon dioxide is placed in an identical vessel at the same pressure and temperature. After one week, 1420 counts have been accumulated. What is the age of the sample?

Solution

(*a*) We first find the number of atoms present in the vessel, using the ideal gas law:

$$N = \frac{PV}{kT} = \frac{(2.00 \times 10^4 \text{ N/m}^2)(2.00 \times 10^{-4} \text{ m}^3)}{(1.38 \times 10^{-23} \text{ J/K})(295 \text{ K})}$$
$$= 9.82 \times 10^{20} \text{ atoms}$$

If the fraction of ^{14}C atoms is 10^{-12}, there are 9.82×10^8 atoms of ^{14}C present. The activity is

$$a = \lambda N = \frac{0.693}{(5730 \text{ y})(3.16 \times 10^7 \text{ s/y})} 9.82 \times 10^8$$
$$= 3.76 \times 10^{-3} \text{ decays/s}$$

In one week the number of decays is 2280.

(*b*) An identical sample that gives only 1420 counts must be old enough for only 1420/2280 of its original activity to remain. With $1420 = 2280e^{-\lambda t}$, we have

$$t = \frac{1}{\lambda} \ln\left(\frac{2280}{1420}\right) = \frac{5730 \text{ y}}{0.693} \ln\left(\frac{2280}{1420}\right) = 3920 \text{ y}$$

Chapter Summary

		Section
Nuclear radius	$R = R_0 A^{1/3}, R_0 = 1.2$ fm	12.2
Nuclear binding energy	$B = [Nm_n + Zm(^1_1\mathrm{H}_0) - m(^A_Z\mathrm{X}_N)]c^2$	12.3
Proton separation energy	$S_p = [m(^{A-1}_{Z-1}\mathrm{X}'_N) + m(^1\mathrm{H}) - m(^A_Z\mathrm{X}_N)]c^2$	12.3
Neutron separation energy	$S_n = [m(^{A-1}_{Z}\mathrm{X}_{N-1}) + m_n - m(^A_Z\mathrm{X}_N)]c^2$	12.3
Range of exchanged particle	$mc^2 = \hbar c/x$	12.4
Activity	$a = \lambda N, \lambda = \ln 2/t_{1/2} = 0.693/t_{1/2}$	12.5
Radioactive decay law	$N = N_0 e^{-\lambda t}, a = a_0 e^{-\lambda t}$	12.5
Q value of decay $\mathrm{X} \rightarrow \mathrm{X}' + \mathrm{x}$	$Q = [m_X - (m_{X'} + m_x)]c^2$	12.6
Q value of alpha decay	$Q = [m(\mathrm{X}) - m(\mathrm{X}') - m(^4\mathrm{He})]c^2$	12.7
Kinetic energy of alpha particle	$K_\alpha \cong Q(A-4)/A$	12.7
Q values of beta decay	$Q_{\beta^-} = [m(^A\mathrm{X}) - m(^A\mathrm{X}')]c^2$, $Q_{\beta^+} = [m(^A\mathrm{X}) - m(^A\mathrm{X}') - 2m_e]c^2$	12.8
Recoil in gamma decay	$K_R = E_\gamma^2/2Mc^2$	12.9

Questions

1. The magnetic dipole moment of a deuterium nucleus is about 0.0005 Bohr magneton. What does this imply about the presence of an electron in the nucleus, as the proton-electron model requires?
2. Suppose we have a supply of 20 protons and 20 neutrons. Do we liberate more energy if we assemble them into a single ^{40}Ca nucleus or into two ^{20}Ne nuclei?
3. Atomic masses are usually given to a precision of about the sixth decimal place in atomic mass units (u). This is true for both stable and radioactive nuclei, even though the uncertainty principle requires that an atom with a lifetime Δt has a rest energy uncertain by $\hbar/\Delta t$. Based on the typical lifetimes given for nuclear decays, are we justified in expressing atomic masses to such precision? At what lifetimes would such precision not be justified?
4. Only two stable nuclei have $Z > N$. (*a*) What are these nuclei? (*b*) Why don't more nuclei have $Z > N$?
5. In a deuterium nucleus, the proton and neutron spins can be either parallel or antiparallel. What are the possible values of the total spin of the deuterium nucleus? (It is not necessary to consider any orbital angular momentum.) The magnetic dipole moment of the deuterium nucleus is measured to be nonzero. Which of the possible spins is eliminated by this measured value?
6. Why is the binding energy per nucleon relatively constant? Why does it deviate from a constant value for low mass numbers? For high mass numbers?
7. A neutron, which has no electric charge, has a magnetic dipole moment. How is this possible?
8. The electromagnetic interaction can be interpreted as an exchange force, in which photons are the exchanged particle. What does Eq. 12.8 imply about the range of such a force? Is this consistent with the conventional interpretation of the electromagnetic force? What would you expect for the rest energy of the exchanged particle that carries the gravitational force?
9. What is meant by assuming that the decay constant λ is a constant, independent of time? Is this a requirement of theory, an axiom, or an experimental conclusion? Under what circumstances might λ change with time?
10. If we focus our attention on a specific nucleus in a radioactive sample, can we know exactly how long that nucleus will live before it decays? Can we predict which half of the nuclei in a sample will decay during one half-life? What part of quantum physics is responsible for this?
11. A certain radioactive sample is observed to undergo 10,000 decays in 10 s. Can we conclude that $a = 1000$ decays/s if (*a*) $t_{1/2} \gg 10$ s; (*b*) $t_{1/2} = 10$ s; (*c*) $t_{1/2} \ll 10$ s?
12. Suppose we wish to do radioactive dating of a sample whose age we guess to be t. Should we choose an isotope whose half-life is (*a*) $\gg t$; (*b*) $\sim t$; or (*c*) $\ll t$?
13. The alpha particle is a particularly tightly bound nucleus. Based on this fact, explain why heavy nuclei alpha decay and light nuclei don't.

14. Can you suggest a possible origin for the helium gas that is part of the Earth's atmosphere?
15. Estimate the recoil kinetic energy of the residual nucleus following alpha decay. (This energy is large enough to drive the residual nucleus out of certain radioactive sources; if the residual nucleus is itself radioactive, there is the chance of spread of radioactive material. A thin coating over the source is necessary to prevent this.)
16. Why does the electron energy spectrum (Figure 12.17) look different from the positron energy spectrum (Figure 12.18) at low energies?
17. Will electron capture always be energetically possible when positron beta decay is possible? Will positron beta decay always be energetically possible when electron capture is possible?
18. All three beta decay processes involve the emission of neutrinos (or antineutrinos). In which processes do the neutrinos have a continuous energy spectrum? In which is the neutrino monoenergetic?
19. Neutrinos always accompany electron capture decays. What other kind of radiation always accompanies electron capture? (*Hint:* It is not nuclear radiation.) What other kind of nonnuclear radiation might accompany β^- or β^+ decays in bulk samples?
20. The positron decay of ^{15}O goes directly to the ground state of ^{15}N; no excited states of ^{15}N are populated and no γ rays follow the beta decay. Yet a source of ^{15}O is found to emit γ rays of energy 0.51 MeV. Explain the origin of these γ rays.
21. Would ^{92}Nb be a convenient isotope to use for determining the age of the Earth by radioactive dating? (See Table 12.4.) What about ^{113}Cd?
22. The natural decay chain $^{238}_{92}\text{U} \rightarrow {}^{206}_{82}\text{Pb}$ consists of several alpha decays, which decrease A by 4 and Z by 2, and negative beta decays, which increase Z by 1. (See Example 12.13.) As shown in Figures 12.27 and 12.28, sometimes a decay chain can proceed through different branches. Does the number of alpha decays and beta decays in the chain depend on this branching?
23. It has been observed that there is an increased level of radon gas ($Z = 86$) in the air just before an earthquake. Where does the radon come from? How is it produced? How is it released? How is it detected?
24. Which of the decay processes discussed in this chapter would you expect to be most sensitive to the chemical state of the radioactive sample?
25. In Figure 12.26, only 1% of the gamma intensity is absorped, even at resonance. For complete resonance, we would expect 100% absorption. What factors might contribute to this small absorption?

Problems

12.1 Nuclear Constituents

1. Give the proper isotopic symbols for: (*a*) the isotope of fluorine with mass number 19; (*b*) an isotope of gold with 120 neutrons; (*c*) an isotope of mass number 107 with 60 neutrons.
2. Tin has more stable isotopes than any other element; they have mass numbers 114, 115, 116, 117, 118, 119, 120, 122, 124. Give the symbols for these isotopes.

12.2 Nuclear Sizes and Shapes

3. (*a*) Compute the Coulomb repulsion energy between two nuclei of ^{16}O that just touch at their surfaces. (*b*) Do the same for two nuclei of ^{238}U.
4. Find the nuclear radius of (*a*) ^{197}Au; (*b*) ^{4}He; (*c*) ^{20}Ne.

12.3 Nuclear Masses and Binding Energies

5. Find the total binding energy, and the binding energy per nucleon, for (*a*) ^{208}Pb; (*b*) ^{133}Cs; (*c*) ^{90}Zr; (*d*) ^{59}Co.
6. Find the total binding energy, and the binding energy per nucleon, for (*a*) ^{4}He; (*b*) ^{20}Ne; (*c*) ^{40}Ca; (*d*) ^{55}Mn.
7. Calculate the total nuclear binding energy of ^{3}He and ^{3}H. Account for any difference by considering the Coulomb interaction of the extra proton of ^{3}He.
8. Find the neutron separation energy of: (*a*) ^{17}O; (*b*) ^{7}Li; (*c*) ^{57}Fe.
9. Find the proton separation energy of: (*a*) ^{4}He; (*b*) ^{12}C; (*c*) ^{40}Ca.

12.4 The Nuclear Force

10. The nuclear attractive force must turn into a repulsion at very small distances to keep the nucleons from crowding too close together. What is the mass of an exchanged particle that will contribute to the repulsion at separations of 0.25 fm?
11. The weak interaction (the force responsible for beta decay) is produced by an exchanged particle with a mass of roughly 80 GeV. What is the range of this force?

12.5 Quantum States in Nuclei

12. Determine the depth of the proton and neutron potential energy wells for (*a*) ^{16}O; (*b*) ^{235}U.
13. The two-neutron separation energies of ^{160}Dy and ^{164}Dy are, respectively, 15.4 MeV and 13.9 MeV, and the two-proton separation energies of ^{158}Dy and ^{162}Dy are, respectively, 12.4 MeV and 14.8 MeV. From these data alone, determine whether alpha decay is energetically allowed for ^{160}Dy and ^{164}Dy.

12.6 Radioactive Decay

14. What fraction of the original number of nuclei present in a sample will remain after (*a*) 2 half-lives; (*b*) 4 half-lives; (*c*) 10 half-lives?
15. A certain sample of a radioactive material decays at a rate of 548 per second at $t = 0$. At $t = 48$ minutes, the counting rate has fallen to 213 per second. (*a*) What is the half-life of the radioactivity? (*b*) What is its decay constant? (*c*) What will be the decay rate at $t = 125$ minutes?
16. What is the decay probability per second per nucleus of a substance with a half-life of 5.0 hours?
17. Tritium, the hydrogen isotope of mass 3, has a half-life of 12.3 y. What fraction of the tritium atoms remains in a sample after 50.0 y?
18. Suppose we have a sample containing 2.00 mCi of radioactive ^{131}I ($t_{1/2} = 8.04$ d). (*a*) How many decays per second occur in the sample? (*b*) How many decays per second will occur in the sample after four weeks?
19. Ordinary potassium contains 0.012 percent of the naturally occurring radioactive isotope ^{40}K, which has a half-life of 1.3×10^9 y. (*a*) What is the activity of 1.0 kg of potassium? (*b*) What would have been the fraction of ^{40}K in natural potassium 4.5×10^9 y ago?

12.7 Alpha Decay

20. Derive Eq. 12.23 from Eqs. 12.21 and 12.22.
21. For which of the following nuclei is alpha decay permitted? (*a*) ^{210}Bi; (*b*) ^{203}Hg; (*c*) ^{211}At.
22. Find the kinetic energy of the alpha particle emitted in the decay of ^{234}U.

12.8 Beta Decay

23. Derive Eqs. 12.29, 12.33, and 12.36.
24. Find the maximum kinetic energy of the electrons emitted in the negative beta decay of ^{11}Be.
25. ^{75}Se decays by electron capture to ^{75}As. Find the energy of the emitted neutrino.
26. ^{15}O decays to ^{15}N by positron beta decay. (*a*) What is the Q value for this decay? (*b*) What is the maximum kinetic energy of the positrons?

12.9 Gamma Decay and Nuclear Excited States

27. The nucleus ^{198}Hg has excited states at 0.412 and 1.088 MeV. Following the beta decay of ^{198}Au to ^{198}Hg, three gamma rays are emitted. Find the energies of these three gamma rays.
28. Compare the recoil energy of a nucleus of mass 200 that emits (*a*) a 5.0-MeV alpha particle, and (*b*) a 5.0-MeV gamma ray.
29. A certain nucleus has the following sequence of rotational states E_L (energies in keV): $E_0 = 0$, $E_1 = 100.1$, $E_2 = 300.9$, $E_3 = 603.6$, and $E_4 = 1010.0$. Assuming that the emitted gamma rays occur only from changes of one or two units in the rotational quantum number, find all possible photon energies that can be emitted from these states. Sketch the excited states, showing the allowed transitions.

12.10 Natural Radioactivity

30. The radioactive decay of ^{232}Th leads eventually to stable ^{208}Pb. A certain rock is examined and found to contain 3.65 g of ^{232}Th and 0.75 g of ^{208}Pb. Assuming all of the Pb was produced in the decay of Th, what is the age of the rock?
31. The $4n$ radioactive decay series begins with $^{232}_{90}$Th and ends with $^{208}_{82}$Pb. (*a*) How many alpha decays are in the chain? (See Question 22.) (*b*) How many beta decays? (*c*) How much energy is released in the complete chain? (*d*) What is the radioactive power produced by 1.00 kg of ^{232}Th ($t_{1/2} = 1.40 \times 10^{10}$ y)?
32. A piece of wood from a recently cut tree shows 12.4 ^{14}C decays per minute. A sample of the same size from a tree cut thousands of years ago shows 3.5 decays per minute. What is the age of this sample?

General Problems

33. Figure 12.2 suggests that the Rutherford scattering formula fails for 60° scattering when K is about 28 MeV. Use the results derived in Chapter 6 to find the closest distance between alpha particle and nucleus for this case, and compare with the nuclear radius of ^{208}Pb. Suggest a possible reason for any discrepancy.
34. Assuming the nucleus to diffract like a circular disk, use the data shown in Figure 12.3 to find the nuclear radius for ^{12}C and ^{16}O. How does changing the electron energy from 360 MeV to 420 MeV affect the deduced radius for ^{16}O? (*Hint:* Use the extreme relativistic approximation from Chapter 2 to relate the electron's energy and momentum to find its de Broglie wavelength.)
35. A radiation detector is in the form of a circular disc of diameter 3.0 cm. It is held 25 cm from a source of radiation, where it records 1250 counts per second. Assuming that the detector records every radiation incident upon it, find the activity of the sample (in curies).
36. What is the activity of a container holding 125 cm^3 of tritium (^{3}H, $t_{1/2} = 12.3$ y) at a pressure of 5.0×10^5 Pa (about 5 atm) at $T = 300$ K?
37. With a radioactive sample originally of N_0 atoms, we could measure the mean, or average, lifetime τ of a nucleus by measuring the number N_1 that live for a time t_1 and then decay, the number N_2 that decay after t_2 and so on:

$$\tau = \frac{1}{N_0}(N_1 t_1 + N_2 t_2 + \cdots)$$

(*a*) Show that this is equivalent to $\tau = \lambda \int_0^\infty e^{-\lambda t} t\, dt$. (*b*) Show that $\tau = 1/\lambda$. (*c*) Is τ longer or shorter than $t_{1/2}$?

38. Complete the following decays:
(*a*) $^{27}\text{Si} \rightarrow {}^{27}\text{Al} +$
(*b*) $^{74}\text{As} \rightarrow {}^{74}\text{Se} +$
(*c*) $^{228}\text{U} \rightarrow \alpha +$
(*d*) $^{93}\text{Mo} + \text{e}^- \rightarrow$
(*e*) $^{131}\text{I} \rightarrow {}^{131}\text{Xe} +$
39. ^{239}Pu decays by alpha emission with a half-life of 2.41×10^4 y. Compute the power output, in watts, that could be obtained from 1.00 gram of ^{239}Pu.
40. ^{228}Th alpha decays to an excited state of ^{224}Ra, which in turn decays to the ground state with the emission of a 217-keV photon. Find the kinetic energy of the alpha particle.
41. By replacing the Coulomb barrier in alpha decay with a flat barrier (see Figure 12.16) of thickness $L = \frac{1}{2}(R' - R)$, equal to half the thickness of the Coulomb barrier that the alpha particle must penetrate, and height $U_0 = \frac{1}{2}(U_\text{B} + K_\alpha)$, equal to half the height of the Coulomb barrier above the energy of the alpha particle, estimate the decay half-lives for ^{232}Th and ^{218}Th and compare with the measured values given in Table 12.2. (*Hint:* In calculating the speed of the alpha particle inside the nucleus, assume that the well depth is 30 MeV.) Although the results of this rough calculation do not agree well with the measured values, the calculation does indicate how barrier penetration is responsible for the enormous range of observed half-lives. How would you refine the calculation to obtain better agreement with the measured values?
42. (*a*) Using the same replacements described in Problem 41, estimate the decay probability of ^{226}Ra for alpha emission and for ^{14}C emission. (See Examples 12.8 and 12.9.) (*b*) Using the results of part (*a*), estimate the number of ^{14}C emitted relative to the number of alpha particles emitted by a source of ^{226}Ra.
43. Compute the recoil proton kinetic energy in neutron beta decay (*a*) when the electron has its maximum energy; (*b*) when the neutrino has its maximum energy.
44. In the beta decay of ^{24}Na, an electron is observed with a kinetic energy of 2.15 MeV. What is the energy of the accompanying neutrino?
45. The first excited state of ^{57}Fe decays to the ground state with the emission of a 14.4-keV photon in a mean lifetime of 141 ns. (*a*) What is the width ΔE of the state? (*b*) What is the recoil kinetic energy of an atom of ^{57}Fe that emits a 14.4-keV photon? (*c*) If the kinetic energy of recoil is made negligible by placing the atoms in a solid lattice, resonant absorptions will occur. What velocity is required to Doppler-shift the emitted photon so that resonance does not occur?
46. What is the probability of a ^{14}C atom in atmospheric CO_2 decaying in your lungs during a single breath? The atmosphere is about 0.03% CO_2. Assume you take in about 0.5 L of air in each breath and exhale it 3.5 s later.

Chapter 13

NUCLEAR REACTIONS AND APPLICATIONS

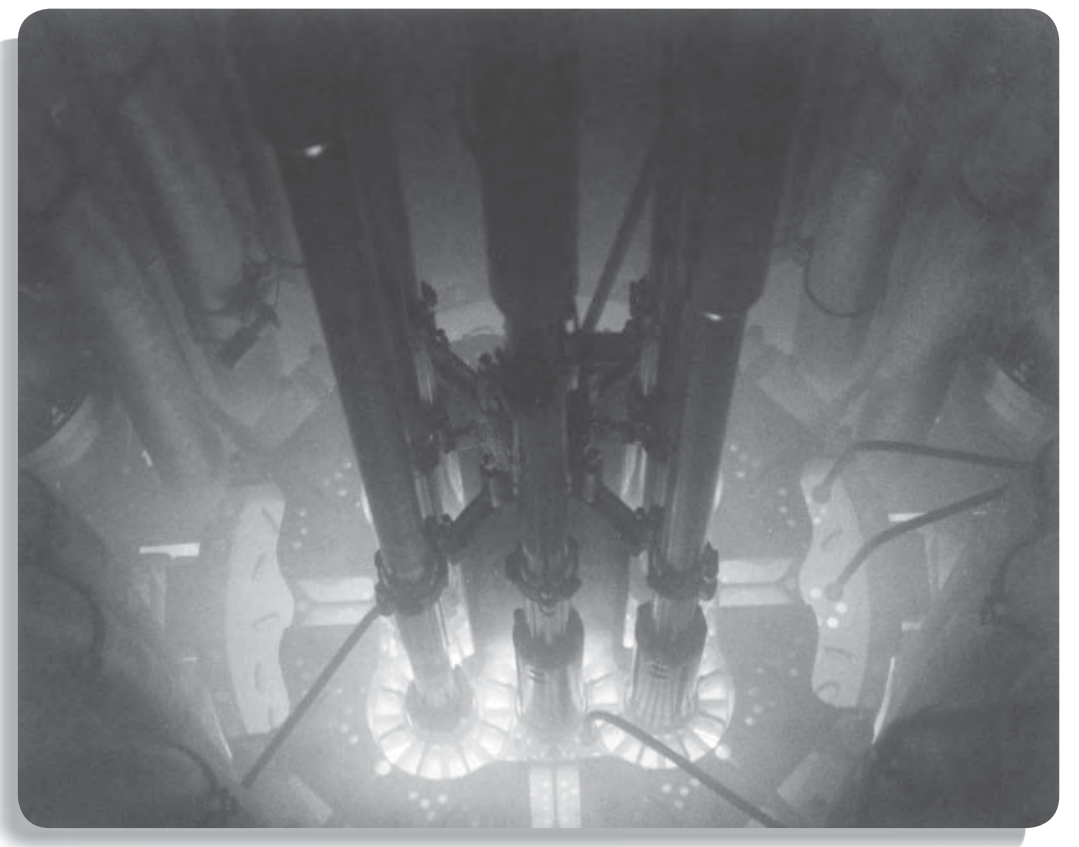

Nuclear reactors produce intense beams of neutrons that can be used to measure how radiation exposure affects various materials. They also produce rare radioisotopes that can be used for medicine and applications in industry. The photo shows the core of a nuclear reactor, which is submerged in water that acts as a neutron moderator. The glow comes from Cerenkov radiation, which is emitted when electrons from radioactive decays move at speeds greater than the speed of light in water.

The knowledge of the nucleus that we can obtain from studying radioactive decays is limited, because only certain radioactive processes occur in nature, only certain isotopes are made in those processes, and only certain excited states of nuclei (those that happen to follow radioactive decays) can be studied. Nuclear reactions, however, give us a controllable way to study *any* nuclear species, and to select any excited states of that species.

In this chapter we discuss some of the different nuclear reactions that can occur, and we study the properties of those reactions. Two nuclear reactions are of particular importance: fission and fusion. We pay special attention to those processes and we discuss how they are useful as sources of energy (or, more correctly, as *converters* of nuclear energy into thermal or electrical energy).

We conclude our study of nuclear physics with an introduction to some of the ways that methods of nuclear physics can be applied to problems in a variety of different areas.

13.1 TYPES OF NUCLEAR REACTIONS

In a typical nuclear reaction laboratory experiment, a beam of particles of type x is incident on a target containing nuclei of type X. After the reaction, an outgoing particle y is observed in the laboratory, leaving a residual nucleus Y. Symbolically, we write the reaction as

$$x + X \rightarrow y + Y$$

For example,

$$^{2}_{1}\mathrm{H}_{1} + ^{63}_{29}\mathrm{Cu}_{34} \rightarrow \mathrm{n} + ^{64}_{30}\mathrm{Zn}_{34}$$

Like a chemical reaction, a nuclear reaction must be balanced—the total number of protons must be the same before and after the reaction, and also the total number of neutrons must remain the same. In the example above, there are 30 protons on each side and 35 neutrons on each side. (The forces responsible for nuclear beta decay can change neutrons into protons or protons into neutrons, but these forces act on a typical time scale of at least 10^{-10} s. The projectile and target nuclei are within the range of one another's nuclear forces for an interval of at most 10^{-20} s, so there is not enough time for this type of proton-neutron conversion to take place.) The protons and neutrons can be rearranged among the reacting nuclei, but their numbers cannot change.

A nuclear reaction takes place under the influence of forces internal to the system of projectile and target. The absence of external forces means that the reaction conserves energy, linear momentum, and angular momentum.

In most experiments, we observe only the outgoing light particle y; the heavy residual nucleus Y usually loses all its kinetic energy (by collisions with other atoms) and therefore stops within the target.

We assume that we produce the reaction by bombarding target nuclei X, initially at rest, with projectiles x of kinetic energy K_x. The product particles then share this kinetic energy, plus or minus any additional energy from the rest energy difference of the initial and final nuclei. (We consider energy in nuclear reactions in Section 13.3.)

The bombarding particles x can be either charged particles, supplied by a suitable nuclear accelerator, or neutrons, whose source may be a nuclear reactor. Accelerators for charged particles, illustrated in Figures 13.1 and 13.2, are of two basic types. In a cyclotron, a particle is held in a circular orbit by a magnetic field and receives a small "kick" by an electric field twice each time it travels around the circle; a particle may make perhaps 100 orbits before finally emerging with a kinetic energy of the order of 10 to 20 MeV per unit of electric charge. In the Van de Graaff accelerator, a particle is accelerated only once from a single high-voltage terminal, which may be at a potential of as much as 25 million volts; the kinetic energy of the particle is then about 25 MeV per unit of charge.

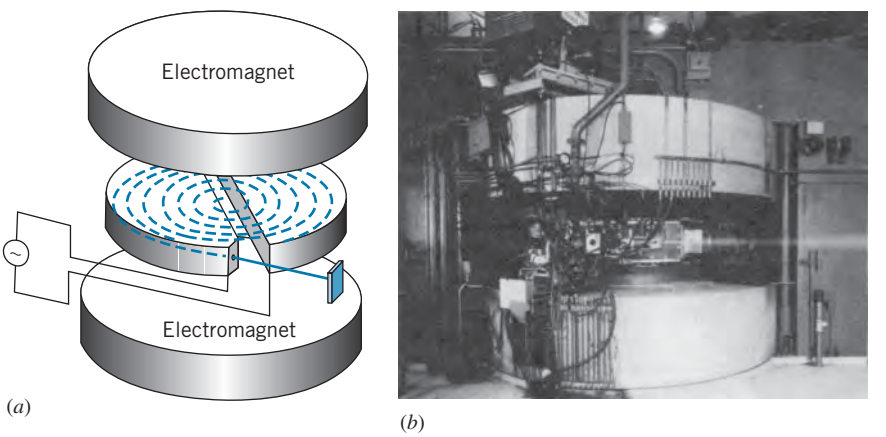

(*a*) (*b*)

FIGURE 13.1 (*a*) Schematic diagram of a cyclotron accelerator. Charged particles are bent in a circular path by a magnetic field and are accelerated by an electric field each time they cross the gap. (*b*) A cyclotron accelerator. The magnets are in the large cylinders at the top and the bottom. The beam of particles is visible as it collides with air molecules after leaving the cyclotron.

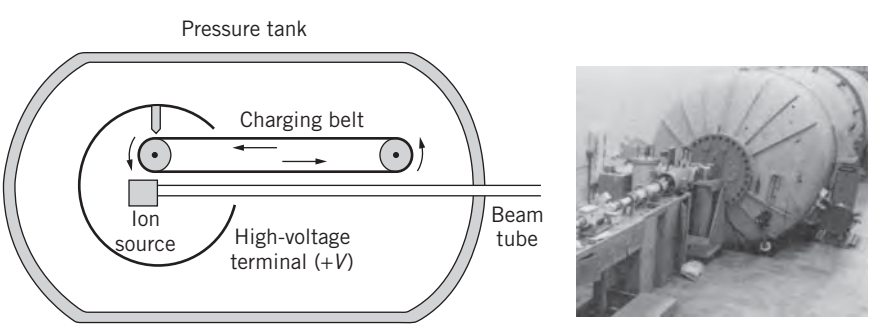

(*a*) (*b*)

FIGURE 13.2 (*a*) Diagram of a Van de Graaff accelerator. Particles from the ion source are accelerated from the high-voltage terminal to ground. (*b*) A typical Van de Graaff accelerator laboratory. The ion source and high-voltage terminal are inside the large pressure tank.

In nuclear reaction experiments, we usually measure two basic properties of the particle y: its energy, and its probability to emerge at a certain angle with a certain energy. We look briefly at these two types of measurements.

1. Measuring the particle energy If neither the residual nucleus Y nor the outgoing particle y had excited states, then by using conservation of energy and momentum, we could calculate exactly the energy of y when measured at a certain angle. If the nucleus Y is left in an excited state, then the kinetic energy of y is reduced by (approximately) the energy of the excited state above the ground state, because the two particles Y and y must still share the same amount of total energy. Each higher excited state of the nucleus Y corresponds to a certain reduced energy of the particle y, and a measurement of the different energies of the particle y tells us about the excited states of the nucleus Y. Figure 13.3 shows an example of a typical set of experimental results and the corresponding deduced excited states of the residual nucleus. Each peak in Figure 13.3 corresponds to a specific energy of y, and therefore to a specific excited state of Y; that is, when particles with energy 9.0 MeV are observed, the nucleus Y is left in the excited state with energy 1.0 MeV.

2. Measuring the reaction probability Notice that the different peaks in Figure 13.3 have different heights. This feature of the results of our experiment tells us that it is more probable for the reaction to lead to one excited state than to another. This is an example of the reaction probability, the second of the properties of y that we can determine. For example, Figure 13.3 shows that the probability of leaving Y in its second excited state (1.0 MeV) is about twice the probability of leaving Y in its first excited state. If it were possible to solve the Schrödinger equation with the nuclear potential energy, we could calculate these reaction probabilities and compare them with experiment. Unfortunately we can't solve this many-body problem, so we must work backward by measuring the reaction probabilities and then trying to infer some properties of the nuclear force.

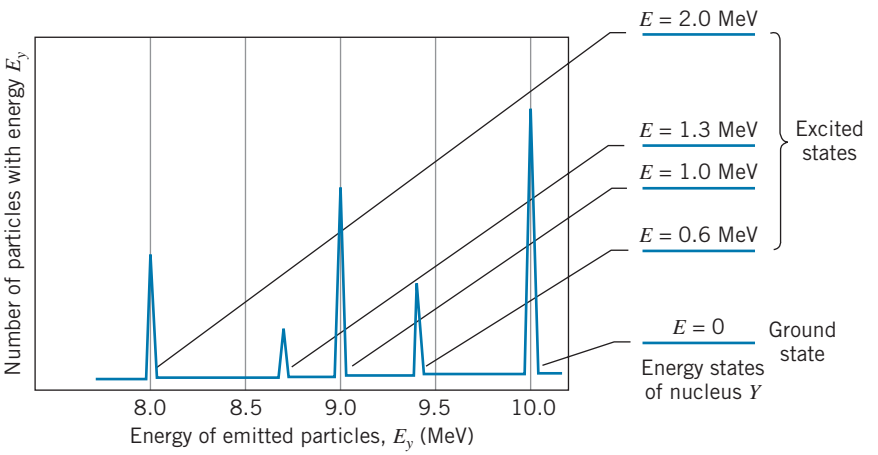

FIGURE 13.3 A sample spectrum of energies of the outgoing particle y, and the corresponding excited states of Y.

The Reaction Cross Section

Reaction probabilities are usually expressed in terms of the *cross section,* which is a sort of effective area presented by the target nucleus to that projectile for a specific reaction, for all possible energies and directions of travel of the outgoing particle y. The larger the reaction probability, the larger is the corresponding cross section. In general, the cross section depends on the energy of the incident particle, K_x.

The cross section σ is expressed in units of area, but the area is a very small one, of the order of $10^{-28}\ \text{m}^2$. Nuclear physicists use this as a convenient unit of measure for cross sections, and it is known as one *barn* (b): 1 barn = $10^{-28}\ \text{m}^2$. Notice that the area of the disc of a single nucleus of medium weight is about 1 barn; however, reaction cross sections often can be very much greater or less than one barn. For example, consider the cross section for these reactions involving certain isotopes of the neighboring elements iodine and xenon:

$$\begin{aligned}
\text{I} + \text{n} &\rightarrow \text{I} + \text{n} \text{ (inelastic scattering)} & \sigma &= 4\ \text{b} \\
\text{Xe} + \text{n} &\rightarrow \text{Xe} + \text{n} \text{ (inelastic scattering)} & \sigma &= 4\ \text{b} \\
\text{I} + \text{n} &\rightarrow \text{I} + \gamma \text{ (neutron capture)} & \sigma &= 7\ \text{b} \\
\text{Xe} + \text{n} &\rightarrow \text{Xe} + \gamma \text{ (neutron capture)} & \sigma &= 10^6\ \text{b}
\end{aligned}$$

You can see that, although the neutron inelastic scattering cross sections of I and Xe are similar, the neutron capture cross sections are very different. These measurements are therefore telling us something interesting and unusual about the properties of the nucleus Xe.

Suppose a beam of particles is incident on a thin target of area S, which contains a total of N nuclei. The effective area of each nucleus is the cross section σ, and so the total effective area of all the nuclei in the target is (ignoring shadowing effects) σN. The fraction of the target area that this represents is $\sigma N/S$, and as long as this ratio is small, shadowing effects are negligible. This fraction is the probability for the reaction to occur.

Suppose the incident particles strike the target at a rate of I_0 particles per second, and suppose the outgoing particles y are emitted at a rate of R per second. (This is also the rate at which the product nucleus Y is formed.) Then the reaction probability can also be expressed as the rate of y divided by the rate of x, or R/I_0. Setting the two expressions for the reaction probability equal to each other, we obtain $\sigma N/S = R/I_0$, or

$$R = \frac{\sigma N}{S} I_0 \tag{13.1}$$

This gives a relationship between the reaction cross section and the rate of emission of y.

In a reactor, the intensity of neutrons is usually expressed in terms of the rate at which neutrons cross a unit area perpendicular to the beam, or *neutron flux* ϕ (neutrons/cm^2/s). The cross section is σ (square centimeter per nucleus per incident neutron). The rate R also depends on the number of target nuclei. Suppose the mass of the target is m; the number of target nuclei is then $N = (m/M)N_\text{A}$, where M is the molar mass, and N_A is Avogadro's constant (6.02×10^{23} atoms per mole). Thus, for neutron-induced reactions, using Eq. 13.1 we obtain

$$R = \phi\sigma N = \phi\sigma \frac{m}{M} N_\text{A} \tag{13.2}$$

Example 13.1

For a certain incident proton energy the reaction $p + {}^{56}Fe \rightarrow n + {}^{56}Co$ has a cross section of 0.40 b. If we bombard a target in the form of a 1.0-cm-square, 1.0-μm-thick iron foil with a beam of protons equivalent to a current of 3.0 μA, and if the beam is spread uniformly over the entire surface of the target, at what rate are the neutrons produced?

Solution

We first calculate the number of nuclei in the target. The volume of the target is $V = (1.0\,\text{cm})^2(1.0\,\mu\text{m}) = 1.0 \times 10^{-4}\,\text{cm}^3$, and (using the density of iron of $7.9\,\text{g/cm}^3$) its mass is $m = \rho V = (7.9\,\text{g/cm}^3)(1.0 \times 10^{-4}\,\text{cm}^3) = 7.9 \times 10^{-4}$ g. The number of atoms (or nuclei) is then

$$N = \frac{mN_A}{M} = \frac{(7.9 \times 10^{-4}\ \text{g})(6.02 \times 10^{23}\ \text{atoms/mole})}{56\ \text{g/mole}}$$
$$= 8.5 \times 10^{18}\ \text{atoms}$$

Next we need to find the number of particles per second in the incident beam. We are given that the current is $3.0 \times 10^{-6}\,\text{A} = 3.0 \times 10^{-6}\,\text{C/s}$, and with each proton having a charge of 1.6×10^{-19} C, the beam intensity is

$$I_0 = \frac{3.0 \times 10^{-6}\ \text{C/s}}{1.6 \times 10^{-19}\ \text{C/particle}} = 1.9 \times 10^{13}\ \text{particles/s}$$

From Eq. 13.1 we can now find R:

$$R = \frac{N\sigma I_0}{S}$$
$$= (8.5 \times 10^{18}\ \text{nuclei})(0.40 \times 10^{-24}\ \text{cm}^2\text{/nucleus})$$
$$\times (1.9 \times 10^{13}\ \text{particles/s})\ (1\ \text{cm}^2)^{-1}$$
$$= 6.5 \times 10^{7}\ \text{particles/s}$$

About 10^8 neutrons per second are emitted from the target.

13.2 RADIOISOTOPE PRODUCTION IN NUCLEAR REACTIONS

Often we use nuclear reactions to produce radioactive isotopes. In this procedure, a stable (nonradioactive) isotope X is irradiated with the particle x to form the radioactive isotope Y; the outgoing particle y is of no interest and is not observed. In this case we don't observe the individual particles Y as they are produced in the reaction; instead, we irradiate the target to produce some number of radioactive Y nuclei that remain within the target. After the irradiation we observe the radioactive decay of the nuclei Y.

We would like now to calculate the activity of the isotope Y that is produced from a given exposure to a certain quantity of the particle x for a certain time t. Let R represent the constant rate at which Y is produced; this quantity is related to the cross section and to the intensity of the beam of x, as given in Eq. 13.1. In a time interval dt, the number of Y nuclei produced is $R\,dt$. The isotope Y is radioactive, so the number of nuclei of Y that decay in the interval dt is $\lambda N\,dt$, where λ is the decay constant ($\lambda = 0.693/t_{1/2}$) and N is the number of Y nuclei present. The net change dN in the number of Y nuclei is

$$dN = R\,dt - \lambda N\,dt \tag{13.3}$$

or

$$\frac{dN}{dt} = R - \lambda N \tag{13.4}$$

The solution to this differential equation is

$$N(t) = \frac{R}{\lambda}(1 - e^{-\lambda t}) \tag{13.5}$$

and the activity is

$$a(t) = \lambda N = R(1 - e^{-\lambda t}) \tag{13.6}$$

Notice that, as expected, $a = 0$ at $t = 0$ (there are no nuclei of type Y present at the start). For large irradiation times $t \gg t_{1/2}$, this expression approaches the constant value R. When t is small compared with the half-life $t_{1/2}$, the activity increases linearly with time:

$$a(t) = R[1 - (1 - \lambda t + \cdots)] \cong R\lambda t \qquad (t \ll t_{1/2}) \tag{13.7}$$

Figure 13.4 shows the relationship between $a(t)$ and t. As you can see, not much activity is gained by irradiating for more than about two half-lives.

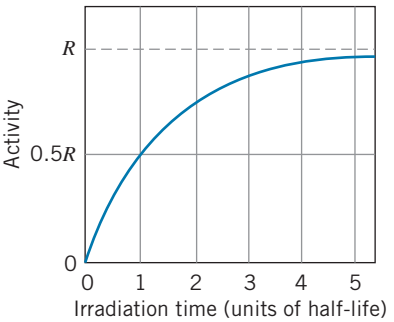

FIGURE 13.4 Formation of activity in a nuclear reaction.

Example 13.2

Thirty milligrams of gold are exposed to a neutron flux of 3.0×10^{12} neutrons/cm^2/s for 1.0 minute. The neutron capture cross section of gold is 99 b. Find the resultant activity of ^{198}Au.

Solution

From Appendix D we find that the stable isotope of gold has a mass number of $A = 197$, and that radioactive ^{198}Au has a half-life of 2.70 d $= 3.88 \times 10^3$ min. Thus, using Eq. 13.2,

$$R = \phi\sigma \frac{m}{M} N_A$$

$$= \left(3.0 \times 10^{12} \frac{\text{neutrons}}{\text{cm}^2 \cdot \text{s}}\right)\left(99 \times 10^{-24} \frac{\text{cm}^2}{\text{neutron} \cdot \text{nucleus}}\right) \times \left(\frac{0.030 \text{ g}}{197 \text{ g/mole}}\right)(6.02 \times 10^{23} \text{ atoms/mole})$$

$$= 2.7 \times 10^{10} \text{ s}^{-1}$$

In this case $t \ll t_{1/2}$, so we can use Eq. 13.7:

$$a = R\lambda t = (2.7 \times 10^{10} \text{ s}^{-1})\left(\frac{0.693}{3.88 \times 10^3 \text{ min}}\right)(1.0 \text{ min})$$

$$= 4.8 \times 10^6 \text{ s}^{-1} = 130 \ \mu\text{Ci}$$

Example 13.3

The radioactive isotope ^{61}Cu ($t_{1/2} = 3.41$ h) is to be produced by alpha particle reactions on a target of ^{59}Co. A foil of cobalt, measuring 1.5 cm $\times$ 1.5 cm in area and 2.5 μm in thickness, is placed in a 12.0-μA beam of alpha particles; the beam uniformly covers the target. For the alpha energy selected, the reaction has a cross section of 0.640 b. (*a*) At what rate is the ^{61}Cu produced? (*b*) What is the resulting activity of ^{61}Cu after 2.0 h of irradiation?

Solution

(*a*) The reaction is $^{59}\text{Co} + {}^4\text{He} \rightarrow {}^{61}\text{Cu} + 2n$. The mass of the target is $m = \rho V = (8.9 \text{ g/cm}^3)(1.5 \text{ cm})^2(2.5 \times 10^{-4} \text{ cm}) = 5.0 \times 10^{-3}$ g and the number of target atoms is

$$N = \frac{mN_A}{M}$$

$$= \frac{(5.0 \times 10^{-3} \text{ g})(6.02 \times 10^{23} \text{ atoms/mole})}{58.9 \text{ g/mole}}$$

$$= 5.12 \times 10^{19} \text{ atoms}$$

The rate at which the beam strikes the target is

$$I_0 = \frac{12.0 \times 10^{-6} \text{ A}}{2 \times 1.60 \times 10^{-19} \text{ C/particle}}$$

$$= 3.75 \times 10^{13} \text{ particles/s}$$

The rate at which the ^{61}Cu is produced is, using Eq. 13.1,

$$R = \frac{N\sigma I_0}{S} = \frac{(5.12 \times 10^{19}\ \text{atoms})(0.640 \times 10^{-24}\ \text{cm}^2)(3.75 \times 10^{13}\ \text{s}^{-1})}{(1.5\ \text{cm})^2} = 5.5 \times 10^8\ \text{s}^{-1}$$

(*b*) The activity is determined from Eq. 13.6:

$$a = R(1 - e^{-\lambda t}) = (5.5 \times 10^8\ \text{s}^{-1})\ (1 - e^{-(0.693)(2.0\ \text{h})/(3.41\text{h})}) = 1.8 \times 10^8\ \text{s}^{-1} = 4.9\,\text{mCi}$$

13.3 LOW-ENERGY REACTION KINEMATICS

We assume for this discussion that the velocities of the nuclear particles are sufficiently small that we can use nonrelativistic kinematics. We consider a projectile x moving with momentum $\vec{\mathbf{p}}_x$ and kinetic energy K_x. The target is at rest, and the reaction products have momenta $\vec{\mathbf{p}}_y$ and $\vec{\mathbf{p}}_Y$ and kinetic energies K_y and K_Y. The particles y and Y are emitted at angles θ_y and θ_Y with respect to the direction of the incident beam. Figure 13.5 illustrates this reaction. We assume that the resultant nucleus Y is not observed in the laboratory (if it is a heavy nucleus, moving relatively slowly, it generally stops within the target).

As we did in the case of radioactive decay, we use energy conservation to compute the Q value for this reaction (assuming X is initially at rest):

initial energy = final energy

$$m_N(x)c^2 + K_x + m_N(X)c^2 = m_N(y)c^2 + K_y + m_N(Y)c^2 + K_Y \tag{13.8}$$

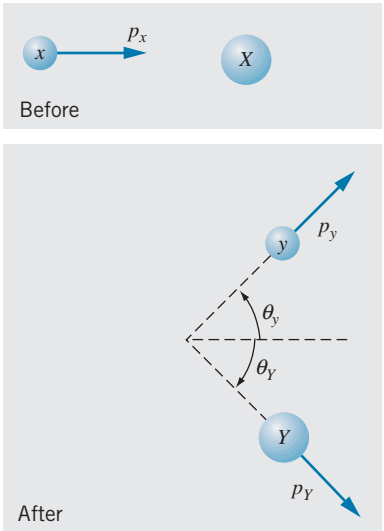

FIGURE 13.5 Momenta of particles before (top) and after (bottom) the reaction.

The m's in Eq. 13.8 represent the *nuclear* masses of the reacting particles. However, as we have discussed, the number of protons must be balanced in a nuclear reaction:

$$Z_x + Z_X = Z_y + Z_Y \tag{13.9}$$

We can therefore add equal numbers of electron masses to each side of Eq. 13.8 and, neglecting as usual the electron binding energy, the nuclear masses become atomic masses with no additional corrections needed. Rewriting Eq. 13.8, we obtain

$$[m(x) + m(X) - m(y) - m(Y)]c^2 = K_y + K_Y - K_x \tag{13.10}$$

The rest energy difference between the initial particles and final particles is defined to be the Q *value* of the reaction

$$Q = (m_\text{i} - m_\text{f})c^2 = [m(x) + m(X) - m(y) - m(Y)]c^2 \tag{13.11}$$

and, combining Eqs. 13.10 and 13.11, we see that the Q value is equal to the difference in kinetic energy between the final particles and initial particle:

$$Q = K_y + K_Y - K_x \tag{13.12}$$

Example 13.4

(*a*) Compute the Q value for the reaction $^2\text{H} + {}^{63}\text{Cu} \rightarrow \text{n} + {}^{64}\text{Zn}$. (*b*) Deuterons of energy 12.00 MeV are incident on a ^{63}Cu target, and neutrons are observed with 16.85 MeV of kinetic energy. Find the kinetic energy of the ^{64}Zn.

Solution

(*a*) The Q value can be found using Eq. 13.11 with masses from Appendix D:

$$Q = [m(^2\text{H}) + m(^{63}\text{Cu}) - m(\text{n}) - m(^{64}\text{Zn})]c^2$$

$$= (2.014102\,\text{u} + 62.929597\,\text{u} - 1.008665\,\text{u} - 63.929142\,\text{u})(931.5\,\text{MeV/u})$$

$$= 5.488\,\text{MeV}$$

(*b*) From Eq. 13.12, we find

$$K_Y = Q + K_x - K_y$$

$$= 5.488\,\text{MeV} + 12.00\,\text{MeV} - 16.85\,\text{MeV}$$

$$= 0.64\,\text{MeV}$$

Reactions for which $Q > 0$ convert nuclear energy to kinetic energy of y and Y. They are called *exothermic* or *exoergic* reactions. Reactions with $Q < 0$ require energy input, in the form of the kinetic energy of x, to be converted into nuclear binding energy. These are known as *endothermic* or *endoergic* reactions.

In an endoergic reaction, we must supply at least enough kinetic energy to provide the additional rest energy of the reaction products. There is thus some minimum, or *threshold*, kinetic energy of x, below which the reaction will not take place. This threshold kinetic energy not only must supply the additional rest energy of the products, but also must supply some kinetic energy of the products; even at the minimum energy, the products cannot be at rest, for that would violate conservation of linear momentum—the momentum p_x before the collision would not be equal to the momentum of the final products after the collision if they were formed at rest.

This problem is most easily analyzed in the center-of-mass reference frame. In the lab frame before the reaction, the center of mass moves with velocity $v = m(x)v_x/[m(x) + m(X)]$. If we travel with that velocity and observe the reaction, we would see x moving with velocity $v_x - v$ and X moving with velocity $-v$, as shown in Figure 13.6. If x has exactly the threshold kinetic energy, in this reference frame the reaction products y and Y would be at rest.

We must conserve total relativistic energy $K + mc^2$ in the reaction, and we restrict our discussion to small velocities $v \ll c$ so that the nonrelativistic expression for the kinetic energy can be used. Energy conservation in the center-of-mass frame gives:

$$\frac{1}{2}m(x)(v_x - v)^2 + \frac{1}{2}m(X)(-v)^2 + m(x)c^2 + m(X)c^2 = m(y)c^2 + m(Y)c^2 \tag{13.13}$$

where v_x represents the threshold velocity in the lab frame. Substituting the value of v and doing a bit of algebra, we can find the threshold kinetic energy (in the laboratory reference frame):

$$K_{\text{th}} = -Q\left(1 + \frac{m(x)}{m(X)}\right) \tag{13.14}$$

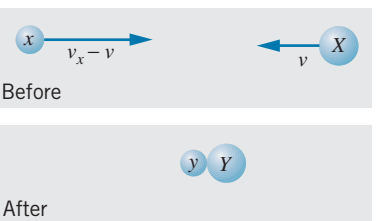

FIGURE 13.6 Reaction at threshold in center-of-mass reference frame.

Example 13.5

Calculate the threshold kinetic energy for the reaction $p + {}^3H \rightarrow {}^2H + {}^2H$ (*a*) if protons are incident on ^3H at rest; (*b*) if ^3H (tritons) are incident on protons at rest.

Solution

The Q value is

$$\begin{aligned} Q &= [m({}^1H) + m({}^3H) - 2m({}^2H)]c^2 \\ &= (1.007825\,u + 3.016049\,u - 2 \times 2.014102\,u) \\ &\quad \times (931.5\,MeV/u) \\ &= -4.033\,MeV \end{aligned}$$

(*a*) When protons are incident on ^3H, the identification is $x = {}^1H, X = {}^3H$, so

$$K_{th} = -Q\left(1 + \frac{m({}^1H)}{m({}^3H)}\right)$$

$$= (4.033\,MeV)\left(1 + \frac{1.007825\,u}{3.016049\,u}\right) = 5.381\,MeV$$

(*b*) When ^3H is incident on protons, the identification of x and X is reversed, so

$$K_{th} = -Q\left(1 + \frac{m({}^3H)}{m({}^1H)}\right)$$

$$= (4.033\,MeV)\left(1 + \frac{3.016049\,u}{1.007825\,u}\right) = 16.10\,MeV$$

This calculation illustrates a general result: Less energy is required for a nuclear reaction if a light particle is incident on a heavy target than if a heavy particle is incident on a light target.

Lise Meitner (1878–1968, Germany-Sweden). Known for her research into radioactivity, Meitner discovered the radioactive element protactinium ($Z = 91$) and was among the first to study the properties of beta decay. Her most important discovery was the explanation for the puzzling results that were observed when uranium was bombarded with neutrons. She suggested that the uranium could split into two pieces, and she proposed the name "fission" for this process. Element 109 is named in her honor.

13.4 FISSION

The massive nucleus ^{254}Cf ($Z = 98$) can be produced in accelerators by collisions between suitably chosen projectiles and targets. This nucleus is of special interest because it is also produced in supernova explosions, and knowledge of its properties provides a key to understanding the formation of the elements in stars, as we discuss later in this chapter. ^{254}Cf is radioactive, decaying with a half-life of 60.5 d. The Q values for positive and negative beta decay of ^{254}Cf are both negative, so that mode of decay is not available. Alpha decay is energetically possible but the Coulomb barrier is very high, making that decay mode improbable. Instead, ^{254}Cf decays by splitting into two pieces of much smaller masses—for example,

$$^{254}_{98}Cf_{156} \rightarrow {}^{140}_{54}Xe_{86} + {}^{110}_{44}Ru_{66} + 4n$$

This mode of decay is known as *nuclear fission*. Fission can occur as a spontaneous radioactive decay process for a relatively small number of massive nuclei, and it can also be induced in other nuclei by adding energy to make the nucleus less stable. In addition to the two fission fragments, some neutrons are usually emitted in the fission process.

We can consider the nucleus to be a mixture of protons and neutrons moving about under the mutual attraction of their nuclear forces and (in the case of the protons) the repulsion of their Coulomb forces. For many nuclei, the result of these interactions is a spherical shape that has often been compared to a drop of liquid floating freely in a region where no external forces act. The equilibrium shape will be close to spherical, and if the nucleus is distorted (for example, by stretching it in one direction) it can vibrate about its equilibrium shape and eventually return to its spherical shape somewhat like a stretched spring or other elastic system returns to its original configuration. Figure 13.7 shows a schematic representation of the energy of the drop as a function of the distortion.

For other nuclei, the equilibrium shape is not spherical but is already distorted; their surfaces are like an ellipse rotated about its long axis. For these nuclei, the major axis might be 30–50% longer than the minor axis. If these nuclei are stretched by a small amount and released, they will usually revert to their distorted equilibrium shape. But if the stretching is sufficiently large, they may not return to equilibrium but instead may split in two, as represented in Figure 13.8.

This occurs because of the rather delicate balance between the nuclear force that keeps the nucleus together and the Coulomb repulsion force, which makes the nucleus less stable. When the stretching is sufficiently large, the total attractive nuclear force is reduced (because on the average the protons and neutrons have fewer "near neighbors" with which to interact), but the Coulomb force, because it has a long range, is not reduced significantly. The center of the distorted shape can be "pinched off" and the delicate balance between the nuclear and Coulomb forces is upset. The Coulomb force can then drive the two fragments apart.

Figure 13.8 shows a kind of "barrier" between the distorted equilibrium shape and the fissioned nucleus. This fission barrier has a height of roughly 6 MeV, but as we know it is possible to "tunnel" through the barrier. Thus nuclei can undergo fission with smaller amounts of excitation energy. It is very unlikely for a nucleus to tunnel through the barrier at its thickest, but as the excitation energy is increased the barrier becomes less thick and fission becomes more probable. For the radioactive decay of ^{254}Cf, the probability to penetrate the fission barrier (99.7%) is greater than the probability to penetrate the barrier to alpha decay (0.3%).

The splitting of a nucleus such as ^{254}Cf into two fragments does not always produce the same set of final nuclei. Many different processes are possible, with the actual outcome determined according to statistical probability. For ^{254}Cf it is most likely that one fragment will have a mass near $A = 110$ and the other near $A = 140$, but other mass distributions can occur. Figure 13.9 shows the mass distribution of the fragments in the fission of ^{254}Cf and ^{235}U.

The number of neutrons emitted in fission can also vary. For ^{254}Cf, the average is about 3.9 neutrons per fission.

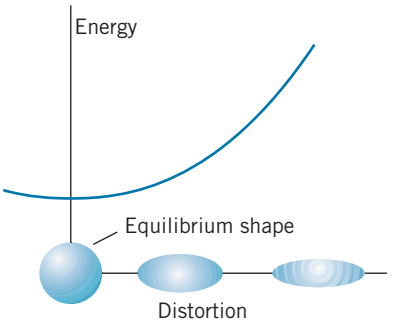

FIGURE 13.7 The energy of a nucleus with a spherical equilibrium shape increases as the distortion increases.

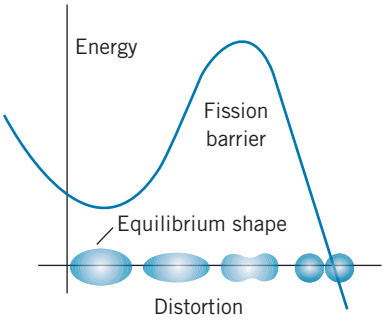

FIGURE 13.8 The energy of a nucleus with a nonspherical equilibrium shape. If enough energy is added, the nucleus can tunnel through the fission barrier and split into two pieces.

Energy Released in Fission

According to Figure 12.4, the binding energy per nucleon of ^{254}Cf is about 7 MeV. If a nucleus of ^{254}Cf splits into two nuclei with $A = 127$, the binding energy per nucleon of the final nuclei would be about 8 MeV. Thus the binding energy of each of those 254 nucleons increases from about 7 MeV to about 8 MeV, which gives an increase in the total binding energy of the nucleus of about 250 MeV. If the final nucleons are more tightly bound, that means that an equivalent amount of energy has been released to some other form.

This energy release from a single nucleus is an enormous quantity. For comparison, chemical processes such as combustion usually release a few eV per atom. In fission we have an energy release at the atomic level that is 10^8 times larger than the energy released in chemical processes!

Where does this energy go? Let's imagine that ^{254}Cf suddenly breaks in half to form two nuclei with $Z = 49$ and $A = 127$ that are just touching at their surfaces. The radius of each of these nuclei is $1.2(127)^{1/3} = 6.0$ fm, and the Coulomb repulsion of these two nuclei would be $U = (49e)^2/4\pi\varepsilon_0(2R) = 286$ MeV, which is quite close to our estimate of the nuclear binding energy released. These two charged objects repel one another, so that the Coulomb energy quickly becomes kinetic energy. Most of the energy released in fission is thus produced as

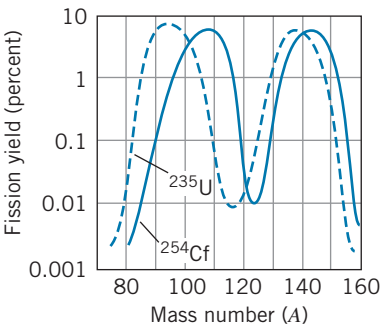

FIGURE 13.9 The mass distribution of fission fragments from ^{254}Cf (solid line) and ^{235}U (dashed line).

Nuclear binding energy
↓
Coulomb potential energy of nuclear fragments
↓
Kinetic energy of fragments

About 80% of the fission energy is released in this form. The fragments do not travel very far before dissipating their kinetic energy through atomic collisions, which are usually observed as a temperature increase of the material. In a power reactor, this temperature increase can be used to produce steam, which can drive a turbine to produce electricity. The remaining 20% of the energy released appears as decay products (betas and gammas) of the highly radioactive fragments and kinetic energies of the neutrons that may also be emitted during fission.

Induced Fission

The radioactive decay of ^{254}Cf is an example of the spontaneous fission of a nucleus that is sufficiently unstable that it can tunnel through the fission barrier with no additional energy needed. However, ^{254}Cf is an artificially produced nucleus that does not occur in nature and in which the energy released in fission is essentially stored in the nucleus by the nuclear reaction that was used to produce the ^{254}Cf. There are other examples of fissionable nuclei that may occur naturally or are produced artificially but that do not fission spontaneously. These nuclei can be made to fission by the addition of some energy, which might be in the form of an absorbed photon but more often occurs with the absorption of a neutron. In these cases the energy input is very small compared with the energy released in the fission process. One such nucleus is ^{235}U, which might absorb a neutron to make ^{236}U and then fission according to

$$^{235}_{92}\mathrm{U}_{143} + \mathrm{n} \rightarrow {}^{93}_{37}\mathrm{Rb}_{56} + {}^{141}_{55}\mathrm{Cs}_{86} + 2\mathrm{n}$$

As in the case of spontaneous fission, many different outcomes are possible, with a statistical distribution of the masses of the fragments. In the fission of ^{235}U, the most probable outcome has fragments of mass numbers near $A = 90$ and $A = 140$ (as in Figure 13.9), and the average number of neutrons is about 2.5. Examples of easily produced fissionable nuclei include ^{239}Pu (obtained from the beta decay of ^{239}U, which is made when ^{238}U absorbs a neutron) and ^{233}U (obtained in a similar manner from ^{232}Th).

In a bulk sample of uranium, each of the neutrons emitted in fission can be absorbed by another nucleus of ^{235}U and thus induce another fission process, resulting in the emission of still more neutrons, followed by more fissions, and so forth. As long as the average number of neutrons available to produce new fissions is greater than 1 per reaction, the number of fissions grows with time. This avalanche or *chain reaction* of fission events, each with the release of about 200 MeV of energy, can either occur under very rapid and uncontrolled conditions, as in a nuclear weapon, or else under slower and carefully controlled conditions, as in a nuclear reactor.

Electrical Power from Fission

Electrical power can be generated using the thermal energy released in fission to boil water. Ordinary uranium by itself cannot serve as fuel for the reactor for several reasons, of which three in particular stand out: enrichment, moderation, and control.

Enrichment To maintain a steady energy production from fission reactions, we would like for one neutron from each fission to be available to produce another fission. Generally the average number of neutrons produced is greater than one, but neutrons can be lost from the reaction in a variety of ways (for example, by non-fission absorption by ^{238}U in uranium fuel). Natural uranium consists of only about 0.7% of ^{235}U and 99.3% ^{238}U, which means that most of the available uranium nuclei generally do not participate in the fission process but instead remove neutrons from being able to produce other fissions. To overcome this problem it is necessary to use *enriched* uranium, in which the abundance of ^{235}U is increased beyond its natural value of 0.7%. Most power reactors use uranium enriched to 3–5% ^{235}U. Enrichment is a difficult process because ^{235}U and ^{238}U are chemically identical. It is achieved only by taking into account the small mass difference between the two isotopes (for example, by forcing gaseous uranium through a porous barrier in which the more massive ^{238}U atoms diffuse more slowly).

Moderation The neutrons produced in fission typically have kinetic energies of a few MeV. Such energetic neutrons have a relatively low probability of inducing new fissions, because the fission cross section generally decreases rapidly with increasing neutron energy. We therefore must slow down, or *moderate*, these neutrons in order to increase their chances of initiating fission events. The fissionable material is surrounded by a *moderator*, and the neutrons lose energy in collisions with the atoms of the moderator. When a neutron is scattered from a heavy nucleus like uranium, the energy of the neutron is changed hardly at all, but in a collision with a very light nucleus, the neutron can lose substantial energy. The most effective moderator is one whose atoms have about the same mass as a neutron; hydrogen is therefore the first choice. Ordinary water is frequently used as a moderator, because collisions with the protons are very effective in slowing the neutrons; however, neutrons have a relatively high probability of being absorbed by the water according to the reaction $\mathrm{p} + \mathrm{n} \rightarrow {}^{2}_{1}\mathrm{H}_{1} + \gamma$. So-called "heavy water," in which the hydrogen is replaced by deuterium, is more useful as a moderator, because it has virtually no neutron absorption cross section. A heavy-water reactor, which has more available neutrons, can use ordinary (nonenriched) uranium as fuel; a reactor using ordinary water as moderator has fewer neutrons available to produce fission, and must therefore have more ^{235}U in its core.

Carbon is a light material that is solid, stable, and abundant, and that has a relatively small neutron absorption cross section. Enrico Fermi and his co-workers built the first nuclear reactor in 1942 at the University of Chicago; this reactor used carbon, in the form of graphite blocks, as moderator.

Control To produce a stable nuclear reactor, the average number of neutrons in each fission reaction that is available to produce the next set of fission reactions must be exactly equal to 1. If it is even slightly greater than 1, the reaction rate will grow exponentially out of control. Control of the reaction rate is usually accomplished by inserting into the core of the reactor control rods made of cadmium, which has a very large cross section for absorbing neutrons and thus removing them from the fission process. However, small fluctuations in the reaction rate occur much too rapidly for any mechanical system to move the control rods in and out to control the number of neutrons emitted in the fission reaction.

Fortunately, nature has provided us with the solution to this problem. About 1% of the neutrons emitted in fission are *delayed neutrons*, produced not at the instant of fission but somewhat later, following the radioactive decays of the fission fragments. For example ^{93}Rb, which might be produced in the fission of

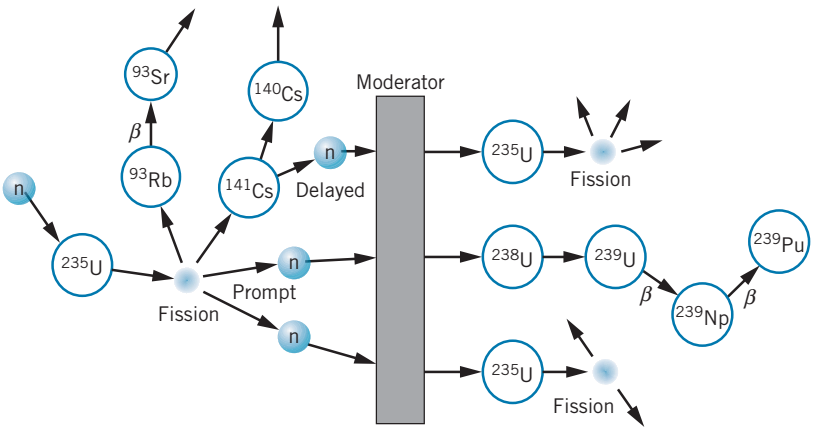

FIGURE 13.10 A typical sequence of processes in fission. A nucleus of ^{235}U absorbs a neutron and fissions; two prompt neutrons and one delayed neutron are emitted. Following moderation, two neutrons cause new fissions and the third is captured by ^{238}U, resulting finally in ^{239}Pu.

^{235}U, beta decays with a half-life of 6 s to ^{93}Sr, which is occasionally (in about 1% of decays) produced in a very high excited state that is unstable to neutron emission. The neutron appears to emerge with the 6-s half-life of the beta decay. This short delay time is enough to allow the control rods to be adjusted to maintain a constant reaction rate. The reactor is designed so that the neutron replication rate is just less than 1 for the prompt neutrons and exactly equal to 1 for prompt + delayed neutrons, which allows the control rods to work effectively.

Figure 13.10 summarizes some of the processes that can occur in fission. A nucleus of ^{235}U captures a neutron and fissions into two heavy fragments and two prompt neutrons; one of the fragments emits a delayed neutron. The three neutrons are slowed by passage through the moderator. Two of the neutrons cause new fissions, and the third is captured by ^{238}U, eventually to form fissionable ^{239}Pu, which can be recovered from the fuel by chemical means. Not shown in this diagram are other processes that can occur: escape of neutrons through the surface of the reactor, capture in the moderator, and fission of ^{238}U by fast (unmoderated) neutrons.

Fission Reactors

In a fission reactor, the heat produced in the fuel must be extracted to generate electrical power. It must also be extracted for reasons of safety, because enough heat is produced to melt the core and cause a serious accident. For this reason, reactors contain an emergency core cooling system that is designed to prevent the core from overheating if the heat extraction system should fail.

Extracting the fission energy from the reactor core can be accomplished through several different techniques. In one design, called the *pressurized water reactor* and illustrated in Figure 13.11, the heat is extracted in a two-step process. Water circulates through the core under great pressure, to prevent its turning to steam. This hot water then in turn heats a second water system, which actually delivers steam to the turbine. The steam never enters the reactor core, so it does not become radioactive, and thus there is no radioactive material in the vicinity of the turbine.

The power reactors in the United States are mostly the pressurized-water type using enriched uranium as fuel and ordinary water as moderator. Canada also

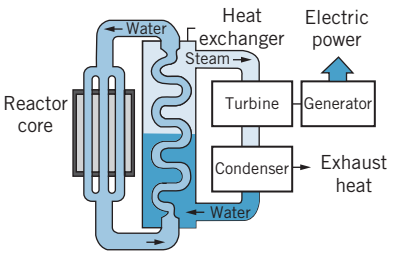

FIGURE 13.11 The components of a pressurized-water reactor.

uses pressurized water reactors, but heavy water and natural uranium are used. In a variation on this design, the pressurized water is replaced with a liquid metal such as sodium, which has the advantages of remaining liquid at much higher temperatures than water and of having a larger thermal conductivity than water. Yet another design uses gas flow through the core to extract the heat; the hot gas is then used to produce steam. Reactors in Great Britain are gas-cooled and graphite-moderated.

There are yet other technological problems associated with nuclear power that are the subjects of active debate and investigation. Some of the radioactive isotopes among the fission fragments have very long half-lives, of the order of many years. The radioactive waste from reactors must be stored in a manner that prevents leakage of radioactive material into the biological environment. Many people are concerned about the safety of nuclear reactors, not only regarding proper design and operation, but also about their resistance to natural disasters such as earthquakes or to acts of terrorism or sabotage.

In 1986, a graphite-moderated power reactor at Chernobyl in the former U.S.S.R. suffered a serious accident due to the disabling of the core cooling system, which is designed to extract the intense heat generated in the reactor core. The resulting temperature rise ignited the graphite moderator and caused an explosion of the reactor containment vessel, releasing radioactive fission products and exposing the inhabitants of the region to life-threatening radiation doses. The water-moderated power reactors used in the United States cannot suffer this kind of accident.

The vulnerability of reactors to natural disasters was dramatically revealed by the earthquake-triggered tsunami that struck Japan's Fukushima reactor complex in 2011. The flooding of the reactor buildings caused the pumps supplying cooling water to fail. As a result, the reactor core overheated due to the radioactive decay of the fission products, and a partial meltdown of the fuel rods occurred. The ensuing release of radioactivity contaminated a wide region of the Japanese countryside.

Finally, as in all heat engines, the disposal of the exhaust or waste heat (primarily from the steam recondensing to water) generates considerable thermal pollution. Nuclear power plants are generally less efficient at converting fuel to electrical power compared with plants that burn fossil fuels, because nuclear plants operate at lower temperatures; while fossil-fuel plants can have efficiencies as large as 40%, nuclear plants are generally in the range of 30 to 35%. A plant operating at 30% efficiency produces 50% more thermal pollution than one that generates the same amount of power at 40% efficiency.

A Naturally Occurring Fission Reactor

We conclude this section with a fascinating example of nature at work—the first sustained nuclear fission reactor on Earth was *not* the one constructed by Fermi in Chicago in 1942, but a *natural* fission reactor in Africa, which is believed to have operated two billion years ago for a period of perhaps several hundred thousand years. This reactor of course used naturally occurring uranium as a fuel and naturally occurring water as a moderator.

It would not be possible to build such a reactor today, because the capture of neutrons by the protons in water results in too few neutrons remaining to sustain a chain reaction in uranium with only 0.7% of ^{235}U. However, two billion years ago, naturally occurring uranium contained a much larger fraction of ^{235}U than does present-day uranium. Both ^{235}U and ^{238}U are radioactive, but the half-life of ^{235}U is only about one-sixth as great as the half-life of ^{238}U. If we go back in

time about 2×10^9 y, which is half of one half-life of ^{238}U, there was about 40% more ^{238}U than there is today, but there was $2^3 = 8$ times as much ^{235}U. Naturally occurring uranium was then about 3% ^{235}U, and, at such enrichments, ordinary water can serve as an effective moderator.

A deposit of such uranium, in a large enough mass and with ground water present to act as moderator, could have "gone critical" and begun to react. The reaction could have been controlled by the boiling of the water—when enough heat had been generated to evaporate some of the water, the reaction would slow down and perhaps stop, because of the lack of a moderator. When the uranium had cooled sufficiently to allow more liquid water to collect, the reactor would have started up again. This cycle could in principle have continued indefinitely, until enough ^{235}U was used up or until geological changes resulted in the removal of the water.

The discovery of this reactor followed the observation that the uranium that was being mined from that region in Africa contained too little ^{235}U. The discrepancy was a very small one—the samples contained 0.7171% ^{235}U, compared with the usual 0.7202%—but it was enough to stimulate the curiosity of the researchers. They guessed that the only mechanism that could result in the consumption of ^{235}U was the nuclear fission process, and this guess was tested by searching in the ore for stable isotopes that result from the radioactive decay of fission products. When such isotopes were found, and in particular when they were found in abundances very different from what would be expected from "natural" mineral deposits, the existence of the natural reactor was confirmed.

13.5 FUSION

Energy may also be released in nuclear reactions in the process of fusion, in which two light nuclei combine to form a heavier nucleus. The energy released in this process is the excess binding energy of the heavy nucleus compared with the lighter nuclei; from Figure 12.4, we see that this process can release energy as long as the final nucleus is less massive than about $A = 60$.

For example, consider the reaction

$$^2_1\mathrm{H}_1 + {}^2_1\mathrm{H}_1 \rightarrow {}^3_1\mathrm{H}_2 + {}^1_1\mathrm{H}_0$$

The Q value is 4.0 MeV, and so this nuclear reaction liberates about 1 MeV per nucleon, roughly the same as the fission reaction. This reaction can occur when a beam of deuterons is accelerated on to a deuterium target. In order to observe the reaction, we must get the incident and target deuterons close enough that the nuclear force can produce the reaction; that is, we must overcome the mutual Coulomb repulsion of the two particles. We can estimate this Coulomb repulsion by calculating the electrostatic repulsion of two deuterons when they are just touching. The radius of a deuteron is about 1.5 fm, and the electrostatic potential energy of the two charges separated by about 3 fm is about 0.5 MeV. A deuteron with 0.5 MeV of kinetic energy can overcome the Coulomb repulsion and initiate a reaction in which 4.5 MeV of energy (0.5 MeV of incident kinetic energy plus the 4-MeV Q value) is released.

Doing this reaction in a typical accelerator, in which the beam currents are typically in the microampere range, would produce only a small amount of energy (of the order of a few watts). To obtain significant amounts of energy from fusion,

it is necessary to work with much larger quantities of deuterium. For example, the fusion energy from the deuterium in a liter of ordinary water (which contains 0.015% D_2O) would be equivalent to the chemical energy obtained from burning about 300 liters of gasoline.

A more promising approach consists of heating deuterium gas to a high enough temperature so that each atom of deuterium has about 0.25 MeV of thermal kinetic energy (hence the name *thermonuclear* fusion). Then in a collision between two deuterium atoms, the total of 0.5 MeV of kinetic energy would be sufficient to overcome the Coulomb repulsion.

The difficulty with this approach is in heating the deuterium gas to a sufficient temperature; from the expression $\frac{1}{2}kT$ for the thermal kinetic energy of a gas molecule, we can calculate that an energy of 0.25 MeV corresponds to a temperature of the order of 10^9 K. Even assuming that barrier penetration (Section 5.6) would allow a reasonable probability to penetrate the Coulomb barrier at lower kinetic energies (perhaps corresponding to one-tenth of the calculated temperature), it is hard to imagine conditions under which these temperatures can be created. However, such conditions do exist in the interiors of stars, which produce their energy through fusion reactions. Fusion processes thus support all life on Earth. Scientists and engineers who are seeking to develop fusion processes for electrical power generation face the challenge of duplicating, for a brief instant of time and on a much smaller scale, the conditions in the interior of stars.

Fusion Processes in Stars

In the basic fusion process that occurs in stars (including our Sun), four protons combine to make one ^{4}He. Stars are composed of ordinary hydrogen rather than deuterium, so it is first necessary to convert the hydrogen to deuterium. This is done according to the reaction

$$ {}_1^1\mathrm{H}_0 + {}_1^1\mathrm{H}_0 \rightarrow {}_1^2\mathrm{H}_1 + \mathrm{e}^+ + \nu $$

This process involves converting a proton to a neutron and is analogous to the beta-decay processes discussed in Chapter 12. Once we have obtained ^{2}H (deuterium), the next reaction that can occur is

$$ {}_1^2\mathrm{H}_1 + {}_1^1\mathrm{H}_0 \rightarrow {}_2^3\mathrm{He}_1 + \gamma $$

followed by

$$ {}_2^3\mathrm{He}_1 + {}_2^3\mathrm{He}_1 \rightarrow {}_2^4\mathrm{He}_2 + 2{}_1^1\mathrm{H}_0 $$

Note that the first two reactions must occur *twice* in order to produce the two ^{3}He we need for the third reaction; see the schematic diagram of Figure 13.12. We can write the net process as

$$ 4{}_1^1\mathrm{H}_0 \rightarrow {}_2^4\mathrm{He}_2 + 2\mathrm{e}^+ + 2\nu + 2\gamma $$

For the calculation of the Q value in terms of *atomic* masses, four electrons must be added to the left side to make four neutral hydrogen atoms. To balance the reaction we must also add four electrons to the right side; two of these are associated with the ^{4}He atom, and the other two can be combined with the two positrons according to the reaction $\mathrm{e}^+ + \mathrm{e}^- \rightarrow 2\gamma$, so that the additional gamma rays are available as energy from the reaction. The two positrons disappear in this

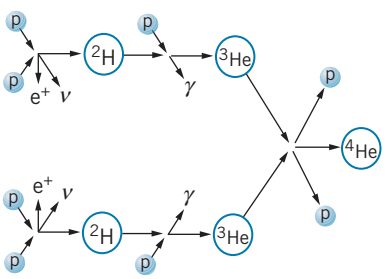

FIGURE 13.12 Schematic diagram of processes in the fusion of protons to form helium.

process; the only masses remaining are four hydrogen *atoms* and the one helium *atom,* and so

$$Q = (m_i - m_f)c^2 = [4m(^1\text{H}) - m(^4\text{He})]c^2$$
$$= (4 \times 1.007825\,\text{u} - 4.002603\,\text{u})(931.5\,\text{MeV/u}) = 26.7\,\text{MeV}$$

Each fusion reaction liberates about 26.7 MeV of energy.

At what rate do these reactions occur in the Sun? About 1.4×10^3 W of solar power is incident on each square meter of the Earth's surface. At our distance of about 1.5×10^{11} m from the Sun, its energy is spread over a sphere of area $4\pi r^2 = 28 \times 10^{22}\,\text{m}^2$, and thus the power output from the Sun is about 4×10^{26} W, which corresponds to about 2×10^{39} MeV/s. Each fusion reaction liberates about 26 MeV, and thus there must be about 10^{38} fusion reactions per second, consuming about 4×10^{38} protons per second. (Don't worry about running out of protons—the Sun's mass is about 2×10^{30} kg, which corresponds to about 10^{57} protons, enough to burn for the next few billion years.)

The sequence of reactions described above is called the *proton-proton* cycle and probably represents the source of the Sun's energy. However, it is probably *not* the primary source of fusion energy in many stars, because the first reaction (in which two protons combine to form a deuteron), which is similar to beta decay, takes place only on a very long time scale (as we discuss in the next chapter), and is therefore very unlikely to occur. A more likely sequence of reactions is the *carbon cycle*:

$$^{12}\text{C} + {}^1\text{H} \rightarrow {}^{13}\text{N} + \gamma$$
$$^{13}\text{N} \rightarrow {}^{13}\text{C} + \text{e}^+ + \nu$$
$$^{13}\text{C} + {}^1\text{H} \rightarrow {}^{14}\text{N} + \gamma$$
$$^{14}\text{N} + {}^1\text{H} \rightarrow {}^{15}\text{O} + \gamma$$
$$^{15}\text{O} \rightarrow {}^{15}\text{N} + \text{e}^+ + \nu$$
$$^{15}\text{N} + {}^1\text{H} \rightarrow {}^{12}\text{C} + {}^4\text{He}$$

A symbolic diagram of the process is shown in Figure 13.13. Notice that the ^{12}C plays the role of catalyst; we neither produce nor consume any ^{12}C in these reactions, but the presence of the carbon permits this sequence of reactions to take place at a much greater rate than the previously discussed proton-proton cycle. The net process is still described by $4\,{}^1\text{H} \rightarrow {}^4\text{He}$, and of course the Q value is the same. The Coulomb repulsion between H and C is larger than the Coulomb repulsion between two H nuclei, so more thermal energy and a correspondingly higher temperature are needed for the carbon cycle. The carbon cycle probably becomes important at a temperature of about 20×10^6 K, while the Sun's interior temperature is "only" 15×10^6 K.

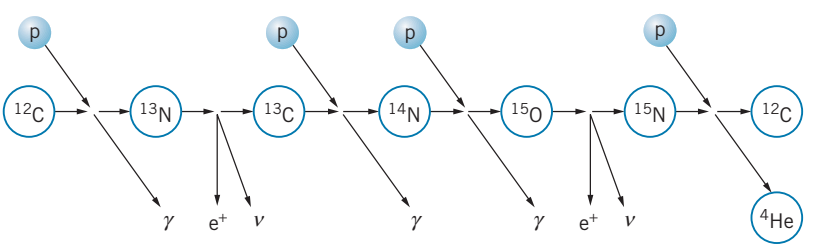

FIGURE 13.13 Sequence of events in the carbon cycle.

Fusion Reactors

For a controlled thermonuclear reactor, several reactions could be used, such as

$$^2\text{H} + {}^2\text{H} \rightarrow {}^3\text{H} + {}^1\text{H} \qquad Q = 4.0\,\text{MeV}$$
$$^2\text{H} + {}^2\text{H} \rightarrow {}^3\text{He} + \text{n} \qquad Q = 3.3\,\text{MeV}$$
$$^2\text{H} + {}^3\text{H} \rightarrow {}^4\text{He} + \text{n} \qquad Q = 17.6\,\text{MeV}$$

The third reaction, known as the D-T (deuterium-tritium) reaction, has the largest energy release and is perhaps the best candidate for a fusion reactor. When deuterium gas (or a deuterium-tritium mixture) is heated to a high temperature, the atoms become ionized; the resulting gas of hot, ionized particles is called a *plasma*. To increase the probability of collisions between the ions that would result in fusion, there are three requirements for the plasma: (1) *a high density n*, so that the particles have a high probability of collision; (2) *a high temperature T*, in the range of 10^8 K, which increases the probability for the particles to penetrate their mutual Coulomb barrier; and (3) *a long confinement time* τ, during which the high temperature and density must be maintained. The first and third of these parameters can be combined using some fairly general considerations based on the power needed to heat the plasma (which is proportional to the density n) and the power derived from fusions in the plasma (which is proportional to $n^2\tau$). For the fusion power to exceed the input power, the product $n\tau$ must exceed a certain minimum value; this condition is

$$n\tau \geq 10^{20}\ \text{s}\cdot\text{m}^{-3} \tag{13.15}$$

which is known as *Lawson's criterion*. The capability of a plasma to produce energy through fusion can be characterized by the value of its Lawson's parameter $n\tau$ and its temperature T.

The electrical repulsion of the ionized particles in a plasma tends to force the ions away from one another and toward the walls of their container, where they would lose energy in collisions with the cooler atoms of the walls. To maintain the density and temperature, two techniques are under development. In *magnetic confinement,* intense magnetic fields are used to trap the motion of the particles, and in *inertial confinement,* the plasma is heated and compressed so quickly that fusion occurs before the fuel can expand and cool.

Magnetic confinement A magnetic field can confine a plasma because the charged particles spiral around the magnetic field lines. Figure 13.14 shows a toroidal magnetic confinement geometry. There are two contributions to the magnetic field: One is along the toroid axis and another is around the axis. The combination of these two fields gives a helical field along the toroid axis, and the charged particles are confined as they spiral about the field lines. This type of device is a called a *tokamak* (from the Russian acronym for "toroidal magnetic chamber"). A current passed through the plasma serves both to heat the plasma and to create one of the magnetic field components. Figure 13.15 shows the Tokamak Fusion Test Reactor at Princeton University, which operated from 1982 to 1997 and achieved an ion temperature of 5.1×10^8 K and a fusion power level of 10.7 MW. This device came very close to reaching Lawson's criterion with a plasma density of $n = 10^{20}$ particles/m^3 (five orders of magnitude smaller than an ordinary gas) and a confinement time of $\tau = 0.2$ s.

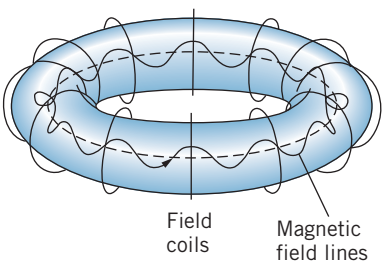

FIGURE 13.14 The toroidal geometry of plasma confinement. The ionized atoms circulate around the ring, trapped by the magnetic field lines. The coils produce a magnetic field along the axis of the toroid (dashed line). Another field component is produced by a current along the axis in the plasma. The two components of the field produce the helical field lines shown.

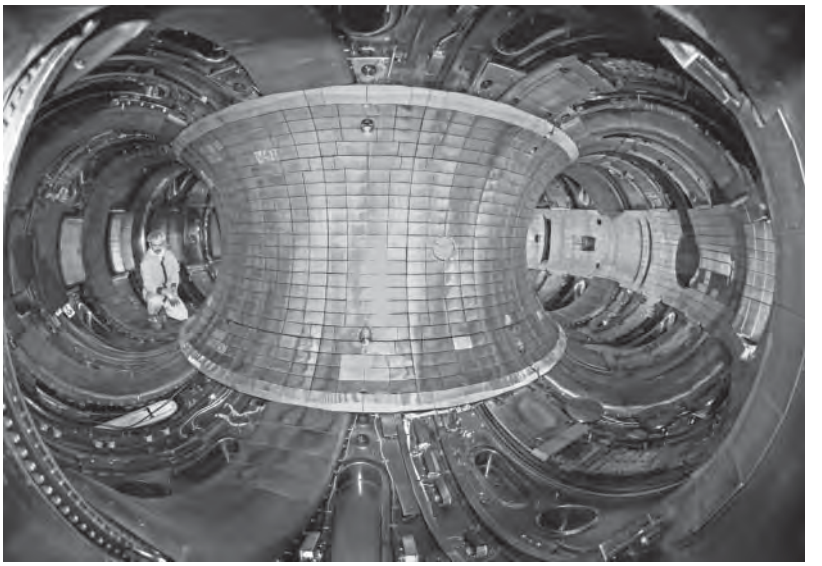

FIGURE 13.15 The inside of the Tokamak Fusion Test Reactor. The technician at the left gives a measure of the size of the toroidal chamber. (Dietmar Krause/Princeton Plasma Physics Laboratory.)

The development of magnetic confinement devices has produced a steady march toward achieving a self-sustaining fusion reactor by increasing the values of both Lawson's parameter $n\tau$ and the temperature, as illustrated in Figure 13.16. Devices have closely approached "breakeven," where the power produced by fusion reactions equals the power necessary to heat the plasma. A true self-sustaining reactor requires the attainment of "ignition," where the power produced by fusion reactions can maintain the reactor with no external source of energy. The next generation of fusion reactor development is the ITER (originally, the International Thermonuclear Experimental Reactor), currently under construction in France as a collaboration among many nations and expected to be operational in the year 2016. The ITER is planned to produce fusion power levels that are 5–10 times what is necessary to heat the plasma (that is, 5–10 times the "breakeven" condition).

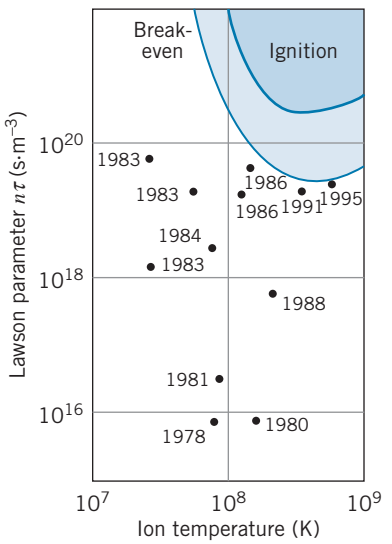

FIGURE 13.16 The approach to breakeven and ignition in fusion reactors, shown as a plot of Lawson's parameter against temperature.

Inertial confinement Inertial confinement takes the opposite approach by compressing the fuel to high densities for very short confinement times. In one method, which is illustrated in Figure 13.17, a small pellet of D-T fuel is struck simultaneously from many directions by intense laser beams that first vaporize the pellet and convert it to a plasma, and then heat and compress it to the point at which fusion can occur. The laser pulses are very short, typically lasting only about 1 ns, and thus according to Lawson's criterion the density must exceed 10^{29} particles/m^3. However, because of inefficiencies of the lasers and other losses a self-sustaining laser fusion reactor must exceed this minimum by perhaps 2–3 orders of magnitude. Figure 13.18 shows the target chamber of the National Ignition Facility at the Lawrence Livermore National Laboratory. Operating for the first time in 2010, it is designed so that a 2-mm diameter pellet of D-T is struck simultaneously by 192 laser beams that deliver an energy of 1 MJ in a pulse lasting a few ns, which is expected to compress the pellet to a central density that is 100 times that of lead.

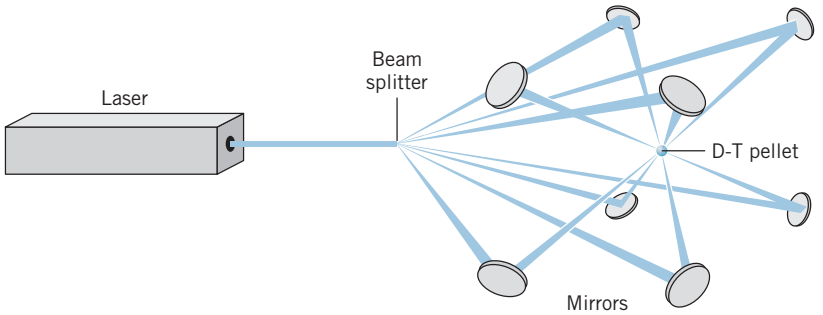

FIGURE 13.17 Inertial confinement fusion initiated by a laser.

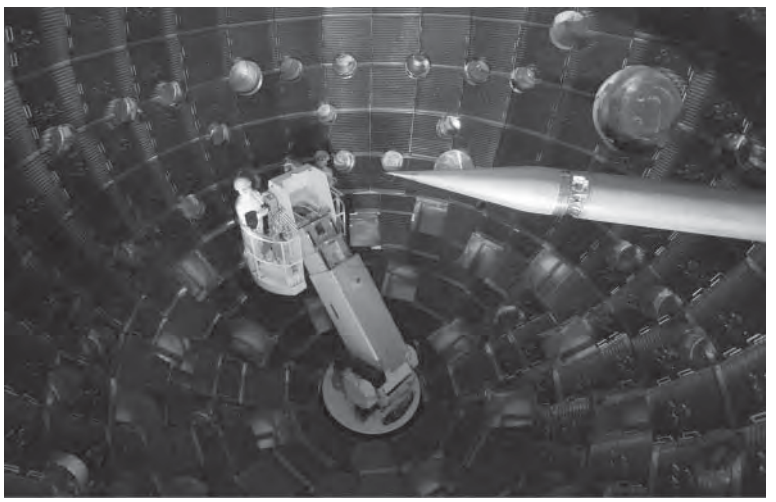

FIGURE 13.18 Workers inside the 10-m-diameter target chamber where 192 laser beams (which enter the chamber through the circular ports) strike the target that is held by the positioning arm at the right. (Courtesy Lawrence Livermore National Laboratory.)

In the D-T fusion reaction, most of the energy is carried by the neutrons (recall that in the fission reaction only a small fraction of the energy went to the neutrons). This presents some difficult problems for the recovery of the energy and its conversion into electrical power. One possibility for a fusion reactor design is shown in Figure 13.19. The reaction area is surrounded by lithium, which captures neutrons by the reaction

$$^{6}_{3}\mathrm{Li}_{3} + \mathrm{n} \rightarrow {}^{4}_{2}\mathrm{He}_{2} + {}^{3}_{1}\mathrm{H}_{2}$$

The kinetic energies of the reaction products are rapidly dissipated as heat, and the thermal energy of the liquid lithium can be used to convert water to steam in order to generate electricity. This reaction has the added advantage of producing tritium (^{3}H), which is needed as a fuel for the fusion reactor.

One difficulty with the D-T fusion process is the large number of neutrons released in the reactions. Although fusion reactors will not produce the radioactive wastes that fission reactors do, the neutrons are sure to make radioactive the immediate area surrounding the reactor, and the structural damage to materials resulting from exposure to large fluxes of neutrons may weaken critical parts of

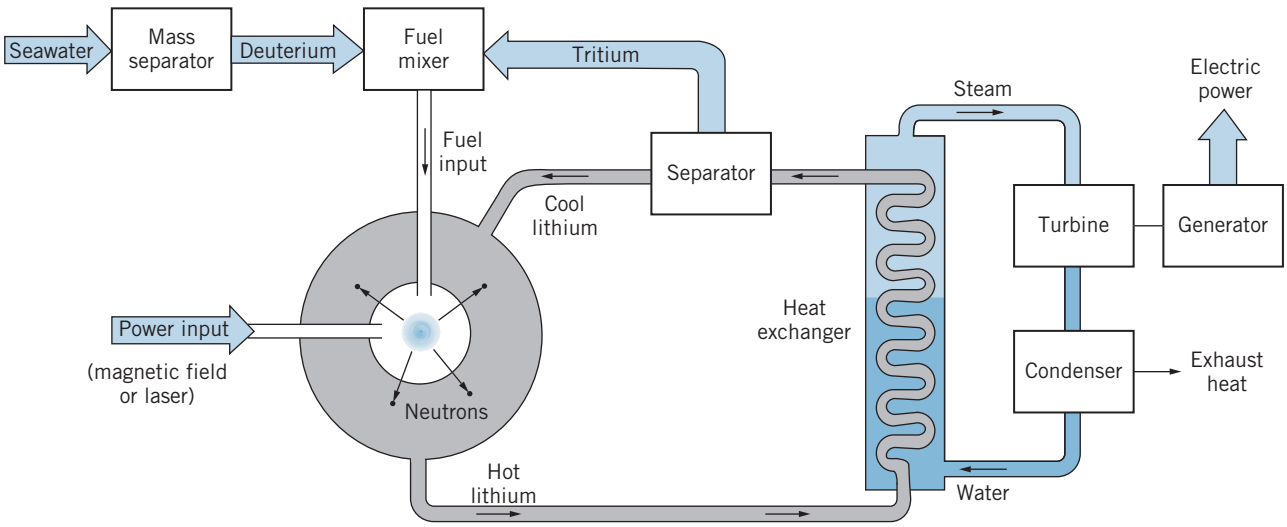

FIGURE 13.19 Design of a fusion reactor.

the reactor vessel. Here once again the lithium is helpful, because a 1-m thickness of lithium should be sufficient to stop essentially all of the neutrons.

Fusion energy is the subject of vigorous research in many laboratories in the United States and around the world; the technological problems are being attacked with a variety of methods, and researchers are hopeful that solutions can be found during the next 20 years so that fusion can help to supply our electrical power needs.

13.6 NUCLEOSYNTHESIS

After a star's hydrogen has been converted to helium through fusion reactions, gravitational collapse can occur that raises the temperature of the core of the star from about 10^7 K to about 10^8 K. At this point there is enough thermal kinetic energy to overcome the Coulomb repulsion of the helium nuclei, and helium fusion can begin. In this process three ^{4}He are converted into ^{12}C by the two-step process

$$^4\text{He} + {}^4\text{He} \rightarrow {}^8\text{Be}$$
$$^8\text{Be} + {}^4\text{He} \rightarrow {}^{12}\text{C}$$

The first reaction is endothermic, with a Q value of 92 keV. The nucleus ^{8}Be is unstable and decays back into two alpha particles in a time of the order of 10^{-16} s. Even so, the Boltzmann factor $e^{-\Delta E/kT}$ suggests that at 10^8 K there will be a small concentration of ^{8}Be. The second reaction has a particularly large cross section; in spite of the rapid breakup of ^{8}Be, there is still a good chance to form ^{12}C. The net Q value for the process is 7.3 MeV, or about 0.6 MeV per nucleon, much less than the 6.7 MeV per nucleon produced by hydrogen burning.

Once enough ^{12}C has formed in the core, other alpha particle reactions become possible, such as

$$^{12}\text{C} + {}^4\text{He} \rightarrow {}^{16}\text{O}$$
$$^{16}\text{O} + {}^4\text{He} \rightarrow {}^{20}\text{Ne}$$
$$^{20}\text{Ne} + {}^4\text{He} \rightarrow {}^{24}\text{Mg}$$

Each of these reactions is exothermic, releasing a few MeV of energy and contributing to the star's energy production. At still higher temperatures (10^9 K) carbon burning and oxygen burning begin:

$$^{12}C + {}^{12}C \rightarrow {}^{20}Ne + {}^{4}He$$
$$^{16}O + {}^{16}O \rightarrow {}^{28}Si + {}^{4}He$$

Eventually ^{56}Fe is reached, at which point no further energy is gained by fusion (Figure 12.4).

If this explanation of the formation of elements is correct, we expect the abundances of the elements to have the following properties:

1. Large relative abundances of the light, even-Z elements; small relative abundances of odd-Z elements.
2. Little or none of the elements between He and C (Li, Be, B), which are not produced in these reactions.
3. Large relative abundance of Fe, the end product of the fusion cycle.

Figure 13.20 shows the relative abundances of the light elements in the solar system, and they are in agreement with all of the three above expectations. Each even-Z element is 10 to 100 times more abundant than its odd-Z neighbors; there is a prominent peak at Fe; the heavy elements with $Z > 30$ *combined* are less abundant than every element but one in the range C to Zn; and the three elements Li, Be, B are far less abundant than the elements in the range C to Zn.

The light odd-Z elements can be produced by alternative reactions among the fusion products, for example:

$$^{12}C + {}^{12}C \rightarrow {}^{23}Na + {}^{1}H$$
$$^{16}O + {}^{16}O \rightarrow {}^{31}P + {}^{1}H$$

The abundance of nitrogen is nearly equal to that of its neighbors C and O, which are the most abundant of elements beyond H and He; nitrogen has a greater abundance than any other odd-Z element shown, and greater than all even-Z elements with $Z > 8$. The formation of nitrogen must therefore be a relatively

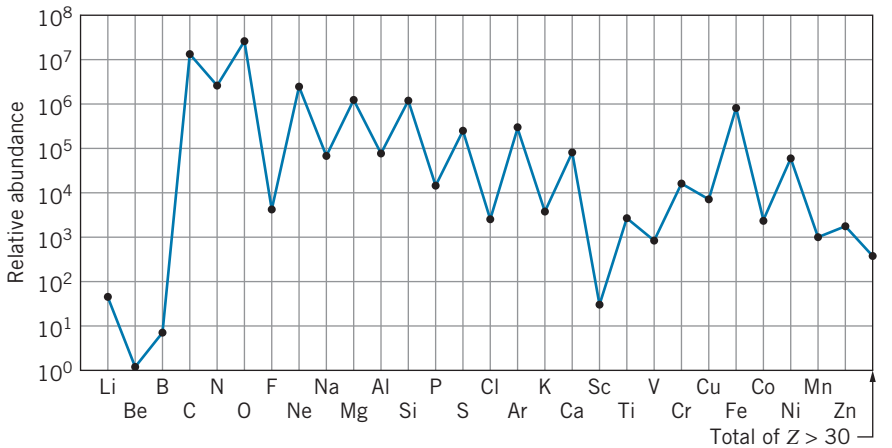

FIGURE 13.20 Relative abundances (by weight) of the elements beyond helium in the solar system.

common process in stars. The element B is rare, so alpha particle reactions are of no help in forming nitrogen. The most likely sources of N are

$$^{12}\mathrm{C} + {}^{1}\mathrm{H} \rightarrow {}^{13}\mathrm{N} + \gamma \qquad\qquad {}^{16}\mathrm{O} + {}^{1}\mathrm{H} \rightarrow {}^{17}\mathrm{F} + \gamma$$
$$^{13}\mathrm{N} \rightarrow {}^{13}\mathrm{C} + \mathrm{e}^{+} + \nu \qquad \text{and} \qquad {}^{17}\mathrm{F} \rightarrow {}^{17}\mathrm{O} + \mathrm{e}^{+} + \nu$$
$$^{13}\mathrm{C} + {}^{1}\mathrm{H} \rightarrow {}^{14}\mathrm{N} + \gamma \qquad\qquad {}^{17}\mathrm{O} + {}^{1}\mathrm{H} \rightarrow {}^{14}\mathrm{N} + {}^{4}\mathrm{He}$$

The stable isotopes ^{13}C and ^{17}O are found in natural carbon and oxygen with abundances of 1.1% and 0.04%, which suggests that these reactions do indeed take place.

The production of the elements beyond iron requires the presence of neutrons, which are not produced in the reactions we have listed so far, because neutrons are likely to be emitted only in reactions with nuclei that have an excess of neutrons. If enough of the heavier isotopes, such as ^{13}C, ^{17}O, or ^{21}Ne, are formed, the following reactions can produce neutrons:

$$^{13}\mathrm{C} + {}^{4}\mathrm{He} \rightarrow {}^{16}\mathrm{O} + \mathrm{n}$$
$$^{17}\mathrm{O} + {}^{4}\mathrm{He} \rightarrow {}^{20}\mathrm{Ne} + \mathrm{n}$$
$$^{21}\mathrm{Ne} + {}^{4}\mathrm{He} \rightarrow {}^{24}\mathrm{Mg} + \mathrm{n}$$

How are the heavy elements built up by neutron capture? Consider the effect of neutron capture on ^{56}Fe:

$$^{56}\mathrm{Fe} + \mathrm{n} \rightarrow {}^{57}\mathrm{Fe} \qquad \text{(stable)}$$
$$^{57}\mathrm{Fe} + \mathrm{n} \rightarrow {}^{58}\mathrm{Fe} \qquad \text{(stable)}$$
$$^{58}\mathrm{Fe} + \mathrm{n} \rightarrow {}^{59}\mathrm{Fe} \qquad (t_{1/2} = 45\ \mathrm{d})$$

What happens next depends on the number of available neutrons. If that number is small, the chances of ^{59}Fe encountering a neutron *before* it decays to ^{59}Co are small, and the process might continue as follows:

$$^{59}\mathrm{Fe} \rightarrow {}^{59}\mathrm{Co} + \mathrm{e}^{-} + \overline{\nu}$$
$$^{59}\mathrm{Co} + \mathrm{n} \rightarrow {}^{60}\mathrm{Co} \qquad (t_{1/2} = 5\ \mathrm{y})$$
$$^{60}\mathrm{Co} \rightarrow {}^{60}\mathrm{Ni} + \mathrm{e}^{-} + \overline{\nu}$$

On the other hand, if the number of neutrons is very large, a different sequence might result:

$$^{59}\mathrm{Fe} + \mathrm{n} \rightarrow {}^{60}\mathrm{Fe} \qquad (t_{1/2} = 3 \times 10^{5}\ \mathrm{y})$$
$$^{60}\mathrm{Fe} + \mathrm{n} \rightarrow {}^{61}\mathrm{Fe} \qquad (t_{1/2} = 6\ \mathrm{m})$$
$$^{61}\mathrm{Fe} \rightarrow {}^{61}\mathrm{Co} + \mathrm{e}^{-} + \overline{\nu}$$
$$^{61}\mathrm{Co} \rightarrow {}^{61}\mathrm{Ni} + \mathrm{e}^{-} + \overline{\nu}$$

If the density of neutrons is so low that the chance of encountering a neutron is, on the average, less than once every 45 days, the first process ought to dominate, with the production of ^{60}Ni. If the chance of encountering a neutron is more like once every few minutes, the second process should dominate, and no ^{60}Ni is produced.

The first type of process, which occurs *slowly* and allows the nuclei time to beta decay, is known as the *s process* (*s* for slow); the second process occurs very *rapidly* and is known as the *r process* (*r* for rapid).

Figure 13.21 illustrates how the *r* and *s* processes can proceed from ^{56}Fe. The *s* process never strays very far from the region of the stable nuclei, while the *r* process can produce many nuclei that have a large excess of neutrons. The larger the excess of neutrons, the shorter is the half-life of these nuclei. Eventually the half-life becomes so short that no neutron is captured before the beta decay occurs to the next higher Z. All nuclei produced in the *r* process will eventually decay toward the stable nuclei, generally moving by beta decays along the diagonal line of constant mass number A.

Some stable nuclei are produced only through the *s* process, others are produced only through the *r* process, and some may be produced through both processes. Often the natural abundance of the isotopes of an element can suggest the relative roles of these two processes. In Figure 13.21, you can see that the stable isotope ^{70}Zn cannot be produced in the *s* process, because the half-life of ^{69}Zn is too short (56 min). Other isotopes for which the *r* process is important are ^{76}Ge, ^{82}Se, ^{86}Kr, ^{96}Zr, and ^{122}Sn. The isotope ^{64}Ni can be produced either through the *s* process (as shown in Figure 13.21) or through the *r* process (such as through beta decays beginning with ^{64}Fe). On the other hand, ^{64}Zn (the most abundant isotope of zinc) is produced *only* through the *s* process, because *r*-process beta decays proceeding along the $A = 64$ line are stopped at stable ^{64}Ni and cannot reach ^{64}Zn.

The heaviest element that can be built up out of *s*-process neutron captures is ^{209}Bi; the half-lives of the isotopes beyond ^{209}Bi are too short to allow the *s* process to continue. The presence in nature of heavier elements such as thorium or uranium suggests that the *r* process must operate in this region as well.

The *r* process most likely occurs during supernova explosions, following the breakdown and implosion of a star that has used up its fusion reserves. In a very short time, lasting of the order of seconds, the star implodes, produces an enormous flux of neutrons (perhaps 10^{32} n/cm^2/s), and builds up all elements to

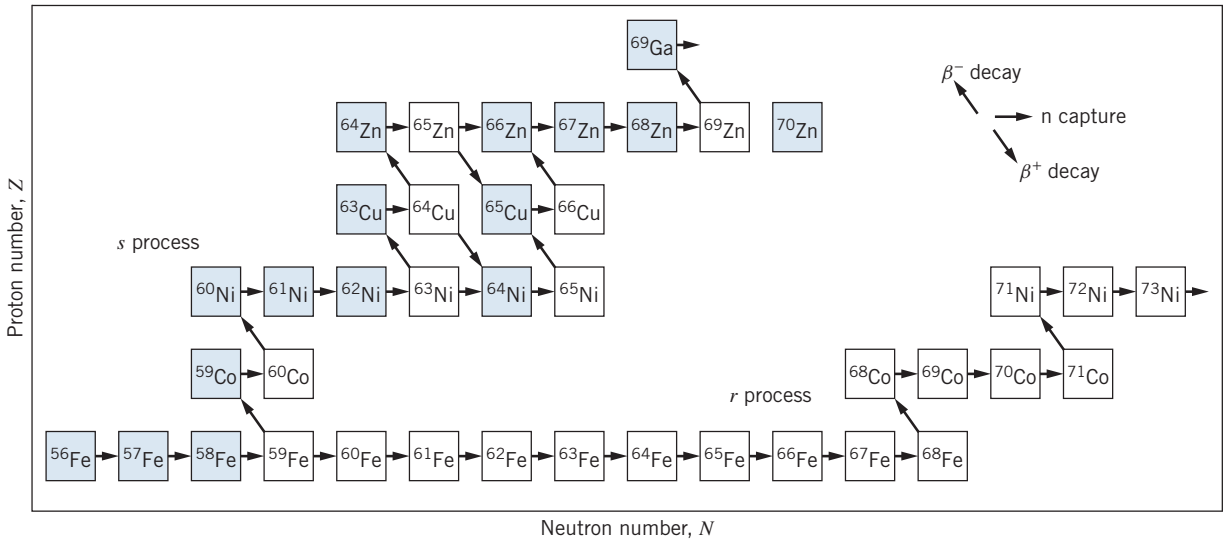

FIGURE 13.21 A section of the chart of the nuclides (Figure 12.11), showing the *s*- and *r*-process paths from ^{56}Fe. Shaded squares represent stable nuclei, and unshaded squares represent radioactive nuclei. Many *r*-process paths are possible, as the short-lived nuclei beta decay; only one of those possible paths is shown. All the nuclei in the *r*-process path are unstable and may beta decay toward the stable nuclei.

about $A = 260$. When the final explosion occurs, these elements are hurled out into space, to become part of new star systems. The heavy atoms of which the Earth is made may have been produced in such an explosion.

13.7 APPLICATIONS OF NUCLEAR PHYSICS

In this chapter, we have discussed how fission and fusion reactions can be used to generate electrical power, and in the previous chapter we discussed how the radioactive decay of various isotopes can be used to date the historical origin of material containing those isotopes. These are but a few of the many ways that nuclear decays and reactions can be applied to the solution of practical problems. In this section we discuss briefly some other applications of the techniques of nuclear physics.

Neutron Activation Analysis

Nearly every radioactive isotope emits characteristic gamma rays, and many chemical elements can be identified by their gamma ray spectra. For example, when ^{59}Co (the only stable isotope of cobalt) is placed in a flux of neutrons (such as is found near the core of a reactor), neutron absorption results in the production of the radioactive isotope ^{60}Co, which beta decays with a half-life of 5.27 years. Following the beta decay, ^{60}Ni emits two gamma rays of energies 1.17 MeV and 1.33 MeV and of equal intensity. If we place in a flux of neutrons a material of unknown composition, and if we observe, following the neutron bombardment, two gamma rays of equal intensity and energies 1.17 MeV and 1.33 MeV, it is a safe bet that the unknown sample contained cobalt. In fact, from the rate of gamma emission we could deduce exactly how much cobalt the material contains, assuming that we know the neutron flux and the neutron capture cross section of ^{59}Co. This technique is known as *neutron activation analysis*, and has been used in many applications in which the elements are present in such small quantities that chemical identification is not practical. Typically, neutron activation analysis can be used to identify elements in quantities of the order of 10^{-9} g, and sensitivity down to 10^{-12} g is often possible.

Such a sensitive and precise technique finds application in a variety of areas, in which the chemical composition must be determined for samples that are available only in microscopic quantities or that must be analyzed in a nondestructive manner. For example, the chemical composition of various types of pottery can help us trace the geographical origin of the clay from which they were made; such analyses of pottery shards can trace the trading routes of prehistoric people. Art forgeries can be detected by a knowledge of the chemical composition of paints, because techniques for producing pigments have changed over the last four centuries with corresponding changes in the level of impurities in paints. The chemical analysis of tiny quantities of material such as paint, gunshot residues, soil, or hair can provide important evidence in criminal investigations. Neutron activation analysis of samples of the hair of such historical figures as Napoleon or Newton has revealed the chemicals to which they were exposed centuries ago. An example of a neutron activation analysis study of a sample of hair is shown in Figure 13.22.

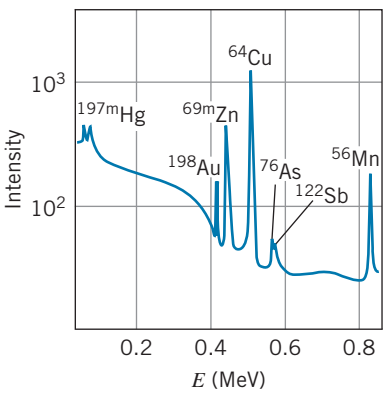

FIGURE 13.22 Gamma-ray spectrum following neutron activation of a sample of human hair. The sample shows traces of mercury, gold, zinc, copper, arsenic, antimony, and manganese. [From D. DeSoete et al., *Neutron Activation Analysis* (Wiley Interscience, 1972).]

Medical Radiation Physics

One of the most important applications of nuclear physics has been in medicine, for both diagnostic and therapeutic purposes. The use of X rays for producing images for medical diagnosis is well known, but X rays are of limited value. They show distinct and detailed images of bones, but they are generally less useful in making images of soft tissue. Radioactive isotopes can be introduced into the body in chemical forms that have an affinity for certain organs, such as bone or the thyroid gland. A sensitive detector (called a "gamma-ray camera") can observe the radiations from the isotopes that are concentrated in the organ and can produce an image that shows how the activity is distributed in the patient. These detectors are capable of determining where each gamma-ray photon originates in the patient. Figure 13.23 shows an image of the brain, taken after the patient was injected with the radioactive isotope ^{99}Tc ($t_{1/2} = 6\,\text{h}$). The images clearly show an area of the brain where the activity has concentrated. Ordinarily the brain does not absorb impurities from the blood, so such concentrations often indicate a tumor or other abnormality.

Another technique that reveals a wealth of information is *positron emission tomography* (PET), in which the patient is injected with a positron-emitting isotope that is readily absorbed by the body. Examples of isotopes used are ^{15}O ($t_{1/2} = 2\,\text{min}$), ^{13}N ($t_{1/2} = 10\,\text{min}$), ^{11}C ($t_{1/2} = 20\,\text{min}$), and ^{18}F ($t_{1/2} = 110\,\text{min}$). These isotopes are produced with a cyclotron, and because of the short half-lives the cyclotron must be present at the site of the diagnostic facility. When a positron emitter decays, the positron quickly annihilates with an electron and produces two 511-keV gamma rays that travel in opposite directions. By surrounding the patient with a ring of detectors, it is possible to determine exactly where the decay occurred, and from a large number of such events, the physician can produce an image that reconstructs the distribution of the radioisotope in the patient. One advantage of the PET scan over X-ray techniques such as the CAT (computerized axial tomography) scan is that it can produce a dynamic image—changes in the patient during the measuring time can be observed. Figure 13.24 shows a brain scan of a patient who was injected with glucose labeled with ^{18}F. Active areas of the brain metabolize glucose more rapidly, and so they become more concentrated with ^{18}F, allowing medical workers to observe regions of the brain associated with different mental activities.

Radiation therapy takes advantage of the effect of radiations in destroying unwanted tissue in the body, such as a cancerous growth or an overactive thyroid gland. The effect of the passage of radiation through matter is often to ionize the

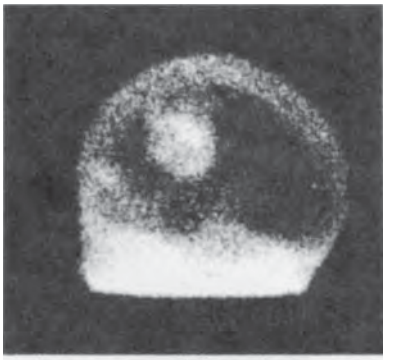

(*a*)

(*b*)

FIGURE 13.23 Scintillation camera image of the brain, following intravenous injection of 20 mCi of ^{99m}Tc. (*a*) Side view, with the patient's face to the left. (*b*) Back view. The bright circular spot shows concentration of blood in a lesion, possibly a tumor. Other bright areas show the scalp and the major veins.

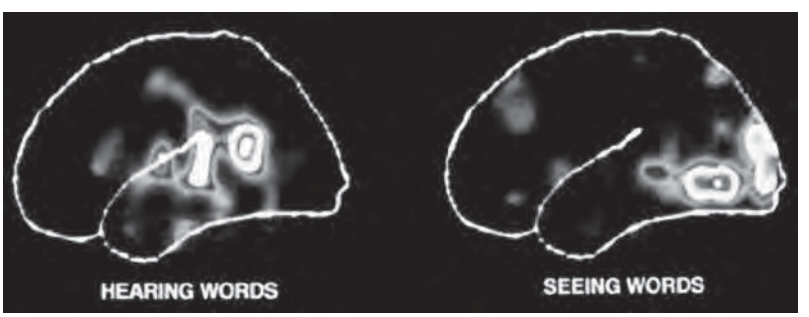

FIGURE 13.24 PET scan showing different areas of the brain that are active when either hearing words or seeing words.

Rosalyn Yalow (1921–2011, United States). After receiving her Ph.D. in nuclear physics, she researched the medical applications of radioactive isotopes. Yalow developed the technique of radioimmunoassay, which uses radioactive tracers to measure small amounts of substances in the blood or other fluids. Her development of this technique was recognized with the award of the Nobel Prize in medicine in 1977.

atoms. The ionized atoms can then participate in chemical reactions that lead to their incorporation into molecules and subsequent alteration of their biological function, possibly the destruction of a cell or the modification of its genetic material. For example, an overactive thyroid gland is often treated by giving the patient radioactive ^{131}I, which collects in the thyroid. The beta emissions from this isotope damage the thyroid cells and ultimately lead to their destruction. Certain cancers are treated by implanting needles or wires containing radium or other radioactive substances. The decays of these radioisotopes cause localized damage to the cancerous cells.

Other cancers can be treated using beams of particles that cause nuclear reactions within the body at the location of the tumor. Pions and neutrons are used for this purpose. The absorption of a pion or a neutron by a nucleus causes a nuclear reaction, and the subsequent emission of particles or decays by the reaction products again causes local damage that is concentrated at the site of the tumor, inflicting maximum damage to the tumor and minimum damage to the surrounding healthy tissue.

Alpha-Scattering Applications

Radioactive sources emitting alpha particles have been used in a variety of applications. Most of these take advantage of the persistence of radioactive decay—the decays can be depended upon to occur at a fixed rate in any location.

Alpha particles from radioactive decay can be absorbed and their energy converted into another form, such as electrical power obtained through thermoelectric conversion. The power levels are not large (of the order of 1 W per gram of material; see Problem 31), but they are sufficient to power many devices, from cardiac pacemakers to the Voyager spacecraft, which photographed Jupiter, Saturn, and Uranus.

Scattering of alpha particles emitted by a radioactive source is the basis of operation of ionization-type smoke detectors; alpha particles from the decay of ^{241}Am are scattered by the ionized atoms that result from combustion. When the smoke detector senses a decrease in the rate at which alphas are counted (due to some of them being scattered away from the detector), the alarm is triggered.

Other applications of alpha-particle scattering are used for materials analysis. In *Rutherford backscattering*, the analysis uses the reduction in energy of an alpha particle that is scattered through an angle of 180°. Although our discussion of Rutherford scattering in Chapter 6 assumed that the target nucleus was infinitely heavy and thus acquired no energy in the scattering, in practice a small amount of energy is given even to a heavy nucleus. By allowing the target nucleus to recoil, we can find the loss in energy ΔK of an alpha particle of kinetic energy K that scatters through 180° (see Problem 29):

$$\Delta K = K\left[\frac{4m/M}{(1+m/M)^2}\right] \tag{13.16}$$

where m is the mass of the alpha particle and M is the mass of the target nucleus. For a heavy nucleus ($m/M = 0.02$), the loss in energy is of order 0.5 MeV, which is easily measurable. Figure 13.25 shows a sample of the spectrum of alpha particles backscattered from a thin foil containing copper, silver, and gold. Note the Z^2 dependence of the scattering probability that characterizes Rutherford scattering (see Eq. 6.14), and also note the sensitivity of the technique even to the two naturally occurring isotopes of copper. (However, the two isotopes of silver cannot be resolved.) The Surveyor spacecraft that landed on the Moon and the

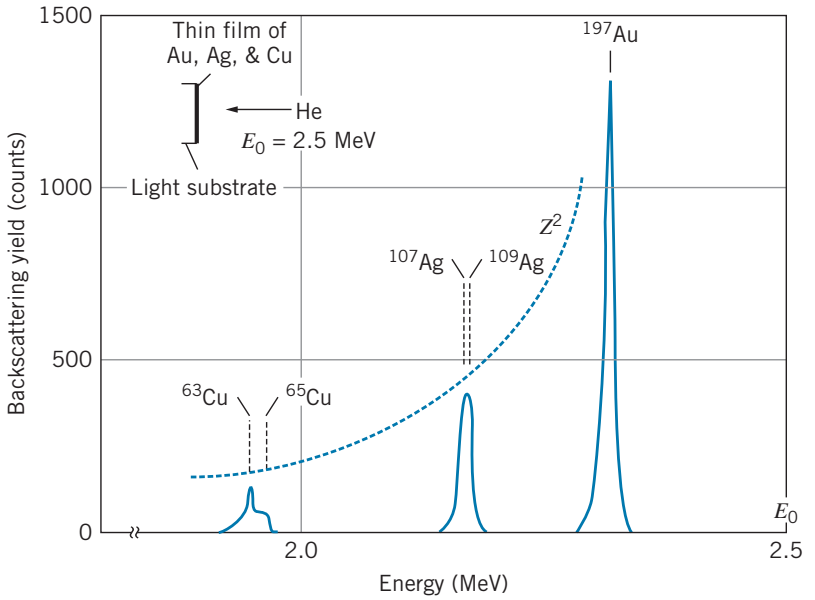

FIGURE 13.25 Backscattering spectrum of 2.5-MeV α particles from a thin film of copper, silver, and gold. The dashed line shows the Z^2 behavior of the cross section expected from the Rutherford formula. Note the appearance of the two isotopes of copper. [From M.-A. Nicolet, J. W. Mayer, and I. V. Mitchell, *Science* **177**, 841 (1972). Copyright ©1972 by the AAAS.]

Viking landers on Mars carried Rutherford backscattering experiments to analyze the chemical composition of the surface of those bodies.

Superheavy Elements

The known atoms beyond uranium ($Z = 92$) are *all* radioactive, with half-lives short compared with the age of the Earth. They are therefore not present in terrestrial matter, but they can be produced in the laboratory. The production process for the series of elements beginning with neptunium ($Z = 93$), called *transuranic* elements, follows the same process outlined in Section 13.6: neutron capture followed by beta decay. Using similar techniques researchers have produced elements up to $Z = 100$ (fermium). Beyond this point, too few atoms are produced for neutron capture to reveal the presence of the next element. Instead, reactions with accelerated charged particles are used.

Many of the elements in this series have half-lives of only minutes or seconds, and thus the production and identification of these elements requires painstaking experimental efforts—the isotopes are often produced in quantities of a few atoms! Although most of these elements have not been produced in sufficient quantity to study their chemical properties, it is expected that their place in the periodic table will be as shown in Figure 13.26, up to the inert gas with $Z = 118$. All elements up to 118 have been observed (although names for elements beyond $Z = 112$ have not yet been chosen—the symbols shown in Figure 13.26 represent placeholder names).

The extreme instability of these transuranic elements results from the increased Coulomb repulsion of the nuclear protons as Z increases; these elements decay by alpha decay or by spontaneous fission. However, strong theoretical evidence

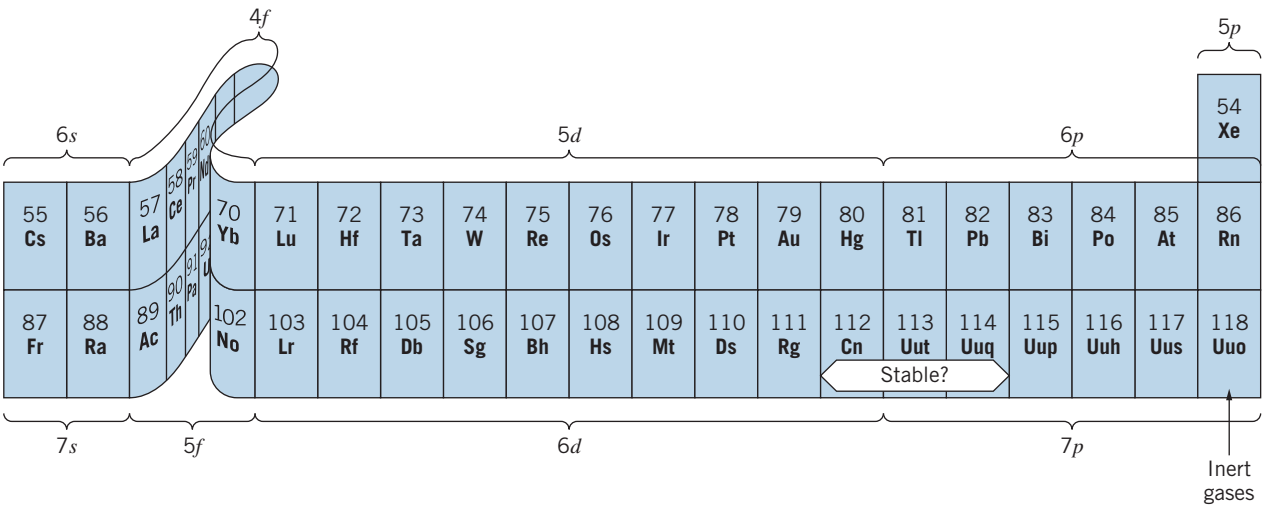

FIGURE 13.26 New massive elements in the periodic table.

suggests that elements around $Z = 114, N = 184$ should be stable against alpha decay, beta decay, and spontaneous fission. This region around element 114 is often called the "island of stability."

Although the production and observation of nuclei of such *superheavy* elements are not likely to have any immediate applications, their study would be of great interest to test our understanding of the ordering of the periodic table, and the comparison of their chemical and physical properties with those of the $5d$ and $6p$ elements would be a test of our ordering of the elements. Many of the artificially produced transuranic elements have already found applications in research and technology. The alpha decays of ^{238}Pu and ^{239}Pu have been used as power sources for spacecraft, and ^{241}Am serves as an alpha source for smoke detectors. The radioisotope ^{254}Cf decays by spontaneous fission; the neutrons released in the decay have many applications, including medical treatment and materials analysis.

Chapter Summary

		Section
Reaction rate	$R = \sigma N I_0/S$ or $R = \phi\sigma N = \phi\sigma m N_A/M$	13.1
Production of activity in reaction	$a(t) = \lambda N = R(1 - e^{-\lambda t})$ $\cong R\lambda t \ (t \ll t_{1/2})$	13.2
Reaction Q value $(x + X \rightarrow y + Y)$	$Q = (m_i - m_f)c^2$ $= [m(x) + m(X) - m(y) - m(Y)]c^2$ $= K_y + K_Y - K_x$	13.3
Threshold kinetic energy	$K_{th} = -Q[1 + m(x)/m(X)]$	13.3
^{235}U fission reaction (sample)	$^{235}_{92}U_{143} + n \rightarrow$ $^{93}_{37}Rb_{56} + {}^{141}_{55}Cs_{86} + 2n$	13.4
D-T fusion reaction	$^2H + {}^3H \rightarrow {}^4He + n$	13.5
Lawson's criterion	$n\tau \geq 10^{20}\ s \cdot m^{-3}$	13.5
Alpha backscattering	$\Delta K = K\left[\frac{4m/M}{(1 + m/M)^2}\right]$	13.7

Questions

1. The cross sections for reactions induced by protons generally increase as the kinetic energy of the proton increases, while cross sections for neutron-induced reactions generally decrease with increasing neutron energy. Explain this behavior.
2. Cross sections for reactions induced by thermal neutrons ($K \sim kT$, where T is room temperature) are often several orders of magnitude larger than cross sections for the same reaction induced by fast neutrons ($K \sim$ MeV). Justify this difference by comparing the time spent in the vicinity of a target nucleus by a thermal neutron and a fast neutron.
3. When two nuclei approach one another in a nuclear reaction, there is a Coulomb repulsion between them. Does this potential energy affect the kinematics of the reaction? Does it affect the cross section?
4. The most abundant component of our atmosphere is ^{14}N. Assuming that cosmic rays supply sufficient high-energy protons and neutrons, explain how the radioactive isotopes ^{14}C and ^{3}H can be formed.
5. Consider the photodisintegration reaction $A + \gamma \rightarrow B + C$. In terms of the binding energies of A, B, and C, what are the requirements for this reaction? Would you expect to observe photodisintegration more readily for light nuclei ($A < 56$) or heavy nuclei ($A > 56$)?
6. Would you expect to observe the radiative capture of an alpha particle $X + \alpha \rightarrow X' + \gamma$ for heavy nuclei?
7. In what sense is photodisintegration (see Question 5) the inverse of radiative capture (see Question 6)? How are the photon energies related?
8. Comment on the following statement: The fission reaction is useful for energy production because of the large kinetic energies given to the neutrons emitted following fission.
9. ^{238}U is fissionable, but only with neutrons in the MeV range. Explain why ^{238}U is not a suitable reactor fuel.
10. What is the difference between a slow neutron and a delayed neutron? Between a fast neutron and a prompt neutron?
11. In a typical fission reaction, which fragment (heavier or lighter) has the larger kinetic energy? The larger momentum? The larger speed?
12. When charged particles travel in a medium faster than light travels in that medium, Cerenkov radiation is emitted. This is the origin of the blue glow of the water that surrounds a reactor core. What might be the identity of these charged particles from a reactor? What velocities and kinetic energies do they need to produce Cerenkov radiation? (The index of refraction of water is 1.33.)
13. In general, would you expect fission fragments to decay by positive or negative beta decay? Why?
14. Among the fission products that build up in reactor fuel elements is xenon, which has an extremely large neutron capture cross section (see Section 13.1). What effect does this buildup have on the operation of the reactor?
15. Helium has virtually no neutron absorption cross section. Would helium be a better reactor moderator than carbon, which has a small but nonzero cross section?
16. Estimate the number of fissions per second that must occur in a 1000-MW power plant, assuming a 30% efficiency of energy conversion.
17. The fission cross section for ^{235}U for slow neutrons is about 10^6 times the fission cross section of ^{238}U for slow neutrons, yet for fast neutrons the fission cross sections of ^{235}U and ^{238}U are roughly the same. Explain this effect.
18. Consider two fragments of uranium fission with atomic numbers Z and $92 - Z$. Estimating their mass numbers as 2.5 times their atomic numbers, find an expression for the Coulomb potential energy of the two fragments when they are just touching, and show that this expression is maximized when the two fragments are identical. Why then is the fission fragment mass distribution, Figure 13.9, not a maximum at $A = 118$?
19. Assume that ^{235}U splits into two fragments with mass numbers of 90 and 145, with each fragment having roughly the same ratio of Z/A as ^{235}U. On this basis, explain why neutrons are emitted in fission.
20. Why is it necessary to convert a proton to a neutron in the first step of the proton-proton fusion cycle? Why can't two protons fuse directly?
21. Explain why a fusion reactor requires a high particle density, a high temperature, and a long confinement time.
22. In the argument leading to Lawson's criterion, Eq. 13.15, it was mentioned that the power necessary to heat the plasma is proportional to the particle density n, while the power obtained from fusion is proportional to n^2. Explain these two proportionalities.
23. Why do radioactive decay power sources use alpha emitters rather than beta emitters?

Problems

13.1 Types of Nuclear Reactions

1. Fill in the missing particle in these reactions:

   (*a*) $^{4}\text{He} + {}^{14}\text{N} \rightarrow {}^{17}\text{O} +$ (*c*) $^{27}\text{Al} + {}^{4}\text{He} \rightarrow \text{n} +$

   (*b*) $^{9}\text{Be} + {}^{4}\text{He} \rightarrow {}^{12}\text{C} +$ (*d*) $^{12}\text{C} + \rightarrow {}^{13}\text{N} + \text{n}$

2. In a certain nuclear reaction, outgoing protons are observed with energies 16.2 MeV, 14.8 MeV, 11.6 MeV, 8.9 MeV, and 6.7 MeV. No energies higher than 16.2 MeV are observed. Construct a level scheme of the product nucleus.

3. In order to determine the cross section for neutron capture, you are irradiating a thin gold foil, in the form of a circular disk of diameter 3.0 mm and thickness 1.81 μm, with neutrons to produce the reaction $n + {}^{197}Au \rightarrow {}^{198}Au + \gamma$. By observing the outgoing gamma-ray photons in a detector, you determine that the gold decays at a rate of 5.37×10^6 per second. From an independent measurement, you have determined the neutron flux to be 7.25×10^{10} neutrons/cm^2/s. What value do you deduce for the cross section for this reaction?
4. The element cobalt is commonly used for measuring the intensity of neutron beams through the reaction $n + {}^{59}Co \rightarrow {}^{60}Co + \gamma$. By observing the radioactive decay of ^{60}Co, it is possible to deduce the rate at which it is produced in the reaction. The cross section for this reaction is 37.0 b. A thin disk of Co-Al alloy has a diameter of 1.00 cm and a mass of 46 mg; the alloy contains 0.44% Co by weight. With neutrons spread uniformly over the surface of the foil, it is concluded that ^{60}Co is produced at the rate of 1.07×10^{12} per second. What is the rate at which neutrons strike the target?
5. A beam of 20.0 μA of protons is incident on 2.0 cm^2 of a target of ^{107}Ag of thickness 4.5 μm producing the reaction $p + {}^{107}Ag \rightarrow {}^{105}Cd + 3n$. Neutrons are observed at a rate of 8.5×10^6 per second. What is the cross section for this reaction at this proton energy?
6. A beam of alpha particles is incident on a target of ^{63}Cu, resulting in the reaction $\alpha + {}^{63}Cu \rightarrow {}^{66}Ga + n$. Assume the cross section for the particular alpha energy to be 1.25 b. The target is in the form of a foil, 2.5 μm thick. The beam has a circular cross section of diameter 0.50 cm and a current of 7.5 μA. Find the rate of neutron emission.

13.2 Radioisotope Production in Nuclear Reactions

7. A radioactive isotope of half-life $t_{1/2}$ is produced in a nuclear reaction. What fraction of the maximum possible activity is produced in an irradiation time of (*a*) $t_{1/2}$; (*b*) $2t_{1/2}$; (*c*) $4t_{1/2}$?
8. List five nuclear reactions, consisting of a light stable projectile nucleus (mass 4 or less) incident on a heavy stable target nucleus, that can produce the radioactive nucleus ^{56}Co.
9. Show that Eq. 13.5 is a solution to Eq. 13.4.
10. The radioisotope ^{15}O ($t_{1/2} = 122$ s) is used to measure respiratory function. Patients inhale the gas, which is made by irradiating nitrogen gas with deuterons (^{2}H). Consider a cubical cell measuring 1.24 cm on each edge, which holds nitrogen gas at a pressure of 2.25 atm and a temperature of 293 K. One face of the cube is uniformly irradiated with a deuteron beam having a current of 2.05 A. At the chosen deuteron energy, the reaction cross section is 0.21 b. (*a*) At what rate is ^{15}O produced in the cell? (*b*) After an irradiation lasting for 60.0 s, what is the activity of ^{15}O in the cell?
11. Neutron capture in sodium occurs with a cross section of 0.53 b and leads to radioactive ^{24}Na ($t_{1/2} = 15$ h). What is the activity that results when 1.0 μg of Na is placed in a neutron flux of 2.5×10^{13} neutrons/cm^2/s for 4.0 h?

13.3 Low-Energy Reaction Kinematics

12. Derive Eq. 13.14 from Eq. 13.13.
13. Find the Q value of the reactions:
    (*a*) $p + {}^{55}Mn \rightarrow {}^{54}Fe + 2n$
    (*b*) $^3He + {}^{40}Ar \rightarrow {}^{41}K + {}^2H$
14. Find the Q value of the reactions:
    (*a*) $^6Li + n \rightarrow {}^3H + {}^4He$
    (*b*) $p + {}^2H \rightarrow 2p + n$
    (*c*) $^7Li + {}^2H \rightarrow {}^8Be + n$
15. In the reaction $^2H + {}^3He \rightarrow p + {}^4He$, deuterons of energy 5.000 MeV are incident on ^{3}He at rest. Both the proton and the alpha particle are observed to travel along the same direction as the incident deuteron. Find the kinetic energies of the proton and the alpha particle.
16. (*a*) What is the Q value of the reaction $p + {}^4He \rightarrow {}^2H + {}^3He$? (*b*) What is the threshold energy for protons incident on ^{4}He at rest? (*c*) What is the threshold energy if ^{4}He are incident on protons at rest?

13.4 Fission

17. (*a*) Find the Q value of the fission decay $^{254}Cf \rightarrow {}^{127}In + {}^{127}In$, in which ^{254}Cf splits in half. (*b*) Find the Q value for the more probable fission process $^{254}_{98}Cf_{156} \rightarrow {}^{140}_{54}Xe_{86} + {}^{110}_{44}Ru_{66} + 4n$. Masses are: $m(^{127}\text{In}) = 126.917353$ u, $m(^{140}\text{Xe}) = 139.921641$ u, $m(^{110}\text{Ru}) = 109.914136$ u.
18. Find the energy released in the fission of 1.00 kg of uranium that has been enriched to 3.0% in the isotope ^{235}U.
19. We can understand why ^{235}U is readily fissionable, and ^{238}U is not, with the following calculation. (*a*) Find the energy difference between $^{235}U + n$ and ^{236}U. We can regard this as the "excitation energy" of ^{236}U. (*b*) Repeat for $^{238}U + n$ and ^{239}U. (*c*) Comparing your results for (*a*) and (*b*), explain why ^{235}U will fission with very low energy neutrons, while ^{238}U requires fast neutrons of 1 to 2 MeV of energy to fission. (*d*) From a similar calculation, predict whether ^{239}Pu requires low-energy or higher-energy neutrons to fission.
20. Find the Q value (and therefore the energy released) in the fission reaction $^{235}U + n \rightarrow {}^{93}Rb + {}^{141}Cs + 2n$. Use $m(^{93}\text{Rb}) = 92.922042$ u and $m(^{141}\text{Cs}) = 140.920046$ u.

13.5 Fusion

21. (*a*) Calculate the Q value for the six reactions or decays of the carbon cycle of fusion. (*b*) By accounting for the electron masses, show that the total Q value for the carbon cycle is identical with that of the proton-proton cycle.
22. Show that the D-T fusion reaction releases 17.6 MeV of energy.
23. In the D-T fusion reaction, the kinetic energies of ^{2}H and ^{3}H are small, compared with typical nuclear binding energies. (Why?) Find the kinetic energy of the emitted neutron.

24. (*a*) If a tokamak fusion reactor were able to achieve a confinement time of 0.60 s, what minimum particle density is required? (*b*) If the reactor were able to achieve 10 times the density found in part (*a*), what is the minimum plasma temperature required for ignition of a self-sustaining fusion reaction?

13.6 Nucleosynthesis

25. Find the energy released when three alpha particles combine to form ^{12}C.
26. To what temperature must helium gas be heated before the Coulomb barrier is overcome and fusion reactions begin?
27. Trace the path of the *s* process from the stable isotope ^{63}Cu to the stable isotope ^{75}As, showing the neutron capture and beta decay processes.
28. Show how the *s* process proceeds from stable ^{81}Br to stable ^{95}Mo.

13.7 Applications of Nuclear Physics

29. An alpha particle of mass m makes an elastic head-on collision with an atom of mass M at rest. Show that the loss in kinetic energy of the alpha particle is given by Eq. 13.16.
30. (*a*) Calculate the energy loss of a 2.50-MeV alpha particle after backscattering from an atom of copper, silver, and gold. Compare your calculated values with the peak energies in Figure 13.25. (*b*) Calculate the expected energy difference between the peaks for the two isotopes of copper and also for the two isotopes of silver. Explain why the silver peaks are closer together than the copper peaks. Can you estimate the relative abundances of the two isotopes of copper from the figure?
31. A radioactive source is to be used to produce electrical power from the alpha decay of ^{238}Pu ($t_{1/2} = 88$ y). (*a*) What is the Q value for the decay? (*b*) Assuming 100% conversion efficiency, how much power could be obtained from the decay of 1.0 g of ^{238}Pu?

General Problems

32. A small sample of paint is placed in a neutron flux of 3.0×10^{12} neutrons/cm^2/s for a period of 2.5 min. At the end of that period the activity of the sample is found to include 105 decays/s of ^{51}Ti ($t_{1/2} = 5.8$ min) and 12 decays/s ^{60}Co ($t_{1/2} = 5.27$ y). Find the amount, in grams, of titanium and cobalt in the original sample. Use the following information: Cobalt is pure ^{59}Co, which has a cross section of 19 b; titanium is 5.25 percent ^{50}Ti, which has a cross section of 0.14 b.
33. A 2.0-mg sample of copper (69% ^{63}Cu, 31% ^{65}Cu) is placed in a reactor where it is exposed to a neutron flux of 5.0×10^{12} neutrons/cm^2/s. After 10.0 min the resulting activities are 72 μCi of ^{64}Cu ($t_{1/2} = 12.7$ h) and 1.30 mCi of ^{66}Cu ($t_{1/2} = 5.1$ min). Find the cross sections of ^{63}Cu and ^{65}Cu.
34. A beam of neutrons of intensity I is incident on a thin slab of material of area A, thickness dx, density ρ, and atomic weight M. The neutron absorption cross section is σ. (*a*) What is the loss in intensity dI of this beam in passing through the material? (*b*) A beam of original intensity I_0 passes through a thickness x of the material. Show that the intensity of the emerging beam is $I = I_0 e^{-n\sigma x}$, where n is the number of absorber nuclei per unit volume. (*c*) Assume that the total cross section for neutrons incident on copper is 5.0 b. What fraction of the intensity of a neutron beam is lost after traveling through copper of thickness 1.0 mm? 1.0 cm? 1.0 m?
35. A reaction in which two particles join to form a single excited nucleus, which then decays to its ground state by photon emission, is known as *radiative capture*. Find the energy of the gamma ray emitted in the radiative capture of an alpha particle by ^{7}Li. Assume alpha particles of very small kinetic energy are incident on ^{7}Li at rest.
36. How much energy is required (in the form of gamma-ray photons) to break up ^{7}Li into $^3\text{H} + {}^4\text{He}$? This reaction is known as *photodisintegration*.
37. The nucleus ^{113}Cd captures a thermal neutron ($K = 0.025$ eV), producing ^{114}Cd in an excited state; the excited state of ^{114}Cd decays to the ground state by emitting a photon. Find the energy of the photon.
38. When a neutron collides head-on with an atom at rest, the loss in its kinetic energy is given by Eq. 13.16. (*a*) What fraction of its energy will a neutron lose in a head-on collision with an atom of hydrogen, deuterium, or carbon? (*b*) Consider a neutron with an initial energy of 2.0 MeV. How many head-on collisions must it make with carbon atoms for its energy to be reduced to the thermal range (0.025 eV)? (*c*) Is the result of part (*b*) an underestimate or an overestimate of the actual number of collisions necessary to "thermalize" the neutrons? Explain.
39. Suppose we have 100.0 cm^3 of water, which is 0.015% D_2O. (*a*) Compute the energy that could be obtained if all the deuterium were consumed in the $^2\text{H} + {}^2\text{H} \rightarrow {}^3\text{H} + \text{p}$ reaction. (*b*) As an alternative, compute the energy released if two-thirds of the deuterium were fused to form ^{3}H, which is then combined with the remaining one-third in the D-T reaction.
40. (*a*) Find the Q value of the reaction $^4\text{He} + {}^4\text{He} \rightarrow {}^8\text{Be}$. (*b*) In a gas of ^{4}He at a temperature of 10^8 K, estimate the relative amount of ^{8}Be present.

Chapter 14

ELEMENTARY PARTICLES

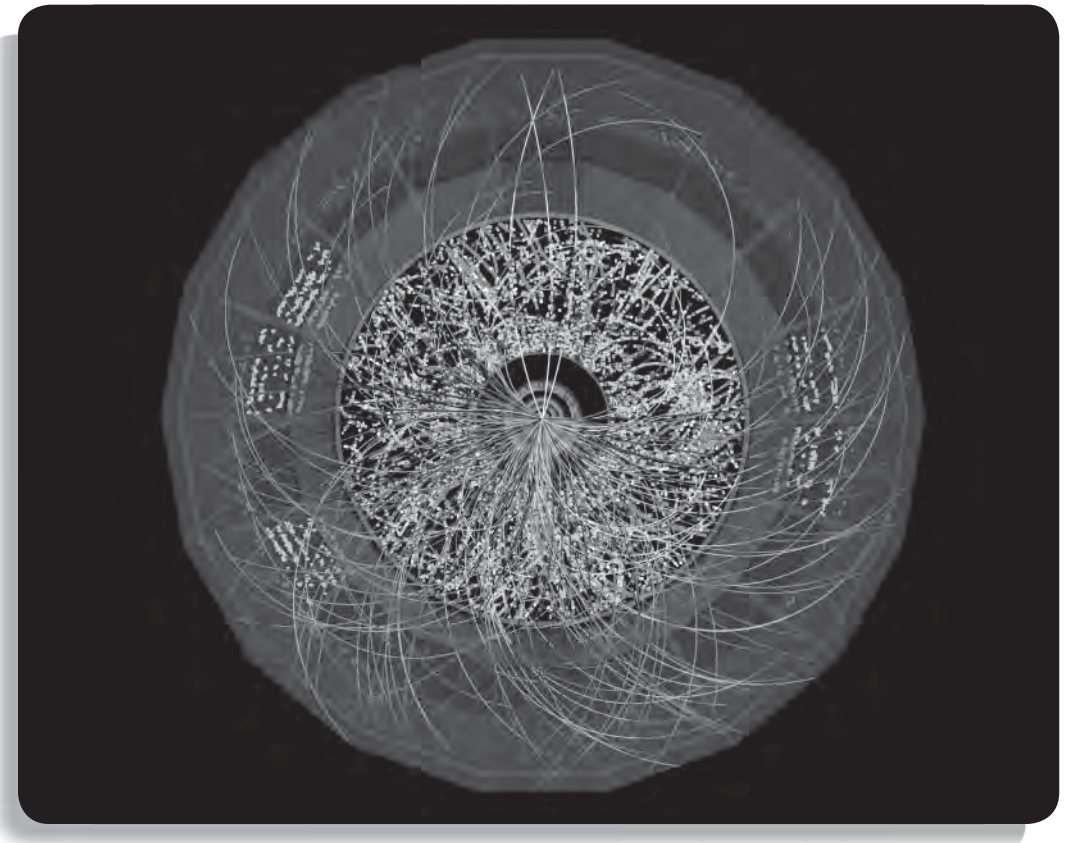

Particle tracks from a head-on collision of two lead ions at the Large Hadron Collider at CERN. Thousands of product particles are produced in each collision. As they travel outward from the collision site at the center, their energy loss and the curvature of their path in a magnetic field help to identify the particles. The goal of this experiment is to produce a ''soup'' of quarks and gluons, which is believed to characterize the universe just microseconds after the Big Bang.

The search for the basic building blocks of nature has occupied the thoughts of scientific investigators since the Greeks introduced the idea of atomism 2500 years ago. As we look carefully at complex structures, we find underlying symmetries and regularities, that help us to understand the laws that determine how they are put together. The regularities of crystal structure, for example, suggest to us that the atoms of which the crystal is composed must follow certain rules for arranging themselves and joining together. As we look more deeply, we find that although nature has constructed all material objects out of roughly 100 different kinds of atoms, we can understand these atoms in terms of only three particles: the electron, proton, and neutron. Our attempts to look further within the electron have been unsuccessful—the electron seems to be a fundamental particle, with no internal structure. However, when nucleons collide at high energy, the result is more complexity rather than simplicity; hundreds of new particles can emerge as products of these reactions. If there are hundreds of basic building blocks, it seems unlikely that we could ever uncover any fundamental dynamic laws of their behavior. However, experiments show a new, underlying regularity that can be explained in terms of a small number of truly fundamental particles called *quarks.*

In this chapter, we examine the properties of many of the particles of physics, the laws that govern their behavior, and the classifications of these particles. We also show how the quark model helps us to understand some properties of the particles.

14.1 THE FOUR BASIC FORCES

All of the known forces in the universe can be grouped into four basic types. In order of increasing strength, these are: *gravitation,* the *weak interaction, electromagnetism,* and the *strong interaction.*

1. The Gravitational Interaction Gravity is of course exceedingly important in our daily lives, but on the scale of fundamental interactions between particles in the subatomic realm, it is of no importance at all. To give a relative figure, the gravitational force between two protons just touching at their surfaces is about 10^{-38} of the strong force between them. The principal difference between gravitation and the other interactions is that, on the practical scale, gravity is cumulative and infinite in range. Tiny gravitational interactions, such as the force exerted by one atom of the Earth on one atom of your body, combine to produce observable effects. The other forces, while much stronger than gravity at the microscopic level, do not affect objects on the large scale, either because they have a short range (the strong and weak forces) or their effect is negated by shielding (electromagnetism).

2. The Weak Interaction The weak interaction is responsible for nuclear beta decay (see Section 12.8) and other similar decay processes involving fundamental particles. It does not play a major role in the binding of nuclei. The weak force between two neighboring protons is about 10^{-7} of the strong force between them, and the range of the weak force is on the scale of 0.001 fm. Nevertheless, the weak force is important in understanding the behavior of fundamental particles, and it is critical in understanding the evolution of the universe.

3. The Electromagnetic Interaction Electromagnetism is important in the structure and the interactions of the fundamental particles. For example, some particles interact or decay primarily through this mechanism. Electromagnetic

forces are of infinite range, but the shielding effect generally diminishes their effect for ordinary objects. Many common macroscopic forces (such as friction, air resistance, drag, and tension) are ultimately due to electromagnetic forces at the atomic level. Within the atom, electromagnetic forces dominate. The electromagnetic force between neighboring protons in a nucleus is about 10^{-2} of the strong force, but within the nucleus the electromagnetic forces can act cumulatively because there is no shielding. As a result, the electromagnetic force can compete with the strong force in determining the stability and the structure of nuclei.

4. The Strong Force The strong force, which is responsible for the binding of nuclei, is the dominant one in the reactions and decays of most of the fundamental particles. However, as we shall see, some particles (such as the electron) do not feel this force at all. It has a relatively short range, on the order of 1 fm.

The relative strength of a force determines the time scale over which it acts. If we bring two particles close enough together for any of these forces to act, then a longer time is required for the weak force to cause a decay or reaction than for the strong force. As we shall see, the mean lifetime of a decay process is often a signal of the type of interaction responsible for the process, with strong forces being at the shortest end of the time scale (often down to 10^{-23} s). Table 14.1 summarizes the four forces and some of their properties.

Particles can interact with one another in decays and reactions through any of the basic forces. Table 14.1 indicates which particles can interact through each of the four forces. All particles can interact through the gravitational and weak forces. A subset of those can interact through the electromagnetic force (for example, the neutrinos are excluded from this category), and a still smaller subset can interact through the strong force. When two strongly interacting particles are within the range of each other's strong force, we can often neglect the effects of the weak and electromagnetic forces in decay and reaction processes; because their relative strengths are so much smaller than that of the strong force, their effects are much smaller than those of the strong force. (However, these forces are not always negligible—the weak interaction between protons is responsible for a critical step in one of the fusion processes that occurs in stars.)

Even though the proton is a strongly interacting particle, a proton and an electron will *never* interact through the strong force. The electron is able to ignore the strong force of the proton and respond only to its weak or electromagnetic force.

Each of the four forces can be represented in terms of the emission or absorption of particles that carry the interaction, just as we represent the force between nucleons in the nucleus in terms of the exchange of pions (see Section 12.4). Associated with each type of force is a field that is carried by its characteristic particle, as shown in Table 14.2.

TABLE 14.1 The Four Basic Forces

Type	Range	Relative Strength	Characteristic Time	Typical Particles
Strong	1 fm	1	$< 10^{-22}$ s	π, K, n, p
Electromagnetic	∞	10^{-2}	$10^{-14} - 10^{-20}$ s	e, μ, π, K, n, p
Weak	10^{-3} fm	10^{-7}	$10^{-8} - 10^{-13}$ s	All
Gravitational	∞	10^{-38}	Years	All

TABLE 14.2 The Field Particles

Force	Field Particle	Symbol	Charge (e)	Spin ($\hbar$)	Rest Energy (GeV)
Strong	Gluon	g	0	1	0
Electromagnetic	Photon	γ	0	1	0
Weak	Weak boson	W^+, W^- Z^0	± 1 0	1 1	80.4 91.2
Gravitational	Graviton		0	2	0

- **The strong force** between quarks is carried by particles called *gluons*, which have been observed through indirect techniques.
- **The electromagnetic force** between particles can be represented in terms of the emission and absorption of *photons*.
- **The weak force** is carried by the *weak bosons* $W^{\pm}$ and Z^0, which are responsible for processes such as nuclear beta decay. For example, the beta decay of the neutron (a weak interaction) can be represented as

$$n \rightarrow p + W^- \qquad \text{followed by} \qquad W^- \rightarrow e^- + \overline{\nu}_e$$

  Because the decay $n \rightarrow p + W^-$ would violate energy conservation, the existence of the W^- is restricted by the uncertainty principle, and its range can be determined in a manner similar to that of the pion (see Eq. 12.8).
- **The gravitational force** is carried by the *graviton*, which is expected to exist based on theories of gravitation but has not yet been observed.

14.2 CLASSIFYING PARTICLES

One way of studying the elementary particles is to classify them into different categories based on certain behaviors or properties and then to look for similarities or common characteristics among the classifications. We have already classified some particles in Table 14.1 according to the types of forces through which they interact. Another way of classifying them might be according to their masses. In the early days of particle physics, it was observed that the lightest particles (including electrons, muons, and neutrinos) showed one type of behavior, the heaviest group (including protons and neutrons) showed a different behavior, and a middle group (such as pions and kaons) showed a still different behavior. The names originally given to these groups are based on the Greek words for light, middle, and heavy: *leptons* for the light particles, *mesons* for the middle group, and *baryons* for the heavier particles. Even though the classification by mass is now obsolete (leptons and mesons have been discovered that are more massive than protons or neutrons), we keep the original names, which now describe instead a group or *family* of particles with similar properties. When we compare our first two ways of classifying particles, we find an interesting result: The leptons do not interact through the strong force, but the mesons and baryons do.

We can also classify particles by their intrinsic spins. Every particle has an intrinsic spin; you will recall that the electron has a spin of $\frac{1}{2}$, as do the proton and neutron. We find that the leptons all have spins of $\frac{1}{2}$, the mesons all have integral spins $(0, 1, 2, \ldots)$, and the baryons all have half-integral spins $(\frac{1}{2}, \frac{3}{2}, \frac{5}{2}, \ldots)$.

Antiparticles

One additional property that is used to classify a particle is the nature of its *antiparticle.** Every particle has an antiparticle, which is identical to the particle in such properties as mass and lifetime, but differs from the particle in the sign of its electric charge (and in the sign of certain other properties, as we discuss later). The antiparticle of the electron is the positron e^+, which was discovered in the 1930s through reactions initiated by cosmic rays. The positron has a charge of $+e$ (opposite to that of the electron) and a rest energy of 0.511 MeV (identical to that of the electron). The antiproton $\bar{p}$ was discovered in 1956 (see Example 2.18); it has a charge of $-e$ and a rest energy of 938 MeV. A stable atom of antihydrogen could be constructed from a positron and an antiproton; the properties of this atom would be identical to those of ordinary hydrogen.

Antiparticles of stable particles (such as the positron and the antiproton) are themselves stable. However, when a particle and its antiparticle meet, the *annihilation reaction* can occur: the particle and antiparticle both vanish, and instead two or more photons can be produced. Conservation of energy and momentum requires that, neglecting the kinetic energies of the particles, when two photons are emitted each must have an energy equal to the rest energy of the particle. Examples of annihilation reactions are:

$$e^- + e^+ \rightarrow \gamma_1 + \gamma_2 \qquad (E_{\gamma_1} = E_{\gamma_2} = 0.511\,\text{MeV})$$
$$p + \bar{p} \rightarrow \gamma_1 + \gamma_2 \qquad (E_{\gamma_1} = E_{\gamma_2} = 938\,\text{MeV})$$

We call the kind of stuff of which we are made *matter* and the other kind of stuff *antimatter.* There may indeed be galaxies composed of antimatter, but we cannot tell by the ordinary techniques of astronomy, because *light and antilight are identical*! To put it another way, the photon and antiphoton are the same particle, so matter and antimatter emit the same photons. The only way to tell the difference is by sending a chunk of our matter to the distant galaxy and seeing whether or not it is annihilated with the corresponding emission of a burst of photons. (It is indeed possible, but *highly unlikely,* that the first astronaut to travel to another galaxy may suffer such a fate! The first intergalactic handshake would indeed be quite an event!)

In our classification scheme it is usually easy to distinguish particles from antiparticles. We begin by defining *particles* to be the stuff of which ordinary matter is made—electrons, protons, and neutrons. Ordinary matter is not composed of neutrinos, so we have no basis for distinguishing a neutrino from an antineutrino, but the conservation laws in the beta decay process can be understood most easily if we define the *antineutrino* to be the particle that accompanies negative beta decay and the *neutrino* to be the particle that accompanies positron decay and electron capture. For a heavy baryon, such as the Λ (lambda), we take advantage of its radioactive decay, which leads eventually to ordinary protons and neutrons; that is, the Λ is the particle that decays to n, and the $\overline{\Lambda}$ ("anti-lambda") therefore decays to $\bar{n}$. Similarly, in the case of the leptons, the μ^- and the μ^+ are antiparticles of one another; because μ^- decays to ordinary e^- (and has many properties in common with the electron) it is the *particle,* while μ^+ is the antiparticle.

---

*We use two systems to indicate antiparticles. Sometimes the symbol for the particle will be written along with the electric charge to indicate particle or antiparticle, as, for example, e^+ and e^-, or μ^+ and μ^-. Other times the antiparticle will be written with a bar over the symbol—for example, ν and $\bar{\nu}$ or p and $\bar{p}$.

Three Families of Particles

Table 14.3 summarizes the three families of material particles.

Leptons The leptons interact only through the weak or electromagnetic interactions. No experiment has yet been able to reveal any internal structure for the leptons; they appear to be truly fundamental particles that cannot be split into still smaller particles. All known leptons have spin $\frac{1}{2}$.

Table 14.4 shows the six known leptons, grouped as three pairs of particles. Each pair includes a charged particle (e^-, μ^-, τ^-) and an uncharged neutrino (ν_e, ν_μ, ν_τ). Each lepton has a corresponding antiparticle. We have already discussed the electron neutrino and antineutrino in connection with beta decay (Section 12.8), and the decay of cosmic-ray muons was discussed as confirming the time dilation effect in special relativity (Section 2.4). The neutrino masses are very small but nonzero. The rest-energy limits shown in Table 14.4 come from attempts at direct measurement, but indirect evidence from astrophysics and cosmology suggests that the rest energies of all three neutrinos are less than 1 eV.

Mesons Mesons are strongly interacting particles having integral spin. A partial list of some mesons is given in Table 14.5. Mesons can be produced in reactions through the strong interaction; they decay to other mesons or leptons through the strong, electromagnetic, or weak interactions. For example, pions can be produced in reaction of nucleons, such as

$$p + n \rightarrow p + p + \pi^- \qquad \text{or} \qquad p + n \rightarrow p + n + \pi^0$$

TABLE 14.3 Families of Particles

Family	Structure	Interactions	Spin	Examples
Leptons	Fundamental	Weak, electromagnetic	Half integral	e, ν
Mesons	Composite	Weak, electromagnetic, strong	Integral	π, K
Baryons	Composite	Weak, electromagnetic, strong	Half integral	p, n

TABLE 14.4 The Lepton Family

Particle	Antiparticle	Particle Charge (e)	Spin ($\hbar$)	Rest Energy (MeV)	Mean Life (s)	Typical Decay Products
e^-	e^+	-1	$\frac{1}{2}$	0.511	∞	
ν_e	$\overline{\nu}_e$	0	$\frac{1}{2}$	< 2 eV	∞	
μ^-	μ^+	-1	$\frac{1}{2}$	105.7	2.2×10^{-6}	$e^- + \overline{\nu}_e + \nu_\mu$
ν_μ	$\overline{\nu}_\mu$	0	$\frac{1}{2}$	< 0.19	∞	
τ^-	τ^+	-1	$\frac{1}{2}$	1777	2.9×10^{-13}	$\mu^- + \overline{\nu}_\mu + \nu_\tau$
ν_τ	$\overline{\nu}_\tau$	0	$\frac{1}{2}$	< 18	∞	

TABLE 14.5 Some Selected Mesons

Particle	Antiparticle	Charge* (e)	Spin ($\hbar$)	Strangeness*	Rest Energy (MeV)	Mean Life (s)	Typical Decay Products
π^+	π^-	+1	0	0	140	2.6×10^{-8}	$\mu^+ + \nu_\mu$
π^0	π^0	0	0	0	135	8.4×10^{-17}	$\gamma + \gamma$
K^+	K^-	+1	0	+1	494	1.2×10^{-8}	$\mu^+ + \nu_\mu$
K^0	$\overline{K}^0$	0	0	+1	498	0.9×10^{-10}	$\pi^+ + \pi^-$
η	η	0	0	0	548	5.1×10^{-19}	$\gamma + \gamma$
ρ^+	ρ^-	+1	1	0	775	4.4×10^{-24}	$\pi^+ + \pi^0$
η'	η'	0	0	0	958	3.2×10^{-21}	$\eta + \pi^+ + \pi^-$
D^+	D^-	+1	0	0	1869	1.0×10^{-12}	$K^- + \pi^+ + \pi^+$
J/ψ	J/ψ	0	1	0	3097	7.1×10^{-21}	$e^+ + e^-$
B^+	B^-	+1	0	0	5279	1.6×10^{-12}	$D^- + \pi^+ + \pi^-$
Υ	Υ	0	1	0	9460	1.2×10^{-20}	$e^+ + e^-$

*The charge and strangeness are those of the particle. Values for the antiparticle have the opposite sign. The spin, rest energy, and mean life are the same for a particle and its antiparticle.

and the pions can decay according to

$$\pi^- \rightarrow \mu^- + \overline{\nu}_\mu \qquad \text{(mean life} = 2.6 \times 10^{-8} \text{ s)}$$
$$\pi^0 \rightarrow \gamma + \gamma \qquad \text{(mean life} = 8.4 \times 10^{-17} \text{ s)}$$

The first decay is caused by the weak interaction (indicated by the lifetime and by the presence of a neutrino among the decay products) and the second is caused by the electromagnetic interaction (indicated by the lifetime and the photons).

Because mesons are not observed in ordinary matter, the classification into particles and antiparticles is somewhat arbitrary. For the charged mesons such as π^+ and π^- or K^+ and K^-, which are not part of ordinary matter, the positive and negative particles are antiparticles of one another but there is no way to choose which is matter and which is antimatter. For some uncharged mesons (such as π^0 and η) the particle and antiparticle are identical, while for others (such as K^0 and $\overline{K}^0$) they may be distinct.

Baryons The baryons are strongly interacting particles with half-integral spins ($1/2, 3/2, \ldots$). A partial listing of some baryons is given in Table 14.6. Like the leptons, the baryons have distinct antiparticles. Like the mesons, the baryons can be produced in reactions with nucleons through the strong interaction; for example, the Λ^0 baryon can be produced in the following reaction:

$$p + p \rightarrow p + \Lambda^0 + K^+$$

The Λ^0 then decays through the weak interaction according to

$$\Lambda^0 \rightarrow p + \pi^- \qquad \text{(mean life} = 2.6 \times 10^{-10} \text{ s)}$$

TABLE 14.6 Some Selected Baryons

Particle	Antiparticle	Charge* (e)	Spin ($\hbar$)	Strangeness*	Rest Energy (MeV)	Mean Life (s)	Typical Decay Products
p	$\bar{p}$	$+1$	$\frac{1}{2}$	0	938	∞	
n	$\bar{n}$	0	$\frac{1}{2}$	0	940	886	$p + e^- + \bar{\nu}_e$
Λ^0	$\overline{\Lambda}^0$	0	$\frac{1}{2}$	-1	1116	2.6×10^{-10}	$p + \pi^-$
Σ^+	$\overline{\Sigma}^+$	$+1$	$\frac{1}{2}$	-1	1189	8.0×10^{-11}	$p + \pi^0$
Σ^0	$\overline{\Sigma}^0$	0	$\frac{1}{2}$	-1	1193	7.4×10^{-20}	$\Lambda^0 + \gamma$
Σ^-	$\overline{\Sigma}^-$	-1	$\frac{1}{2}$	-1	1197	1.5×10^{-10}	$n + \pi^-$
Ξ^0	$\overline{\Xi}^0$	0	$\frac{1}{2}$	-2	1315	2.9×10^{-10}	$\Lambda^0 + \pi^0$
Ξ^-	$\overline{\Xi}^-$	-1	$\frac{1}{2}$	-2	1322	1.6×10^{-10}	$\Lambda^0 + \pi^-$
Δ^*	$\overline{\Delta}^*$	$+2, +1, 0, -1$	$\frac{3}{2}$	0	1232	5.6×10^{-24}	$p + \pi$
Σ^*	$\overline{\Sigma}^*$	$+1, 0, -1$	$\frac{3}{2}$	-1	1385	1.8×10^{-23}	$\Lambda^0 + \pi$
Ξ^*	$\overline{\Xi}^*$	$-1, 0$	$\frac{3}{2}$	-2	1533	7.2×10^{-23}	$\Xi + \pi$
Ω^-	$\overline{\Omega}^-$	-1	$\frac{3}{2}$	-3	1672	8.2×10^{-11}	$\Lambda^0 + K^-$

*The charge and strangeness are those of the particle. Values for the antiparticle have the opposite sign. The spin, rest energy, and mean life are the same for a particle and its antiparticle.

Even though neutrinos are not produced in this decay process, the lifetime indicates that the decay proceeds through the weak interaction. Other baryons can be identified in Table 14.6 that decay through the strong, electromagnetic, or weak interactions.

14.3 CONSERVATION LAWS

In the decays and reactions of elementary particles, conservation laws provide a way to understand why some processes occur and others are not observed, even though they are expected on the basis of other considerations. We frequently use the conservation of energy, linear momentum, and angular momentum in our analysis of physical phenomena. These conservation laws are closely connected with the fundamental properties of space and time; we believe those laws to be absolute and inviolable.

We also use other kinds of conservation laws in analyzing various processes. For example, when we combine two elements in a chemical reaction, such as hydrogen + oxygen → water, we must balance the reaction in the following way:

$$2H_2 + O_2 \rightarrow 2H_2O$$

The process of balancing a reaction can also be regarded as a way of accounting for the electrons that participate in the process: A molecule of water contains 10 electrons, and so the atoms that combine to make up the molecule must likewise include 10 electrons.

In nuclear processes, we are concerned not with electrons but with protons and neutrons. In the alpha decay of a nucleus, such as

$$^{235}_{92}\mathrm{U}_{143} \rightarrow {}^{231}_{90}\mathrm{Th}_{141} + {}^{4}_{2}\mathrm{He}_{2}$$

or in a reaction such as

$$\mathrm{p} + {}^{63}_{29}\mathrm{Cu}_{34} \rightarrow {}^{63}_{30}\mathrm{Zn}_{33} + \mathrm{n}$$

we balance the number of protons and also the number of neutrons. We might be tempted to conclude that nuclear processes conserve both proton number and neutron number, but the separate conservation laws are not satisfied in beta decays, for example

$$\mathrm{n} \rightarrow \mathrm{p} + \mathrm{e}^{-} + \overline{\nu}_{\mathrm{e}}$$

which does not conserve either neutron number or proton number. However, it does conserve the total neutron number plus proton number, which is equal to 1 both before and after the decay. (This conservation law of total nucleon number includes the separate laws of conservation of proton number and neutron number as a special case.)

Emmy Noether (1882–1935, Germany-United States). Known both as a mathematician and a theoretical physicist, she explored the role of conservation laws in physics. In an important result now known as Noether's theorem, she discovered that each symmetry of the mathematical equations describing a phenomenon gives a conserved quantity. For example, the symmetry of equations to translations in time leads to conservation of energy, and the invariance to translations in space leads to conservation of linear momentum.

Lepton Number Conservation

In negative beta decay we always find an antineutrino emitted, never a neutrino. Conversely, in positron beta decay, it is the neutrino that is always emitted. We account for these processes by assigning each particle a *lepton number L*. The electron and neutrino are assigned lepton numbers of +1, and the positron and antineutrino are assigned lepton numbers of −1; all mesons and baryons are assigned lepton numbers of zero. Lepton number conservation in positive and negative beta decay then works as follows:

$$\begin{array}{rccccccc} & \mathrm{n} & \rightarrow & \mathrm{p} & + & \mathrm{e}^{-} & + & \overline{\nu}_{\mathrm{e}} \\ L: & 0 & \rightarrow & 0 & + & 1 & + & (-1) \end{array}$$

$$\begin{array}{rccccccc} & \mathrm{p} & \rightarrow & \mathrm{n} & + & \mathrm{e}^{+} & + & \nu_{\mathrm{e}} \\ L: & 0 & \rightarrow & 0 & + & (-1) & + & 1 \end{array}$$

You can see that the total lepton number is 0 both before and after these decays, which accounts for the appearance of the antineutrino in negative beta decay and the neutrino in positron decay.

According to the lepton conservation law, these processes are forbidden:

$$\begin{array}{rccccccc} & \mathrm{e}^{-} & + & \mathrm{p} & \rightarrow & \mathrm{n} & + & \overline{\nu}_{\mathrm{e}} \\ L: & 1 & + & 0 & \rightarrow & 0 & + & (-1) \end{array}$$

$$\begin{array}{rccccc} & \mathrm{p} & \rightarrow & \mathrm{e}^{+} & + & \gamma \\ L: & 0 & \rightarrow & -1 & + & 0 \end{array}$$

In keeping track of leptons, we must count each type of lepton (e, μ, τ) separately. Evidence for this comes from a variety of experiments. For example, the distinction between electron-type and muon-type leptons is clear from an experiment in which a beam of muon-type antineutrinos is incident on a target of protons:

$$\overline{\nu}_{\mu} + \mathrm{p} \rightarrow \mathrm{n} + \mu^{+}$$

If there were no difference between electron-type and muon-type leptons, the following reaction would be possible: $\overline{\nu}_\mu + \mathrm{p} \rightarrow \mathrm{n} + \mathrm{e}^+$. However, this outcome is never observed, which indicates the distinction between the two types of leptons and the need to account separately for each type.

Another example of the difference between the types of leptons comes from the failure to observe the decay $\mu^- \rightarrow \mathrm{e}^- + \gamma$. If there were only one common type of lepton number, this decay would be possible. The failure to observe this decay (in comparison with the commonly observed decay $\mu^- \rightarrow \mathrm{e}^- + \overline{\nu}_\mathrm{e} + \nu_\mu$, which conserves both muon-type and electron-type lepton number) suggests the need for the different kinds of lepton numbers. We call these lepton numbers L_e, L_μ, and L_τ, and we have the following conservation law for leptons:

In any process, the lepton numbers for electron-type leptons, muon-type leptons, and tau-type leptons must each remain constant.

The following examples illustrate the conservation of these lepton numbers.

$$\begin{array}{rccccccc} & \overline{\nu}_\mathrm{e} & + & \mathrm{p} & \rightarrow & \mathrm{e}^+ & + & \mathrm{n} \\ L_\mathrm{e}: & -1 & + & 0 & \rightarrow & -1 & + & 0 \end{array}$$

$$\begin{array}{rccccccc} & \nu_\mu & + & \mathrm{n} & \rightarrow & \mu^- & + & \mathrm{p} \\ L_\mu: & 1 & + & 0 & \rightarrow & 1 & + & 0 \end{array}$$

$$\begin{array}{rccccccc} & \mu^- & \rightarrow & \mathrm{e}^- & + & \overline{\nu}_\mathrm{e} & + & \nu_\mu \\ L_\mathrm{e}: & 0 & \rightarrow & 1 & + & (-1) & + & 0 \\ L_\mu: & 1 & \rightarrow & 0 & + & 0 & + & 1 \end{array}$$

$$\begin{array}{rccccc} & \pi^- & \rightarrow & \mu^- & + & \overline{\nu}_\mu \\ L_\mu: & 0 & \rightarrow & 1 & + & (-1) \end{array}$$

Studying these examples, we can understand why sometimes neutrinos appear and sometimes antineutrinos appear.

Baryon Number Conservation

Baryons are subject to a similar conservation law. All baryons are assigned a baryon number $B = +1$, and all antibaryons are assigned $B = -1$. All nonbaryons (mesons and leptons) have $B = 0$. We then have the law of conservation of baryon number:

In any process, the total baryon number must remain constant.

(The conservation of nucleon number A is a special case of conservation of baryon number, in which all the baryons are nucleons. In particle physics, it is customary to use B instead of A to represent all baryons, including the nucleons.) No violation of the law of baryon conservation has ever been observed, although the Grand Unified Theories (see Section 14.8) suggest that the proton can decay in a way that would violate conservation of baryon number.

As an example of conservation of baryon number, consider the reaction that was responsible for the discovery of the antiproton:

$$\mathrm{p} + \mathrm{p} \rightarrow \mathrm{p} + \mathrm{p} + \mathrm{p} + \overline{\mathrm{p}}$$

On the left side, the total baryon number is $B = +2$. On the right side, we have three baryons with $B = +1$ and one antibaryon with $B = -1$, so the total baryon number is $B = +2$ on the right side also. On the other hand, the

reaction $p + p \rightarrow p + p + \bar{n}$ violates baryon number conservation and is therefore forbidden.

Strangeness Conservation

The number of mesons that can be created or destroyed in decays or reactions is not subject to a conservation law like the number of leptons or baryons. For example, the following reactions can be used to produce pions:

$$p + p \rightarrow p + n + \pi^+ \qquad p + p \rightarrow p + n + \pi^+ + \pi^0$$
$$p + p \rightarrow p + p + \pi^0 \qquad p + p \rightarrow p + p + \pi^+ + \pi^-$$

As long as enough energy is available, any number of pions can be produced in these reactions.

If we try the same type of reaction to produce K mesons, a different type of behavior is observed. The reactions $p + p \rightarrow p + n + K^+$ and $p + p \rightarrow p + p + K^0$ never occur, even though the incident proton is given enough energy to produce this particle. We do, however, observe reactions such as $p + p \rightarrow p + n + K^+ + \overline{K}^0$ and $p + p \rightarrow p + p + K^+ + K^-$, which are very similar to the reactions that produce two pions. Why do reactions producing π mesons give any number (odd or even) but reactions producing K mesons give them only in pairs?

Here's another example of this unusual behavior. The reaction $\pi^- + p \rightarrow \pi^+ + \Sigma^-$ conserves electric charge and baryon number and so would be expected to occur, but it does not. Instead, the following reaction is easily observed: $\pi^- + p \rightarrow K^+ + \Sigma^-$. Usually when we fail to observe a reaction or decay process that is expected to occur, we look for the violation of some conservation law such as electric charge or baryon number. Is there a new conserved quantity whose violation prohibits the reaction from occurring?

There are also decay processes that suggest that our labeling of the particles is incomplete. The uncharged η and π^0 mesons decay very rapidly ($10^{-16} - 10^{-18}$ s) into two photons; on the basis of the systematic behavior of mesons, we would expect the K^0 to decay similarly to two photons in a comparable time. The observed decay of the K^0 takes place much more slowly (10^{-10} s); moreover, the decay products are not photons, but π mesons and leptons. Is a new conservation law responsible for restricting the decay of the K^0?

As a final example of the need for a new conservation law, the heavy charged mesons are all strongly interacting particles, and we expect them to decay into the lighter mesons through the strong interaction with very short lifetimes. For example, the decay $\rho^+ \rightarrow \pi^+ + \pi^0$ occurs in a lifetime of about 10^{-23} s. But the decay $K^+ \rightarrow \pi^+ + \pi^0$ occurs very slowly, in a time of the order of 10^{-8} s, and in fact the different decay mode $K^+ \rightarrow \mu^+ + \nu_\mu$ is more probable. What is responsible for slowing the decay of the K meson by 15 orders of magnitude?

These unusual behaviors are explained by the introduction of a new conserved quantity. This quantity is called the *strangeness* S, and we can use it to explain the properties of the K-meson decays. The K^0 and K^+ are assigned strangeness of $S = +1$; the π mesons and leptons are nonstrange particles ($S = 0$). The decay $K^0 \rightarrow \gamma + \gamma$, which is an electromagnetic decay (as indicated by the photons), is forbidden because the electromagnetic interaction conserves strangeness ($S = +1$ on the left, $S = 0$ on the right). The decay $K^+ \rightarrow \pi^+ + \pi^0$ does not occur in the typical strong interaction time of 10^{-23} s because the strong interaction cannot change strangeness. It occurs in the typical weak interaction time of 10^{-8} s (and the

corresponding weak interaction decay $K^+ \rightarrow \mu^+ + \nu_\mu$ occurs as often) because the weak interaction *does not* conserve strangeness; decays that are caused by the weak interaction can change the strangeness by one unit.

We can summarize these results in the *law of conservation of strangeness*:

> *In processes governed by the strong or electromagnetic interactions, the total strangeness must remain constant. In processes governed by the weak interaction, the strangeness either remains constant or changes by one unit.*

The strangeness quantum numbers of the mesons and baryons are given in Tables 14.5 and 14.6. The strangeness of an antiparticle has the opposite sign to that of the corresponding particle.

Conservation of strangeness in the strong interaction explains why the K mesons are always produced in pairs in proton-proton collisions. The protons and neutrons are non-strange particles ($S = 0$), so the only way to conserve strangeness in the collisions that produce K mesons is to produce them in pairs, always one with $S = +1$ and the other with $S = -1$.

The baryons also come in strange and nonstrange varieties. Looking at the lifetimes in Table 14.6, we see that the Λ^0 decays into $p + \pi^-$ with a lifetime of about 10^{-10} s, while we would expect a strongly interacting particle to decay to other strongly interacting particles with a lifetime of about 10^{-23} s. If the strangeness of the Λ^0 is assigned as -1, these decays change S and are forbidden to go by the strong interaction, and so must be due to the weak interaction, with the characteristic 10^{-10} s lifetime. The strangeness violation also tells us why the electromagnetic decay $\Lambda^0 \rightarrow n + \gamma$ does not occur (while the decay $\Sigma^0 \rightarrow \Lambda^0 + \gamma$ does occur, with a typical electromagnetic lifetime of 10^{-19} s). It also explains why the reaction $\pi^- + p \rightarrow \pi^+ + \Sigma^-$, which is permitted by all other conservation laws. is never observed—the initial state has $S = 0$ and the final state has $S = -1$, so it violates strangeness conservation.

The weak interaction can change the strangeness by at most *one* unit. As a result, processes such as $\Xi^0 \rightarrow n + \pi^0$ ($S = -2 \rightarrow S = 0$) are absolutely forbidden, even by the weak interaction.

Example 14.1

The Ω^- baryon has $S = -3$. (*a*) It is desired to produce the Ω^- using a beam of K^- incident on protons. What other particles are produced in this reaction? (*b*) How might the Ω^- decay?

Solution

(*a*) Reactions usually proceed only through the strong interaction, which conserves strangeness. We consider the reaction

$$K^- + p \rightarrow \Omega^- + ?$$

On the left side, we have $S = -1, B = +1$, and electric charge $Q = 0$. On the right side, we have $S = -3$, $B = +1$, and $Q = -1$. We must therefore add to the right side particles with $S = +2$, $B = 0$, and $Q = +1$. Scanning through the tables of mesons and baryons, we find that we can satisfy these criteria with K^+ and K^0, so one possible reaction is

$$K^- + p \rightarrow \Omega^- + K^+ + K^0$$

(*b*) The Ω^- cannot decay by the strong interaction, because no $S = -3$ final states are available. It must therefore decay to particles having $S = -2$ through the weak interaction, which can change S by one unit. One of the product particles must be a baryon in order to conserve baryon number. Two possibilities are

$$\Omega^- \rightarrow \Lambda^0 + K^- \quad \text{and} \quad \Omega^- \rightarrow \Xi^0 + \pi^-$$

14.4 PARTICLE INTERACTIONS AND DECAYS

In this section we briefly summarize the properties of the elementary particles and how they are measured.

Atoms and molecules can be taken apart relatively easily and nonviolently, enabling us to study their structure. However, the elementary particles, most of which are unstable and do not exist in nature, must be created in violent collisions. (The particle theorist Richard Feynman once compared this process with studying fine Swiss watches by smashing them together and looking at the pieces that emerge from the collision.) For this purpose we need a high-energy beam of particles and a suitable target of elementary particles. The only strongly interacting, stable elementary particle is the proton, and thus a hydrogen target is a logical choice. To get a reasonable density of target atoms, researchers often use liquid, rather than gaseous, hydrogen.

For a suitable beam, we must be able to accelerate a particle to very high energies (so that the energy of the particle may be hundreds of times its rest energy mc^2). A stable charged particle is the logical choice for the beam; stability is required because of the relatively long time necessary to accelerate the particle to high energies, and a charged particle is required so that electromagnetic fields may be used to accelerate the particle. Once again the proton is a convenient choice, and thus many particle physics reactions are produced using beams of high-energy protons. For example, at the Fermi National Accelerator Laboratory (Fermilab) near Chicago protons are accelerated to 1000 GeV ($v/c = 0.9999996$) around a track of radius 1000 m (Figure 14.1).

One type of particle physics reaction can thus be represented as

$$\mathrm{p} + \mathrm{p} \rightarrow \text{product particles}$$

FIGURE 14.1 An aerial view of the Tevatron at the Fermi National Accelerator Laboratory. Beams of protons and antiprotons circulate in opposite directions around the 1-km ring and collide at two locations, at the upper center and lower left. (Courtesy Fermi National Accelerator Laboratory.)

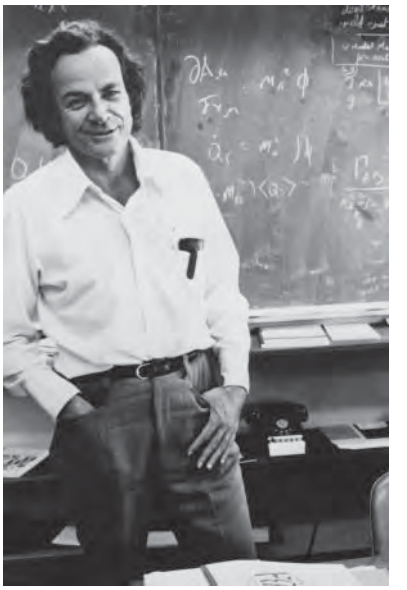

Richard P. Feynman (1918–1988, United States). Seldom is one person known for both exceptional insights into theoretical physics and exceptional methods of teaching first-year physics. He received the Nobel Prize for his work on the theory that couples quantum mechanics to electromagnetism, and his text and film *Lectures on Physics* give unusual perspectives to many areas of basic physics for undergraduates.

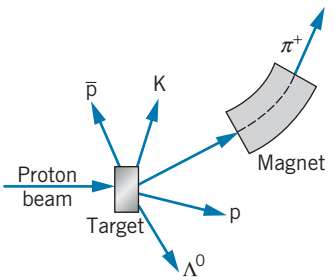

FIGURE 14.2 The production of secondary particle beams. The magnet helps to select the mass and momentum of the desired particle.

Among the product particles may be a variety of mesons or even heavier particles of the baryon family, of which the nucleons are the lightest members. The study of the nature and properties of these particles is the goal of particle physics.

In many cases, conservation laws restrict the nature of the product particles, and it would be desirable to have other types of beams available. One possibility is indicated in Figure 14.2. A proton beam is incident on a target—the nature of the target is not important. Like Feynman's Swiss watch parts, many different particles emerge. By suitable focusing and selection of the momentum, we can extract a beam of the *secondary* particles created in the reactions. The particle must live long enough to be delivered to a second target, which might be tens of meters away; even if the particle were traveling at the speed of light, it would need about 10^{-7} s to make its journey. Although this is a very short time interval by ordinary standards, on the time scale of elementary particles, it is a very long time—in fact, none of the unstable mesons or baryons (except the neutron) lives that long.

Although our efforts to make a secondary beam would seem to be in vain, we have forgotten one very important detail. The lifetime of the particle is measured in its rest frame, while we are observing its flight in the laboratory frame, in which the particle is moving at speeds extremely close to the speed of light. The *time dilation* factor results in a lifetime, observed in our frame of reference, which might be hundreds of times longer than the *proper lifetime.* This factor extends the range of available secondary beams to those particles with lifetimes as short as 10^{-10} s, and makes it possible to obtain secondary beams to study such reactions as

$$\pi + \mathrm{p} \rightarrow \text{particles}$$

and

$$\mathrm{K} + \mathrm{p} \rightarrow \text{particles}$$

even though the proper lifetimes of the π and K are in the range of 10^{-10} to 10^{-8} s.

Detecting Particles

Observing the products of these reactions, which may involve dozens of high-energy charged and uncharged particles, poses a great technological problem for the experimenter. The detector must completely surround the reaction area, so that particles are recorded no matter what direction they travel after the reaction. The particles must produce visible tracks in the detector, so that their identity and direction of travel can be determined. The detector must provide sufficient mass to stop the particles and measure their energy. A magnetic field must be present, so that the resulting curved trajectory of a charged particle can be used to determine its momentum and the sign of its charge. Figure 14.3 shows tracks left in a *bubble chamber*, a large tank filled with liquid hydrogen in which the passage of a charged particle causes microscopic bubbles resulting from the ionization of the hydrogen atoms. The bubbles can be illuminated and photographed to reveal the tracks. Figure 14.4 shows a large detector system that is used both to display the tracks of particles and to measure their energies; Figure 14.5 shows a sample of the results that are obtained with this type of detector.

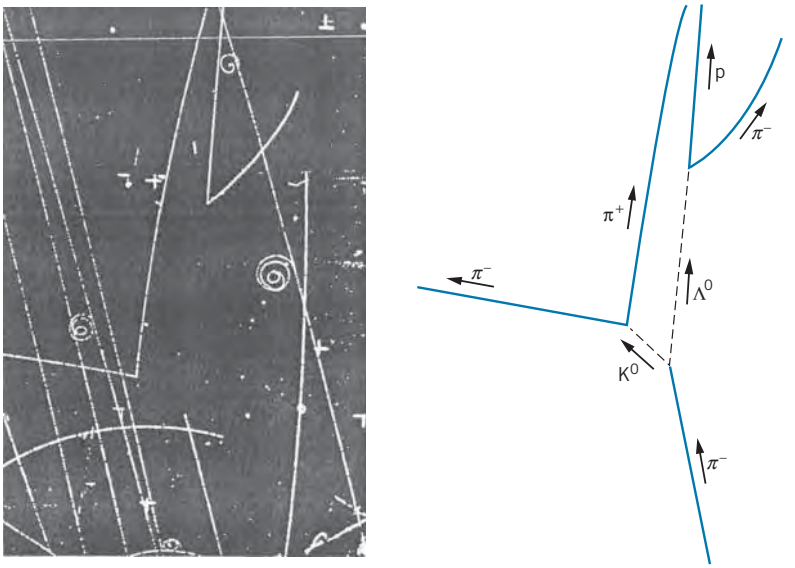

FIGURE 14.3 A bubble chamber photograph of a reaction between particles. At right is shown a diagram indicating the particles that participate in the reaction. An incident pion collides with a proton in the liquid hydrogen, producing a K^0 and a Λ^0, both of which subsequently decay. (Photo Courtesy Lawrence Berkeley National Laboratory.)

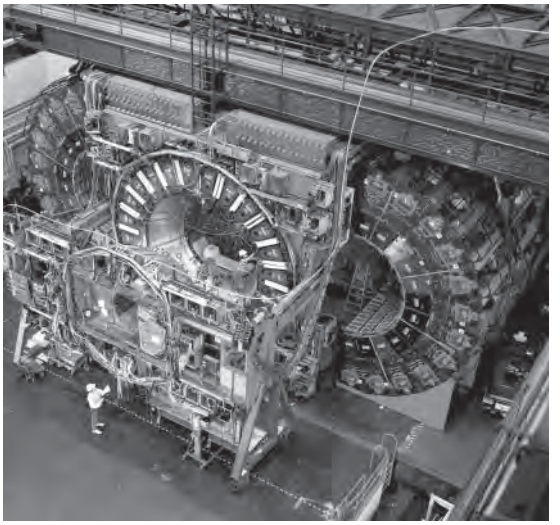

FIGURE 14.4 A large detector at the Tevatron at Fermilab. The proton and antiproton beams travel along the central axis of the detector and collide in its interior. The arches that have been removed on either side are the calorimeter detectors that in operation are pushed together so they can record the energies of all particles that leave the reaction. The inner detectors record the tracks of the particles. (Courtesy Fermi National Accelerator Laboratory.)

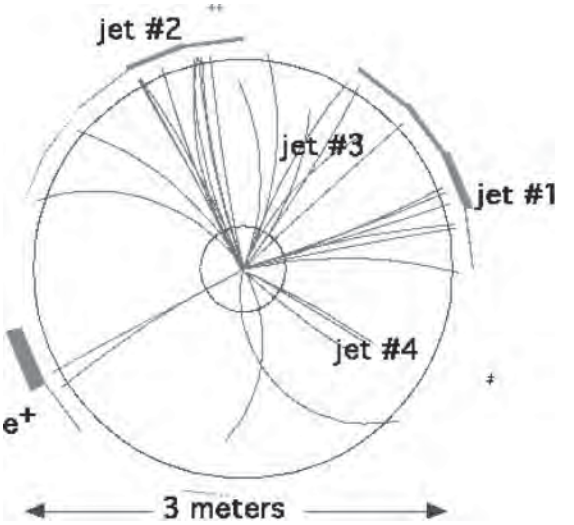

FIGURE 14.5 A sample of the tracks left by a multitude of particles from a single proton-antiproton collision recorded with the detector of Figure 14.4. A magnetic field causes the tracks to curve; the radius of curvature determines the momentum of the particle, and the direction of curvature determines the sign of the charge of the particle. The jets are showers of particles resulting from a quark or antiquark that is produced in the reaction. In this case the jets come from the top and antitop quarks. (Courtesy Fermi National Accelerator Laboratory.)

From a careful analysis of the paths of particles, such as those of Figures 14.3 or 14.5, we can deduce the desired quantities of mass, linear momentum, and energy. The other important property we would like to know is the lifetime of the decay of the product particles, because many of the products are often unstable. If we know the speed of a particle, we can find its lifetime by simply observing the length of its track in a bubble chamber photograph. (Even for uncharged particles, which leave no tracks, we can use this method to deduce the lifetime, because the subsequent decay of the uncharged particle into two charged particles defines the length of its path rather clearly, as shown in Figure 14.3.)

This method works well if the lifetime is of the order of 10^{-10} s or so, such that the particle leaves a track long enough to be measured (millimeters to centimeters). With careful experimental technique and clever data analysis, this can be extended to track lengths of the order of 10^{-6} m, and so lifetimes down to about 10^{-16} s can be measured in this way (with a little help from the time dilation factor). But many of our particles have lifetimes of only 10^{-23} s, and a particle moving at even the speed of light travels only the diameter of a nucleus in that time! How can we measure such a lifetime? Furthermore, how do we even know such a particle exists at all? Consider the reaction

$$\pi + \mathrm{p} \rightarrow \pi + \mathrm{p} + \mathrm{x}$$

where x is an unknown particle with a lifetime of about 10^{-23} s, which decays into two π mesons according to $\mathrm{x} \rightarrow \pi + \pi$. How do we distinguish the above reaction from the reaction

$$\pi + \mathrm{p} \rightarrow \pi + \mathrm{p} + \pi + \pi$$

which leads to the same particles as actually observed in the laboratory?

Experimental evidence suggests that the two π mesons in this type of reaction may combine for an instant (10^{-23} s) to form an entity with all of the usual properties of a particle—a definite mass, charge, spin, lifetime, etc. These states are known as *resonance particles*, and we now look at the indirect evidence from which we infer their existence.

Suppose you receive a package in the mail from a friend. When you open it, you find it contains many small, irregular pieces of broken glass. How do you learn whether your friend sent you a beautiful glass vase that was broken in shipment or a package of broken glass as a practical joke? You try to put the pieces together! If the pieces fit together, it is a good assumption that the vase was once whole, although the mere fact that they fit together doesn't *prove* that it was once whole. It's just the simplest possible assumption *consistent with our experience*. (An alternative assumption that the pieces were manufactured separately and just happen by chance to fit together is highly improbable.)

How then do we detect a "particle" that lives for only 10^{-23} s? We look at its decay products (which live long enough to be seen in the laboratory), and putting the pieces back together, we infer that they once may have been a whole particle.

For example, suppose in the laboratory we observe two π mesons emitted as shown in Figure 14.6. We measure the direction of travel and the linear momentum of the π mesons as shown. A second and a third event each produces two π mesons as also shown in the figure. Are these three events consistent with the existence of the same resonance particle?

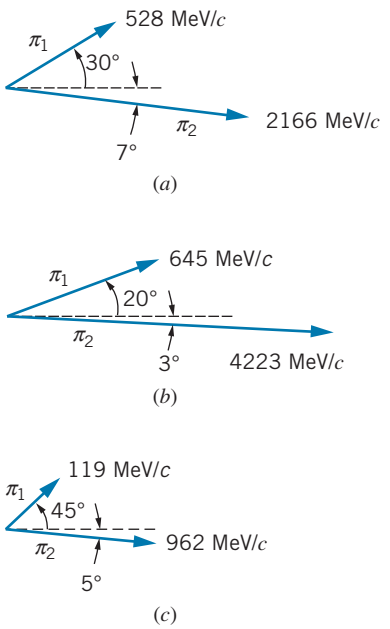

FIGURE 14.6 Three possible decays of an unknown particle into two π mesons. The direction and momentum of each π meson are indicated.

Let us assume that in each case, a particle moving at an unknown speed decayed into the two particles as shown, one with energy E_1 and momentum $\vec{\mathbf{p}}_1$ and the other with energy E_2 and momentum $\vec{\mathbf{p}}_2$. Each decay must conserve energy and momentum, so we can use the decay information to find the energy $E = E_1 + E_2$ and momentum $\vec{\mathbf{p}} = \vec{\mathbf{p}}_1 + \vec{\mathbf{p}}_2$ of the decaying particle, and then we can find its rest energy according to $mc^2 = \sqrt{E^2 - c^2\vec{\mathbf{p}}^2} = \sqrt{(E_1 + E_2)^2 - c^2(\vec{\mathbf{p}}_1 + \vec{\mathbf{p}}_2)^2}$. Carrying out the calculation, we find that, for the decay shown in part (*a*) of Figure 14.6, $mc^2 = 764$ MeV, while for part (*b*), $mc^2 = 775$ MeV. It is therefore possible that these two events result from the decays of identical particles. Part (*c*) of the figure gives $mc^2 = 498$ MeV, which differs considerably from parts (*a*) and (*b*).

Of course, these two events are not sufficient to identify conclusively the existence of a resonance particle with a rest energy in the range of 770 MeV. It could be a mere accident, just like the chance fitting together of two pieces of broken glass. What is needed is a large (statistically significant) number of events, in which we can combine the energy and momenta of the two emitted π mesons in such a way that the deduced mass of the resonance particle is always the same. Figure 14.7 is an example of such a result. There is a background of events with a continuous distribution of energies, like beta decay electrons; these come from events like part (*c*) of Figure 14.6. There is also present a very prominent peak at 775 MeV. We identify this energy as the rest energy of the resonance particle, which is known as the ρ (rho) meson. (How do we know it is a meson? It must be a strongly interacting particle, because it decays so rapidly. Therefore the only possibilities are mesons, with integral spin, or baryons, with half-integral spin. Pi mesons have integral spin, and two integral spins can combine to give only another integral spin, so it must be a meson.)

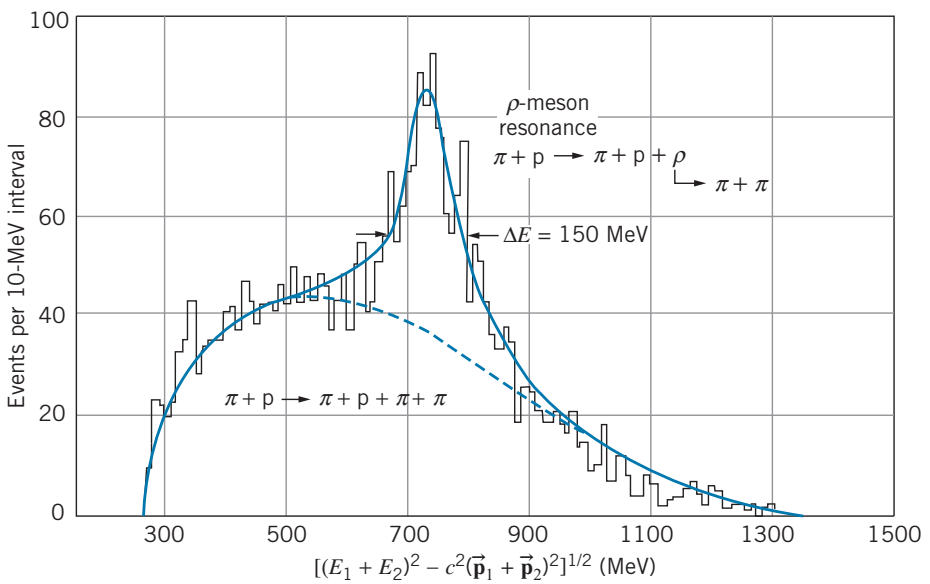

FIGURE 14.7 The resonance identified as the ρ meson. The horizontal axis shows the energy and momentum of the two decay π mesons, combined to be equivalent to the mass of the resonance particle.

We can also infer the lifetime of the particle from Figure 14.7. The particle lives only for about 10^{-23} s, and so if we are to measure its rest energy we have only 10^{-23} s in which to do it. But the uncertainty principle requires that an energy measurement made in a time interval Δt be uncertain by an amount roughly $\Delta E \cong \hbar/\Delta t$. This energy uncertainty ΔE is observed as the *width* of the peak in Figure 14.7. We don't always deduce the same value 775 MeV for the rest energy of the ρ meson; sometimes our value is a bit larger and sometimes a bit smaller. *The width of the resonance peak tells us the lifetime of the particle.* (The width is not really precisely defined, but physicists usually take as the width the interval between the two points where the height of the resonance is one-half its maximum value above the background, as shown in Figure 14.7.) The width of $\Delta E = 150\,\text{MeV}$ leads to a value of $\Delta t = \hbar/\Delta E = 4.4 \times 10^{-24}$ s for the lifetime of the ρ meson.

14.5 ENERGY AND MOMENTUM IN PARTICLE DECAYS

In analyzing the decays and reactions of elementary particles, we apply many of the same laws that we used for nuclear decays and reactions: energy, linear momentum, and total angular momentum must be conserved, and the total value of the quantum numbers associated with electric charge, lepton number, and baryon number (which we previously called nucleon number) must be the same before and after the decay or reaction. In reactions of elementary particles, we are often concerned with the production of new varieties of particles. The energy necessary to manufacture these particles comes from the kinetic energy of the reaction constituents (usually the incident particle); this energy is usually quite large (hence the name *high-energy physics* for this type of research), so *relativistic equations* must be used for energy and momentum.

The decays of elementary particles can be analyzed in a way similar to the decays of nuclei, following the same two basic rules:

1. The energy available for the decay is the difference in rest energy between the initial decaying particle and the particles that are produced in the decay. By analogy with our study of nuclear decays, we call this the Q value:

$$Q = (m_\text{i} - m_\text{f})c^2 \tag{14.1}$$

   where $m_\text{i}c^2$ is the rest energy of the initial particle and $m_\text{f}c^2$ is the total rest energy of all the final product particles. (Of course, the decay will occur only if Q is positive.)
2. The available energy Q is shared as kinetic energy of the decay products in such a way as to conserve linear momentum. As in the case of nuclear decays, for a decay of a particle at rest into two final particles, the particles have equal and opposite momenta, and we can find unique values for the energies of the two final particles. For decays into three or more particles, each particle has a spectrum or distribution of energies from zero up to some maximum value (as was the case with nuclear beta decay).

Example 14.2

Compute the energies of the proton and π meson that result from the decay of a Λ^0 at rest.

Solution

The decay process is $\Lambda^0 \rightarrow \mathrm{p} + \pi^-$. Using the rest energies from Tables 14.5 and 14.6, we have:

$$\begin{aligned} Q &= (m_{\Lambda^0} - m_\mathrm{p} - m_{\pi^-})c^2 \\ &= 1116\,\mathrm{MeV} - 938\,\mathrm{MeV} - 140\,\mathrm{MeV} \\ &= 38\,\mathrm{MeV} \end{aligned}$$

and so the total kinetic energy of the decay products must be:

$$K_\mathrm{p} + K_\pi = 38\,\mathrm{MeV}$$

Using the relativistic formula for kinetic energy, we can write this as

$$\begin{aligned} K_\mathrm{p} + K_\pi = &\left(\sqrt{c^2p_\mathrm{p}^2 + m_\mathrm{p}^2c^4} - m_\mathrm{p}c^2\right) \\ &+ \left(\sqrt{c^2p_\pi^2 + m_\pi^2c^4} - m_\pi c^2\right) = 38\,\mathrm{MeV} \end{aligned}$$

Conservation of momentum requires $p_\mathrm{p} = p_\pi$. Substituting for one of the unknown momenta in the above equation and solving algebraically for the other, we obtain

$$p_\pi = p_\mathrm{p} = 101\,\mathrm{MeV}/c$$

The kinetic energies can be found by substituting these momenta into the relativistic formula:

$$K_\pi = 33\,\mathrm{MeV} \qquad \text{and} \qquad K_\mathrm{p} = 5\,\mathrm{MeV}$$

Example 14.3

What is the maximum kinetic energy of the electron emitted in the decay $\mu^- \rightarrow \mathrm{e}^- + \overline{\nu}_\mathrm{e} + \nu_\mu$?

Solution

The Q value for this decay is $Q = m_\mu c^2 - m_\mathrm{e}c^2 = 105.2\,\mathrm{MeV}$, because the neutrinos have negligible rest energy. If the μ^- is at rest, this energy is shared by the electron and the neutrinos: $Q = K_\mathrm{e} + E_{\overline{\nu}_\mathrm{e}} + E_{\nu_\mu}$. When the electron has its maximum kinetic energy, the two neutrinos carry away the minimum energy. This minimum cannot be zero, because that would violate momentum conservation: the electron would be carrying momentum that would not be balanced by the neutrino momenta to give a net of zero (the μ^- is at rest, so $\sum \vec{\mathbf{p}}_\mathrm{i} = \sum \vec{\mathbf{p}}_\mathrm{f} = 0$). We assume that the electron has its maximum energy when the neutrinos are emitted in exactly the opposite direction to the electron; otherwise some of the decay energy is "wasted" by providing transverse momentum components for the neutrinos, and not as much energy will be available for the electron. It does not matter which of the neutrinos carry the energy and momentum (they may even share it in any proportion), so we let E_ν and p_ν be the total neutrino energy and momentum; these are of course related by $E_\nu \cong cp_\nu$, because neutrinos are presumed to be of negligible mass and thus to travel at nearly the speed of light. If we let E_e and p_e represent the energy and momentum of the electron, then linear momentum conservation gives

$$p_\mathrm{e} - p_\nu = 0$$

For the electron, $E_\mathrm{e} = \sqrt{c^2p_\mathrm{e}^2 + m_\mathrm{e}^2c^4}$. Together, these equations give:

$$\begin{aligned} Q = K_\mathrm{e} + E_\nu &= E_\mathrm{e} - m_\mathrm{e}c^2 + cp_\nu = E_\mathrm{e} - m_\mathrm{e}c^2 + cp_\mathrm{e} \\ &= E_\mathrm{e} - m_\mathrm{e}c^2 + \sqrt{E_\mathrm{e}^2 - m_\mathrm{e}^2c^4} \end{aligned}$$

Solving, we find $E_\mathrm{e} = Q/2m_\mu c^2 + m_\mathrm{e}c^2$ and so

$$K_\mathrm{e} = E_\mathrm{e} - m_\mathrm{e}c^2 = Q^2/2m_\mu c^2 = 52.3\,\mathrm{MeV}$$

The original rest energy of the μ^- is shared essentially equally by the electron and the two neutrinos in this case: $(K_\mathrm{e})_\mathrm{max} = (E_\nu)_\mathrm{max} \cong Q/2$. Note how different this is from the case of the beta decay of the neutron, where the heavy proton resulting from the decay could absorb considerable recoil momentum at a cost of very little energy, so nearly all of the available energy could be given to the electron, and in that case $(K_\mathrm{e})_\mathrm{max} \cong Q$.

Example 14.4

Find the maximum energy of the positrons and of the π mesons produced in the decay $K^+ \rightarrow \pi^0 + e^+ + \nu_e$.

Solution

The Q value for this decay is

$$Q = (m_K - m_\pi - m_e)c^2 = 494\,\text{MeV} - 135\,\text{MeV} - 0.5\,\text{MeV} = 358.5\,\text{MeV}$$

This energy must be shared among the three products:

$$Q = K_\pi + K_e + E_\nu$$

The electron and π meson have their maximum energies when the neutrino has negligible energy: $Q = K_\pi + K_e$, and conservation of momentum in this case (if the neutrino has negligible momentum) requires $p_\pi = p_e$. Using relativistic kinetic energy, we have

$$Q = K_\pi + K_e = \sqrt{(pc)^2 + (m_\pi c^2)^2} - m_\pi c^2 + \sqrt{(pc)^2 + (m_e c^2)^2} - m_e c^2$$

where $p = p_e = p_\nu$. Inserting the numbers, we obtain

$$494\,\text{MeV} = \sqrt{(pc)^2 + (135\,\text{MeV})^2} + \sqrt{(pc)^2 + (0.5\,\text{MeV})^2}$$

Clearing the two radicals involves quite a bit of algebra, but we can simplify the problem if we inspect this expression and notice that the solution must have a large value of pc, certainly greater than 100 MeV. (Otherwise the two terms could not sum to nearly 500 MeV.) Thus $(pc)^2 \gg (0.5\,\text{MeV})^2$, and we can neglect the electron rest energy term in the second radical, which simplifies the equation somewhat:

$$494\,\text{MeV} = \sqrt{(pc)^2 + (135\,\text{MeV})^2} + pc$$

Solving, we find $pc = 229$ MeV, which gives $(E_e)_{max} = 229$ MeV and $(E_\pi)_{max} = 266$ MeV. Figure 14.8 shows the observed energy spectra of e^+ and π^0 from the K^+ decay, and the energy maxima are in agreement with the calculated values. (The shapes of the energy distributions are determined by statistical factors, as in the case of nuclear beta decay. The statistical factors are different for e^+ and π^0, because the π^0 also has its maximum energy when the e^+ appears at rest and the ν carries the recoil momentum.)

You should repeat this calculation and convince yourself that (1) the π^0 has its maximum energy also when $K_e = 0$ ($E_e = m_e c^2$) and (2) the e^+ does *not* have its maximum energy when $K_\pi = 0$.

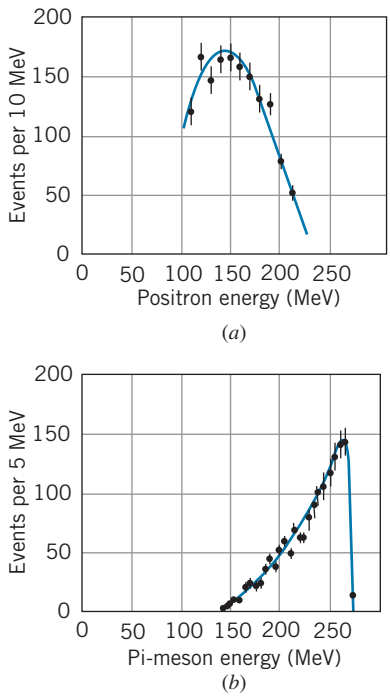

FIGURE 14.8 The spectrum of positrons and π mesons from the decay of the K^+ meson.

14.6 ENERGY AND MOMENTUM IN PARTICLE REACTIONS

The basic experimental technique of particle physics consists of studying the product particles that result from a collision between an incident particle (accelerated to high energies) and a target particle (often at rest). The kinematics of the reaction

process must be analyzed using relativistic formulas, because the kinetic energies of the particles are usually comparable to or greater than their rest energies. In this section we derive some of the relationships that are needed to analyze these reactions, using the formulas for relativistic kinematics we obtained in Chapter 2. An important purpose of these reactions is the production of new varieties of particles, so we concentrate on calculating the threshold energy needed to produce these particles. (You might find it helpful to review the discussion in Chapter 13 on *nonrelativistic* reaction thresholds.)

Consider the following reaction:

$$m_1 + m_2 \rightarrow m_3 + m_4 + m_5 + \cdots$$

where the m's represent both the particles and their masses. Any number of particles can be produced in the final state. Here m_1 is the incident particle, which has total energy E_1, kinetic energy $K_1 = E_1 - m_1c^2$, and momentum $cp_1 = \sqrt{E_1^2 - m_1^2c^4}$ in the *laboratory* frame of reference. The target particle m_2 is at rest in the laboratory. Figure 14.9 illustrates this reaction in the laboratory frame of reference.

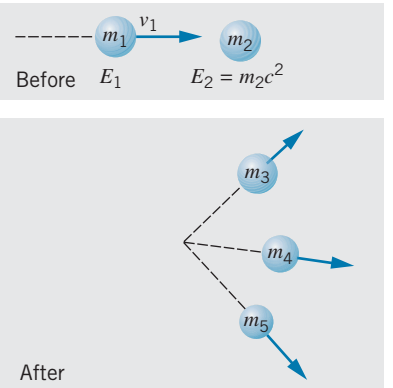

FIGURE 14.9 A reaction between particles in the laboratory reference frame.

Just as we did for nuclear reactions, we define the Q value to be the difference between the initial and final rest energies:

$$Q = (m_i - m_f)c^2 = [m_1 + m_2 - (m_3 + m_4 + m_5 + \cdots)]c^2 \qquad (14.2)$$

If Q is positive, rest energy is turned into kinetic energy, so that the product particles $m_3, m_4, m_5, \ldots$ have more combined kinetic energy than the initial particles m_1 and m_2. If Q is negative, some of the initial kinetic energy of m_1 is turned into rest energy.

Example 14.5

Compute the Q values for the reactions (*a*) $\pi^- + p \rightarrow K^0 + \Lambda^0$; (*b*) $K^- + p \rightarrow \Lambda^0 + \pi^0$.

Solution

(*a*) Using rest energies from Tables 14.5 and 14.6,

$$\begin{aligned} Q &= [m_{\pi^-} + m_p - (m_{K^0} + m_{\Lambda^0})]c^2 \\ &= 140\,\text{MeV} + 938\,\text{MeV} - 498\,\text{MeV} - 1116\,\text{MeV} \\ &= -536\,\text{MeV} \end{aligned}$$

This reaction has a negative Q value, and energy must be supplied in the form of initial kinetic energy to produce the additional rest energy of the products.

(*b*)

$$\begin{aligned} Q &= [m_{K^-} + m_p - (m_{\Lambda^0} + m_{\pi^0})]c^2 \\ &= 494\,\text{MeV} + 938\,\text{MeV} - 1116\,\text{MeV} - 135\,\text{MeV} \\ &= 181\,\text{MeV} \end{aligned}$$

A positive Q value indicates that there is enough rest energy in the initial particles to produce the final particles; in fact there is 181 MeV of energy (plus the kinetic energy of the incident particle) left over for kinetic energy of the Λ^0 and π^0.

Threshold Energy

When the Q value is negative, there is a minimum kinetic energy that m_1 must have in order to initiate the reaction. As in the non-relativistic nuclear physics case, this *threshold kinetic energy* K_{th} is larger than the magnitude of Q. The Q value is the energy necessary to create the additional mass of the product particles,

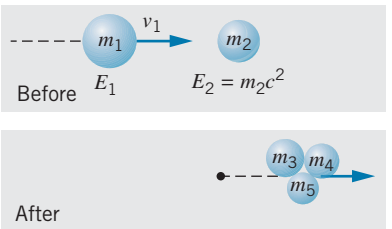

FIGURE 14.10 The reaction of Figure 14.9 when m_1 has the threshold kinetic energy. The product particles move together as a unit in the direction of the original momentum.

but to conserve momentum the product particles cannot be formed at rest, so the threshold energy must not only create the additional particles but must also give them sufficient kinetic energy so that linear momentum is conserved in the reaction.

If Figure 14.9 represents a reaction with a negative Q value, clearly the reaction is not being done at the threshold kinetic energy. In the reaction as it is drawn, not only have the new particles been created, they have been given both forward momentum (to the right in the figure), which is necessary to conserve the initial momentum of m_1, as well as transverse momentum. This transverse momentum, which must sum to zero in order to conserve momentum, is not necessary either to create the particles or to satisfy conservation of momentum. At the minimum or threshold condition, this transverse momentum is zero.

Also at threshold, the most efficient way to provide momentum to the final particles is to have them all moving together with the same speed, as in Figure 14.10. (This is equivalent to creating the particles at rest if we examine the collision from a reference frame in which the total initial momentum is zero, such as in a head-on collision of two particles.) Let's represent the bundle of final particles, all moving as a unit, as a total mass M. Then conservation of momentum ($p_{\text{initial}} = p_{\text{final}}$) gives $p_1 = p_M$ and conservation of total relativistic energy ($E_{\text{initial}} = E_{\text{final}}$) gives $E_1 + E_2 = E_M$, where p_M and E_M represent the momentum and total relativistic energy of the final bundle of particles. Then

$$\sqrt{(p_1c)^2 + (m_1c^2)^2} + m_2c^2 = \sqrt{(p_Mc)^2 + (m_Mc^2)^2} = \sqrt{(p_1c)^2 + (m_Mc^2)^2} \tag{14.3}$$

Squaring both sides and solving, we obtain

$$\sqrt{(p_1c)^2 + (m_1c^2)^2} = \frac{(Mc^2)^2 - (m_1c^2)^2 - (m_2c^2)^2}{2m_2c^2} \tag{14.4}$$

The threshold kinetic energy of m_1 is then

$$\begin{aligned} K_{\text{th}} &= E_1 - m_1c^2 = \sqrt{(p_1c)^2 + (m_1c^2)^2} - m_1c^2 \\ &= \frac{(Mc^2)^2 - (m_1c^2)^2 - (m_2c^2)^2}{2m_2c^2} - m_1c^2 \\ &= \frac{(Mc^2 - m_1c^2 - m_2c^2)(Mc^2 + m_1c^2 + m_2c^2)}{2m_2c^2} \end{aligned} \tag{14.5}$$

With $Q = m_1c^2 + m_2c^2 - Mc^2$ and $M = m_3 + m_4 + m_5 + \cdots$, this becomes

$$K_{\text{th}} = (-Q)\frac{m_1 + m_2 + m_3 + m_4 + m_5 + \cdots}{2m_2} \tag{14.6}$$

This can also be written as

$$K_{\text{th}} = (-Q)\frac{\text{total mass of all particles involved in reaction}}{2 \times \text{mass of target particle}} \tag{14.7}$$

In the limit of low speeds, the relativistic threshold formula reduces to the non-relativistic formula for nuclear reactions derived in Chapter 13 (see Problem 20).

Example 14.6

Calculate the threshold kinetic energy to produce π mesons from the reaction $p + p \rightarrow p + p + \pi^0$.

Solution

The Q value is

$$Q = m_p c^2 + m_p c^2 - (m_p c^2 + m_p c^2 + m_\pi c^2)$$
$$= -m_\pi c^2 = -135\,\text{MeV}$$

Using Eq. 14.7 we can find the threshold kinetic energy:

$$K_{th} = (-Q)\frac{4m_p + m_\pi}{2m_p}$$
$$= (135\,\text{MeV})\frac{4(938\,\text{MeV}) + 135\,\text{MeV}}{2(938\,\text{MeV})} = 280\,\text{MeV}$$

Such energetic protons are produced at many accelerators throughout the world, and as a result the properties of the π mesons can be carefully investigated.

Example 14.7

In 1956 an experiment was performed at Berkeley to search for the antiproton, which could be produced in the reaction $p + p \rightarrow p + p + p + \bar{p}$. What is the threshold energy for this reaction?

Solution

The rest energy of the antiproton is identical to the rest energy of the proton (938 MeV), so the Q value is

$$Q = m_p c^2 + m_p c^2 - 4(m_p c^2) = -2m_p c^2$$

Thus

$$K_{th} = (2m_p c^2)\frac{6m_p c^2}{2m_p c^2} = 6m_p c^2 = 5628\,\text{MeV}$$
$$= 5.628\,\text{GeV}$$

For the discovery of the antiproton produced in this reaction, Owen Chamberlain and Emilio Segrè were awarded the Nobel Prize in physics in 1959.

It is interesting to compute the "efficiency" of these reactions—that is, how much of the initial kinetic energy we supply actually goes into producing the final particles, and how much is "wasted" in the laboratory kinetic energies of the reaction products. In the first example, we supply 280 MeV of kinetic energy to produce 135 MeV of rest energy, for an efficiency of about 50%. In the second example, $6m_p c^2$ of kinetic energy produces only $2m_p c^2$ of rest energy, for an efficiency of only 33%. As the rest energies of the product particles become larger, the efficiency decreases, and relatively more energy must be supplied. For example, to produce a particle with a rest energy of 50 GeV in a proton-proton collision, we need to supply about 1250 GeV of initial kinetic energy. Only 4% of the energy supplied actually goes into producing the new particles; the remaining 96% must go to kinetic energy of the products in order to balance the large initial momentum of the incident particle. To produce a 100-GeV particle requires not twice as much energy, but four times as much. This is obviously not a pleasant situation for particle physicists, who must build increasingly more powerful accelerators to accomplish their goals of producing more massive particles.

One way out of this difficulty would be to do an experiment in which two particles with equal and opposite momentum collide head-on. In effect, we would be doing this experiment in the center-of-mass (CM) frame, where at threshold the production of new particles is 100% efficient—*none* of the initial kinetic energy

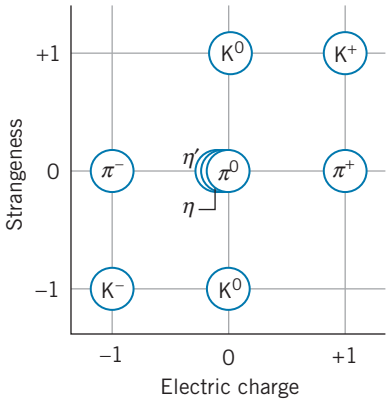

FIGURE 14.11 The relationship between electric charge and strangeness for the spin-0 mesons.

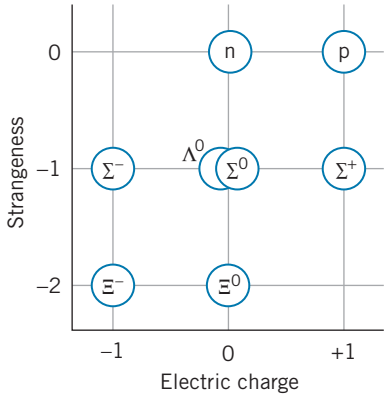

FIGURE 14.12 The relationship between electric charge and strangeness for the spin-$\frac{1}{2}$ baryons.

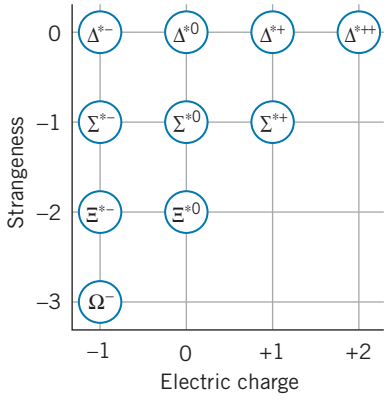

FIGURE 14.13 The relationship between electric charge and strangeness for the spin-$\frac{3}{2}$ baryons.

goes into kinetic energy of the products, which are produced at rest in the CM frame. Thus a 50-GeV particle could be produced by a head-on collision between two protons with as little as 25 GeV of kinetic energy. Of course, this great gain in efficiency is at a cost of the technological difficulty of making such collisions occur.

There are now *colliding beam* accelerators in operation, in which beams of particles (such as electrons or protons) can occasionally be made to collide. For example, in the Fermilab accelerator (Figure 14.1), beams of protons and antiprotons (each of energy 1 TeV = 1000 GeV) circulate around the ring in opposite directions and collide twice during each revolution. The Large Hadron Collider (hadron meaning strongly interacting particles), which is on the border between Switzerland and France, became operational in 2009; it collides two beams of protons each at an energy of 7 GeV in order to search for new particles in an even higher range of rest energies. Other colliding beam accelerators bring together electrons and positrons at energies of 50 to 100 GeV. In each case, all of the available energy can go into the production of new particles.

14.7 THE QUARK STRUCTURE OF MESONS AND BARYONS

Although the classifications and properties of the elementary particles seem like a complicated and disordered collection, there is an underlying order that suggests that a scheme of remarkable simplicity is at work. We can illustrate this order if we plot a diagram that has strangeness along the y axis and electric charge along the x axis. If the families of particles are placed in their proper locations on the graphs, regular geometrical patterns begin to emerge. Figures 14.11 to 14.13 show such plots for the lower mass spin-0 mesons, the spin-$\frac{1}{2}$ baryons, and the spin-$\frac{3}{2}$ baryons. In 1964, Murray Gell-Mann and George Zweig independently and simultaneously recognized that such regular patterns are evidence of an underlying structure in the particles. They showed that they could duplicate these patterns if the mesons and baryons were composed of three fundamental particles, which soon became known as *quarks*. These three quarks, known as up (u), down (d), and strange (s), have the properties listed in Table 14.7. We will shortly see that we now believe that six quarks are necessary to account for all known mesons and baryons.

Let us see how the quark model works in the case of the spin-0 mesons. The quarks have spin $\frac{1}{2}$, so the simplest scheme to form a spin-0 meson would be to combine two quarks, with their spins directed oppositely. However the mesons have baryon number $B = 0$, while a combination of two quarks would have $B = \frac{1}{3} + \frac{1}{3} = \frac{2}{3}$. A combination of a quark and an antiquark, on the other hand, would have $B = 0$, because the antiquark has $B = -\frac{1}{3}$.

For example, suppose we combine a u quark with a $\bar{\text{d}}$ ("antidown") quark, obtaining the combination $\text{u}\bar{\text{d}}$. This combination has spin zero and electric charge $\frac{2}{3}e + \frac{1}{3}e = +e$. (A d quark has charge $-\frac{1}{3}e$, so $\bar{\text{d}}$ has charge $+\frac{1}{3}e$.) The properties of this combination are identical with the π^+ meson, and so we identify the π^+ with the combination $\text{u}\bar{\text{d}}$. Continuing in this way, we find nine possible combinations of one of the three original quarks from Table 14.7 with an antiquark, as listed in Table 14.8, and plotting those nine combinations on a graph of strangeness against electric charge, we obtain Figure 14.14, which looks identical to Figure 14.11.

TABLE 14.7 Properties of the Three Original Quarks

Name	Symbol	Charge (e)	Spin ($\hbar$)	Baryon Number	Strangeness	Antiquark
Up	u	$+\frac{2}{3}$	$\frac{1}{2}$	$+\frac{1}{3}$	0	$\bar{u}$
Down	d	$-\frac{1}{3}$	$\frac{1}{2}$	$+\frac{1}{3}$	0	$\bar{d}$
Strange	s	$-\frac{1}{3}$	$\frac{1}{2}$	$+\frac{1}{3}$	-1	$\bar{s}$

Values shown for the charge, baryon number, and strangeness are those for the quark; values for the antiquark have the opposite sign.

TABLE 14.8 Possible Quark-Antiquark Combinations

Combination	Charge (e)	Spin ($\hbar$)	Baryon Number	Strangeness
$u\bar{u}$	0	0, 1	0	0
$u\bar{d}$	+1	0, 1	0	0
$u\bar{s}$	+1	0, 1	0	+1
$d\bar{u}$	−1	0, 1	0	0
$d\bar{d}$	0	0, 1	0	0
$d\bar{s}$	0	0, 1	0	+1
$s\bar{u}$	−1	0, 1	0	−1
$s\bar{d}$	0	0, 1	0	−1
$s\bar{s}$	0	0, 1	0	0

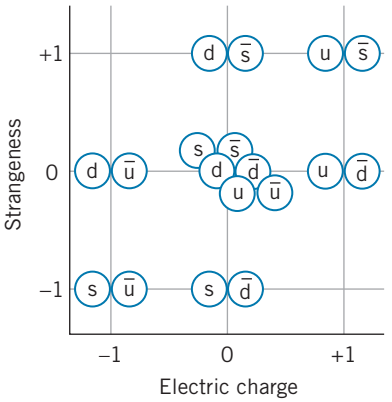

FIGURE 14.14 Spin-0 quark-antiquark combinations; compare with Figure 14.11.

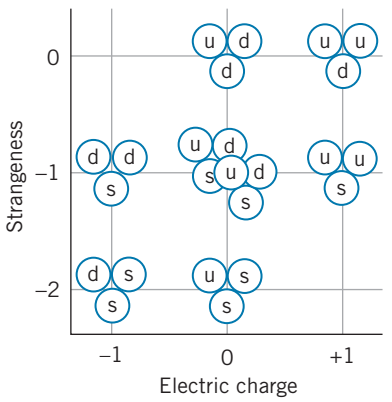

FIGURE 14.15 Spin-$\frac{1}{2}$ three-quark combinations; compare with Figure 14.12.

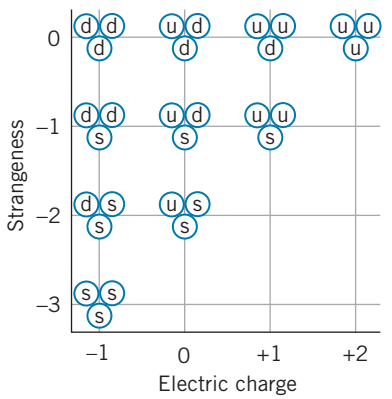

FIGURE 14.16 Spin-$\frac{3}{2}$ three-quark combinations; compare with Figure 14.13.

The baryons have $B = +1$ and spin $\frac{1}{2}$ or $\frac{3}{2}$, which suggests immediately that three quarks make a baryon. The 10 possible combinations of the three original quarks are listed in Table 14.9, and we can arrange them into two patterns as shown in Figures 14.15 and 14.16, which are identical to those for the spin-$\frac{1}{2}$ and spin-$\frac{3}{2}$ baryons.

Using the quark model, we can analyze the decays and reactions of the elementary particles, based on two rules:

1. Quark-antiquark pairs can be created from energy quanta, and conversely can annihilate into energy quanta. For example,

$$\text{energy} \rightarrow u + \bar{u} \qquad \text{or} \qquad d + \bar{d} \rightarrow \text{energy}$$

   This energy can be in the form of gamma rays (as in electron-positron annihilation), or else it can be transferred to or from other particles in the decay or reaction.
2. The weak interaction can change one type of quark into another through emission or absorption of a W^+ or W^-, for example $s \rightarrow u + W^-$. The W then decays by the weak interaction, such as $W^- \rightarrow \mu^- + \bar{\nu}_\mu$ or $W^- \rightarrow d + \bar{u}$. The strong and electromagnetic interactions cannot change one type of quark into another.

TABLE 14.9 Possible Three-Quark Combinations

Combination	Charge (e)	Spin ($\hbar$)	Baryon Number	Strangeness
uuu	$+2$	$\frac{3}{2}$	$+1$	0
uud	$+1$	$\frac{1}{2}, \frac{3}{2}$	$+1$	0
udd	0	$\frac{1}{2}, \frac{3}{2}$	$+1$	0
uus	$+1$	$\frac{1}{2}, \frac{3}{2}$	$+1$	-1
uss	0	$\frac{1}{2}, \frac{3}{2}$	$+1$	-2
uds	0	$\frac{1}{2}, \frac{3}{2}$	$+1$	-1
ddd	-1	$\frac{3}{2}$	$+1$	0
dds	-1	$\frac{1}{2}, \frac{3}{2}$	$+1$	-1
dss	-1	$\frac{1}{2}, \frac{3}{2}$	$+1$	-2
sss	-1	$\frac{3}{2}$	$+1$	-3

Example 14.8

Analyze (*a*) the reaction $\pi^- + \mathrm{p} \rightarrow \Lambda^0 + \mathrm{K}^0$ and (*b*) the decay $\pi^+ \rightarrow \mu^+ + \nu_\mu$ in terms of the constituent quarks.

Solution

(*a*) The reaction $\pi^- + \mathrm{p} \rightarrow \Lambda^0 + \mathrm{K}^0$ can be rewritten as follows:

$$\mathrm{d}\bar{\mathrm{u}} + \mathrm{uud} \rightarrow \mathrm{uds} + \mathrm{d}\bar{\mathrm{s}}$$

Each side contains one u quark and two d quarks, which don't change in the reaction. Removing these "spectator" quarks from each side of the reaction, we are left with the remaining transformation:

$$\bar{\mathrm{u}} + \mathrm{u} \rightarrow \mathrm{s} + \bar{\mathrm{s}}$$

The u and $\bar{\mathrm{u}}$ annihilate, and from the resulting energy s and $\bar{\mathrm{s}}$ are created.

(*b*) The π^+ has the quark composition $\mathrm{u}\bar{\mathrm{d}}$. There are no quarks in the final state ($\mu^+ + \nu_\mu$), so we must find a way to get rid of the quarks. One possible way is to change the u quark into a d quark: $\mathrm{u} \rightarrow \mathrm{d} + \mathrm{W}^+$. The net process can thus be written as

$$\mathrm{u}\bar{\mathrm{d}} \rightarrow \mathrm{d} + \bar{\mathrm{d}} + \mathrm{W}^+$$

with the products then undergoing the following processes to produce the final observed particles:

$$\mathrm{d} + \bar{\mathrm{d}} \rightarrow \text{energy} \quad \text{and} \quad \mathrm{W}^+ \rightarrow \mu^+ + \nu_\mu$$

You may have noticed that some of the heavier mesons listed in Table 14.5 were not included in Figure 14.11, and they cannot be accounted for among the quark-antiquark combinations listed in Table 14.8. Where do these particles fit in our scheme?

In 1974, a new meson called J/ψ was discovered at a rest energy of 3.1 GeV. (It was given different names J and ψ by the two competing experimental groups that first reported its discovery.) This new meson was expected to decay to lighter mesons in a characteristic strong interaction time of around 10^{-23} s. Instead, its lifetime was stretched by 3 orders of magnitude to about 10^{-20} s, and its decay products were e^+ and e^-, which are more characteristic of an electromagnetic process. Why is the rapid, strong interaction decay path blocked for this particle? This was soon explained by assuming the J/ψ to be composed of a new quark c, called the *charm* quark, and its antiquark $\bar{\mathrm{c}}$. The existence of the c quark had been predicted 4 years earlier as a way to explain the failure to observe the decay $\mathrm{K}^0 \rightarrow \mu^+ + \mu^-$, which violates no previously known law but is nevertheless not observed.

The c quark, which carries a charge of $+\frac{2}{3}e$, has a property, charm, that operates somewhat like strangeness. We assign a charm quantum number $C = +1$ to the c quark (and assign $C = -1$ to its antiquark $\bar{c}$). All other quarks are assigned $C = 0$. We can now construct a new set of mesons by combining the c quark with the $\bar{u}, \bar{d}$, and $\bar{s}$ antiquarks and by combining the $\bar{c}$ antiquark with the u, d, and s quarks. Instead of nine spin-0 mesons, there are now 16, and the two-dimensional graphs of Figures 14.11 and 14.14 must be extended to a third dimension to show the C axis (Figure 14.17). All of these new mesons, called D, have been observed in high-energy collision experiments. Baryons containing this new quark have also been discovered, analogous to the Λ, Σ, Ξ, and Ω particles but with an s quark replaced by a c quark.

In 1977, the same sequence of events was repeated with another meson, Υ (upsilon). The rest energy was determined to be about 9.5 GeV, and again its decay was slowed to about 10^{-20} s and occurred into $e^+ + e^-$ rather than into mesons. Once again, a new quark was postulated: the b (bottom) quark with a new quantum "bottomness" number $B = -1$ and a charge of $-\frac{1}{3}e$. (The letter B is used to represent baryon number as well as bottomness. It should always be apparent from the discussion which one is meant.) The Υ is assigned as the combination $b\bar{b}$. Many new particles containing the b quark have been discovered, including B mesons (in which a b quark is paired with a different antiquark) and baryons similar to Λ, Σ, and Ξ with a b quark replacing one of the s quarks.

A sixth quark was discovered in 1994 in proton-antiproton collisions at Fermilab. These collisions created this new quark and its antiquark, both of which decayed into a shower of secondary particles (as in Figure 14.5). By measuring the energy and momentum of the secondary particles, the experimenters were able to determine the mass of the new quark to be 172 GeV (roughly the mass of a tungsten atom). This new quark is known as t (top) and has a new associated property of "topness" with a quantum number $T = +1$.

It may now seem that we are losing sight of our goal to achieve simplicity (to add the "bottomness" axis to Figure 14.17 we would need to depict a four-dimensional space!) and that we are moving toward replacing a complicated array of particles with an equivalently complicated array of quarks. However, there is good reason to believe that there are no more than six fundamental quarks. In the next section, we discuss how we are indeed on the path to a simple explanation of the fundamental particles.

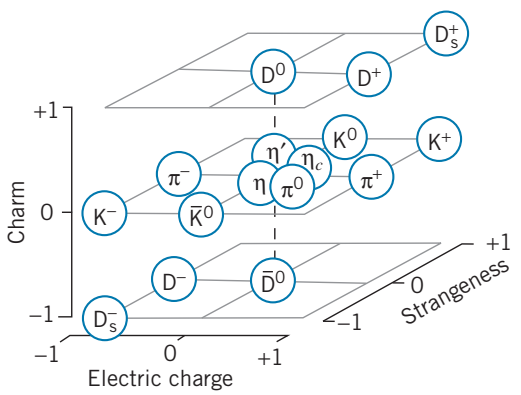

FIGURE 14.17 The relationship among electric charge, strangeness, and charm for the spin-0 mesons.

TABLE 14.10 Properties of the Quarks

Type	Symbol	Antiparticle	Charge (e)	Spin ($\hbar$)	Baryon Number	Rest Energy (MeV)	Properties			
							C	S	T	B
Up	u	$\bar{u}$	$+\frac{2}{3}$	$\frac{1}{2}$	$+\frac{1}{3}$	330	0	0	0	0
Down	d	$\bar{d}$	$-\frac{1}{3}$	$\frac{1}{2}$	$+\frac{1}{3}$	330	0	0	0	0
Charm	c	$\bar{c}$	$+\frac{2}{3}$	$\frac{1}{2}$	$+\frac{1}{3}$	1500	+1	0	0	0
Strange	s	$\bar{s}$	$-\frac{1}{3}$	$\frac{1}{2}$	$+\frac{1}{3}$	500	0	−1	0	0
Top	t	$\bar{t}$	$+\frac{2}{3}$	$\frac{1}{2}$	$+\frac{1}{3}$	172,000	0	0	+1	0
Bottom	b	$\bar{b}$	$-\frac{1}{3}$	$\frac{1}{2}$	$+\frac{1}{3}$	4700	0	0	0	−1

Table 14.10 shows the six quarks and their properties. The masses of the quarks cannot be directly determined, because a free quark has yet to be observed. The rest energies shown in Table 14.10 are estimates based on the "apparent" masses that quarks have when bound in various particles. For example, the observed rest energy of the proton is the sum of the rest energies of its three quark constituents less the binding energy of the quarks. Since we don't know the binding energy, we can't determine the rest energy of a free quark. The rest energies shown in Table 14.10 are often called those of *constituent* quarks.

The quark model does a great deal more than allow us to make geometrical arrangements of particles such as Figure 14.17. It can be used to explain many observed properties of the particles, such as their masses and magnetic moments, and to account for their decay lifetimes and reaction probabilities. Nevertheless, a free quark has never been observed, despite heroic experiments to search for them. How can we be sure that they exist? In experiments that scatter high-energy electrons from protons, we observe more particles scattered at large angles than we would expect if the electric charge of the proton were uniformly distributed throughout its volume, and from the analysis of the distribution of the scattered electrons we conclude that inside the proton are three point-like objects that are responsible for the scattering. This experiment is exactly analogous to Rutherford scattering, in which the presence of the nucleus as a compact object inside the atom was revealed by the distribution of scattered alpha particles at angles larger than expected. Like Rutherford's experiment, the observed cross section depends on the electric charge of the object doing the scattering, and from these experiments we can deduce charges of magnitude $\frac{1}{3}e$ and $\frac{2}{3}e$ for these point-like objects. These experiments give clear evidence for the presence of quarks inside the proton.

We don't yet know why free quarks have not been observed. Perhaps they are so massive that no accelerator yet built has enough energy to liberate one. Perhaps the force between quarks increases with distance (in contrast with electromagnetism or gravitation, which *decrease* with separation distance), so that an infinite amount of energy would be required to separate a quark from a nucleon. Or (as is now widely believed) perhaps the basic theory of quark structure forbids the existence of free quarks.

Quarkonium

The theoretical analysis of the structure of baryons poses mathematical difficulties that are characteristic of all three-body mechanical or quantum-mechanical systems. Instead, we can learn a bit about the interactions of quarks from

examining the properties of two-body systems, especially the quark-antiquark combinations in mesons.

We'll look briefly at the combination of a quark with its own antiquark. The binding energies of quarks in mesons are very large (hundreds of MeV), so the quark-antiquark pairs of the light quarks (u, d, s) must be treated relativistically, because the binding energies and thus the kinetic energies in the bound state are roughly the same as the rest energies. However, for the more massive quarks (c, b, t), the binding energies are small compared with the rest energies and we can use nonrelativistic methods (such as the Schrödinger equation) for the analysis.

There is a well-studied analogy for the properties of a quark-antiquark combination. When a positron travels through matter, before it annihilates it forms an atom-like bound state with an electron. This bound electron-positron system is called *positronium*. The positron and the electron each orbit about their center of mass, in states that are similar to atomic states in hydrogen. We can label these states by the values of their total spin angular momentum S and orbital angular momentum L, as we did for atomic states in Chapter 8. (Don't confuse these labels with strangeness and lepton number.) The spins of the two particles can be parallel (hence with total spin $S = 1$) or antiparallel ($S = 0$). The total orbital angular momentum of the two particles about the center of mass can be $L = 0$ for s states, $L = 1$ for p states, etc. Finally, the system can exist with different radial wave functions that we can label with principal quantum number $n = 1, 2, 3, \ldots$, exactly as we did in the hydrogen atom. Figure 14.18*a* shows some of the bound states in positronium.

The positronium structure is very similar to the bound states in a quark-antiquark system, which is correspondingly known as *quarkonium*. Figure 14.18*b* shows the quarkonium excited states for the $c\bar{c}$ system, and the states for the $b\bar{b}$ system are shown in Figure 14.18*c*. There is a great similarity between the excited states of the two quarkonium systems. Note in particular the states with $S = 1$ and $L = 0$ in $c\bar{c}$ and $b\bar{b}$. (These would be equivalent to the $1s$, $2s$, $3s$, and $4s$ states

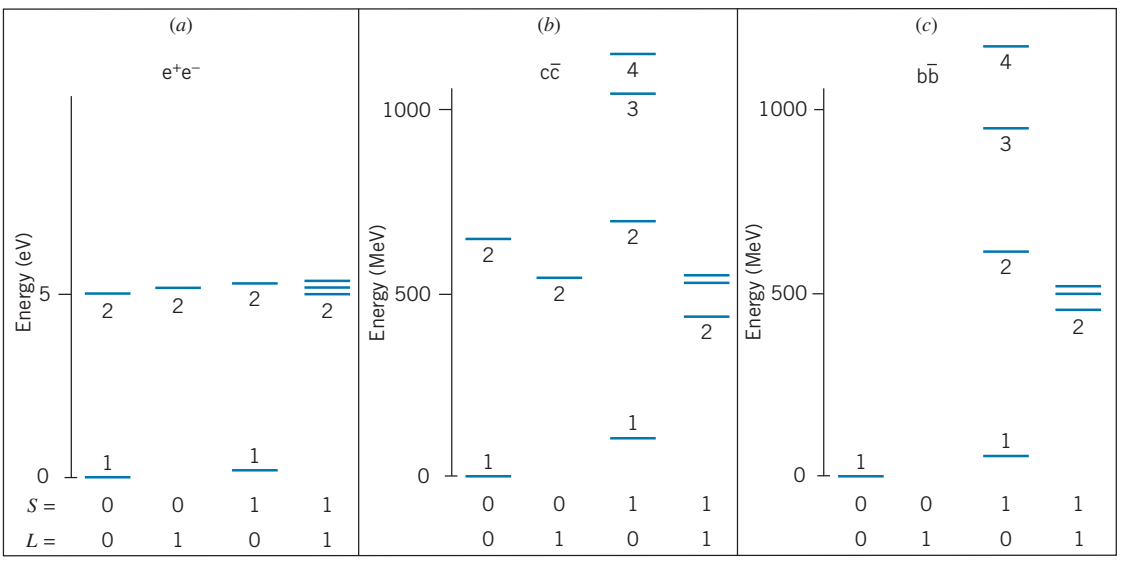

FIGURE 14.18 The energy levels of (*a*) positronium (e^+e^-), (*b*) $c\bar{c}$ quarkonium, and (*c*) $b\bar{b}$ quarkonium. The atom-like states are labeled with the value of the principal quantum number n. The zero of the energy scale is at 2980 MeV for $c\bar{c}$ and 9389 MeV for $b\bar{b}$. The $n = 2$ states with $S = 0, L = 0$ and $S = 0, L = 1$ in $b\bar{b}$ have not yet been discovered.

in a hydrogenic system. The lowest $S = 1, L = 0$ $c\bar{c}$ state is the J/ψ meson, and the corresponding $b\bar{b}$ state is the Υ meson.) Moreover, the overall structure of the excited states of the quarkonium systems is very similar to that of positronium (especially the $n = 2$ states of positronium and $c\bar{c}$).

Knowledge of the excited states of quarkonium allows us to guess at an effective potential energy for which we can solve the Schrödinger equation to try to calculate the energies of the states. The similarity with positronium certainly suggests that we try a Coulomb-like potential energy that depends on $1/r$. However, it cannot be an electromagnetic interaction—the electromagnetic interaction between two quarks separated by a distance on 0.5 fm (a typical size of a meson) is at most about 1 MeV, which is less than 1% of the energy differences of the quarkonium excited states shown in Figure 14.18. (Moreover, the $c\bar{c}$ electromagnetic interaction should be 4 times stronger than the $b\bar{b}$ electromagnetic interaction, but there is no evidence of this in Figure 14.18.) The $1/r$ interaction grows weaker with increasing separation, so we must add another term that grows stronger with separation, which accounts for the failure to produce a free quark. Several different potential energies have been tried for this additional term, the simplest being a term that is linear in the separation r. The net effective potential energy is then of the form

$$U(r) = -\frac{a}{r} + br \tag{14.8}$$

The Schrödinger equation can be solved numerically for this potential energy, with the constants a and b adjusted to give best agreement with experiment. The constant b turns out to have a value of about 1 GeV/fm. This large value is consistent with the failure to observe a free quark—to separate the quarks in a meson even to an atom-sized distance would require about 10^5 GeV, far greater than the beam energy of any accelerator.

One of the especially interesting features of the quarkonium excited states shown in Figure 14.18 is the rough agreement between the energies of the $c\bar{c}$ and $b\bar{b}$ states. (See especially the four states with $S = 1$ and $L = 0$.) This is surprising, because in a simple two-body hydrogen-like system, the energies should depend on the masses of the orbiting particles, and the b quark is three times as massive as the c quark. It would be interesting to continue this comparison for the bound states of the $t\bar{t}$ system involving the top quark, but the difficulty of producing this particle in significant quantities (owing to its large mass) has so far prevented a study of the excited states of the $t\bar{t}$ system.

14.8 THE STANDARD MODEL

Ordinary matter is composed of protons and neutrons, which are in turn composed of u and d quarks. Ordinary matter is also composed of electrons. In the radioactive decay of ordinary matter, electron-type neutrinos are emitted. Our entire world can thus be regarded as composed of four spin-$\frac{1}{2}$ particles (and their antiparticles), which can be grouped into a pair of leptons and a pair of quarks:

$$(e, \nu_e) \qquad \text{and} \qquad (u, d)$$

Within each pair, the charges of the two particles differ by one unit: -1 and 0, $+\frac{2}{3}$ and $-\frac{1}{3}$.

When we do experiments with high-energy accelerators, we find new types of particles: muons and muon neutrinos, plus mesons and baryons with the new properties of strangeness and charm. We can account for the structure of these particles with another pair of leptons and another pair of quarks:

$$(\mu, \nu_\mu) \qquad \text{and} \qquad (\text{c, s})$$

Once again, the particles come in pairs differing by one unit of charge.

At even higher energies, we find a new generation of particles consisting of another pair of leptons (tau and its neutrino) and a new pair of quarks (top and bottom), which permits us to continue the symmetric arrangement of the fundamental particles in pairs:

$$(\tau, \nu_\tau) \qquad \text{and} \qquad (\text{t, b})$$

Is it possible that there are more pairs of leptons and quarks that have not yet been discovered? At this point, we strongly believe the answer to be "No." Every particle so far discovered can be fit into this scheme of 6 leptons and 6 quarks. Furthermore, the number of lepton generations can be determined by the decay rates of the heaviest particles, and a limit of 3 emerges from these experiments. Finally, according to present theories the evolution of the universe itself would have proceeded differently if there had been more than three types of neutrinos. For these reasons, it is generally believed that there are no more than three generations of particles.

The strong force between quarks is carried by an exchanged particle, called the *gluon*, which provides the "glue" that binds quarks together in mesons and baryons. (There are actually eight different gluons in the model.) A theory known as *quantum chromodynamics* describes the interactions of quarks and the exchange of gluons. In this theory, the internal structure of the proton consists of three quarks "swimming in a sea" of exchanged gluons. Like the quarks, the gluons cannot be observed directly, but there is indirect evidence of their existence from a variety of experiments.

The theory of the structure of the elementary particles we have described so far is known as the *Standard Model.* It consists of 6 leptons and 6 quarks (and their antiparticles), plus the field particles (photon, 3 weak bosons, 8 gluons) that carry the various forces. It is remarkably successful in accounting for the properties of the fundamental particles, but it lacks the unified treatment of forces we would expect from a complete theory.

The first step toward unification was taken in 1967 with the development of the *electroweak* theory by Stephen Weinberg and Abdus Salam. In this theory, the weak and electromagnetic interactions are regarded as separate aspects of the same basic force (the electroweak force), just as electric and magnetic forces are distinct but part of a single phenomenon, electromagnetism. The theory predicted the existence of the W and Z particles; their discovery in 1983 provided a dramatic confirmation of the theory.

The next-higher level of unification would be to combine the strong and electroweak forces into a single interaction. Theories that attempt to do this are called *Grand Unified Theories* (GUTs). By incorporating leptons and quarks into a single theory, the GUTs explain many observed phenomena: the fractional electric charge of the quarks and the difference of one unit of charge between the members of the quark and lepton pairs within each generation. The GUTs also predict new phenomena, such as the conversion of quarks into leptons, which would permit the proton (which we have so far assumed to be an absolutely stable

particle) to decay into lighter particles with a lifetime of at least 10^{31} y. Searches for photon decay (by looking for evidence of decays in a large volume of matter; see Figure 14.19) have so far been unsuccessful and have placed lower limits on the proton lifetime of at least 10^{32} y.

A missing part of the Standard Model is an explanation of why the particles have the masses that we observe. A complete theory ought to be able to calculate the masses of the particles. It has been proposed that there is a field pervading the entire universe and that particles acquire their particular masses as a result of the strength of their interactions with this field, somewhat like a particle moving through a viscous medium seems to have more inertia and thus a greater "effective" mass. This field is known as the *Higgs field* and the particle that carries the field interaction is called the *Higgs boson*. This particle has been searched for but not yet found; estimates of its expected mass are in excess of 100 GeV/c^2. The Large Hadron Collider, the world's most powerful particle accelerator, is currently searching for evidence of the Higgs boson by colliding beams of protons at an energy of 7000 GeV.

Another shortcoming of the Standard Model is that it is based on massless neutrinos. Although the upper limit (see Table 14.4) on the mass of the electron neutrino is very small (2 eV), the limits on the other neutrino masses are much larger. Measurements of the flux of neutrinos reaching Earth from the Sun, produced in the fusion reactions discussed in Chapter 13, have consistently revealed a large deficit—the intensity of electron neutrinos observed on Earth is only about 1/3 of what is predicted based on models of how fusion reactions occur in the Sun's interior. Recent measurements at the Sudbury Neutrino Observatory in Canada have revealed that, although the intensity of electron neutrinos from the Sun is only 1/3 of the expected value, the total intensity

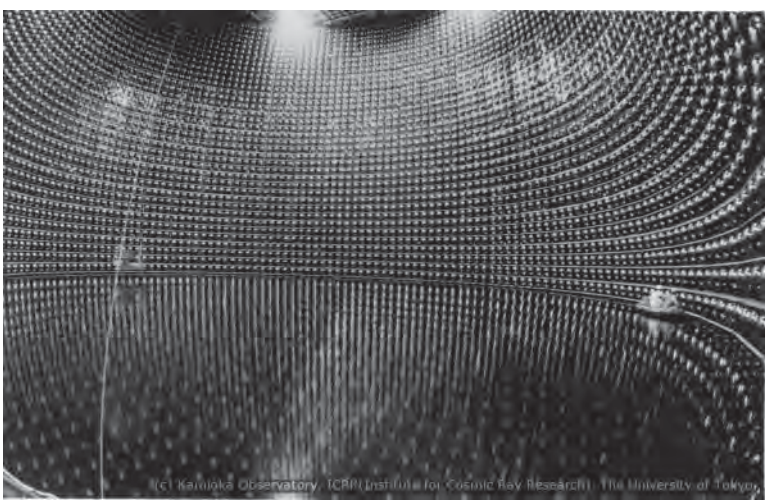

FIGURE 14.19 The Superkamiokande detector system in Japan was designed to search for proton decay. The water tank, 40 m in diameter and located 1000 m underground, holds 50,000 tons of water. The tank is lined with more than 10,000 photomultiplier detectors that respond to flashes of light that would be emitted when one of the protons in the water decayed. Here the tank has been partly emptied so that the technicians (in the boat) can service the photomultipliers.

of *all* neutrinos (including muon and tau neutrinos) reaching us from the Sun agrees with the predicted rate. This is very puzzling, because the fusion reactions in the Sun should produce only electron neutrinos; the reacting particles in the solar interior are not sufficiently energetic to produce mu and tau leptons. This mystery has been explained by proposing that the electron neutrinos are produced in the solar interior at the expected rate, but that during their journey from the Sun to Earth, the purely electron neutrinos become a mixture of roughly equal parts electron, muon, and tau neutrinos. This nicely explains why the rate of electron neutrinos from the Sun appears to be only about 1/3 of what is expected (the other 2/3 of the electron neutrinos having been converted into muon or tau neutrinos). This phenomenon of *neutrino oscillation* (which refers to neutrinos oscillating from one type to another) can occur only if the neutrinos have mass. The required masses are very small, well within the experimental limits, but the neutrino masses are definitely not zero. The Standard Model must be extended to include nonzero neutrino masses, and the rules for conservation of lepton number must be modified to allow one type of neutrino to transform into another.

The search for a consistent explanation of the elementary particles has led physicists to work with exotic theories. In *string theory* the particles are replaced by tiny (10^{-33} cm) strings, whose vibrations give rise to the properties we observe as particles. These theories exist in spacetimes with 10 or more dimensions, and at present seem to be far beyond any possible experimental test. Another extension of the Standard Model is called *supersymmetry*; this theory proposes that there is a higher symmetry between the spin-$\frac{1}{2}$ particles (such as the quarks and leptons) and particles with integral spin, so that under this theory there would be electrons and quarks with a spin of 0 and W and Z particles and photons with a spin of $\frac{1}{2}$. The masses of these supersymmetric particles are estimated to be very much larger than their ordinary partners, perhaps in the range of 100 GeV/c^2, but even in this range they should be observable through experiments currently planned at the Large Hadron Collider.

There is so far no conclusive verification for any of the GUTs, nor is there a successful theory that incorporates the remaining force, gravity, into a unified theory. The quest for unification and its experimental tests remains an active area of research in particle physics.

Chapter Summary

		Section
Forces	Strong, electromagnetic, weak, gravitational	14.1
Field particles	Gluon (g), photon (γ), weak boson ($W^{\pm}, Z^0$), graviton	14.1
Leptons	e^-, ν_e, μ^-, ν_μ, τ^-, ν_τ	14.2
Mesons	$\pi^{\pm}$, π^0, $K^{\pm}$, K^0, $\overline{K}^0$, η, $\rho^{\pm}$, η', $D^{\pm}$, ψ, $B^{\pm}$, Υ, ...	14.2
Baryons	p, n, Λ^0, $\Sigma^{\pm,0}$, $\Xi^{-,0}$, Ω^-, ...	14.2
Conservation of lepton number L	*In any process, L_e, L_μ, and L_τ remain constant.*	14.3
Conservation of baryon number B	*In any process, B remains constant.*	14.3
Conservation of strangeness S	*In strong and electromagnetic processes, S remains constant; in weak processes, $\Delta S = 0$ or ± 1.*	14.3
Q value in decays or reactions	$Q = (m_i - m_f)c^2$	14.5, 14.6
Threshold energy in reactions	$K_{th} = -Q(m_1 + m_2 + m_3 + m_4 + m_5 + \cdots)/2m_2$	14.6
Quarks	u, d, c, s, t, b	14.7

Questions

1. Some conservation laws are based on fundamental properties of nature, while others are based on systematics of decays and reactions and have as yet no fundamental basis. Give the basis for the following conservation laws: energy, linear momentum, angular momentum, electric charge, baryon number, lepton number, strangeness.
2. Does the presence of neutrinos among the decay products of a particle always indicate that the weak interaction is responsible for the decay? Do all weak interaction decays have neutrinos among the decay products? Which decay product indicates an electromagnetic decay?
3. Do all strongly interacting particles also feel the weak interaction?
4. In what ways would physics be different if there were another member of the lepton family less massive than the electron? What if there were another lepton more massive than the tau?
5. Suppose a proton is moving with high speed, so that $E \gg mc^2$. Is it possible for the proton to decay, such as into $n + \pi^+$ or $p + \pi^0$?
6. On planet anti-Earth, antineutrons beta decay into antiprotons. Is a neutrino or an antineutrino emitted in this decay?
7. List some experiments that might distinguish antineutrons from neutrons. Among others, you might consider (*a*) neutron capture by a nucleus; (*b*) beta decay; (*c*) the effect of a magnetic field on a beam of neutrons.
8. The Σ^0 can decay to Λ^0 without changing strangeness, so it goes by the electromagnetic interaction; the charged $\Sigma^\pm$ decay to p or n by the weak interaction in characteristic lifetimes of 10^{-10} s. Why can't $\Sigma^\pm$ decay to Λ^0 by the strong interaction in a much shorter time?
9. The Ω^- particle decays to $\Lambda^0 + K^-$. Why doesn't it also decay to $\Lambda^0 + \pi^-$?
10. Explain why we do not account for the number of mesons in decays or reactions with a "meson number" in analogy with lepton number or baryon number.
11. Consider that leptons and baryons both obey conservation laws and are both fermions; mesons do not obey a conservation law and are bosons. Can you think of another particle (other than a meson) that has integral spin and can be emitted or absorbed in unlimited numbers?
12. Can antibaryons be produced in reactions between baryons and mesons?
13. List some similarities and differences between the properties of photons and neutrinos.
14. Is it reasonable to describe a resonance as a definite particle, when its mass is uncertain (and therefore variable) by 20%?
15. Why are most particle physics reactions endothermic ($Q < 0$)?
16. Although doubly charged baryons have been found, no doubly charged mesons have yet been found. What would be the effect on the quark model if a meson with charge $+2e$ were found? How could such a meson be interpreted within the quark model?
17. All direct quark transformations must involve a change of charge; for example, $u \rightarrow d$ is allowed (accompanied by the emission of a W^-), but $s \rightarrow d$ is not. Can you suggest a two-step process that might permit the transformation of an s quark into a d?
18. The decay $K^+ \rightarrow \pi^+ + e^+ + e^-$ is at least five orders of magnitude less probable than the decay $K^+ \rightarrow \pi^0 + e^+ + \nu_e$. Based on Question 17, can you explain why?
19. The D mesons decay to π and K mesons with a lifetime of 10^{-13} s. (*a*) Why is the lifetime so much slower than a typical strong interaction lifetime? Is a quantum number not conserved in the decay? (*b*) What interaction is responsible for the decay?
20. The Δ^* baryons are found with electric charges $+2, +1, 0$, and -1. Based on the quark model, why do we expect no Δ^* with charge -2?
21. Although we cannot observe quarks directly, indirect evidence for quarks in nucleons comes from the scattering of high-energy particles, such as electrons. When the de Broglie wavelength of the electrons is small compared with the size of a nucleon (~ 1 fm), the electrons appear to be scattered from massive, compact objects much smaller than a nucleon. To which phenomenon discussed previously in this text is this similar? Can the scattering be used to deduce the mass of the struck object? How does the scattering depend on the electric charge of the struck object? What would be the difference between scattering from a particle of charge e and one of charge $\frac{2}{3}e$?

Problems

14.1 The Four Basic Forces

1. Identify the interaction responsible for the following decays (approximate half-lives are given in parentheses):

   (*a*) $\Delta^* \rightarrow p + \pi$ (10^{-23} s)
   (*b*) $\eta \rightarrow \gamma + \gamma$ (10^{-18} s)
   (*c*) $K^+ \rightarrow \mu^+ + \nu_\mu$ (10^{-8} s)
   (*d*) $\Lambda^0 \rightarrow p + \pi^-$ (10^{-10} s)
   (*e*) $\eta' \rightarrow \eta + 2\pi$ (10^{-21} s)
   (*f*) $K^0 \rightarrow \pi^+ + \pi^-$ (10^{-10} s)

2. What is the range of the W^- particle that is responsible for the weak interaction of a proton and a neutron?

14.2 Classifying Particles

3. Give one possible decay mode of the following mesons:
   (*a*) π^- (*b*) ρ^- (*c*) D^- (*d*) $\overline{\mathrm{K}}^0$
4. Give one possible decay mode of the following antibaryons:
   (*a*) $\overline{\mathrm{n}}$ (*b*) $\overline{\Lambda}^0$ (*c*) $\overline{\Omega}^-$ (*d*) $\overline{\Sigma}^0$
5. Suggest a possible decay mode for the K^0 meson that involves the emission of:
   (*a*) ν_e (*b*) $\overline{\nu}_\mathrm{e}$ (*c*) ν_μ (*d*) $\overline{\nu}_\mu$
   Is it possible to have a decay mode of the K^0 that involves the emission of ν_τ or $\overline{\nu}_\tau$?

14.3 Conservation Laws

6. Name the conservation law that would be violated in each of the following decays:
   (*a*) $\pi^+ \rightarrow \mathrm{e}^+ + \gamma$
   (*b*) $\Lambda^0 \rightarrow \mathrm{p} + \mathrm{K}^-$
   (*c*) $\Omega^- \rightarrow \Sigma^- + \pi^0$
   (*d*) $\Lambda^0 \rightarrow \pi^- + \pi^+$
   (*e*) $\Lambda^0 \rightarrow \mathrm{n} + \gamma$
   (*f*) $\Omega^- \rightarrow \Xi^0 + \mathrm{K}^-$
   (*g*) $\Xi^0 \rightarrow \Sigma^0 + \pi^0$
   (*h*) $\mu^- \rightarrow \mathrm{e}^- + \gamma$
7. Each of the following reactions violates one (or more) of the conservation laws. Name the conservation law violated in each case:
   (*a*) $\nu_\mathrm{e} + \mathrm{p} \rightarrow \mathrm{n} + \mathrm{e}^+$
   (*b*) $\mathrm{p} + \mathrm{p} \rightarrow \mathrm{p} + \mathrm{n} + \mathrm{K}^+$
   (*c*) $\mathrm{p} + \mathrm{p} \rightarrow \mathrm{p} + \mathrm{p} + \Lambda^0 + \mathrm{K}^0$
   (*d*) $\pi^- + \mathrm{n} \rightarrow \mathrm{K}^- + \Lambda^0$
   (*e*) $\mathrm{K}^- + \mathrm{p} \rightarrow \mathrm{n} + \Lambda^0$
8. Supply the missing particle in each of the following decays:
   (*a*) $\mathrm{K}^- \rightarrow \pi^0 + \mathrm{e}^- +$
   (*b*) $\mathrm{K}^0 \rightarrow \pi^0 + \pi^0 +$
   (*c*) $\eta \rightarrow \pi^+ + \pi^- +$
9. Each of the reactions below is missing a single particle. Supply the missing particle in each case.
   (*a*) $\mathrm{p} + \mathrm{p} \rightarrow \mathrm{p} + \Lambda^0 +$
   (*b*) $\mathrm{p} + \overline{\mathrm{p}} \rightarrow \mathrm{n} +$
   (*c*) $\pi^- + \mathrm{p} \rightarrow \Xi^0 + \mathrm{K}^0 +$
   (*d*) $\mathrm{K}^- + \mathrm{n} \rightarrow \Lambda^0 +$
   (*e*) $\overline{\nu}_\mu + \mathrm{p} \rightarrow \mathrm{n} +$
   (*f*) $\mathrm{K}^- + \mathrm{p} \rightarrow \mathrm{K}^+ +$

14.4 Particle Interactions and Decays

10. Carry out the calculations of mc^2 for the three decays of Figure 14.6.
11. Determine the energy uncertainty or width of (*a*) η; (*b*) η'; (*c*) Σ^0; (*d*) Δ^*.

14.5 Energy and Momentum in Particle Decays

12. A Σ^- baryon is produced in a certain reaction with a kinetic energy of 3642 MeV. If the particle decays after one mean lifetime, what is the longest possible track this particle could leave in a detector?
13. Repeat the calculation of Example 14.4 for the case in which the π meson has zero kinetic energy, and show that the electron energy in this case is less than the maximum value.
14. Find the Q values of the following decays:
   (*a*) $\pi^0 \rightarrow \gamma + \gamma$
   (*b*) $\Sigma^+ \rightarrow \mathrm{p} + \pi^0$
   (*c*) $\mathrm{D}^+ \rightarrow \mathrm{K}^- + \pi^+ + \pi^+$
15. Find the Q values of the following decays:
   (*a*) $\pi^- \rightarrow \mu^- + \overline{\nu}_\mu$
   (*b*) $\mathrm{K}^0 \rightarrow \pi^+ + \pi^-$
   (*c*) $\Sigma^0 \rightarrow \Lambda^0 + \gamma$
16. Find the kinetic energies of each of the two product particles in the following decays (assume the decaying particle is at rest):
   (*a*) $\mathrm{K}^0 \rightarrow \pi^+ + \pi^-$
   (*b*) $\Sigma^- \rightarrow \mathrm{n} + \pi^-$
17. Find the kinetic energies of each of the two product particles in the following decays (assume the decaying particle is at rest):
   (*a*) $\Omega^- \rightarrow \Lambda^0 + \mathrm{K}^-$
   (*b*) $\pi^+ \rightarrow \mu^+ + \nu_\mu$
18. A Σ^- with a kinetic energy of 0.250 GeV decays into π^- + n. The π^- moves at 90° to the original direction of travel of the Σ^-. Find the kinetic energies of π^- and n and the direction of travel of n.
19. A K^0 with a kinetic energy of 276 MeV decays in flight into π^+ and π^-, which move off at equal angles with the original direction of the K^0. Find the energies and directions of motion of the π^+ and π^-.

14.6 Energy and Momentum in Particle Reactions

20. Show Eq. 14.6 reduces to Eq. 13.14 in the nonrelativistic limit.
21. Determine the Q values of the following reactions:
   (*a*) $\mathrm{K}^- + \mathrm{p} \rightarrow \Lambda^0 + \pi^0$
   (*b*) $\pi^+ + \mathrm{p} \rightarrow \Sigma^+ + \mathrm{K}^+$
   (*c*) $\mathrm{p} + \mathrm{p} \rightarrow \mathrm{p} + \pi^+ + \Lambda^0 + \mathrm{K}^0$
22. Determine the Q values of the following reactions:
   (*a*) $\gamma + \mathrm{n} \rightarrow \pi^- + \mathrm{p}$
   (*b*) $\mathrm{K}^- + \mathrm{p} \rightarrow \Omega^- + \mathrm{K}^+ + \mathrm{K}^0$
   (*c*) $\mathrm{p} + \mathrm{p} \rightarrow \mathrm{p} + \Sigma^+ + \mathrm{K}^0$
23. Find the threshold kinetic energy for the following reactions. In each case the first particle is in motion and the second is at rest.
   (*a*) $\mathrm{p} + \mathrm{p} \rightarrow \mathrm{n} + \Sigma^+ + \mathrm{K}^0 + \pi^+$
   (*b*) $\pi^- + \mathrm{p} \rightarrow \Sigma^0 + \mathrm{K}^0$
24. Find the threshold kinetic energy for the following reactions. In each case the first particle is in motion and the second is at rest.
   (*a*) $\mathrm{p} + \mathrm{n} \rightarrow \mathrm{p} + \Sigma^- + \mathrm{K}^+$
   (*b*) $\pi^+ + \mathrm{p} \rightarrow \mathrm{p} + \mathrm{p} + \overline{\mathrm{n}}$

14.7 The Quark Structure of Mesons and Baryons

25. Analyze the following reactions in terms of the quark content of the particles and reduce them to fundamental processes involving the quarks:
   (*a*) $\mathrm{K}^- + \mathrm{p} \rightarrow \Omega^- + \mathrm{K}^+ + \mathrm{K}^0$
   (*b*) $\pi^+ + \mathrm{p} \rightarrow \Sigma^+ + \mathrm{K}^+$
   (*c*) $\gamma + \mathrm{n} \rightarrow \pi^- + \mathrm{p}$

26. Analyze the following reactions in terms of the quark content of the particles and reduce them to fundamental processes involving the quarks:
(*a*) $K^- + p \rightarrow \Lambda^0 + \pi^0$
(*b*) $p + p \rightarrow p + \pi^+ + \Lambda^0 + K^0$
(*c*) $\gamma + p \rightarrow D^+ + \overline{D}^0 + n$

27. Analyze the following decays in terms of the quark content of the particles and reduce them to fundamental processes involving the quarks:
(*a*) $\Omega^- \rightarrow \Lambda^0 + K^-$
(*b*) $n \rightarrow p + e^- + \overline{\nu}_e$
(*c*) $\pi^0 \rightarrow \gamma + \gamma$
(*d*) $D^+ \rightarrow K^- + \pi^+ + \pi^+$

28. Analyze the following decays in terms of the quark content of the particles and reduce them to fundamental processes involving the quarks:
(*a*) $K^0 \rightarrow \pi^+ + \pi^-$
(*b*) $\Delta^{*++} \rightarrow p + \pi^+$
(*c*) $\Sigma^- \rightarrow n + \pi^-$
(*d*) $\overline{D}^0 \rightarrow K^+ + \pi^-$

29. Based on Figure 14.17, give the quark content of the six D mesons.

General Problems

30. Table 14.5 lists the most likely decay mode of the K^+ meson; Example 14.4 gives another possible decay. List four other possible decays that are allowed by the conservation laws.

31. It is desired to form a beam of Λ^0 particles to use for the study of reactions with protons. The Λ^0 are produced by reactions at one target and must be transported to another target 2.0 m away so that at least half of the original Λ^0 remain in the beam. Find the speed and the kinetic energy of the Λ^0 for this to occur.

32. Find a decay mode, other than that listed in Table 14.6, for (*a*) Ω^-; (*b*) Λ^0; (*c*) Σ^+ that satisfies the applicable conservation laws.

33. Consider the reaction $p + p \rightarrow p + p + \pi^0$ discussed in Example 14.6, but viewed instead from a frame of reference in which the two protons collide head-on with equal velocities. (*a*) At threshold in this frame of reference, the product particles are formed at rest. Find the proton velocities in this case. (*b*) Use the Lorentz velocity transformation to switch to the laboratory frame of reference in which one of the protons is at rest, and find the velocity of the other proton. (*c*) Find the kinetic energy of the incident proton in the laboratory frame and compare with the value found in Example 14.6.

34. The D_s^+ meson (rest energy = 1969 MeV, $S = +1, C = +1$; see Figure 14.17) has a lifetime of 0.5×10^{-12} s. (*a*) Which interaction is responsible for the decay? (*b*) Among the possible decay modes are $\phi + \pi^+$, $\mu^+ + \nu_\mu$, and $K^+ + \overline{K}^0$. How do the S and C quantum numbers change in these three decays? (The ϕ meson has a spin of 1, a rest energy of 1020 MeV, and a quark content of $s\bar{s}$.) (*c*) Analyze the three decay modes according to the quark content of the initial and final particles. (*d*) Why is the decay into $K^+ + \pi^+ + \pi^-$ allowed, while the decay into $K^- + \pi^+ + \pi^+$ is forbidden?

35. In the decay $K^+ \rightarrow \pi^+ + \pi^+ + \pi^-$ with the initial K meson at rest, what is the maximum kinetic energy of the pi mesons?

36. A beam of π^- mesons with a speed of $0.9980c$ is incident on a target of protons at rest. The reaction produces two particles, one of which is a K^0 meson that is observed to travel with momentum 1561 MeV/c in a direction that makes an angle of 20.6° with the direction of the incident pions. (*a*) Find the momentum and the direction of the second product particle. (*b*) Find the energy of that particle. (*c*) Find the rest energy of the second particle and deduce its identity.

Chapter 15

COSMOLOGY: THE ORIGIN AND FATE OF THE UNIVERSE

Today we scan the skies at all wavelengths from the very short (X rays and gamma rays) to the very long (radio waves). New and unexpected discoveries have occurred at these wavelengths: quasars, pulsars, supernovas, black holes — all of which suggest that the universe is not at all static and eternal, as was once believed, but instead is active, evolving, and teeming with radiation. Van Gogh's painting *The Starry Night* suggests exactly that view, even though it was painted in 1889, long before any of these discoveries were made.

In the short time of a few hundred years, developments in astronomy have taken us from the belief that the Earth and its human population were the center of the universe, to a role that approaches insignificance. Before the 16th century, it was widely believed that the planets, Sun, Moon, and stars revolved about a central Earth. By the early 20th century, astronomers had discovered that we inhabit one minor star of a vast number in our galaxy, and that the universe contains an equally vast number of other galaxies.

Gravity is the dominant force that determines the structure of the present universe, but Newton's theory is insufficient to explain a number of observations of the motion of celestial objects. For this purpose we need a different theory, the *general theory of relativity,* which was proposed by Albert Einstein in 1916. Although the mathematics of this theory is beyond the level of this text, we can summarize some of its features and discuss its experimental predictions and their verification. Like the special theory, the general theory of relativity offers us a new way of thinking about space and time.

In this chapter, we briefly survey the field of *cosmology*, the study of the universe on the large scale, including its origin, evolution, and future. For this study we must rely not only on relativity (special and general) and quantum theory, but also on fundamental results from atomic and molecular physics, statistical physics, thermodynamics, nuclear physics, and particle physics.

We begin with three discoveries that fundamentally altered our concept of the universe: it is expanding, it is filled with electromagnetic radiation, and most of its mass is mysteriously hidden from our view. We show how these discoveries have been incorporated, using results from general relativity, into a theory of the origin of the universe known as the Big Bang theory. We then consider other measurements that support this theory, and we conclude with some speculations on the future of the universe.

15.1 THE EXPANSION OF THE UNIVERSE

The evidence for the expansion of the universe comes from the change in wavelength of the light emitted by distant galaxies. In Chapter 2, we analyzed a similar effect as the relativistic Doppler shift (Eq. 2.22), which we can write in terms of wavelength as

$$\lambda' = \lambda\sqrt{\frac{1+v/c}{1-v/c}} = \lambda\frac{1+v/c}{\sqrt{1-v^2/c^2}} \tag{15.1}$$

where v represents the relative velocity between the source of the light and the observer. Here λ' is the wavelength we measure on Earth and λ is the wavelength emitted by the moving star or galaxy in its own rest frame.

The light emitted by a star such as the Sun has a continuous spectrum. As light passes through the star's atmosphere, some of it is absorbed by the gases in the atmosphere, so the continuous *emission* spectrum has a few dark *absorption* lines superimposed (see Figure 6.15). Comparison between the known wavelengths of these lines (measured on Earth for sources at rest relative to the observer) and the Doppler-shifted wavelengths allows the speed of the star to be deduced from Eq. 15.1.

Of the stars in our galaxy, some are found to be moving toward us, with their light shifted toward the shorter wavelengths (blue), and others are moving

away from us, with their light shifted toward the longer wavelengths (red). The average speed of these stars relative to us is about 30 km/s ($10^{-4}c$). The change in wavelength for these stars is very small. Light from nearby galaxies, those of our "local" group, again shows either small blue shifts or small red shifts.

However, when we look at the light from distant galaxies, we find it to be systematically red shifted, and by a large amount. Some examples of these measurements are shown in Figure 15.1. We do *not* see a comparable number of red and blue shifts, as we would expect if the galaxies were in random motion. All of the galaxies beyond our local group seem to be moving away from us.

The *cosmological principle* asserts that the universe must look the same from any vantage point, and so we must conclude that any other observer in the universe would draw the same conclusion: *The galaxies would be observed to recede from every point in the universe.*

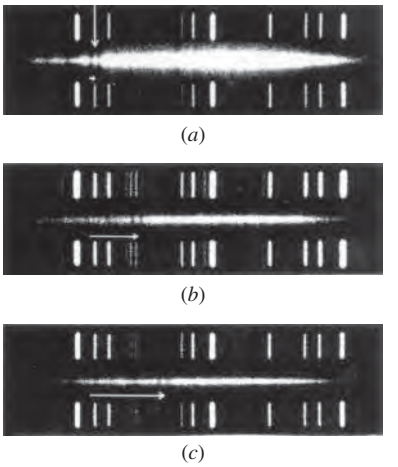

(*a*)

(*b*)

(*c*)

FIGURE 15.1 Red shifts of galaxies. (*a*) The horizontal band in the center shows a continuous spectrum with two dark lines superimposed (vertical arrow near left side), which represent absorption by calcium. Above and below the absorption spectrum are emission spectra for calibration. The recessional speed of this galaxy (which is in our local group) is 1200 km/s, so the red shift is very small. (*b*) The absorption spectrum of a galaxy with a recessional speed of 15,000 km/s. The red shift of the two calcium lines (indicated by the horizontal arrow) is significant. (*c*) The red shift of a galaxy with a recessional speed of 22,000 km/s. (Data courtesy Hale Observatories.)

Hubble's Law

In the 1920s, astronomer Edwin Hubble was using the 100-inch telescope on Mount Wilson in California to study the wispy nebulae. By resolving individual stars in the nebulae, Hubble was able to show that they are galaxies like the Milky Way, composed of hundreds of billions of stars. When Hubble measured the wavelength shifts of the light from the galaxies and deduced their speeds, he made two remarkable conclusions: the galaxies are moving away from us, and *the farther away a galaxy is from us, the faster it is moving.* This proportionality between the speed of the galaxy and its distance d is known as *Hubble's law*:

$$v = H_0 d \tag{15.2}$$

The proportionality constant H_0 is known as the *Hubble parameter*.

Figure 15.2*a* shows a plot of Hubble's data for the deduced speeds against the distance. Although the points scatter quite a bit (due primarily to uncertainties in the distance measurements), there is a definite indication of a linear relationship. (Hubble's distance calibration was incorrect, so the labels on the horizontal axis do not correspond to the actual distances to the galaxies.) More modern data based on observing supernovas in distant galaxies are shown in Figure 15.2*b*. There is again clear evidence for a linear relationship, and the slope of the line gives a value of the Hubble parameter of about 72 km/s/Mpc*, within a range of about ±10%. The Hubble parameter can also be determined from a variety of other cosmological experiments. These agree with the supernova data, and the best current value is

$$H_0 = 72 \frac{\text{km/s}}{\text{Mpc}}$$

The uncertainty in this value is on the order of ±4%.

The Hubble parameter has the dimension of inverse time. As we show later, H_0^{-1} is a rough measure of the age of the universe. The best value of H_0 gives an age of 14×10^9 y. If the speed of recession has been changing, the true age can be less than H_0^{-1}.

*A parsec, pc, is a measure of distance on the cosmic scale; it is the distance that corresponds to one angular second of parallax. Because parallax is due to the Earth's motion around the Sun, the parallax angle 2α is the diameter $2R$ of the Earth's orbit divided by the distance d to the star or galaxy. Thus $\alpha = R/d$ radians, which gives 1 pc = 3.26 light-years = 3.084×10^{13} km. One megaparsec, Mpc, is 10^6 pc.

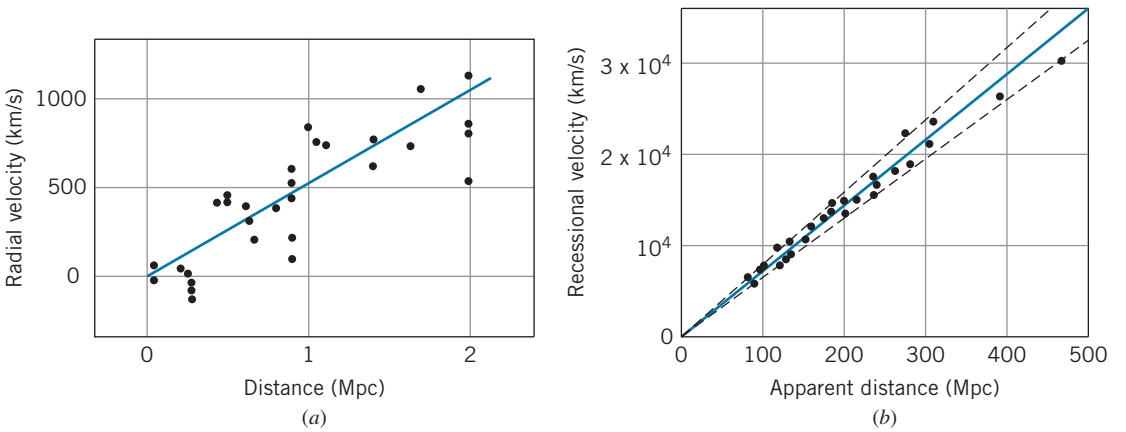

FIGURE 15.2 (*a*) Hubble's original data showing the linear relationship between the recessional speed of a galaxy and its distance from Earth. (*b*) Modern data showing Hubble's law. Data are based on observations of supernovas in distant galaxies using the Hubble Space Telescope. The solid line represents a Hubble parameter of 72 km/s/Mpc, and the dashed lines show the limits corresponding to ±7 km/s/Mpc. [Data from W. L. Freedman et al., *Astrophysical Journal* **553**, 47 (2001).]

How does the Hubble law show that the universe is expanding? Consider the unusual universe represented by the three-dimensional coordinate system shown in Figure 15.3*a*, where each point represents a galaxy. With the Earth at the origin, we can determine the distance d to each galaxy. If this universe were to expand, with all the points becoming further apart, as in Figure 15.3*b*, the distance to each galaxy would be increased to d'. Suppose the expansion were such that every dimension increased by a constant ratio k in a time t; that is, $x' = kx$, and so forth. Then $d' = kd$, and a given galaxy moves away from us by a distance $d' - d$ in a time t, so its apparent recessional speed is

$$v = \frac{d' - d}{t} = d\frac{k - 1}{t} \tag{15.3}$$

If we compare two galaxies 1 and 2,

$$\frac{v_1}{v_2} = \frac{d_1}{d_2} \tag{15.4}$$

a relationship identical with Hubble's law, Eq. 15.2. Thus, in an expanding universe, it is perfectly natural that the further away from us a galaxy might be, the faster we observe it to be receding.

Notice also from Figure 15.3 that this is true no matter which point we happen to choose as our origin. From *any* point in the "universe" of Figure 15.3, the other points would be observed to satisfy Eq. 15.4 and thus also Hubble's law. We can further demonstrate this with two analogies. If we glue some spots to a balloon (Figure 15.4) and then inflate it, *every* spot observes all other spots to be moving away from it, and the farther away a spot is from any point, the faster its separation grows. For a three-dimensional analogy, consider the loaf of raisin bread shown in Figure 15.5 rising in an oven. As the bread rises, every raisin observes all the others to be moving away from it, and the speed of recession increases with the separation.

Edwin Hubble (1889–1953, United States). His observational work with large telescopes revealed the existence of galaxies, and he was the first to measure their size and distance. Hubble's discovery of the recessional motion of the galaxies was one of the most exciting and important in the history of astronomy.

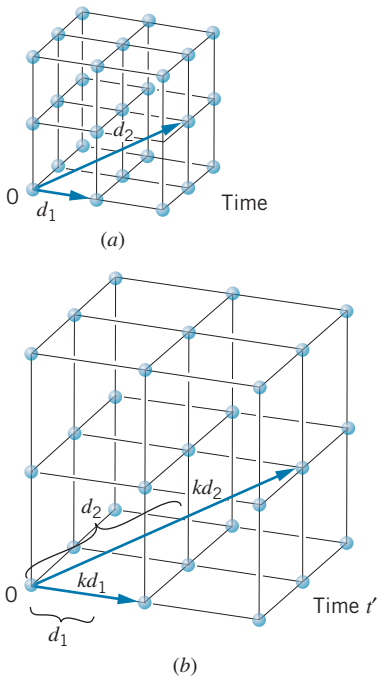

FIGURE 15.3 The expansion of a coordinate space, showing that the apparent speed of recession depends on the distance; d_2 is greater than d_1, and d_2 increases faster than d_1.

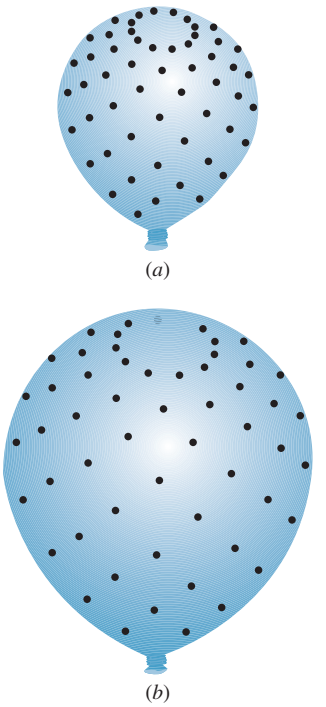

FIGURE 15.4 As a balloon is inflated, every observer on the surface experiences a velocity-distance relationship of the form of the Hubble law.

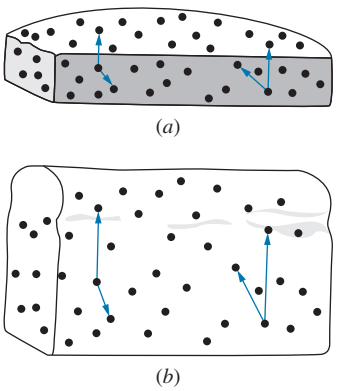

FIGURE 15.5 Another system in which the Hubble law is valid.

The correct interpretation of the cosmological redshifts requires the techniques of *general* relativity, which we discuss later in this chapter. According to general relativity, the shift in wavelength is caused by a stretching of the entire fabric of spacetime. Imagine small photos of galaxies glued to a rubber sheet. As the sheet is stretched, the distance between the galaxies increases, but they are not "in motion" according to the terms we usually use in physics to describe motion. However, the stretching of the space between the galaxies causes the wavelength of a light signal from one galaxy to increase by the total amount of the stretching before it is received at another galaxy. This is very different from the usual interpretation of the Doppler formula (Eq. 15.1). (In fact, for some galaxies the wavelength shift is so large that the special relativity formula would imply a recessional speed greater than the speed of light!) At low speeds, the Doppler interpretation of the redshift (that is, calculating a speed from the Doppler formula and using that speed in Hubble's law) gives results that correspond with those based on an expansion of spacetime. However, for very large cosmological redshifts, a more correct analysis must be based on the stretching model:

$$\frac{\lambda'}{\lambda} = \frac{R_0}{R} \tag{15.5}$$

where R_0 represents a "size" or distance scale factor of the universe at the present time and R represents a similar factor at the time the light was emitted.

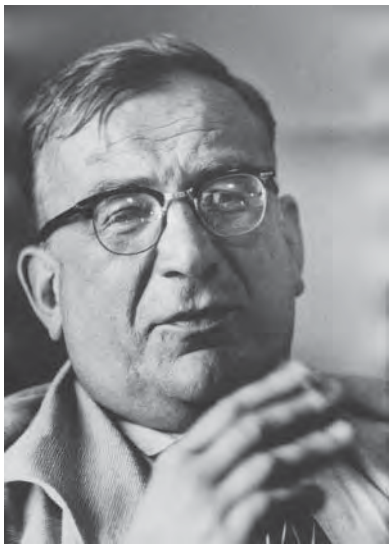

George Gamow (1904–1969, United States). His significant contributions to nuclear physics (theories of alpha decay, beta decay, and nuclear structure), astrophysics (nucleosynthesis, stellar structure), and cosmology (the Big Bang theory) place him among the first rank of scientists. Gamow was also one of the most successful writers of popular science, to which he brought unusual and amusing perspectives.

The expansion of the universe has been widely accepted since Hubble's discoveries in the 1920s. There are, however, two interpretations of this expansion. (1) If the galaxies are separating, long ago they must have been closer together. The universe was much denser in its past history, and if we look back far enough we find a single point of infinite density. This is the "Big Bang" hypothesis, developed in 1948 by George Gamow and his colleagues. (2) The universe has always had about the same density it does now. As the galaxies separate, additional matter is continuously created in the empty space between the galaxies, to keep the density more or less constant. This is the "Steady State" hypothesis, proposed also in 1948 by astronomer Fred Hoyle and others. New galaxies created from this new matter would make the universe look the same not only from all vantage points, but also *at all times* in the present and future. (To keep the density constant, the rate of creation need be only about one hydrogen atom per cubic meter every billion years.)

Both hypotheses had their supporters, and during the 1940s and 1950s the experimental evidence did not seem to favor either one over the other. In the 1960s, the new field of radio astronomy revealed the presence of a universal background radiation in the microwave region, which is believed to be the remnant radiation from the Big Bang. This single observation has propelled the Big Bang theory to the forefront of cosmological models.

15.2 THE COSMIC MICROWAVE BACKGROUND RADIATION

When a gas expands adiabatically, it cools. The same is true for the universe: the expansion is accompanied by cooling. As we go back in time, we find a hotter, denser universe. Far enough back in time, the universe would have been too hot for stable matter to form. Its composition was then a "gas" of particles and photons. The unstable particles eventually decayed to stable ones, and the stable particles eventually clumped together to form matter. The photons that filled the universe remained, but their wavelengths were stretched by the continuing expansion. Today those photons have a much lower temperature, but they still uniformly fill the universe.

The wavelength spectrum of those photons is that of an isolated object (blackbody) emitting thermal radiation at the temperature T that characterizes the universe at a particular time. The wavelengths change as the universe expands, but the radiation retains an ideal thermal spectrum at a temperature that decreases with time. In the 1940s, the Big Bang cosmologists (Gamow and others) predicted that this "fireball" would today be at a temperature of the order of 5 to 10 K; such photons would have a typical energy kT of the order of 10^{-3} eV or a wavelength of order 1 mm, in the microwave region of the spectrum.

The properties of this background radiation can be described using the formulas for thermal radiation we developed in Section 10.6. The number of photons dN in the energy interval dE at E (that is, with energies between E and $E + dE$) was given by Eq. 10.38. Writing that equation as the number per unit volume (number density), we get

$$\frac{N(E)\,dE}{V} = \frac{8\pi E^2}{(hc)^3}\frac{1}{e^{E/kT} - 1}\,dE \tag{15.6}$$

To find the *total* number of photons of all energies per unit volume we integrate Eq. 15.6 over energy:

$$\frac{N}{V} = \frac{1}{V}\int_0^\infty N(E)\,dE = \frac{8\pi}{(hc)^3}\int_0^\infty \frac{E^2\,dE}{e^{E/kT}-1} = \frac{8\pi}{(hc)^3}(kT)^3\int_0^\infty \frac{x^2\,dx}{e^x-1} \tag{15.7}$$

where we have substituted $x = E/kT$. The definite integral is a standard form with a value approximately equal to 2.404. Equation 15.7 shows that the total number of photons per unit volume is proportional to the cube of the temperature, and evaluating the constants we find

$$N/V = (2.03 \times 10^7 \text{ photons/m}^3\cdot\text{K}^3)T^3 \tag{15.8}$$

We can write Eq. 10.41 for the energy density (energy per unit volume) in the same form by evaluating the constants:

$$U = \frac{8\pi^5 k^4}{15(hc)^3}T^4 = (4.72 \times 10^3\ \text{eV/m}^3\cdot\text{K}^4)T^4 \tag{15.9}$$

and the mean (average) energy per photon at temperature T is obtained from the ratio of Eqs. 15.9 and 15.8:

$$E_\text{m} = \frac{U}{N/V} = (2.33 \times 10^{-4}\ \text{eV/K})T \tag{15.10}$$

We now look at the experimental evidence for the existence of this microwave radiation and the determination of its temperature. From Eq. 10.42 we see that the measurement of the radiant energy density at *any* wavelength is enough for a determination of the temperature T, although to demonstrate that the radiation actually has an ideal thermal spectrum requires measurement over a range of wavelengths.

The first experimental evidence for this radiation was obtained in a 1965 experiment by Arno Penzias and Robert Wilson, who used a microwave antenna tuned to a wavelength of 7.35 cm. At this wavelength they recorded an annoying "hiss" from their antenna that could not be eliminated, no matter how much care they took in refining the measurement. After painstaking efforts to eliminate the "noise," they concluded that it was coming from no identifiable source and was striking their antenna from all directions, day and night, summer and winter. From the radiant energy at that wavelength they deduced a temperature of 3.1 ± 1.0 K, and it was later concluded that the radiation was the present remnant of the Big Bang "fireball." For this experiment, Penzias and Wilson shared the 1978 Nobel Prize in physics.

Since that original experiment there have been many additional studies, at various wavelengths in the range 0.05 to 100 cm, all giving about the same temperature. The most recent measurements were made with the Cosmic Background Explorer (COBE) satellite, which was launched into Earth orbit 1989, and the Wilkinson Microwave Anisotropy Probe (WMAP) satellite, which was launched into solar orbit in 2001. Previously, no precise data from Earth-bound observations were available below a wavelength of 1 cm because of atmospheric absorption. The COBE and WMAP satellites were able to obtain very precise data on the intensity of the background radiation in the wavelength range between 1 cm and 0.05 cm (0.0001 eV and 0.0025 eV).

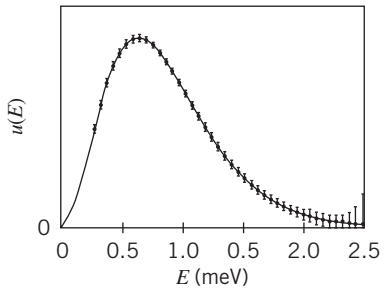

FIGURE 15.6 Energy density of the microwave background. The data points are from the COBE satellite, and the error bars have been multiplied by a factor of 400 to make them visible. The solid curve is the expected thermal radiation spectrum (Eq. 10.39) for a temperature of 2.725 K. (Data from Legacy Archive for Microwave Background Data Analysis, NASA Office of Space Science.)

The results from the COBE satellite are summarized in Figure 15.6. The data points fall precisely on the solid line, which is calculated from Eq. 10.39 for a temperature $T = 2.725\,\text{K}$. For these spectacularly beautiful data, experimenters John Mather and George Smoot were awarded the 2006 Nobel Prize in physics.

Other experiments show that the radiation has a uniform intensity in all directions. It comes from no particular source, but instead fills the universe today as it did in the early times just after the Big Bang.

Using the deduced temperature of 2.7 K, we can calculate from Eqs. 15.8 to 15.10 that there are about 4.0×10^8 of these photons in every cubic meter of space, that they contribute to the universe an energy density of about $2.5 \times 10^5\,\text{eV/m}^3$ (about half the rest energy of an electron), and that each photon has an average energy of about 0.00063 eV. The number of photons is particularly important, because for nearly all of the last 14×10^9 y the *ratio* of the number of nucleons (protons and neutrons) to photons has been almost constant. This has important consequences for the Big Bang cosmology.

15.3 DARK MATTER

Figure 15.7 shows spiral galaxies that are similar to our Milky Way galaxy, in which about 10^{11} stars are bound together by the gravitational force. The diameter of a typical galaxy might be 10–50 kpc ($0.3-1.5 \times 10^{18}$ km). Many galaxies have this spiral structure, with a bright central region (containing most of the galaxy's mass) and several spiral arms in a flat disk. The entire structure rotates about an axis perpendicular to the plane of the disk. The Sun, which is in one of the spiral arms of our galaxy at a distance of 8.5 kpc from the center (about 2/3 of the radius of the disk), has a tangential velocity of 220 km/s. At this speed, it takes about 240 million years for a complete rotation; during the lifetime of the solar system of about 4.5 billion years, the Sun has made about 20 revolutions.

Because the stars in the galaxy are bound by the gravitational force, we can use Kepler's laws to analyze the motion. We assume that the gravitational force on the Sun is due primarily to the dense region at the center of the galaxy; the total

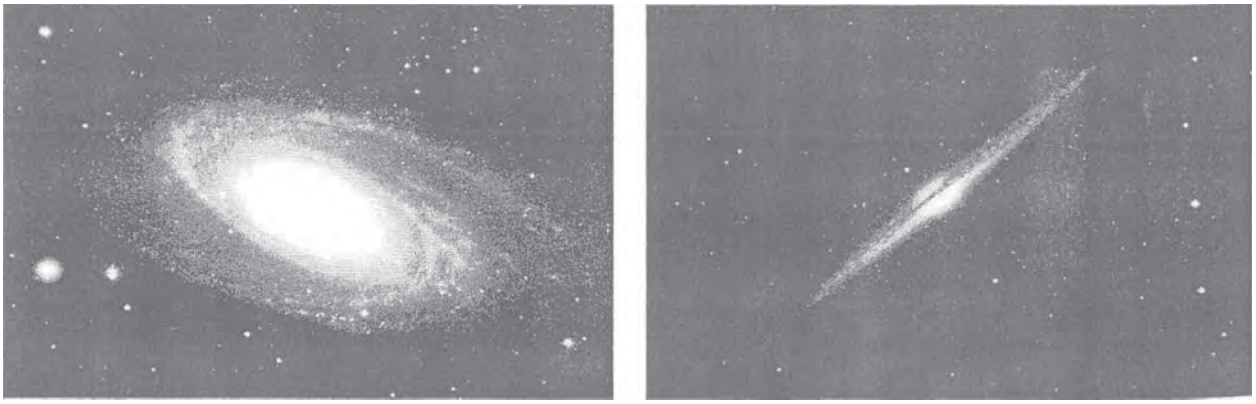

FIGURE 15.7 Spiral galaxies similar to the Milky Way, viewed from two different perspectives—one normal to the plane and one along the plane.

mass of the other stars in the spiral arm is much smaller than the central mass, so they make a negligible contribution to the force on the Sun. Kepler's third law relates the period T of the orbit to the radius:

$$T^2 = \left(\frac{4\pi^2}{GM}\right) r^3 \tag{15.11}$$

With $T = 2\pi r/v$, where v is the tangential velocity, we obtain

$$v = \sqrt{\frac{GM}{r}} \tag{15.12}$$

Here M refers to the mass contained within the region of radius r. The Sun's tangential velocity suggests that a mass equivalent to 10^{11} solar masses lies within the Sun's orbit.

According to this model, we expect stars beyond the Sun to have tangential velocities that decrease with increasing radius like $r^{-1/2}$. (The planets in the solar system follow this expectation to very high precision.) However, we observe that for the rotation of the galaxy v is constant or perhaps increases slightly for stars beyond the Sun (Figure 15.8).

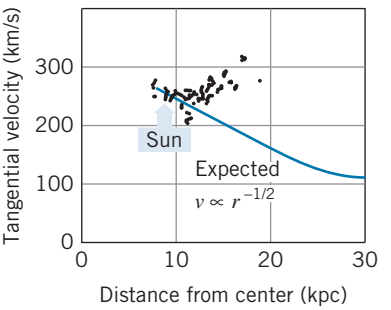

FIGURE 15.8 Tangential velocities of stars in our galaxy, determined from the Doppler shift of their light. The solid line is the prediction based on Kepler's third law, Eq. 15.12.

Other spiral galaxies show the same effect. The tangential speeds of stars in distant galaxies can be measured by the Doppler shift of their light. If we are viewing a galaxy along the plane of the disk, then one side will always be moving toward us and the other will always be moving away from us. The *difference* between the Doppler shifts of the light from the two sides of the galaxy then tells us about its rotational speed, independently of the net motion of the entire galaxy. From this measurement, we can determine how the tangential velocity of the galaxy depends on the distance from its center. A typical set of results is shown in Figure 15.9. Once again, the velocity fails to follow the expected relationship and instead remains constant throughout the visible part of the galaxy.

These results are not consistent with Kepler's law, which is based on a large central mass attracting each star toward the center of the galaxy. On the contrary, to explain a velocity that is constant as a function of radius we must have a mass M that increases linearly with r (see Eq. 15.12). However, this explanation is inconsistent with visual observations of the galaxies, which clearly show that most of the light, and therefore presumably most of the mass, is concentrated in the central region.

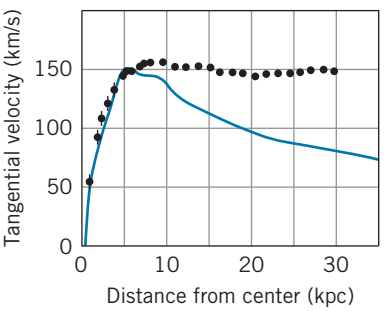

FIGURE 15.9 The tangential rotational velocity of a distant galaxy as a function of the distance from its center. The solid line is the expected $r^{-1/2}$ dependence at distances beyond the central concentration of stars.

To resolve this dilemma, it has been concluded that there is a large quantity of invisible matter in galaxies—matter that must be present in the galaxy to supply the gravitational force, but that does not give off any light (or other electromagnetic radiation). To supply the required gravitational force, this *dark matter* must have a mass at least 10 times the mass of the visible matter in the galaxy. That is, more than 90% of the matter in the galaxy is in some unknown and invisible form. This dark matter permeates the region of space occupied by the galaxy and may surround it in the form of a halo.

Galaxies are observed in gravitationally bound clusters of typically 100 members. The size of a cluster is perhaps 1 Mpc, about 100 times as large as a typical galaxy. Because these clusters rotate about their common center, we can perform similar measurements to compare the rotational speed of a galaxy with its distance from the center. As with individual galaxies, the clusters follow the dependence shown in Figure 15.9, suggesting that there is more matter in the

Vera Rubin (1928–, United States). An observational astronomer, she has made pioneering discoveries about the motion of stars and galaxies. By observing the Doppler shifts of stars in galaxies, she deduced that their rotational velocities are not consistent with attraction only by a large concentration of mass at the galactic center. Rubin's work has been among the leading contributions to understanding the existence and amount of dark matter in the universe. She was awarded the National Medal of Science in 1993.

clusters than we can account for from the galaxies alone. We conclude that dark matter also surrounds clusters of galaxies.

Support for the existence of dark matter comes from the observation of light from distant galaxies that passes by a cluster of galaxies on its way to Earth. This light is deflected by the gravitational field of the cluster in a process known as "gravitational lensing." From the amount of the deflection of the light, it is possible to deduce the quantity of matter in the cluster. The results of these observations show that there is much more matter in the cluster than we would deduce from the luminous matter alone, suggesting the presence of relatively large amounts of dark matter. A dramatic illustration of this effect occurs in the colliding galaxies of the "Bullet Cluster," first analyzed in 2006, in which the distribution of ordinary matter (revealed by the glowing interstellar gas) is different from the distribution of dark matter (revealed by the gravitational lensing effect).

What kinds of objects make up this dark matter? Speculations about its nature are divided loosely into two categories: MACHOs (Massive Compact Halo Objects) and WIMPs (Weakly Interacting Massive Particles). Possible MACHOs include massive black holes, neutron stars, burnt-out white dwarf stars, or brown dwarf stars (Jupiter-sized objects of too small a mass to become a star). The WIMPs include neutrinos, magnetic monopoles, and other exotic types of stable elementary particles produced during the Big Bang. The major difference between the two types of objects is that MACHOs are made from baryons (protons and neutrons, like ordinary matter), while WIMPs are made from some other, more exotic type of non-baryonic matter. Current theories suggest that most of the dark matter is of the non-baryonic form, but (aside from neutrinos) no examples of this type of matter have yet been produced in any laboratory on Earth.

15.4 THE GENERAL THEORY OF RELATIVITY

The interpretation of the observational data describing our universe must be done using methods from the general theory of relativity, which is in essence a theory of gravitation developed by Albert Einstein between 1911 and 1915. The mathematical level of this theory is beyond the level of this text, but we will try to appreciate how the theory helps us to understand the structure and evolution of the universe.

The special theory of relativity arose from a thought experiment of Einstein's in which he imagined trying to catch up with a light beam. The general theory also arose from a thought experiment. Here are Einstein's words:

> *I was sitting in a chair in the patent office at Bern when all of a sudden a thought occurred to me: If a person falls freely he will not feel his own weight. This simple thought made a deep impression on me. It impelled me toward a theory of gravitation.*

Figure 15.10 illustrates a freely falling person in two situations: in the Earth's gravity and in interstellar space where the gravitational field is negligibly weak. In both cases the person is in an isolated chamber and therefore unable to use outside objects to deduce the motion of the chamber. From within the chamber

(*a*) (*b*)

FIGURE 15.10 The effects of freely falling appear identical from within the chamber in (*a*) the Earth's gravity and (*b*) interstellar space.

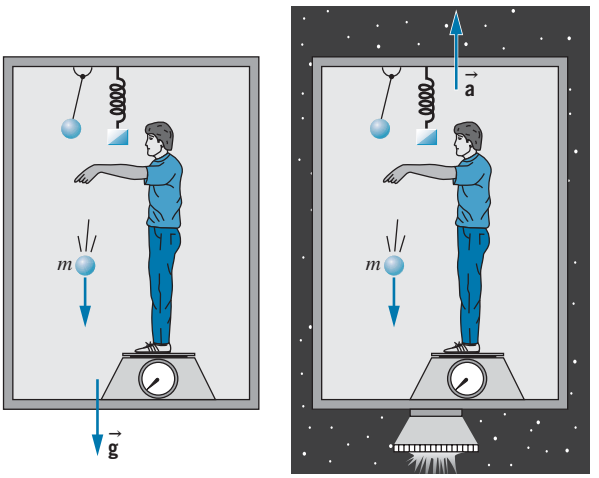

(*a*) (*b*)

FIGURE 15.11 The effects appear identical when the chamber is (*a*) at rest in a uniform gravitational field and (*b*) accelerating in interstellar space.

the two cases look exactly equivalent; no measuring instrument operating entirely within the chamber can distinguish between the two cases. An acceleration $\vec{\mathbf{a}} = \vec{\mathbf{g}}$ in a gravitational field $\vec{\mathbf{g}}$ is equivalent to an acceleration of 0 in a negligible gravitational field.

It appears that an acceleration is able to "cancel out" the effects of a gravitational field. Let us go one step further and ask whether an acceleration can *produce* the effects of a gravitational field. Consider the situations illustrated in Figure 15.11. In one case the observer is at rest near the Earth, where the gravitational field is $\vec{\mathbf{g}}$. In the other case, the observer is in empty space where the gravitational field is negligibly small, but the rocket engines are firing so that the chamber has an acceleration $\vec{\mathbf{a}} = -\vec{\mathbf{g}}$. There are various experiments in the chamber: a scale displays the weight of the observer (actually, the normal force exerted on the observer by the scale), a ball drops to the floor, a mass stretches a spring, and a pendulum oscillates. All of these experiments give identical results in the two chambers. Once again, there is no experiment that can be done within the chamber to distinguish the two cases.

This leads us to the *principle of equivalence:*

> *There is no local experiment that can be done to distinguish between the effects of a uniform gravitational field in a nonaccelerating inertial frame and the effects of a uniformly accelerating (noninertial) reference frame.*

By "local" we mean that the experiments must be done within the chamber, and also that the chamber must be sufficiently small that the gravitational field is uniform. Near the surface of the Earth, for example, not all $\vec{\mathbf{g}}$ vectors inside the chamber would be parallel; they point toward the center of the Earth, so there would be a slight angle between the $\vec{\mathbf{g}}$ vectors on opposite sides of the chamber. If we make the chamber small, this effect is negligible and the $\vec{\mathbf{g}}$ vectors everywhere

in the chamber, like the $\vec{\mathbf{a}}$ vectors in the accelerating chamber, are parallel to one another.

The principle of equivalence appears in a slightly different (and weaker) form in introductory physics, where it is stated in terms of the equivalence of *inertial* and *gravitational* mass. That is, the mass m that appears in the expression $F = ma$ (inertial mass) is identical to the mass m that appears in the expression $F = GMm/r^2$ (gravitational mass). It follows from this form of the principle of equivalence that all objects, regardless of their masses, fall with the same acceleration in the Earth's gravity. This was first tested by Galileo in the famous (and perhaps apocryphal) experiment in which he dropped two different masses from the top of the leaning tower of Pisa and observed them to fall at the same rate. In recent years other more precise experiments have established the equivalence of gravitational and inertial mass to about 1 part in 10^{11}.

Einstein realized that the principle of equivalence applied not only to mechanical experiments but to all experiments, even ones based on electromagnetic radiation. Consider the arrangement shown in Figure 15.12. At the top of the chamber is a light source that emits a wave of frequency f. At the bottom of the chamber and a distance H away is a detector that observes the wave and measures its frequency. When the light wave is emitted in the accelerating chamber, the source has speed v, which we assume to be small compared with the speed of light c. When it is detected, after a time of flight $t \approx H/c$, the floor is moving with a speed $v + at$. In effect there is a relative speed $\Delta v = at$ between the source and the detector, so there is a Doppler shift in the frequency given by Eq. 2.22:

$$f' = f\sqrt{\frac{1 + \Delta v/c}{1 - \Delta v/c}} \approx f(1 + \Delta v/c) \tag{15.13}$$

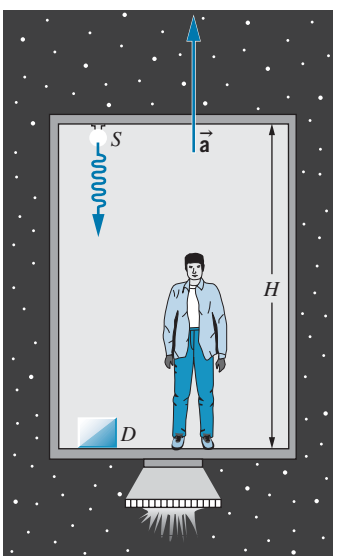

FIGURE 15.12 A source S emits a light wave that is recorded by a detector D in a chamber that is accelerating upward.

or, in terms of the frequency difference $\Delta f = f' - f$,

$$\frac{\Delta f}{f} = \frac{\Delta v}{c} = \frac{at}{c} = \frac{aH}{c^2} \tag{15.14}$$

Now let us compare the result of this experiment with a similar one done in a chamber at rest in a uniform gravitational field g. If the results of the two experiments are to be identical (as required by the principle of equivalence), there must be a frequency shift given by Eq. 15.14 with $a = g$:

$$\frac{\Delta f}{f} = \frac{gH}{c^2} \tag{15.15}$$

The principle of equivalence thus predicts a change in frequency of a light wave falling in the Earth's gravity.

In 1959, R. V. Pound and G. A. Rebka allowed 14.4-keV photons from the radioactive decay of ^{57}Co to fall down the Harvard tower, a distance of 22.6 m. The expected fractional change in frequency, $\Delta f/f = gH/c^2$, was 2.46×10^{-15}; that is, to detect the effect, they had to measure the frequency or energy of the photon at the bottom of the tower to a precision of about 1 part in 10^{15}! The Mössbauer effect (Section 12.9) makes it possible to achieve such a level of precision, and the measured result was $\Delta f/f = (2.57 \pm 0.26) \times 10^{-15}$, consistent with the equivalence principle. Similar experiments based on comparisons between the

frequency of radiation emitted by satellites and received by ground stations have confirmed the predictions of the principle of equivalence to a precision of about 1 part in 10^4.

Because the Global Positioning System (GPS) relies on frequency measurements on the surface of the Earth from transmitters in orbiting satellites, its accuracy depends on applying a correction due to the gravitational frequency shift predicted by general relativity. Without this correction, errors in the GPS locating system of roughly 10 km per day would accumulate.

Note that in Eq. 15.15 the frequency shift depends on the difference in gravitational potential ΔV (potential energy per unit mass) between the source and the detector:

$$\Delta V = \frac{\Delta U}{m} = \frac{(mgH - 0)}{m} = gH \tag{15.16}$$

For the satellite, even though the gravitational field through which the radiation travels is not uniform, the same conclusion holds: the frequency shift depends on the difference in gravitational potential between the source and the observer. Consider, for example, light leaving the surface of a star of mass M and radius R. The gravitational potential at the surface is $V = -GM/R$. If the light is observed on the Earth, where the gravitational potential is negligible compared with that of the star, the frequency shift is

$$\frac{\Delta f}{f} = \frac{\Delta V}{c^2} = -\frac{GM}{Rc^2} \tag{15.17}$$

Photons climbing out of a star's gravitational field lose energy and are therefore shifted to smaller frequencies or longer wavelengths (red shifted). This effect is difficult to observe for two reasons: (1) the motion of the star causes a Doppler shift that is generally greater than the gravitational shift, and (2) the spectral lines are Doppler broadened by the thermal motion of the atoms near the surface of a star (see Section 10.4). Nevertheless, the effect has been confirmed for a few stars including the Sun.

Example 15.1

The Lyman α line in the hydrogen spectrum has a wavelength of 121.5 nm. Find the change in wavelength of this line in the solar spectrum due to the gravitational shift.

Solution

From Eq. 15.17, we have

$$\begin{aligned}\frac{\Delta\lambda}{\lambda} = -\frac{\Delta f}{f} &= \frac{GM}{Rc^2} \\ &= \frac{(6.67 \times 10^{-11}\,\mathrm{N \cdot m^2/kg^2})(1.99 \times 10^{30}\,\mathrm{kg})}{(6.96 \times 10^{8}\,\mathrm{m})(3.00 \times 10^{8}\,\mathrm{m/s})^2} \\ &= 2.12 \times 10^{-6}\end{aligned}$$

The shift in wavelength is

$$\begin{aligned}\Delta\lambda &= (2.12 \times 10^{-6})(121.5\,\mathrm{nm}) \\ &= 0.257\,\mathrm{pm}\end{aligned}$$

This shift in wavelength is small in comparison with the Doppler shifts due to the Sun's rotation and the thermal broadening of its spectral lines (see Problem 6).

Space and Time in General Relativity

From *special* relativity we learn that the laws of physics must be the same in all inertial frames, and that there is no preferred inertial frame relative to which it is possible to determine the absolute velocity of an observer. From this point of view, it seems that an accelerated (noninertial) frame is a preferred frame, because it is possible to determine the absolute acceleration. In the *general* theory, Einstein sought to remove this restriction, so that motion would be relative for *all* observers, even accelerated ones. The principle of equivalence, which tells us that we can't distinguish between acceleration and a gravitational field, removes acceleration from its privileged role.

Ultimately, general relativity is a theory of geometry. The motion of a particle is determined by the properties of the space and time coordinates through which it moves. Because space and time are intimately coupled in relativity (see, for example, the Lorentz transformation in Section 2.5), we regard them as components of a combined coordinate system called *spacetime.*

The equivalence between accelerated motion and gravity suggests a relationship between spacetime coordinates and gravity. In the classical description, we would say that the presence of matter sets up a gravitational field, which then determines how objects move in response to that field. According to general relativity, we say that the presence of matter (and energy) causes spacetime to warp or curve; the motion of particles is then determined by the shape of the coordinate system. It is sometimes said that "Geometry tells matter how to move, and matter tells geometry how to curve." From the configuration of mass and energy, general relativity gives us a procedure for calculating the curvature of spacetime, and the motion of a particle or a light beam then follows directly.

Let's consider the simple case of a particle that moves in only one dimension—for example, a bead sliding without friction on a straight wire. We can plot the motion of the bead on an xt coordinate system, which is the two-dimensional spacetime of the bead. For example, if the bead moves with constant velocity along the wire from position x_A at time t_A to position x_B at time t_B, the motion in spacetime is represented by the straight line shown in Figure 15.13*a*.

Now suppose the wire is mounted vertically in an accelerating chamber in a gravity-free environment. To an observer in the chamber, the bead will appear to accelerate downward as the chamber is accelerated upward. The path in spacetime is now curved, as suggested by Figure 15.13*b*.

If the acceleration is replaced by the equivalent gravitational field, the motion of the bead, as observed from inside the chamber, is exactly the same—the bead appears to accelerate downward. General relativity describes this situation as a change in the shape of spacetime; the presence of matter (which classically we would describe as the source of the gravitational field) distorts the xt spacetime as indicated in Figure 15.13*c*. If we imagine the spacetime coordinate system as a grid laid out on a rubber sheet, the gravitating matter stretches the sheet, and the particle moves from A to B along the most direct path in the curved spacetime.

It is convenient to define the *spacetime interval* ds, in effect the separation between two events (such as the particle passing through successive points) in two-dimensional spacetime, as

$$(ds)^2 = (c\,dt)^2 - (dx)^2 \tag{15.18}$$

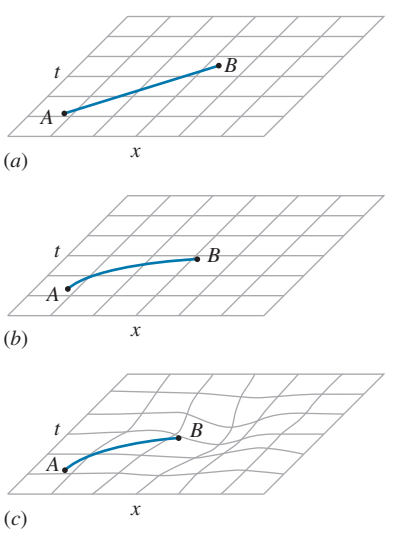

FIGURE 15.13 (*a*) The path through flat spacetime of a particle moving at constant velocity. (*b*) The path through flat spacetime of an accelerating particle. (*c*) The path of a particle through spacetime curved by matter.

This quantity is invariant under the Lorentz transformation, as you can prove by substituting dx' and dt' from Eq. 2.23. The trajectory of the particle in spacetime can be regarded as a collection of infinitesimal intervals. The particle is merely following the contour of spacetime, so the interval serves both to define the trajectory and to represent the shape of spacetime. The extension to three spatial dimensions gives an interval

$$(ds)^2 = (c\,dt)^2 - (dx)^2 - (dy)^2 - (dz)^2 \tag{15.19}$$

To characterize a "curved" four-dimensional spacetime, we might write the interval as

$$(ds)^2 = g_0(c\,dt)^2 - g_1(dx)^2 - g_2(dy)^2 - g_3(dz)^2 \tag{15.20}$$

where the four coefficients g_i describe the curvature of the spacetime and its deviation from a Euclidian nature (for which all $g_i = 1$).

The interval of Eq. 15.19 is characteristic of our familiar Euclidian space, which we call "flat." Figure 15.14 summarizes some of the characteristics of that space: a straight line is the shortest distance between two points, the sum of the angles of a triangle is 180°, parallel lines never meet, the ratio between the circumference and the diameter of a circle is π, and so forth.

Figure 15.15 shows a curved non-Euclidian geometry, the surface of a sphere. Here the shortest distance between points is an arc of a great circle, the sum of the angles of a triangle is greater than 180°, parallel lines can meet, and the ratio between the circumference and the diameter of a circle is less than π. The saddle-shaped geometry shown in Figure 15.16 has a different kind of curvature, in which the ratio between the circumference and the diameter of a circle is greater than π.

To appreciate the importance of curved spacetime, consider the experiment illustrated in Figure 15.17. A light beam is emitted by a source in the chamber and travels across the chamber to the opposite wall. If the chamber is in an inertial frame and free from gravitational fields, the beam travels horizontally across the chamber and strikes the opposite wall at the same height above the floor as the source. (This holds even if the chamber moves at constant velocity, as you can prove using special relativity.) Observers inside and outside the chamber agree on this conclusion.

If the chamber accelerates, the situation is different. Suppose the light is emitted when the chamber is at rest, relative to a particular inertial frame. The light beam then has no transverse component of velocity in this frame and moves horizontally. As the chamber accelerates, the light beam acquires no transverse velocity component, but the chamber's velocity increases. To the inertial observer, the beam travels along a horizontal straight line, but the chamber accelerates forward so that the beam strikes the opposite wall at a lower height than the source. To an observer in the chamber, the beam appears to follow the curved path shown in Figure 15.17*a* and strikes the wall at a lower height than the source.

According to the principle of equivalence, the observer in the chamber should record the same outcome if the chamber is at rest in a uniform gravitational field (Figure 15.17*b*). General relativity explains this observation through the curvature

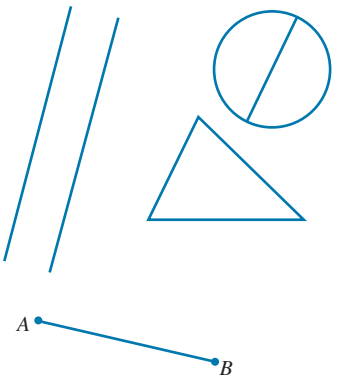

FIGURE 15.14 A flat space and its Euclidian geometrical properties.

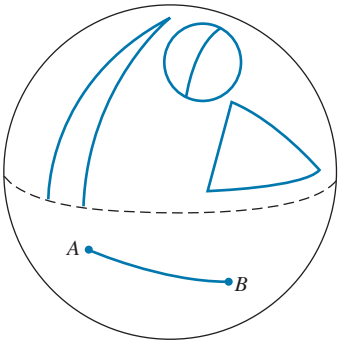

FIGURE 15.15 A curved space and its non-Euclidian geometrical properties.

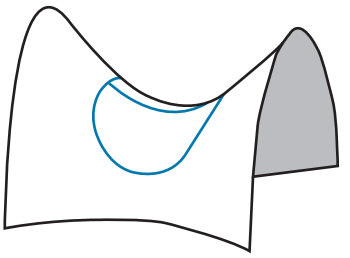

FIGURE 15.16 Another non-Euclidian curved space.

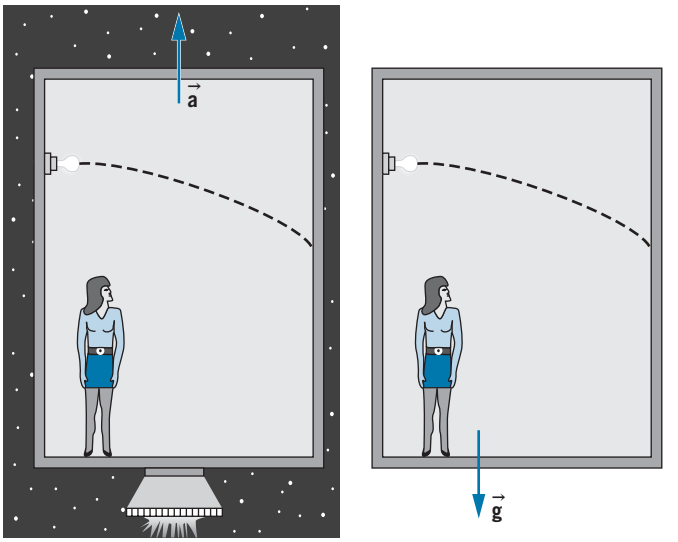

FIGURE 15.17 (*a*) According to an observer in an accelerating chamber, the light beam follows a curved path. (*b*) An observer at rest in a uniform gravitational field finds the same outcome.

of spacetime in the vicinity of the mass that is responsible for the gravitational field. The light beam is merely seeking out the shortest possible path in the curved spacetime, just like an ant crawling along a line on the spherical surface of Figure 15.15. All paths in the curved spacetime are curved.

It is tempting to seek an alternative explanation for the outcome shown in Figure 15.17*b*. For instance, we can assume each photon in the light beam to have an effective mass $m = E/c^2$ and then calculate its trajectory in the gravitational field as we would that of any classical particle of mass m. However, as we discuss in the next section, this method gives results that do not agree with observations for the path of photons in a gravitational field. The curvature of spacetime, which provides the correct explanation, is an inescapable consequence of the principle of equivalence.

General relativity gives a relationship between curvature and the density of mass and energy in space, which can be written symbolically as

$$\text{curvature of space} = \frac{8\pi G}{c^4}(\text{mass-energy density}) \tag{15.21}$$

Note that this expression incorporates gravitation (Newton's constant G) and special relativity (the speed of light c). If no matter or energy is present, the right-hand side is zero; as a result, the curvature is zero and space is flat. In the limit of classical kinematics ($c \to \infty$) and in the limit of weak gravitational fields ($G \to 0$), space is nearly flat and we can safely use the Newtonian gravitational theory. This is equivalent to saying that if we take a small enough region of the sphere of Figure 15.15, or if we increase its radius to a sufficiently large value,

the geometry is approximately Euclidian. Just as classical kinematics can be regarded as the limiting case of *special* relativity (for low speeds), so can classical gravitation be regarded as the limiting case of *general* relativity (for weak fields). In calculating the orbit of an Earth satellite or the trajectory of a space probe to Mars, Newton's theory gives entirely satisfactory results. Close to the Sun and to compact or massive stars, the curving of space can lead to observable effects, as we discuss in the next section.

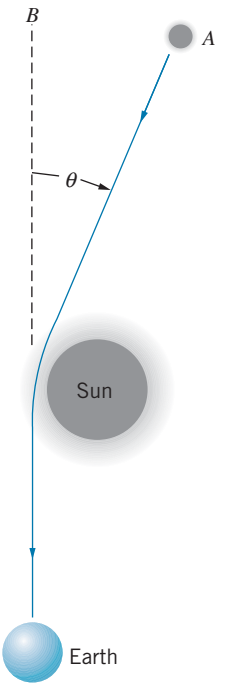

FIGURE 15.18 A light beam passing near the Sun is deflected. To an observer on Earth, the star at A appears to be at B.

15.5 TESTS OF GENERAL RELATIVITY

Newtonian gravitation and Einstein's general relativity each give predictions that can be tested against experiment, but under most circumstances the differences between the two predictions are extremely small. At the surface of the Earth, space is curved by only about 1 part in 10^9; even at the surface of the Sun, the curvature is only about 1 part in 10^6.

Nevertheless, there are experiments we can do that are precise enough to detect the difference between flat spacetime and curved spacetime. In this section we discuss several of these experiments.

Deflection of Starlight

When a beam of light from a star passes close to the Sun, it is deflected from its original direction, as shown in Figure 15.18. The star appears to be displaced from its true position by an angle θ.

It is possible to analyze this situation using Newtonian gravitation and special relativity by assigning the photons in the beam an effective mass $m = E/c^2$ and assuming them to be deflected by the Newtonian gravitational force. The experiment then looks very much like Rutherford scattering, and by analogy with the Rutherford scattering formula (see Problem 9) it is possible to calculate the deflection angle (in radians):

$$\theta = \frac{2GM}{Rc^2} \tag{15.22}$$

where M is the mass of the Sun and R is its radius. Substituting the numbers gives $\theta = 0.87''$ as the prediction of special relativity and Newtonian gravitation.

General relativity gives a different view. Spacetime in the vicinity of the Sun is curved, and the light beam is simply following the most direct path along the curved spacetime (Figure 15.19 is a two-dimensional representation of this effect). According to general relativity, the expected deflection is $1.74''$, exactly twice the value predicted by the Newtonian formula.

Measuring this effect requires the observation of a beam of light, such as from a star, that passes near the edge of the Sun. Starlight near the Sun can be observed only during a total solar eclipse. In 1919, just a few years after Einstein completed his general theory, two expeditions of British astronomers traveled to Africa and to South America to observe the solar eclipse and to measure the apparent changes in positions of stars whose light grazed the Sun. Their results for the deflection

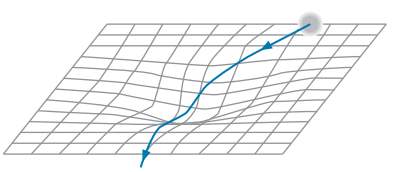

FIGURE 15.19 The path of a light beam from a star through curved spacetime.

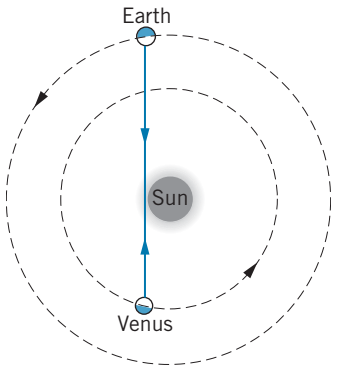

FIGURE 15.20 An electromagnetic signal travels between Earth and Venus at superior conjunction.

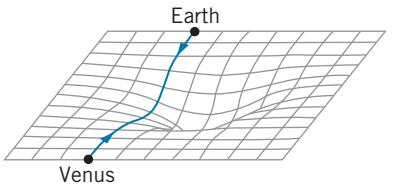

FIGURE 15.21 Path of signal between Earth and Venus in curved spacetime.

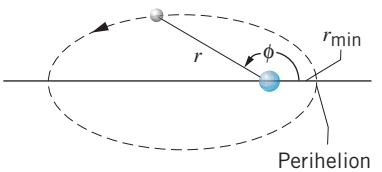

FIGURE 15.22 The elliptical orbit of a planet about a star.

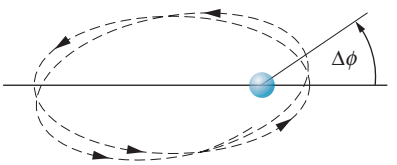

FIGURE 15.23 Precession of the perihelion (greatly exaggerated). After each orbit, the perihelion advances by an angle $\Delta\phi$.

angles, $1.98'' \pm 0.18''$ and $1.69'' \pm 0.45''$, gave strong support for the new general theory. In the years since those early results, this experiment has been repeated at nearly every total solar eclipse, and the overall agreement with general relativity is within 10%. Radio emission from quasars has also been used to confirm this effect, and here the agreement with general relativity is within 2%.

These experimental results give a clear distinction between Newtonian gravity (even with special relativity included) and general relativity.

Delay of Radar Echoes

When a line joining Earth and another planet (Venus, for example) passes through the Sun, the situation is known as "superior conjunction" and is illustrated in Figure 15.20. Based on the orbits of Earth and Venus, we can calculate how long it takes a radar signal sent from Earth to be reflected from Venus and return to Earth (about 20 minutes). Near superior conjunction, the signal passes close to the Sun, and therefore, according to general relativity, it does not travel in a Euclidian straight line, but instead follows a path through curved spacetime (Figure 15.21). It therefore takes the signal a bit longer than the expected time to make the round trip (think of the time intervals as extended as the beam passes close to the Sun, thus lengthening the time to travel the path). This time delay is expected to be about 10^{-4} s, and it has been confirmed to within a few percent (the limit on precision being uncertainties in the surface of Venus, since we don't know if the signal is being reflected from a mountain or a valley). More precise experiments were done in the late 1970s using a signal sent between Earth and the Viking landers on Mars. In this case, the result was consistent with general relativity to within about 0.1%. Signals from NASA's Cassini spacecraft, which entered orbit around Saturn in 2004, have provided the most sensitive test of the time delay, agreeing with the predictions of general relativity to within 0.002%.

Precession of Perihelion of Mercury

Consider a simple planetary system, shown in Figure 15.22, consisting of a single planet in orbit about a star of mass M such as the Sun. According to Newtonian gravitation, the orbit is a perfect ellipse with the star at one focus. The equation of the ellipse is

$$r = r_{\text{min}} \frac{1 + e}{1 + e\cos\phi} \tag{15.23}$$

where r_{min} is the minimum distance between planet and star and e is the *eccentricity* of the orbit (the degree to which the ellipse is noncircular; $e = 0$ for a circle). When $r = r_{\text{min}}$, the planet is said to be at *perihelion*; this occurs regularly, at exactly the same point in space, whenever $\phi = 0, 2\pi, 4\pi, \ldots$. According to general relativity, the orbit is not quite a closed ellipse; the curved spacetime near the star causes the perihelion direction to *precess* somewhat, as shown in Figure 15.23. After completing one orbit, the planet returns to r_{min}, but at a slightly different ϕ. The difference $\Delta\phi$ can be computed from general relativity, according to which the orbit is

$$r = r_{\text{min}} \frac{1 + e}{1 + e\cos(\phi - \Delta\phi)} \tag{15.24}$$

where

$$\Delta\phi = \frac{6\pi GM}{c^2 r_{\min}(1+e)} \tag{15.25}$$

For the Sun, $6\pi GM/c^2 = 27.80\,\text{km}$, and thus even for the smallest value of $r_{\min}$ (for Mercury, 46×10^6 km) $\Delta\phi$ is of order 10^{-6} rad, an extremely small quantity. However, this effect is *cumulative*; that is, it builds up orbit after orbit, and after N orbits, the perihelion has advanced by $N\Delta\phi$. We usually express this precession in terms of the total precession per century (per 100 Earth years), and some representative values are shown in Table 15.1.

The expected precessions are very small, of the order of seconds of arc per century, but nevertheless have been measured with great accuracy; for the three planets closest to the Sun, and for the asteroid Icarus, the measured values are in agreement with the predictions of general relativity. In the best case, the agreement is within about 1%.

These experiments are very difficult to do because (except for Mercury and Icarus) the eccentricities are small and locating the perihelion is difficult. A more serious problem is that other effects, not associated with general relativity, also cause an apparent precession of the perihelion. In the case of Mercury, the observed precession is actually about 5601″ per century; of that, 5026″ are due to the precession of the Earth's equinox (a classical Newtonian effect of the spinning Earth) and 532″ are due to the gravitational pull of the other planets on Mercury (also a classical Newtonian effect). Only the difference of 43″ is due to general relativity.

Gravitational Radiation

Just as an accelerated charge emits electromagnetic radiation that travels with the speed of light, an accelerated mass emits gravitational radiation that also travels with the speed of light. In effect, gravity waves are ripples that travel through spacetime. Waves produced by such motions as the planets around the Sun are exceedingly weak and beyond any hope of detection. Cataclysmic events in the universe, such as supernova explosions, and highly accelerated systems, such as compact binary objects, may produce observable gravitational waves. Detection

TABLE 15.1 Precession of Perihelia

Planet	N (orbits per century)	e	$r_{\min}$ (10^6km)	$N\Delta\phi$ (arc seconds per century)	
				General Relativity	Observed
Mercury	415.2	0.206	46.0	43.0	43.1 ± 0.5
Venus	162.5	0.0068	107.5	8.6	8.4 ± 4.8
Earth	100.0	0.017	147.1	3.8	5.0 ± 1.2
Mars	53.2	0.093	206.7	1.4	
Jupiter	8.43	0.048	740.9	0.06	
Icarus	89.3	0.827	27.9	10.0	9.8 ± 0.8

of these waves would provide another important confirmation of the general relativity theory.

In analogy with the effect of a passing electromagnetic wave on a charge, a passing gravitational wave could be detected by its effect on matter. Several antennas have been built to search for gravity waves, but no conclusive experimental evidence has yet been obtained. Indirect evidence has come from the observations of the change in the orbital period of a binary pulsar (see next section). Interferometric techniques are being used to build new detectors to search for gravity waves. The Laser Interferometer Gravitational-wave Observatory (LIGO), which began operation in 2001, consists of two installations (located in the states of Washington and Louisiana) whose interferometer arms are 4 km in length. A passing gravitational wave would cause a small change in the length of one arm relative to the other, which would be detected through a change in the fringe pattern similar to that of the Michelson interferometer (Section 2.2).

15.6 STELLAR EVOLUTION AND BLACK HOLES

Although the large gravitational field of the Sun has provided several good tests of general relativity, the most stringent tests will come from measurements in even larger gravitational fields, where the curvature of spacetime is significantly greater. Such large gravitational fields can occur following the collapse of a star into a more compact object: a white dwarf, a neutron star, or a black hole.

We considered the collapse of an ordinary star like the Sun to a white dwarf star as an example of the application of Fermi-Dirac statistics in Section 10.7. As the supply of hydrogen fuel in a star begins to be used up, the star will contract because the radiation pressure that opposes gravitational collapse is reduced. Eventually the stable white dwarf stage can be reached, at which the Pauli principle applied to the electrons prevents further collapse. The average density of a white dwarf star such as Sirius B is about $10^9\ \text{kg/m}^3$, which is about 10^6 times the average density of the Sun.

If the star has a mass greater than about 1.4 solar masses (the *Chandrasekhar limit*), the gravitational force is sufficient to overcome the Pauli repulsion of the electrons, and further collapse can occur. For a star of this mass, the Fermi energy of the electrons (Eq. 10.50) is 0.30 MeV. Higher-energy electrons in the tail of the Fermi-Dirac distribution will have sufficient energy to produce the inverse beta-decay reaction:

$$e^- + p \rightarrow n + \nu_e$$

for which the threshold energy is 0.782 MeV, not too far above E_F. This reaction removes some electrons from the star, reducing the effects of Pauli repulsion, and allowing the star to collapse a bit. The Fermi energy *increases*, pushing more electrons above the 0.782-MeV threshold, resulting in more electrons being lost, and so on, until all (or very nearly all) of the electrons vanish. The star is now composed of neutrons, instead of protons and electrons. The Pauli repulsion of the

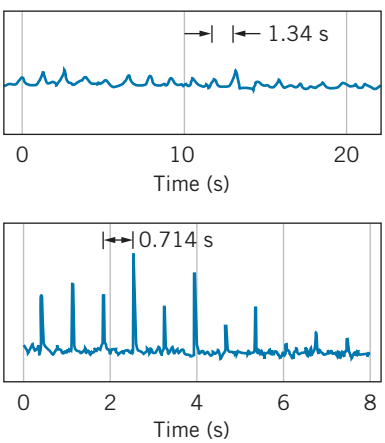

FIGURE 15.24 The radio signals from two different pulsars. The top signal is the record of the first pulsar discovered.

electrons no longer can oppose gravitational collapse, and so the star contracts until the Pauli principle applied to the *neutrons* (which also obey Fermi-Dirac statistics) prevents further collapse. As we calculated in Section 10.7, a neutron star of 1.5 solar masses would have a radius of 11 km and a density of about 5×10^{17} kg/m^3.

Are these neutron stars merely figments of the physicist's imagination or do they really exist? In 1967, radio astronomers at Cambridge University discovered an unusual signal among their observations—a regular pulsation, such as is shown in Figure 15.24, with a period of 1.34 s. No previously known astronomical object could produce such sharp and regular pulses, and at first the Cambridge group suspected that they might have discovered signals from an extraterrestrial intelligent civilization. (The object emitting the pulses was at first called LGM-1; LGM stands for "Little Green Men.") This notion was later discarded (unfortunately) and the object became known as a *pulsar.* Since 1967, hundreds of other pulsars have been discovered; all have extremely regular periods typically in the range 0.01–1 s.

The connection between pulsars and neutron stars was made soon after their discovery. The collapse of a rotating star to a neutron star causes the neutron star to rotate much more rapidly. Angular momentum is conserved during the collapse (see Problem 11), so the rotational angular velocity increases as the rotational inertia decreases. A relatively slow rotation rate of the original star can become a very rapid rotation rate for the neutron star.

The intense magnetic field of such a rapidly rotating object traps any emitted charged particles and accelerates them to high speeds, especially near the magnetic poles, where they give off radiation (Figure 15.25). As the star rotates, this beam of emitted radiation sweeps around like a searchlight or a lighthouse, and we see a pulse of radiation whenever the beam sweeps through the Earth. The observed interval between the pulses is, according to this interpretation, the rotational period of the neutron star.

If this explanation of a pulsar as a rotating neutron star is correct, we ought to see the pulsars slowing down somewhat, as the radiated energy is compensated by a decrease in the neutron star's rotational kinetic energy. This effect has been seen for nearly all pulsars, and amounts to about 1 part in 10^9 per day.

Pulsars have now been observed at many different wavelengths (optical, X ray, γ ray, radio) and with such great precision of timing that the slowing down of 10^{-9} per day is easily observable.

Although the exact mechanism of the collapse of a star to a neutron star is not yet understood, we suspect that the violent explosions known as *supernovas* leave a neutron star as a remnant. In 1054, Chinese astronomers observed a supernova explosion (which they called a "guest star") that was visible in the daytime over many days. Today we see the expanding shell of that explosion as the Crab Nebula (Figure 15.26). At the center of the Crab Nebula is a pulsar, rotating with a frequency of 30 Hz. It is remarkable that none of the many photographs of the Crab that were taken before 1967 revealed this pulsar blinking on and off every 0.033 s; all of these photographs were taken over long exposure times, and so the pulsations were not observable. When careful measures are taken, however, the blinking effect can be seen quite clearly (Figure 15.27). This suggests that, at least in this instance, pulsars may be identified as supernova remnants.

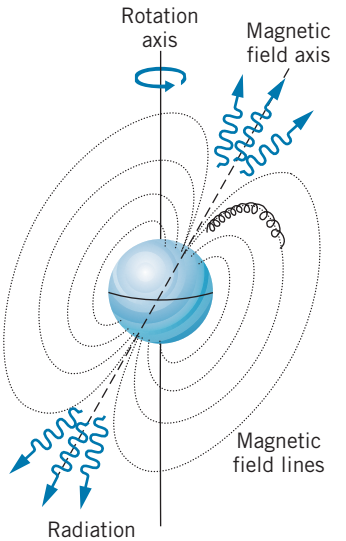

FIGURE 15.25 Charged particles trapped by the magnetic field lines of a neutron star are given large accelerations near the magnetic poles, from which a directional radiation beam emerges. If this radiation beam intercepts the Earth as the neutron star rotates, we see it as a pulse of radiation.

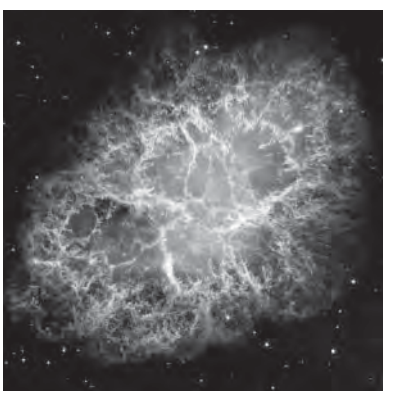

FIGURE 15.26 The Crab Nebula, remnant of a supernova observed in the year 1054.

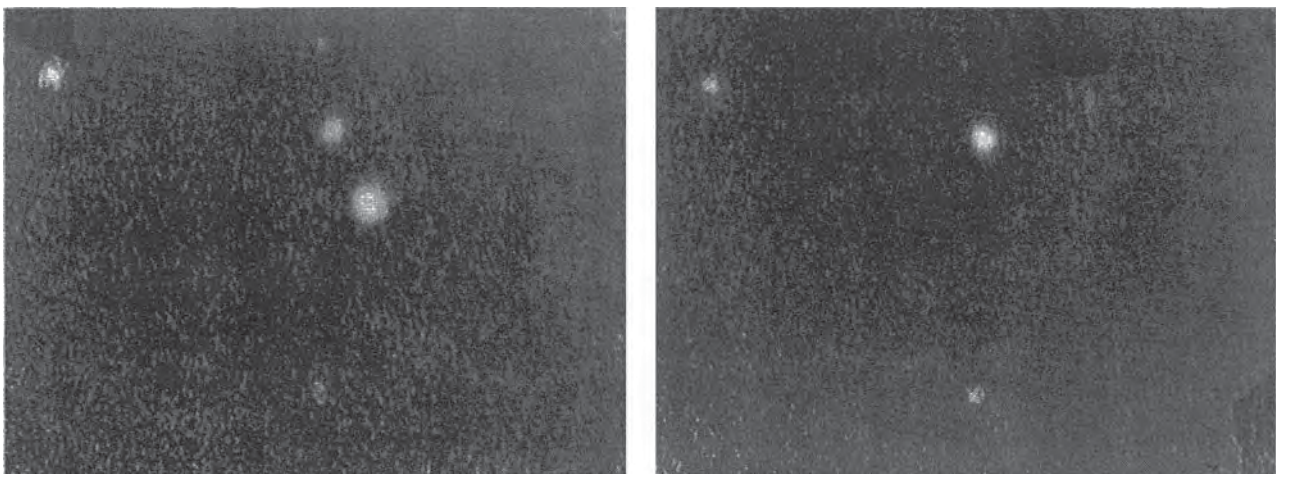

FIGURE 15.27 The visible pulsar of the Crab Nebula. The two exposures show the pulsar blinking on and off relative to the other stars in the photograph.

A Binary Pulsar

In 1974, an unusual pulsar was discovered. The period of the pulsar was measured to be 59 ms, making it among the fastest observed up to that time. More surprising, the pulse rate appeared to be slowing down by about 0.1% per hour, but later was observed to be *increasing* by about the same amount. It was quickly realized that the decrease and increase of the pulse rate could be explained as a Doppler shift if the neutron star were moving first away from and later toward the Earth. To move in this way, the pulsar must be in orbit around an unseen companion. Thus we have a pulsar as part of a binary star system, or a "binary pulsar."

The orbital period of the binary system was determined to be about 8 hours. This is an extremely short period; for example, it is more than 250 times shorter than the orbital period of Mercury, the fastest moving planet in our solar system. To have such a short orbital period, the pulsar must be orbiting very close to its companion (which is believed to be another neutron star). At such close distances, the curvature of spacetime is large and the effects of general relativity should be measurable. In effect, the binary pulsar provides us with a "general relativity laboratory."

Among the general relativity effects that have been observed in the binary pulsar system is the delay of the pulses due to the curvature of spacetime. This situation is similar to Figures 15.20 and 15.21, except that the pulsar (instead of Venus) is the origin of the signals and the curvature is due to the companion star (instead of the Sun). An effect analogous to the precession of Mercury's perihelion has also been observed (except that, in the case of a star, the point of closest approach is called *periastron* rather than perihelion). The periastron of the binary pulsar changes by 4.23° per year, about 35,000 times more rapidly than that of Mercury; the change of the periastron is known to an accuracy of about 1 part in 10^5, three orders of magnitude more precisely than Mercury's.

The most remarkable observation from the binary pulsar is the slowing of its orbital period, which general relativity explains as caused by the emission of gravitational radiation. Because of its large centripetal acceleration (its orbital

speed is about $0.001c$), the binary pulsar should emit gravity waves, and the energy radiated away is compensated by a loss in the orbital energy. This loss amounts of $76\,\mu$s per year or 67 ns per orbit, and the measured change in the orbital rate confirmed the prediction of general relativity to within 1%. In the absence of direct observation, this is the strongest evidence yet obtained for the existence of gravitational radiation. For the discovery of the binary pulsar and its contributions to the study of gravitation, Joseph Taylor and Russell Hulse were awarded the 1993 Nobel Prize in physics.

Black Holes

A neutron star is not the ultimate fate of the collapse of massive stars. Stars with masses less than two or three solar masses probably do end up as white dwarf stars or neutron stars. For more massive stars, the gravitational force is strong enough to overcome even the Pauli principle applied to the neutrons, and there is nothing to prevent the material in the star from suffering complete collapse down to a single point in space. To understand gravitational collapse, we must turn again to general relativity.

Within a year after Einstein's 1916 publication of the general theory, Karl Schwarzschild worked out the solutions to the equations for the curvature of spacetime near a spherically symmetric mass M. In spherical coordinates (r, θ, ϕ), the spacetime interval for this solution is

$$(ds)^2 = c^2\left[1 - \frac{2GM}{c^2 r}\right](dt)^2 - \frac{(dr)^2}{\left[1 - \dfrac{2GM}{c^2 r}\right]} - r^2(d\theta)^2 - r^2\sin^2\theta(d\phi)^2 \tag{15.26}$$

(Note that in the classical and zero-gravity limits $c \to \infty$ and $G \to 0$, the two factors in square brackets disappear, leaving us with an interval in spherical coordinates that is the exact analog of the three-dimensional interval expressed in Cartesian coordinates, Eq. 15.19.) The radial part of this solution (the dr term) has what appears to be a serious problem: the factor in the denominator can become zero for a particular r, causing that term in the equation to "blow up." This occurs when r has the value

$$r_S = \frac{2GM}{c^2} \tag{15.27}$$

which is known as the *Schwarzschild radius.* None of the physical coordinates actually "blows up" at $r = r_S$, and an object falling toward M would notice no change in its motion as it crossed the Schwarzschild radius.

For external observers watching the falling object, the situation is very different. As the object falls, general relativity predicts that its clocks would appear to run ever more slowly, stopping completely when the object reaches r_S. The object appears to be frozen forever at that location! While the object is falling, the light it emits becomes increasingly red shifted, and the red shift becomes infinite at $r = r_S$, so the object disappears from view! The outside observer can obtain no information about the object once it passes through the Schwarzschild radius. For that reason, the Schwarzschild radius is often called the *event horizon*; no external observer can see into that horizon.

The falling object does encounter one crisis at r_S. At any time before crossing r_S, the object could reverse its fall and escape from the gravitational pull of M—for example, by firing its rockets. Once it passes r_S, no escape is possible. Inside r_S, the escape speed exceeds the speed of light, and nothing (*not even light*) can escape. No travel or communication is permitted from inside r_S to the outside world. However, the object inside r_S can continue to exert a gravitational force on external objects or, in the language of general relativity, to curve spacetime beyond r_S.

An object whose mass M lies totally within the corresponding radius r_S is said to be a *black hole.* To form such an object requires that matter be compressed to exceptional densities. Table 15.2 shows some values of r_S for representative objects. For the Earth to become a black hole, we would need to compress it into a sphere of radius less than 1 cm, and the Sun would become a black hole only if compressed to a 3-km radius! Nevertheless, it has been speculated that black holes are the end products of the collapse of massive stars, and that tiny (atom-sized) black holes may have been formed by the extreme densities and pressures in the early universe.

Far from a black hole, the gravitational field is Newtonian in character; the effects of curved spacetime are small, and the black hole cannot be distinguished from any other gravitating object. Close to a black hole (or close to any massive, compact object), the effects of curved spacetime can become significant. The discovery of a massive black hole could therefore provide another "laboratory" for testing the predictions of general relativity where the effects may be substantially larger than in the vicinity of the Sun.

Many stars are members of binary systems, in which two stars orbit about their common center of mass. In many cases, a visible star appears to orbit with an invisible companion, and gases from the visible star emit intense X rays as they are accelerated toward the invisible companion. It is believed that these invisible companions in binary systems are black holes. Many such systems have been observed in our galaxy.

By observing the rotational motion of galaxies, it is possible to deduce the mass at the galactic center. For some galaxies, this mass turns out to be greater than 10^9 times the mass of the Sun. No known phenomenon other than a black hole permits so much mass to be concentrated in so small a region. Similar evidence derived from rotational motions suggests that even our near neighbor,

TABLE 15.2 Black Hole Event Horizons

Object	Mass (kg)	Ordinary Radius (m)	r_S (m)
^{238}U nucleus	4×10^{-25}	7×10^{-15}	6×10^{-52}
Physics book	1	0.1	1.5×10^{-27}
Earth	6×10^{24}	6×10^{6}	8.9×10^{-3}
Sun	2×10^{30}	7×10^{8}	3×10^{3}
Galaxy	$\sim 2 \times 10^{41}$	$\sim 10^{20}$	3×10^{14}
Universe	$\sim 10^{51}$	10^{26}(?)	$\sim 10^{24}$

the Andromeda galaxy, has a black hole of a few million solar masses at its center. Radio emissions from the center of our own Milky Way galaxy also suggest a black hole of a few million solar masses.

A surprising development in black hole theory occurred in 1974, when Steven Hawking showed that black holes could be sources of particle emission. According to quantum mechanics, particle-antiparticle pairs can spontaneously appear, as long as they exist for a short enough time that the uncertainty principle is not violated. That is, the particles can "borrow" an energy of $2mc^2$ as long as the loan is repaid (the particles vanish) within a time of at most $\Delta t \sim \hbar/2mc^2$. If a particle-antiparticle pair arises outside the event horizon of a black hole, its gravitational field can provide the energy necessary to repay the loan so that the particle and antiparticle can become real. Usually the particle and antiparticle fall back into the black hole, restoring the energy balance. However, one of the members of the pair may have enough energy to escape into the outside world. The black hole thus appears to be emitting particles. In the process, the black hole loses mass. The rate of mass loss is inversely proportional to the mass of the black hole; massive black holes that result from the collapse of stars emit particles at too low a rate to be observed. However, tiny black holes of atomic or nuclear size, which may have been formed in the early evolution of the universe, could be very bright sources of radiation.

Black holes provide both a fertile area for theoretical speculation and a challenge for the skill of experimenters. It has been suggested that material that falls into a black hole reappears at another time and place in the universe, or perhaps in another universe. Thus a black hole, if this speculation is correct, could be used for time travel or to travel between different universes. Other proposals suggest harnessing a black hole as an energy source. It has been estimated that, if black holes are indeed the end products of the evolution of massive stars, there could be as many as 10^9 massive black holes in our galaxy, which makes it likely that many black holes are within our observational reach. Or, perhaps we will someday observe a minihole ending its existence with a burst of radiation. As we continue to refine our ability to study the skies at visible, X-ray, and γ-ray wavelengths, black holes will figure prominently in our investigations.

15.7 COSMOLOGY AND GENERAL RELATIVITY

General relativity can be applied to calculate the properties of the universe as a whole. For this case, the mass-energy density term in Eq. 15.21 must describe the entire universe. We are not interested in the "local" variations in density on a scale of galactic size, but rather in the average density of the entire universe, evaluated over a distance that is large compared with the spacing between galaxies. (In a similar way, when we speak of the density of a solid we are interested not in the variations on the atomic scale but rather in the average density of the entire material, evaluated over a distance that is large compared with the spacing between atoms.) The density of the universe is not a constant; it changes with time as the universe expands.

Solving the equations of general relativity for the large-scale structure of the universe gives the following result, which is known as the Friedmann equation:

$$\left(\frac{dR}{dt}\right)^2 = \frac{8\pi}{3}G\rho R^2 - kc^2 \tag{15.28}$$

Here $R(t)$ represents the size or distance scale factor of the universe at time t, and ρ represents the total mass-energy density at the same time. (The density is expressed in mass units, such as kg/m^3, even if it represents radiation.)

The constant k that appears in Eq. 15.28 specifies the overall geometrical structure of the universe: $k = 0$ if the universe is flat, like Figure 15.14; $k = +1$ if the universe is curved and closed, like Figure 15.15; $k = -1$ if the universe is curved and open, like Figure 15.16. When $k = +1$, the distance factor $R(t)$ is directly related to the size or "radius" of the universe, but its meaning is not so apparent when $k = 0$ or $k = -1$, because in both of the latter cases the universe is infinite in extent. In these cases $R(t)$ should be regarded as a scale factor that represents the expansion of space; the absolute magnitude of R in this case is not significant, and only its variation with time is of interest, because any particular length (such as the distance between two galaxies) will vary with time just as R does.

To solve Eq. 15.28, we must therefore specify the constant k. On the large scale, our universe seems quite close to being flat (as we discuss in Section 15.10), and we therefore take $k = 0$. This simplifies the mathematics and gives results that are not too far different from what we obtain with $k = \pm 1$, so for rough estimates our calculation should be acceptable.

The density ρ in Eq. 15.28 must include both the matter and the radiation present in the universe. The present universe is dominated by matter; the contribution of radiation to the total density is negligible. As the universe expands, the amount of matter remains constant but the volume increases like R^3. Thus the matter density ρ_m decreases with increasing R according to $\rho_m \propto R^{-3}$. Putting this result into Eq. 15.28 and integrating, we find

$$R(t) = At^{2/3} \tag{15.29}$$

where A is a constant. Using this result to eliminate R from Eq. 15.28, we obtain

$$t = \frac{1}{\sqrt{6\pi G\rho_m}} \tag{15.30}$$

In contrast, the early universe was dominated by radiation; the mass density of the matter was negligible. From Eq. 10.42 we see that the energy density of the radiation depends on $d\lambda/\lambda^5$. All wavelengths scale with R, so we have $d\lambda \propto R$ and $\lambda^5 \propto R^5$. Thus the energy density of radiation ρ_r decreases with increasing R according to $\rho_r \propto R^{-4}$. Inserting this result into Eq. 15.28 and integrating, we obtain

$$R(t) = A't^{1/2} \tag{15.31}$$

where A' is a constant, and so

$$t = \sqrt{\frac{3}{32\pi G\rho_r}} \tag{15.32}$$

The Hubble parameter can be defined in terms of the time variation of the scale factor:

$$H = \frac{1}{R}\frac{dR}{dt} \tag{15.33}$$

As the universe evolves, the value of H changes. Its present value H_0 is revealed in experiments with Hubble's law (Eq. 15.2).

If the universe has been expanding at a constant rate ($R \propto t$), then H^{-1} is the age of the universe. In the two cases we derived above, the age is less than H^{-1}. A matter-dominated universe expanding since $t = 0$ has an age of $\frac{2}{3}H^{-1}$, while a radiation-dominated universe has an age of $\frac{1}{2}H^{-1}$. In either case we can take H^{-1} as a rough measure of the age at any time.

We can therefore characterize the universe by several parameters: a shape parameter k, which describes whether it is flat or curved, open or closed; a radius or scale parameter $R(t)$, which measures the size of the universe as a function of time; the density ρ, which represents both matter and energy, and which is also a function of time; the Hubble parameter H, which is proportional to the rate of expansion; and also a deceleration parameter q, which tells us the rate at which the expansion is slowing down (see Problem 12). The challenge to the observational astronomer is to obtain data on the distribution and motion of the stars and galaxies that can be analyzed to obtain values for these parameters.

15.8 THE BIG BANG COSMOLOGY

The present universe is characterized by a relatively low temperature and a low density of particles. Its structure and evolution are dominated by the gravitational force. Because the universe has been expanding and cooling, in the distant past it must have been characterized by a higher temperature and a greater density of particles. Let us imagine we could run the cosmic clock backward and examine the universe at earlier times, even before the formation of stars and galaxies. At some point in its history, the temperature of the universe must have been high enough to ionize atoms; at that time the universe consisted of a plasma of electrons and positive ions, and the electromagnetic force was important in determining the structure of the universe. At still earlier times, the temperature was hot enough that collisions between the ions would have knocked loose individual nucleons, so the universe consisted of electrons, protons, and neutrons, along with radiation. In this era the strong nuclear force was important in determining the evolution of the universe. At still earlier times the weak interaction played a significant role.

If we try to go back still further, we reach a time when the matter of the universe consisted only of quarks and leptons. Because we have never observed a free quark, we don't know much about their individual interactions, and so we can't describe this very early state of the universe. If someday we are able to understand the interactions of free quarks, we can penetrate this barrier and look to still earlier times. Eventually we reach a fundamental barrier when the universe had an age of only 10^{-43} s, which is known as the *Planck time* (see Problem 26). Before this time, quantum theory and gravity are hopelessly intertwined, and none of our present theories gives us any clue about the structure of the universe.

Later than the Planck time, but still before the condensation of bulk matter, the universe consisted of particles, antiparticles, and radiation in approximate thermal

equilibrium at temperature T. The universe at this time was radiation-dominated: the energy density of the radiation exceeded the energy density of the matter. In a radiation-dominated universe, we can use Eq. 15.32 to find a relationship between the temperature and the age. Inserting the radiation density from Eq. 15.9, remembering to convert to mass units such that $\rho_r = U/c^2$, and evaluating all numerical factors, we obtain

$$T = \frac{1.5 \times 10^{10}\ \text{s}^{1/2} \cdot \text{K}}{t^{1/2}} \tag{15.34}$$

where the temperature T is in K and the time t is in seconds. This equation relates the age of the early universe to its temperature.

The radiation of the early universe consisted of high-energy photons, whose average energy at the temperature T can be roughly estimated as kT, where k is the Boltzmann constant. The interactions between the radiation and the matter can be represented by two processes:

$$\text{photons} \rightarrow \text{particle} + \text{antiparticle}$$
$$\text{particle} + \text{antiparticle} \rightarrow \text{photons}$$

That is, photons can engage in pair production, in which their energy becomes the rest energy of a particle-antiparticle pair, or a particle and antiparticle can annihilate into photons. In each case, the energy of the photons must be at least as large as the rest energy of the particle and antiparticle.

Example 15.2

(*a*) At what temperature is the thermal radiation in the universe energetic enough to produce nucleons and antinucleons? (*b*) What is the age of the universe when it cools to that temperature?

Solution

(*a*) Let us consider the formation of proton-antiproton or neutron-antineutron pairs by photons:

$$\gamma + \gamma \rightarrow \text{p} + \overline{\text{p}} \quad \text{and} \quad \gamma + \gamma \rightarrow \text{n} + \overline{\text{n}}$$

To produce these reactions, the photons must have an energy at least as great as the nucleon rest energy, or about 940 MeV. The temperature of the photons must then be

$$T = \frac{E}{k} = \frac{mc^2}{k}$$
$$= \frac{940\ \text{MeV}}{8.6 \times 10^{-5}\ \text{eV/K}} = 1.1 \times 10^{13}\ \text{K}$$

(*b*) From Eq. 15.34 we can find the age of the universe when the photons have this temperature:

$$t = \left(\frac{1.5 \times 10^{10}\ \text{s}^{1/2} \cdot \text{K}}{T}\right)^2$$
$$= \left(\frac{1.5 \times 10^{10}\ \text{s}^{1/2} \cdot \text{K}}{1.1 \times 10^{13}\ \text{K}}\right)^2 = 2 \times 10^{-6}\ \text{s}$$

That is, at times earlier than 2 μs, the universe was hot enough for the photons to produce nucleon-antinucleon pairs, but after 2 μs the photons were not energetic enough to produce nucleon-antinucleon pairs. The annihilation reaction continues to occur, but after this time nucleon-antinucleon pair production ceases.

In this calculation we are using average photon energies as estimates. Photons in the tail of the thermal spectrum are sufficiently energetic to produce nucleon-antinucleon pairs even after 2 μs, but *on the average* the photons have too little energy. More precisely, we could state that the rate of nucleon-antinucleon pair production drops rapidly at around 2 μs and becomes negligible at times much greater than 2 μs.

Let us now look at some of the major developments in the evolution of the universe.

$t = 10^{-6}$ s We begin the story at a time of 1 μs. From Eq. 15.34 we find $T = 1.5 \times 10^{13}$ K or $kT = 1300$ MeV. The scale factor is smaller than that of the present universe by the red shift, $2.7\,\text{K}/1.5 \times 10^{13}\,\text{K} = 1.8 \times 10^{-13}$. If the universe were closed and finite, its radius would be smaller than the present observable radius (10^{26} m) by this factor, so the universe at that time is about the present size of the solar system (10^{13} m). At 1 μs, the universe consists of p, $\overline{\text{p}}$, n, $\overline{\text{n}}$, e^-, e^+, μ^-, μ^+, π^0, π^-, π^+, and perhaps other particles, plus photons, neutrinos, and antineutrinos. Because both pair production and annihilation can occur, the number of particles is roughly equal to the number of antiparticles for each species. Furthermore, the number of photons is roughly equal to the number of nucleons, which is in turn roughly equal to the number of electrons. The relative number of neutrons and protons is determined by three factors:

1. *The Boltzmann factor* $e^{-\Delta E/kT}$. Protons have less rest energy than neutrons, so there are more of them at any given temperature. The energy difference ΔE is $(m_\text{n} - m_\text{p})c^2 = 1.3$ MeV, so the neutron-to-proton ratio can be expressed as $e^{-1.5\times10^{10}/T}$ with T in Kelvins. For $T \sim 10^{13}$ K, this ratio is very nearly 1, but it becomes different from 1 as T approaches 10^{10} K.
2. *Nuclear reactions.* Reactions such as $\text{n} + \nu_\text{e} \rightleftarrows \text{p} + \text{e}^-$ and $\text{n} + \text{e}^+ \rightleftarrows \text{p} + \overline{\nu}_\text{e}$ can go in either direction and tend to make it easy for protons to turn into neutrons or neutrons into protons, as long as there are plenty of e^-, e^+, ν_e, and $\overline{\nu}_\text{e}$ around.
3. *Neutron decay.* The neutron half-life is about 10 min, which is going to be important only at later times. For $t < 1$ s, there has not yet been enough time for an appreciable number of neutrons to decay.

At $t = 1$ μs, all three of these factors keep the neutron-to-proton ratio very close to 1.

$t = 10^{-2}$ s Between 10^{-6} s and 10^{-2} s, the temperature drops from 1.5×10^{13} K ($kT = 1300$ MeV) to 1.5×10^{11} K ($kT = 13$ MeV), and the distance scale factor increases by a factor of 100. The photons have on the average too little energy (13 MeV) to produce pions and muons, and because the pion and muon lifetimes are much shorter than 10^{-2} s, they have decayed into electrons, positrons, and neutrinos. Pair production of nucleons and antinucleons no longer occurs, but nucleon-antinucleon annihilation continues. As we discuss later, there is very slight imbalance of matter over antimatter of perhaps 1 part in 10^9. During this interval, all of the antimatter and most (99.9999999%) of the matter is annihilated. Pair production of electrons and positrons can still occur, so the universe consists of p, n, e^-, e^+, photons, and neutrinos. The neutron-to-proton ratio remains about 1.

$t = 1$ s Between 10^{-2} s and 1 s, the temperature drops to 1.5×10^{10} K ($kT = 1.3$ MeV). In this interval, the Boltzmann factor, which determines the neutron-to-proton ratio, becomes different from 1; by $t = 1$ s, the nucleons consist of about 73% protons and 27% neutrons. During this period, the influence of the neutrinos has been decreasing; to convert a proton to a neutron by capturing an antineutrino

($\bar{\nu}_e + p \rightarrow n + e^+$) requires an antineutrino of at least 1.8 MeV, above the mean neutrino energy (1.3 MeV) at this temperature. This begins the time of "neutrino decoupling," when the interactions of matter and primordial neutrinos no longer occur. From this time on, the neutrinos continue to fill the universe, cooling along with the expansion of the universe. These primordial neutrinos presently have roughly the same density as the microwave photons, but a slightly lower temperature (about 2 K).

***t* = 6 s** Between 1 s and 6 s ($T = 6 \times 10^9$ K or $kT = 0.5$ MeV), the average photon energy decreases and becomes insufficient to produce electron-positron pairs. Electron-positron annihilation continues, and as a result all of the positrons and nearly all (99.9999999%) of the electrons are annihilated. The electrons have too little energy to convert protons to neutrons ($e^- + p \rightarrow n + \nu_e$ no longer occurs), and so the only remaining weak interaction process that influences the relative number of protons and neutrons is the radioactive decay of the neutron, which has a half-life of 10 minutes and so has not appreciably occurred by this time. The nucleons are now about 84% protons and 16% neutrons, or about 5 times as many protons as neutrons.

The composition of the universe after $t = 6$ s consists of some number N protons, the same number N electrons, and about $0.2N$ neutrons. There are no remaining positrons or antinucleons. Because particle-antiparticle annihilation has substantially reduced the number of nucleons while the number of photons remained stable, there are about $10^9 N$ photons (and about the same number of neutrinos).

Example 15.3

Estimate the relative number of neutrons and protons among the nucleons at $t = 1$ s.

Solution

At this time, the temperature is 1.5×10^{10} K. The neutron-to-proton ratio is determined by the Boltzmann factor, $e^{-\Delta E/kT}$, where ΔE is the neutron-proton rest energy difference. The exponent in the Boltzmann factor is

$$\frac{\Delta E}{kT} = \frac{1.3\ \text{MeV}}{(8.62 \times 10^{-5}\ \text{eV/K})(1.5 \times 10^{10}\ \text{K})} = 1.0$$

so the ratio of neutrons to protons is

$$\frac{N_n}{N_p} = e^{-\Delta E/kT} = e^{-1.0} = 0.37$$

The relative number of protons is then

$$\frac{N_p}{N_p + N_n} = \frac{1}{1 + N_n/N_p} = \frac{1}{1 + 0.37} = 0.73$$

The nucleons consist of 73% protons and 27% neutrons.

15.9 THE FORMATION OF NUCLEI AND ATOMS

Let's review developments in the Big Bang cosmology up to $t = 6$ s. (1) A hot, dense universe, full of photons and elementary particles of all varieties, has cooled to below 10^{10} K. (2) Most of the unstable particles have decayed away. (3) All of the original antimatter and most of the original matter annihilated one another, leaving a small number of protons, an equal number of electrons, and about

one-fifth as many neutrons. (4) Neutrinos, which have about the same density as photons, decoupled at about 1 s and will continue cooling as the universe expands.

As the neutrons and protons collide with one another, it is possible to form a deuteron (^{2}H nucleus):

$$\mathrm{n} + \mathrm{p} \rightarrow {}^2\mathrm{H} + \gamma$$

but the high density of photons can also produce the inverse reaction:

$$\gamma + {}^2\mathrm{H} \rightarrow \mathrm{n} + \mathrm{p}$$

We recall from Chapter 12 that the deuteron binding energy is 2.22 MeV. In order to have any appreciable buildup of deuterons, the photons present must first cool until their energies are below 2.22 MeV; otherwise the deuterons will be broken up as quickly as they can be formed. The energy 2.22 MeV corresponds to a temperature $T = 2.5 \times 10^{10}$ K, and we therefore might expect deuterons to be formed as soon as the temperature drops below 2.5×10^{10} K. However, this does not happen. The radiation does not have a single energy, but rather has a thermal spectrum. A small fraction of the photons has energies *above* 2.22 MeV, and these photons continue to break apart the deuterons (Figure 15.28).

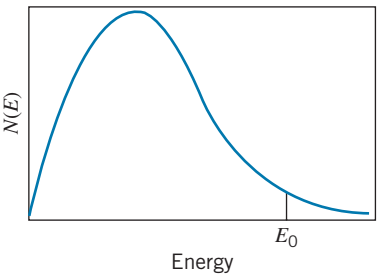

FIGURE 15.28 The thermal radiation spectrum. The photons above $E_0 =$ 2.22 MeV are sufficiently energetic to break apart deuterium nuclei.

Before matter-antimatter annihilation occurred, there were about as many photons as nucleons and antinucleons, but after $t = 0.01$ s, the ratio of nucleons to photons is about 10^{-9}; about $\frac{1}{6}$ of the nucleons are neutrons. If the fraction of photons above 2.22 MeV is greater than $\frac{1}{6} \times 10^{-9}$, there will be at least one energetic photon per neutron, which effectively prevents deuteron formation. Our next job is to calculate to what temperature the photons must cool before fewer than $\frac{1}{6} \times 10^{-9}$ of them are above 2.22 MeV.

The number density of thermal photons was given by Eq. 15.6. We expect that the temperature must be much less than 2.5×10^{10} K, and so we are interested in the distribution where $E \gg kT$, for which it is approximately

$$\frac{N(E)\,dE}{V} = \frac{8\pi E^2}{(hc)^3} e^{-E/kT}\,dE \tag{15.35}$$

and the total number density above some energy E_0 is determined by integrating the number density from E_0 to ∞: $N_{E>E_0}/V = \int_{E_0}^{\infty} N(E)dE/V$, which can be shown to be

$$\frac{N_{E>E_0}}{V} = \frac{8\pi}{(hc)^3}(kT)^3 e^{-E_0/kT}\left[\left(\frac{E_0}{kT}\right)^2 + 2\left(\frac{E_0}{kT}\right) + 2\right] \tag{15.36}$$

Equation 15.8 gives the *total* number density of photons, and thus the fraction f above E_0 is $(N_{E>E_0}/V)/(N/V)$, which can be evaluated to be

$$f = \frac{N_{E>E_0}/V}{N/V} = 0.42 e^{-E_0/kT}\left[\left(\frac{E_0}{kT}\right)^2 + 2\left(\frac{E_0}{kT}\right) + 2\right] \tag{15.37}$$

For $f = \frac{1}{6} \times 10^{-9}$, corresponding to the number needed to prevent deuteron formation, Eq. 15.37 gives $E_0/kT = 28$. With $E_0 = 2.22$ MeV, the required temperature is thus about 9×10^8 K; when $T > 9 \times 10^8$ K, the number of photons with $E > 2.22$ MeV is greater than the number of neutrons, and deuteron (^{2}H) formation is prevented. When T drops below 9×10^8 K (which occurs at about $t = 250$ s), deuterons can be produced.

From 6 s to 250 s, very little (except expansion and the corresponding temperature decrease) happens in the universe, but after $t = 250\,\text{s}$ things happen very quickly. Deuterons form and then react with the many protons and neutrons available to give

$$^2\text{H} + \text{p} \rightarrow {}^3\text{He} + \gamma \qquad \text{and} \qquad {}^2\text{H} + \text{n} \rightarrow {}^3\text{H} + \gamma$$

The energies of formation of these nuclei are, respectively, 5.49 MeV and 6.26 MeV, well above the 2.22 MeV threshold of the deuteron formation. If the photons are not energetic enough to break apart the deuterons, they are certainly not energetic enough to break apart ^{3}He and ^{3}H. The final steps in the formation of the heavier nuclei are

$$^3\text{He} + \text{n} \rightarrow {}^4\text{He} + \gamma \qquad \text{and} \qquad {}^3\text{H} + \text{p} \rightarrow {}^4\text{He} + \gamma$$

There are no stable nuclei with $A = 5$, so no further reactions of this sort are possible. Nor is it possible to have ^{4}He $+^4$He reactions because ^{8}Be is highly unstable. (It would be possible to form stable ^{6}Li and ^{7}Li, but these are made in very small quantities relative to H and He; from Li further reactions are possible, such as $^7\text{Li} + {}^4\text{He} \rightarrow {}^{11}\text{B}$, and so forth, but these occur in still smaller quantities. The end products ^{2}H and He, along with the leftover original protons, make up about 99.9999% of the nuclei after the era of nuclear reactions.)

By $t = 250\,\text{s}$, the original 16% neutrons present at $t = 6\,\text{s}$ had beta-decayed to about 12%, leaving 88% protons. Most of the ^{2}H, ^{3}H, and ^{3}He were "cooked" into heavier nuclei, so we can assume the universe to be composed mostly of ^{1}H and ^{4}He nuclei. Of the N nucleons present at $t = 250\,\text{s}$, 12% ($0.12N$) were neutrons and $0.88N$ were protons. The $0.12N$ neutrons combined with $0.12N$ protons, forming $0.06N$ ^{4}He, and leaving $0.88N - 0.12N = 0.76N$ protons. The universe then consisted of $0.82N$ nuclei, of which $0.06N$ (7.3%) were ^{4}He and $0.76N$ (92.7%) were protons. Helium is about four times as massive as hydrogen, so by *mass* the universe is about 24% helium.

At this point the universe began a long and uneventful period of cooling, during which the *strong* interactions ceased to be of importance.

The final step in the evolution of the primitive universe is the formation of neutral hydrogen and helium atoms from the ^{1}H, ^{2}H, ^{3}He, and ^{4}He nuclei and the free electrons. In the case of hydrogen, this takes place when the photon energy drops below 13.6 eV; otherwise any atoms that might happen to form will be immediately ionized by the radiation. There are still about 10^9 photons for every proton, and so we must wait for the radiation to cool until the fraction of photons above 13.6 eV is less than about 10^{-9}. We can solve Eq. 15.37 for $f = 10^{-9}$ to obtain $E_0/kT = 26$. With $E_0 = 13.6\,\text{eV}$, the corresponding temperature is $T = 6070\,\text{K}$, which occurs at time $t = 6.1 \times 10^{12}\,\text{s} = 190,000\,\text{y}$. These final estimates are actually not quite correct. We have been considering only the energy density of radiation present in the universe. As the universe cools, the contribution of the matter to the total energy density becomes more significant, and so the temperature drops more slowly than we would estimate. This contribution may increase this time by about a factor of 2 to about 380,000 y, and the radiation temperature is decreased by about a factor of $\sqrt{2}$, to $T = 4300\,\text{K}$.

After neutral atoms have formed, there are virtually no charged particles left in the universe, and the radiation field is not energetic enough to ionize the atoms. This is the time of the decoupling of the radiation field from the matter, and now

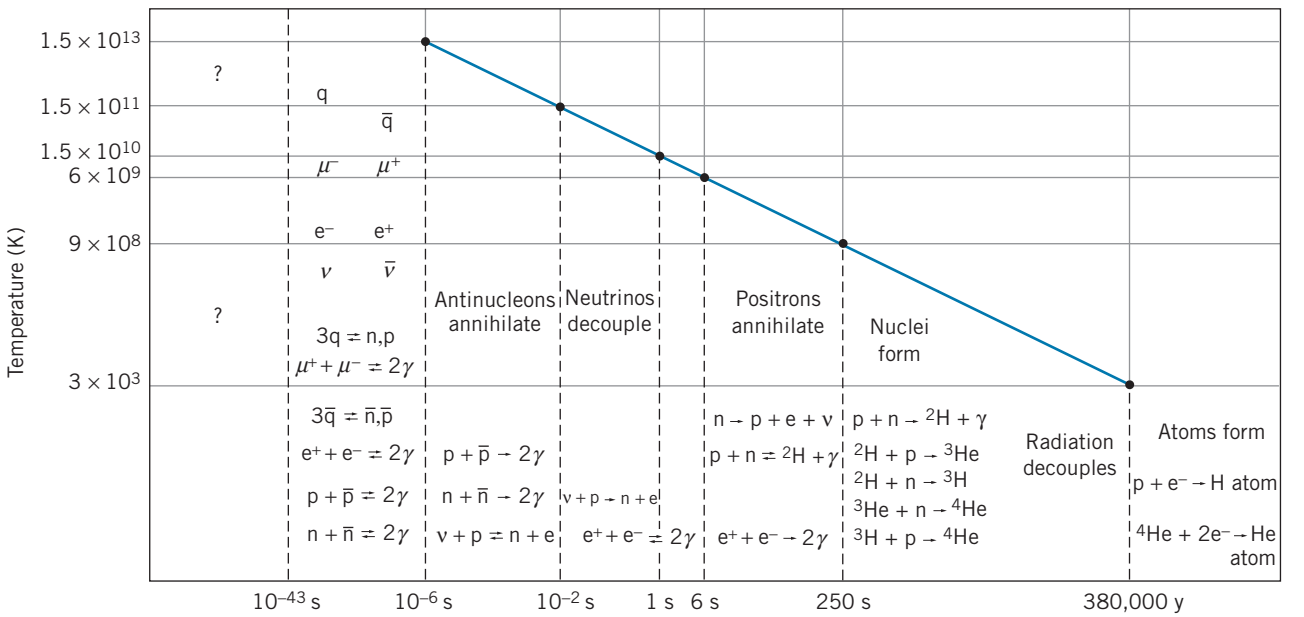

FIGURE 15.29 Evolution of the universe according to the Big Bang cosmology. The blue line shows the temperature and time in the radiation-dominated era before decoupling. The most important reactions in each era are shown.

electromagnetism, the third of the four basic forces, is no longer important in shaping the evolution of the universe. The large-scale development of the universe is from this point governed only by gravity.

The time after $t = 380{,}000$ y has been comparatively uneventful, at least from the point of view of cosmology. Density fluctuations of the hydrogen and helium triggered the condensation of galaxies, and then first-generation stars were born. Supernova explosions of the material from these stars permitted the formation of second generation systems, among which planets formed from the rocky debris.

Meanwhile, the decoupled radiation field, unaffected by the gravitational coming and going of matter, began the long journey that eventually took it, cooled again by a factor of 1600, to the radio telescopes of 20th-century Earth.

The details of the Big Bang cosmology are summarized in Figure 15.29. It is a remarkable story, all the more so because we can understand most of its details—with the possible exception of the first instant—with nothing more than some basic theories of modern physics, most of which we can study (on a much smaller scale!) in our laboratories on Earth.

15.10 EXPERIMENTAL COSMOLOGY

Far from being a science that involves only speculations about the distant past or the indefinite future, cosmology has in recent decades become a precise experimental science, involving observational results from high-resolution observatories on Earth and in space, as well as laboratory measurements of nuclear and particle properties that provide insight into cosmological phenomena. Here are a few of the observations and their implications.

Matter and Antimatter

In the early universe, there was roughly one nucleon and one antinucleon for each photon. If the numbers of nucleons and antinucleons had been exactly equal, there would have been either complete annihilation of both (in which case we would not be around to comment on the outcome) or else the clumping of matter and antimatter into galaxies and antigalaxies. Our telescopes can't tell the difference between galaxies made of matter and antimatter (because both emit the same light), but if there were large quantities of antimatter in the universe we should occasionally find a galaxy and an antigalaxy colliding, and their annihilation would light up the sky. We observe many galaxies in the process of colliding with their neighbors, but none show the intense annihilation radiation that would signal a matter-antimatter collision. Our conclusion is that the universe is made of matter and contains no significant concentrations of antimatter. For every 1,000,000,000 nucleons in the early universe there were 999,999,999 antinucleons; following the annihilation all of the antinucleons disappeared, leaving 1 out of the original 10^9 nucleons to make up the current universe.

After the matter-antimatter annihilation in the early universe, the ratio of the number of remaining nucleons to photons was about 10^{-9}. This number, which has remained constant since the annihilation era, is deduced from the measurement of the relative density of ^{2}H and ^{3}He in sites such as "first-generation" stars or interstellar gas, where no significant additional amounts of those atoms have been subsequently produced by fusion. The observed relative abundances of these atoms gives a nucleon to photon ratio in the range of $5-7 \times 10^{-10}$.

Where did the 10^{-9} excess of matter over antimatter in the early universe come from? We don't yet know the answer to this question, but evidence gathered in particle physics experiments may provide a clue. The first indication of an asymmetry between matter and antimatter was a 1964 experiment studying the decay of the neutral K meson, which shows a difference in behavior between K^0 and $\overline{K}^0$ only at the very low level of 1 part in 10^3 in the weak interaction or thus at a level of 10^{-10} relative to the strong interaction. (J. W. Cronin and V. L. Fitch received the 1980 Nobel Prize in physics for their work on this experiment.) Following the discovery of the b quark, it was hypothesized that the B^0 meson would show a similar effect, and so accelerators were built in the U. S. and Japan that produced the B^0 in large enough quantities to verify the asymmetry. Beginning in about 2001, scientists at these accelerators announced results that verified the matter-antimatter asymmetry previously observed only in the K^0 decay.

The distinction between matter and antimatter occurred at an early stage in the evolution of the universe, during the quark-antiquark era. The Grand Unified Theories (GUTs) include this asymmetry between quarks and antiquarks in a natural way, although there is as yet no accepted version of the GUTs that yields a convincing explanation for the K^0 and B^0 experiments.

Helium Abundance

Much of the matter in the universe has been formed and reformed, and so has lost its "memory" of the Big Bang. There is, however, "first generation" matter in stars and galaxies, that should show the roughly 24% helium abundance that characterized the formation of matter.

A variety of experiments suggests that the abundance of helium in the universe is 23 to 27% by mass, in excellent agreement with our rough estimate of 24%. These experiments include the emission of visible light from gas clouds near stars

and the emission of radio waves by interstellar gas, both of which permit us to compare the amounts of hydrogen and helium present. In addition, the dynamics of stellar formation depends on the initial hydrogen and helium concentrations; present theories permit us to estimate their ratio from the observed properties of stars. The 24% abundance seems to be rather constant throughout the universe, as we would expect if it were predetermined by the Big Bang. (Not enough helium has been produced by nuclear fusion in stars in the last 14×10^9 y to change this ratio significantly.)

In fact (and here physics comes nearly full circle, from the very old and large to the very new and small), the early helium abundance is a function of the conditions before 10^{-6} s, when quarks and leptons filled the universe. The evolutionary rate in this era depends on the number of different kinds of quarks and leptons that can participate in reactions. It has been calculated that the helium abundance is probably not consistent with the existence of more than three generations of quarks and leptons. It is remarkable that extrapolations to an unobservable state of the universe can yield such insight into the fundamental structure of matter.

The Horizon Problem

Our telescopes permit us to look outward by about 10 billion light-years in any direction. No matter in what direction we look, the universe (which we are viewing as it looked 10 billion years ago) appears pretty much the same—the same types of galaxies and the same temperature of the background radiation. This is surprising, because regions that we observe in opposite directions are separated by 20 billion light years, while the universe is only 14 billion years old. If the universe had been expanding throughout its history at a uniform rate, those opposite regions of the sky could never have been connected by any signal and thus had no way to achieve the common characteristics that we now observe. (Imagine finding a block of copper that had been assembled from a random collection of copper atoms. If all parts of the block were at the same temperature, you would conclude that the block had been in existence for a long enough time for thermal energy to propagate throughout its volume. If we learned that the time since the block's assembly was less than that propagation time, it would be very puzzling to explain the achievement of thermal equilibrium in so short a time.)

This paradox is solved by a hypothesis called "inflation," which proposes that in the early universe rather than a constant expansion rate there was a sudden rapid growth (by perhaps 50 orders of magnitude) in a short interval of time between 10^{-35} s and 10^{-32} s. Before the time of inflation, the size of the universe was less than the distance through which distant parts could exchange energy since the time of the Big Bang. Thus all parts of the universe were able to achieve a common set of characteristics. After inflation, the size of the universe exceeded the maximum range of communication signals, but the homogeneous characteristics had already been achieved. The inflationary hypothesis thus neatly solves the horizon problem.

The Flatness Problem

For a flat universe ($k = 0$), we can combine Eqs. 15.28 and 15.33 to give

$$\rho_{\text{cr}} = \frac{3H^2}{8\pi G} = 0.97 \times 10^{-26}\ \text{kg/m}^3 \tag{15.38}$$

This is the critical density corresponding to a flat universe. If the density is greater than this critical value, the universe is closed, and if it is less than this value, the

universe is open. In discussing the density of the universe, it is useful to define the ratio between the actual density and this critical value:

$$\Omega = \frac{\rho}{\rho_{\text{cr}}} \tag{15.39}$$

As the universe expands, the gravitational interaction among its components slows the expansion rate. If $\Omega > 1$, the gravitational interaction will eventually halt and reverse the expansion. If $\Omega < 1$, the expansion will continue until the components are separated by infinite distances. If Ω is exactly equal to one, the expansion will also continue forever, but the components will arrive at their infinite separation just as they lose the last bit of kinetic energy.

By carefully measuring the variations in the temperature of regions of the microwave background, the WMAP satellite and other experiments have concluded that Ω is very close to 1, probably within 1%. It is of considerable interest to know whether Ω is *exactly* equal to 1 (for a flat universe), or just happens to be very close to 1 (for an open or closed universe).

By way of analogy, consider a projectile that is thrown upward from the surface of the Earth (ignore the gravity of the Sun and all other objects). The parameter Ω in effect measures the ratio between the gravitational potential energy and the kinetic energy: $\Omega = |U_{\text{grav}}|/K$. If the initial value of Ω is greater than 1, the gravitational energy exceeds the kinetic energy, so the projectile will rise to a maximum height and then fall back to Earth. When it reaches its maximum height, $K = 0$ and Ω becomes infinite. During the entire ascent, the value of Ω increases because the kinetic energy decreases more rapidly than the magnitude of the gravitational energy. If the projectile is launched so that $\Omega < 1$, there is more than enough kinetic energy to overcome the Earth's gravity, and the projectile will escape the pull of the Earth. When it reaches infinite separation, $\Omega = 0$ because $U_{\text{grav}} = 0$. During its entire outward journey, Ω decreases from its initial value and approaches zero. If we choose the initial velocity such that $\Omega = 1$, there is just enough energy to escape, and the projectile reaches infinite separation with $K = 0$. Throughout the entire journey, Ω remains exactly 1.

For the projectile as well as for the evolution of the universe, the conclusions are identical: If $\Omega = 1$ initially, it remains exactly 1 always, but if either $\Omega > 1$ or $\Omega < 1$, it grows further away from 1. If the early universe had $\Omega = 1.000001$, after the passage of 14 billion years Ω would have grown very large; similarly, if the initial value of Ω were 0.999999, by now it would be very close to 0. It has been calculated that for Ω to be within 1% of 1 today, it must have originally been in the range 1 ± 10^{-62}. Here again the inflation hypothesis is essential. Prior to the inflation era, the universe may have been open, flat, or closed, with any value of Ω. During inflation, the universe grew by so many orders of magnitude that the curvature became flat, much as the surface of a balloon becomes nearly flat when it is inflated by many orders of magnitude. As a result, Ω was indeed very close to 1 just after inflation, and we continue today to observe an Ω that remains close to 1.

The Composition and Age of the Universe

During the past 10 years, researchers have made enormous strides in determining the composition of the universe and its age. These determinations are based mostly on measurements of the properties of the cosmic microwave background radiation, in particular its geometrical distribution and its polarization properties. Among the most detailed experiments are those of the WMAP satellite (2001) and the

Boomerang balloon flights over Antarctica (1998 and 2003). These experiments, along with others, indicate that the universe is very nearly flat; that is, $\Omega = 1.00$ (so that $\rho = \rho_{cr}$) to within about 1%. They are also able to measure the relative densities of the various components of the mass-energy content of the universe. Ordinary baryonic matter contributes about 4.6% of the critical density, and dark (nonbaryonic) matter contributes 23%. Together, the two kinds of matter make up 28% of the critical density. If the density of the universe is equal to the critical density, what makes up the other 72%?

Beginning in about 1998, two teams of researchers were investigating the Hubble law by studying the exploding stars known as supernovas in the most distant galaxies (corresponding to large redshifts, with $\Delta\lambda/\lambda$ close to 0.9). Both teams found systematic and consistent departures from the Hubble law. The supernovas in these distant galaxies were fainter than expected, indicating that the galaxies were 10 to 15% farther from us than the Hubble law predicts. The research groups concluded that a mysterious force is accelerating the expansion of the universe. Generally we would expect that the expansion would be slowing down, owing to the gravitational interactions of its components. What could be responsible for increasing the rate of the expansion?

This unknown interaction is called "dark energy," and it represents the missing 72% of the composition of the universe. Although there are several theories about the nature of the dark energy, there is no convincing explanation of its origin or its role in the physical world. It has been suggested that the dark energy density does not diminish as the universe expands, so that as the densities of matter (both baryonic and non-baryonic) decrease with the expansion, eventually the dark energy begins to dominate and accelerates the expansion. We live at a time when this acceleration is dominant (which has occurred for about the past 5 billion years).

Another finding based on the observation of the background radiation is the age of the universe. There is general agreement that the age is 13.7×10^9 years, with an uncertainty of about 1%. The accelerated expansion solves a problem associated with the Hubble age. In a matter-dominated universe (which our universe has been for most of its existence), the present Hubble age should be $\frac{2}{3}H_0^{-1}$, which works out to be about 9×10^9 years. If the expansion has been accelerating, then the actual age can be greater than the Hubble age, which certainly seems to be the case.

It is fitting that this story ends where it began, with Einstein. When Einstein produced the general relativity theory in 1916 (a decade before Hubble's work), it was widely believed that the universe was static. In order for the equations of general relativity to allow a static solution, Einstein introduced into his equations an additional term, called the cosmological constant. After learning of Hubble's discovery of the expansion of the universe, Einstein called the introduction of the cosmological constant his "greatest blunder." It now appears that the cosmological constant is one possible explanation for the dark energy, and the term has been restored to the equations.

The increasing role of the dark energy suggests a sad fate for the universe. An open universe will expand forever, but in an accelerating open universe each observer's horizon will shrink increasingly rapidly. The most distant galaxies will separate from us at speeds greater than the speed of light (which is *not* a violation of special relativity, because no signals are being exchanged). The light from these distant galaxies will not be able to reach us, and the galaxies will gradually disappear. Future astronomers might be able to observe only local galaxies and might learn nothing of the expansion or the properties of the universe!

Chapter Summary

		Section
Hubble's law	$v = H_0 d$	15.1
Number density of photons	$N/V = (2.03 \times 10^7 \text{photons/m}^3 \cdot \text{K}^3) T^3$	15.2
Energy density of photons	$U = (4.72 \times 10^3 \text{ eV/m}^3 \cdot \text{K}^4) T^4$	15.2
Gravitational frequency change	$\Delta f/f = gH/c^2$	15.4
Deflection of starlight	$\theta = 2GM/Rc^2$	15.5
Perihelion precession	$\Delta\phi = \dfrac{6\pi GM}{c^2 r_{\min}(1+e)}$	15.5
Schwarzschild radius	$r_S = 2GM/c^2$	15.6
Age of matter-dominated universe	$t = 1/\sqrt{6\pi G\rho_m}$	15.7
Age of radiation-dominated universe	$t = \sqrt{3/32\pi G\rho_r}$	15.7
Temperature of universe at age t	$T = \dfrac{1.5 \times 10^{10}\,\text{s}^{1/2} \cdot \text{K}}{t^{1/2}}$	15.8
Fraction of photons above E_0	$f = 0.42 e^{-E_0/kT} \times \left[\left(\frac{E_0}{kT}\right)^2 + 2\left(\frac{E_0}{kT}\right) + 2\right]$	15.9
Critical density of universe	$\rho_{cr} = \dfrac{3H^2}{8\pi G} = 0.97 \times 10^{-26}\,\text{kg/m}^3$	15.10

Questions

1. If we were to measure the equivalence of gravitational and inertial mass, would we show that $m_{\text{inertial}} = m_{\text{gravitational}}$ or merely that $m_{\text{inertial}} \propto m_{\text{gravitational}}$?
2. Do tidal effects distinguish between Newtonian gravity and curved spacetime? What would be the shape of a drop of liquid following a path in a curved spacetime? Can such a drop distinguish between a uniform gravitational field and a uniform acceleration?
3. Suppose that the first measurement of deflection of starlight during a solar eclipse had been done after 1905, when the special theory of relativity was introduced, but before 1916, when the general theory was introduced. What would have been the effect of this measurement on the special theory?
4. If we could make a precise comparison of light from the Sun with light from the Moon, would the moonlight be red shifted, blue shifted, or unshifted relative to sunlight?
5. What difficulties might arise in the Pound and Rebka experiment on the gravitational red shift if the temperature of the source or the absorber varied?
6. Why are the abundances of Li, Be, and B so small?
7. Can we look out into the distant universe without also looking back into time?
8. Is Hubble's parameter a constant? Does it vary over large distances of space? Over long intervals of time?
9. Explain why the age of the universe must be less than H^{-1}.
10. Why is it difficult to obtain precise values for the Hubble parameter?
11. All natural processes are governed by the rule that the entropy must increase; the increase of entropy, as the universe "runs down," defines for us a direction of time. If the universe begins to contract and therefore to heat up, will the entropy of natural processes therefore decrease? Will the inhabitants of that universe observe time to be running backward?
12. The hydrogen in the universe contains a small fraction of deuterium. Assuming the deuterium originated in the Big Bang, what era of the Big Bang would we learn about by measuring the deuterium abundance? Can we accomplish this measurement using terrestrial hydrogen? What properties of deuterium could we use to determine its presence in distant regions of the galaxy?
13. Between $t = 1\,\text{s}$ and $t = 6\,\text{s}$, the neutron fraction should drop from 27 to 8%; instead it drops only to about 16%. Why don't more neutrons turn into protons during this era? Is it as difficult for protons to turn into neutrons?
14. If we were able to observe the neutrinos from the early universe, would they have a spectrum determined by the Planck distribution?

Problems

15.1 The Expansion of the Universe

1. Use Hubble's law to estimate the wavelength of the 590.0 nm sodium line as observed emitted from galaxies whose distance from us is (*a*) 1.0×10^6 light-years; (*b*) 1.0×10^9 light-years.
2. The light from a certain galaxy is red-shifted so that the wavelength of one of its characteristic spectral lines is doubled. Assuming the validity of Hubble's law, calculate the distance to this galaxy.

15.2 The Cosmic Microwave Background Radiation

3. (*a*) Taking $u(E) = EN(E)$ as the energy density of the thermal radiation, with $N(E)$ given in Eq. 15.6, differentiate to find the energy at which the maximum of the radiation energy spectrum occurs. (*b*) Evaluate the peak photon energy of the 2.7-K microwave background.
4. Starting with Eqs. 15.7 and 10.41, show how to evaluate the numerical constants that appear in Eqs. 15.8 and 15.9.

15.3 Dark Matter

5. Suppose an observer in a distant galaxy were observing the light from our Sun as the Sun moves directly toward the observer. Neglecting any net relative motion of the two galaxies, calculate the change in wavelength of the 121.5-nm Lyman series line due to the rotation of our galaxy.

15.4 The General Theory of Relativity

6. In Example 15.1 we calculated the change in wavelength of the Lyman α line due to the gravitational red shift. Compare this value with (*a*) the special relativistic Doppler shift due to the rotation of the Sun and (*b*) the thermal Doppler broadening (see Eq. 10.30). The Sun's radius is 6.96×10^8 m, its rotational period is 26 days, and it surface temperature is 6000 K.
7. A satellite is in orbit at an altitude of 150 km. We wish to communicate with it using a radio signal of frequency 10^9 Hz. What is the gravitational change in frequency between a ground station and the satellite? (Assume g doesn't change appreciably.)
8. According to the uncertainty principle, what is the minimum time interval necessary to measure a change in frequency of the magnitude observed in the Pound and Rebka experiment?

15.5 Tests of General Relativity

9. By drawing analogies between the Coulomb force law and the gravitational force law, use Eq. 6.8 for the deflection in Rutherford scattering to obtain Eq. 15.22 for the deflection of photons. Assume the photon behaves as if it has a mass $m = E/c^2$. (*Hint:* Write Eq. 6.8 in terms of the velocity of the particle instead of kinetic energy.)
10. In the binary star system known as PSR 1913 + 16, two neutron stars move about their common center of mass in highly elliptical orbits. Locate the orbital parameters for this motion, and add a row to Table 15.1 showing the precession angle expected from general relativity. (Hint: In Eq. 15.25, M is the total mass of the orbiting body and the central body.)

15.6 Stellar Evolution and Black Holes

11. (*a*) Show that Eq. 10.57 for the radius of a neutron star of mass M can be written $R = (12.3\,\text{km})(M/M_\odot)^{-1/3}$ where $M_\odot$ is the mass of the Sun. (*b*) Consider a star 1.5 times as massive as the Sun with a radius of 7×10^5 km (equal to the present radius of the Sun), rotating on its axis about once per year. (This is quite a slow rate of rotation—our Sun rotates about once per month.) If angular momentum is conserved in the collapse, what will be the final angular velocity? Assume the star can be represented as a sphere of uniform density, with rotational inertia $I = \frac{2}{5}MR^2$.

15.7 Cosmology and General Relativity

12. The rate of change of the cosmic expansion can be described in terms of a *deceleration parameter* $q = -R(d^2R/dt^2)/(dR/dt)^2$. (*a*) Evaluate q for the matter-dominated universe (Eq. 15.29) and the radiation-dominated universe (Eq. 15.31). (*b*) By differentiating Eq. 15.28, show that in a matter-dominated universe $q = 4\pi G\rho_\text{m}/3H^2$. (*Hint:* Use $\rho_\text{m} \propto R^{-3}$ to relate $d\rho_\text{m}/dt$ to dR/dt.)

15.8 The Big Bang Cosmology

13. Derive Eq. 15.34.
14. At what age did the universe cool below the threshold temperature for (*a*) nucleon production; (*b*) pi meson production?
15. (*a*) At what temperature was the universe hot enough to permit the photons to produce K mesons ($mc^2 = 500$ MeV)? (*b*) At what age did the universe have this temperature?

15.9 The Formation of Nuclei and Atoms

16. Derive Eqs. 15.36 and 15.37.
17. Suppose the difference between matter and antimatter in the early universe were 1 part in 10^8 instead of 1 part in 10^9. (*a*) Evaluate the temperature at which deuterium begins to form. (*b*) At what age does this occur? (*c*) Evaluate the temperature and the corresponding time of radiation decoupling (when hydrogen atoms form).
18. What was the age of the universe when the nucleons consisted of 60% protons and 40% neutrons?

15.10 Experimental Cosmology

19. Assuming that the density of the universe is equal to its critical value and that 4.6% of the universe is baryonic

matter, calculate the average number of baryons (nucleons) per cubic meter in the universe.

20. (*a*) Suppose the baryonic matter in the universe were composed of uniformly distributed stars of the mass of the Sun (2.0×10^{30} kg). What would be the average spacing between the stars? Express your answer in light-years. (*b*) Suppose instead that the baryonic matter were composed of uniformly distributed galaxies of the mass of the Milky Way (1.2×10^{42} kg). Expressed in light-years, what would be the average distance between the galaxies?
21. Suppose the non-baryonic dark matter consists entirely of neutrinos. What is the average rest energy of the neutrinos that could account for this part of the mass of the universe? As a rough estimate, assume that the neutrino density is the same as the present photon density.

General Problems

22. Photons of visible light have energies between about 2 and 3 eV. (*a*) Compute the number density of photons from the 2.73-K background radiation in that interval. (It is sufficient to characterize the visible region as $E = 2.5$ eV with $dE = 1.0$ eV.) (*b*) Assume the eye can detect about 100 photons/cm^3. At what temperature would the background radiation be visible? At what age of the universe would this have occurred?
23. Consider the universe at a temperature of 5000 K. (*a*) At what age did this occur, and during which stage of the evolution of the universe? (*b*) Evaluate the average photon energy at that time. (*c*) If there are 10^9 photons per nucleon, evaluate the ratio between the radiation density and the mass density at that time.
24. The early universe was radiation dominated, and the present universe is matter dominated. (*a*) At what temperature were the radiation and matter densities equal? (*b*) What was the age of the universe when this occurred?
25. A neutron star of 2.00 solar masses is rotating at a rate of 1.00 revolutions per second. (*a*) What is the radius of the neutron star? (See Problem 11.) (*b*) Find its rotational kinetic energy. (*c*) If its rotational speed slows by 1 part in 10^9 per day, find the loss in rotational kinetic energy per day. (*d*) Assuming that the entire energy loss goes into radiation, find the radiative power. (*e*) If the star is 10^4 light-years from Earth, what would be the average power received by an antenna of area 10 m^2 if the star's energy were distributed uniformly in space instead of concentrated in a narrow beam?
26. Because we don't yet have a quantum theory of gravity, we cannot analyze the properties of the universe before the Planck time, about 10^{-43} s. If we assume that the properties of the universe during that era were determined by quantum theory, relativity, and gravity, the Planck time should be characterized by the fundamental constants of those three theories: h, c, and G. We can therefore write $t \propto h^i c^j G^k$, where i, j, and k are exponents to be determined. (*a*) Using a dimensional analysis, determine i, j, and k. (*b*) Assuming the proportionality parameter is of order unity, evaluate t. (*c*) What was the size of the observable universe at the Planck time?
27. Show that the spacetime interval given by Eq. 15.18 is invariant with respect to the Lorentz transformation. That is, show that $(ds)^2 = (ds')^2$, where $(ds')^2 = (c\,dt')^2 - (dx')^2$.
28. Light from star S in Figure 15.30 passes a distance b from a galaxy L, where it is deflected by an angle α and then reaches the observer O, who sees an image of the star at I. (For simplicity, assume the gravitational deflection takes place at a single point, and assume all angles in the figure are very small.) The galaxy (of mass M) is a distance d_L from the observer, and the star is a distance d_S from the observer. (*a*) For small angles, show that $\theta d_S = \beta d_S + (4GM/\theta d_L c^2)(d_S - d_L)$. (Hint: Use Eq. 15.22 for the deflection angle α when the impact parameter is b instead of R, but double the value to account for the difference between the special and general relativity predictions.) (*b*) Solve the resulting quadratic equation for θ and show that there are two image positions whose locations differ by $\Delta\theta = \sqrt{\beta^2 + 4\theta_E^2}$, where the Einstein angle θ_E is $\sqrt{4GM(d_S - d_L)/c^2 d_S d_L}$. This is an example of *gravitational lensing*, an effect of general relativity that has been observed for distant objects that appear in multiple images when their light travels a path through spacetime that is curved by an intervening galaxy. (*c*) When the star, lensing galaxy, and observer lie along a single line, something other than two images appears. Given the symmetry of the figure when $\beta = 0$, what do you expect to be observed in this case?

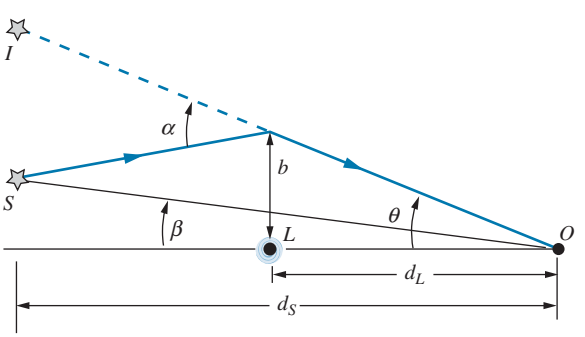

FIGURE 15.30 Problem 28.

Appendix A

CONSTANTS AND CONVERSION FACTORS*

CONSTANTS

Speed of light	c	2.99792458×10^{8} m/s
Charge of electron	e	$1.60217657 \times 10^{-19}$ C
Boltzmann constant	k	1.380649×10^{-23} J/K $= 8.617332 \times 10^{-5}$ eV/K
Planck's constant	h	$6.62606957 \times 10^{-34}$ J · s $= 4.13566752 \times 10^{-15}$ eV · s
	$\hbar = h/2\pi$	$1.054571726 \times 10^{-34}$ J · s $= 6.58211928 \times 10^{-16}$ eV · s
	hc	1239.8419 eV · nm (or MeV · fm)
	$\hbar c$	197.326972 eV · nm (or MeV · fm)
Gravitational constant	G	6.67384×10^{-11} N · m^2/ kg^2
Avogadro's constant	N_A	6.0221413×10^{23} mole^{-1}
Universal gas constant	R	8.314462 J/mole · K
Stefan-Boltzmann constant	σ	5.67037×10^{-8} W/m^2 · K^4
Rydberg constant	R_∞	$1.097373156854 \times 10^{7}$ m^{-1}
Hydrogen ionization energy	$\lvert E_1 \rvert$	13.6056925 eV
Bohr radius	a_0	$5.291772109 \times 10^{-11}$ m
Bohr magneton	μ_B	$9.2740097 \times 10^{-24}$ J/T $= 5.78838181 \times 10^{-5}$ eV/T
Nuclear magneton	μ_N	$5.0507835 \times 10^{-27}$ J/T $= 3.15245126 \times 10^{-8}$ eV/T
Fine structure constant	α	1/137.03599907
Electric constant	$e^2/4\pi\varepsilon_0$	1.4399645 eV · nm (or MeV · fm)

*The number of significant figures given for the numerical constants indicates the precision to which they have been determined; there is an experimental uncertainty, typically of a few parts in the last or next-to-last digit, except for the speed of light (which is exact).

SOME PARTICLE MASSES

	kg	u	MeV/c^2
Electron	$9.1093829 \times 10^{-31}$	$5.485799095 \times 10^{-4}$	0.51099893
Proton	$1.67262178 \times 10^{-27}$	1.0072764668	938.27205
Neutron	$1.67492735 \times 10^{-27}$	1.0086649160	939.56538
Deuteron	$3.3435835 \times 10^{-27}$	2.0135532127	1875.61286
Alpha	$6.6446568 \times 10^{-27}$	4.001506179	3727.3792

CONVERSION FACTORS

$1\,\text{eV} = 1.60217657 \times 10^{-19}\,\text{J}$

$1\,\text{u} = 931.49406\,\text{MeV}/c^2$

$= 1.66053892 \times 10^{-27}\,\text{kg}$

$1\,\text{y} = 3.156 \times 10^{7}\,\text{s} \cong \pi \times 10^{7}\,\text{s}$

$1\ \text{barn (b)} = 10^{-28}\,\text{m}^2$

$1\ \text{curie (Ci)} = 3.7 \times 10^{10}\ \text{decays/s}$

$1\ \text{light-year} = 9.46 \times 10^{15}\,\text{m}$

$1\ \text{parsec} = 3.26\ \text{light-year}$

Appendix B

COMPLEX NUMBERS

The imaginary number i is defined as $\sqrt{-1}$. A *complex number or function* can be represented as having a real part, which does not depend on i, and an imaginary part, which depends on i. We can write a complex variable as $z = x + iy$, where the real part x and the imaginary part y are both real numbers or real functions. A complex wave function ψ can be written in terms of its real and imaginary parts as $\psi = \mathrm{Re}(\psi) + i\mathrm{Im}(\psi)$.

The complex conjugate of a complex number is obtained by substituting $-i$ for i, as in $z^* = x - iy$ or $\psi^* = \mathrm{Re}(\psi) - i\mathrm{Im}(\psi)$.

The squared magnitude of a complex number is defined as the product of the number and its complex conjugate, as in $|z|^2 = zz^*$ or $|\psi|^2 = \psi\psi^*$, and is equal to the sum of the squares of its real and imaginary parts:

$$|z|^2 = x^2 + y^2 \qquad \text{or} \qquad |\psi|^2 = [\mathrm{Re}(\psi)]^2 + [\mathrm{Im}(\psi)]^2$$

The complex exponential $e^{i\theta}$ can be represented in terms of real trigonometric functions as

$$e^{i\theta} = \cos\theta + i\sin\theta \qquad \text{and} \qquad e^{-i\theta} = \cos\theta - i\sin\theta$$

The squared magnitude of the complex exponential is equal to 1:

$$|e^{i\theta}|^2 = e^{i\theta}e^{-i\theta} = (\cos\theta + i\sin\theta)(\cos\theta - i\sin\theta) = \cos^2\theta + \sin^2\theta = 1$$

We can write the ordinary trigonometric functions in terms of these complex functions:

$$\sin\theta = \frac{1}{2i}(e^{i\theta} - e^{-i\theta}) \qquad \text{and} \qquad \cos\theta = \frac{1}{2}(e^{i\theta} + e^{-i\theta})$$

It is sometimes convenient to write the wave function in terms of a complex exponential as:

$$\psi = |\psi|e^{i\alpha}$$

where $|\psi|$ gives the magnitude of the wave function and α is its phase.

Periodic Table of the Elements

Group I	Group II	Transition elements										Group III	Group IV	Group V	Group VI	Group VII	Group 0
H 1 1.00794 $1s^1$																	He 2 4.00260 $1s^2$
Li 3 6.941 $2s^1$	Be 4 9.01218 $2s^2$											B 5 10.81 $2p^1$	C 6 12.011 $2p^2$	N 7 14.0067 $2p^3$	O 8 15.9994 $2p^4$	F 9 18.9984 $2p^5$	Ne 10 20.180 $2p^6$
Na 11 22.9898 $3s^1$	Mg 12 24.305 $3s^2$											Al 13 26.9815 $3p^1$	Si 14 28.0855 $3p^2$	P 15 30.9738 $3p^3$	S 16 32.065 $3p^4$	Cl 17 35.453 $3p^5$	Ar 18 39.948 $3p^6$
K 19 39.0983 $4s^1$	Ca 20 40.08 $4s^2$	Sc 21 44.9559 $3d^14s^2$	Ti 22 47.867 $3d^24s^2$	V 23 50.9415 $3d^34s^2$	Cr 24 51.996 $3d^54s^1$	Mn 25 54.9380 $3d^54s^2$	Fe 26 55.845 $3d^64s^2$	Co 27 58.9332 $3d^74s^2$	Ni 28 58.693 $3d^84s^2$	Cu 29 63.546 $3d^{10}4s^1$	Zn 30 65.38 $3d^{10}4s^2$	Ga 31 69.723 $4p^1$	Ge 32 72.64 $4p^2$	As 33 74.9216 $4p^3$	Se 34 78.96 $4p^4$	Br 35 79.904 $4p^5$	Kr 36 83.798 $4p^6$
Rb 37 85.4678 $5s^1$	Sr 38 87.62 $5s^2$	Y 39 88.9059 $4d^15s^2$	Zr 40 91.224 $4d^25s^2$	Nb 41 92.9064 $4d^45s^1$	Mo 42 95.96 $4d^55s^1$	Tc 43 (98) $4d^55s^2$	Ru 44 101.07 $4d^75s^1$	Rh 45 102.906 $4d^85s^1$	Pd 46 106.42 $4d^{10}5s^0$	Ag 47 107.868 $4d^{10}5s^1$	Cd 48 112.41 $4d^{10}5s^2$	In 49 114.82 $5p^1$	Sn 50 118.71 $5p^2$	Sb 51 121.76 $5p^3$	Te 52 127.60 $5p^4$	I 53 126.904 $5p^5$	Xe 54 131.29 $5p^6$
Cs 55 132.905 $6s^1$	Ba 56 137.33 $6s^2$	57–71	Hf 72 178.49 $5d^26s^2$	Ta 73 180.948 $5d^36s^2$	W 74 183.84 $5d^46s^2$	Re 75 186.207 $5d^56s^2$	Os 76 190.2 $5d^66s^2$	Ir 77 192.22 $5d^76s^2$	Pt 78 195.08 $5d^96s^2$	Au 79 196.967 $5d^{10}6s^1$	Hg 80 200.59 $5d^{10}6s^2$	Tl 81 204.383 $6p^1$	Pb 82 207.2 $6p^2$	Bi 83 208.980 $6p^3$	Po 84 (209) $6p^4$	At 85 (210) $6p^5$	Rn 86 (222) $6p^6$
Fr 87 (223) $7s^1$	Ra 88 (226) $7s^2$	89–103	Rf 104 (265) $6d^27s^2$	Db 105 (268) $6d^37s^2$	Sg 106 (271) $6d^47s^2$	Bh 107 (272) $6d^57s^2$	Hs 108 (270) $6d^67s^2$	Mt 109 (276) $6d^77s^2$	Ds 110 (281) $6d^97s^2$	Rg 111 (280) $6d^{10}7s^1$	Cn 112 (285) $6d^{10}7s^2$	Uut 113 (284) $7p^1$	Uuq 114 (289) $7p^2$	Uup 115 (288) $7p^3$	Uuh 116 (293) $7p^4$	Uus 117 (292) $7p^5$	Uuo 118 (294) $7p^6$

Symbol — Cl 17 — Atomic number
Atomic mass* — 35.453
Electron configuration — $3p^5$

Lanthanide series	La 57 138.906 $5d^16s^2$	Ce 58 140.12 $4f^15d^16s^2$	Pr 59 140.908 $4f^36s^2$	Nd 60 144.24 $4f^46s^2$	Pm 61 (145) $4f^56s^2$	Sm 62 150.36 $4f^66s^2$	Eu 63 151.96 $4f^76s^2$	Gd 64 157.25 $5d^14f^76s^2$	Tb 65 158.925 $4f^96s^2$	Dy 66 162.50 $4f^{10}6s^2$	Ho 67 164.930 $4f^{11}6s^2$	Er 68 167.26 $4f^{12}6s^2$	Tm 69 168.934 $4f^{13}6s^2$	Yb 70 173.05 $4f^{14}6s^2$	Lu 71 174.967 $5d^14f^{14}6s^2$
Actinide series	Ac 89 (227) $6d^17s^2$	Th 90 232.038 $6d^27s^2$	Pa 91 231.036 $5f^26d^17s^2$	U 92 238.029 $5f^36d^17s^2$	Np 93 (237) $5f^46d^17s^2$	Pu 94 (244) $5f^67s^2$	Am 95 (243) $5f^77s^2$	Cm 96 (247) $5f^76d^17s^2$	Bk 97 (247) $5f^97s^2$	Cf 98 (251) $5f^{10}7s^2$	Es 99 (252) $5f^{11}7s^2$	Fm 100 (257) $5f^{12}7s^2$	Md 101 (258) $5f^{13}7s^2$	No 102 (259) $5f^{14}7s^2$	Lr 103 (262) $6d^15f^{14}7s^2$

* Atomic mass values are averaged over isotopes according to the percentages that occur on the earth's surface. For unstable elements, the mass number of the most stable known isotope is given in parentheses. Electron configurations of elements above 103 are tentative assignments based on the corresponding elements in the 6th row (period).
Source: IUPAC Commission on Atomic Weights and Isotopic Abundances, 2001.

Appendix C

Appendix D

TABLE OF ATOMIC MASSES

The table gives the atomic masses of some isotopes of each element. All naturally occurring stable isotopes are included (with their natural abundances shown in italics in the last column). Some of the longer-lived radioactive isotopes of each element are also included, with their half-lives. Each element has many other radioactive isotopes that are not included in this table. More complete listings can be found in the sources from which this table was derived: *Table of Isotopes* (8th Edition), edited by R. B. Firestone and V. S. Shirley (Wiley, 1999); G. Audi, A. H. Wapstra, and C. Thibault, "The 2003 Atomic Mass Evaluation," *Nuclear Physics* **A729,** 129 (2003).

In the half-life column, My $= 10^6$ y.

	Z	*A*	Atomic mass (u)	*Abundance* or Half-life
H	1	1	1.0078250	*99.985%*
		2	2.014102	*0.015%*
		3	3.016049	12.3 y
He	2	3	3.016029	*0.000137%*
		4	4.002603	*99.999863%*
Li	3	6	6.015123	*7.59%*
		7	7.016005	*92.41%*
		8	8.022487	0.84 s
Be	4	7	7.016930	53.2 d
		8	8.005305	0.07 fs
		9	9.012182	*100%*
		10	10.013534	1.5 My
		11	11.021658	13.8 s
B	5	8	8.024607	0.77 s
		9	9.013329	0.85 as
		10	10.012937	*19.8%*
		11	11.009305	*80.2%*
		12	12.014352	20.2 ms
C	6	10	10.016853	19.3 s
		11	11.011434	20.3 m
		12	12.000000	*98.89%*
		13	13.003355	*1.11%*
		14	14.003242	5730 y
		15	15.010599	2.45 s
N	7	13	13.005739	9.96 m
		14	14.003074	*99.63%*
		15	15.000109	*0.37%*
		16	16.006102	7.1 s
		17	17.008450	4.2 s
O	8	14	14.008596	70.6 s
		15	15.003066	122 s
		16	15.994915	*99.76%*
		17	16.999132	*0. 038%*
		18	17.999161	*0.200%*
		19	19.003580	26.9 s
		20	20.004077	13.5 s
F	9	17	17.002095	64.5 s
		18	18.000938	1.83 h
		19	18.998403	*100%*
		20	19.999981	11 s
		21	20.999949	4.2 s
Ne	10	18	18.005708	1.7 s
		19	19.001880	17.2 s
		20	19.992440	*90.48%*
		21	20.993847	*0.27%*
		22	21.991385	*9.25%*
		23	22.994467	37.2 s
		24	23.993611	3.4 m

	Z	*A*	Atomic mass (u)	*Abundance* or Half-life
Na	11	21	20.997655	22.5 s
		22	21.994436	2.60 y
		23	22.989769	*100%*
		24	23.990963	15.0 h
		25	24.989954	59 s
		26	25.992633	1.1 s
Mg	12	22	21.999574	3.88 s
		23	22.994124	11.3 s
		24	23.985042	*78.99%*
		25	24.985837	*10.00%*
		26	25.982593	*11.01%*
		27	26.984341	9.46 m
		28	27.983877	20.9 h
Al	13	25	24.990428	7.18 s
		26	25.986892	0.72 My
		27	26.981539	*100%*
		28	27.981910	2.24 m
		29	28.980445	6.56 m
Si	14	26	25.992330	2.23 s
		27	26.986705	4.16 s
		28	27.976927	*92.23%*
		29	28.976495	*4.68%*
		30	29.973770	*3.09%*
		31	30.975363	2.62 h
		32	31.974148	132 y
P	15	29	28.981801	4.14 s
		30	29.978314	2.50 m
		31	30.973762	*100%*
		32	31.973907	14.3 d
		33	32.971726	25.3 d
S	16	30	29.984903	1.18 s
		31	30.979555	2.57 s
		32	31.972071	*95.02%*
		33	32.971459	*0.75%*
		34	33.967867	*4.21%*
		35	34.969032	87.5 d
		36	35.967081	*0.02%*
		37	36.971126	5.05 m
Cl	17	33	32.977452	2.51 s
		34	33.973763	1.53 s
		35	34.968853	*75.77%*
		36	35.968307	0.30 My
		37	36.965903	*24.23%*
		38	37.968010	37.2 m
		39	38.968008	55.6 m

	Z	*A*	Atomic mass (u)	*Abundance* or Half-life
Ar	18	34	33.980271	0.844 s
		35	34.975258	1.78 s
		36	35.967545	*0.337%*
		37	36.966776	35.0 d
		38	37.962732	*0.063%*
		39	38.964313	269 y
		40	39.962383	*99.60%*
		41	40.964501	1.82 h
		42	41.963046	32.9 y
K	19	37	36.973376	1.23 s
		38	37.969081	7.64 m
		39	38.963707	*93.26%*
		40	39.963998	1.25 Gy
		41	40.961826	*6.73%*
		42	41.962403	12.3 h
		43	42.960716	22.3 h
Ca	20	38	37.976318	0.44 s
		39	38.970720	0.86 s
		40	39.962591	*96.94%*
		41	40.962278	0.103 My
		42	41.958618	*0.647%*
		43	42.958767	*0.135%*
		44	43.955482	*2.09%*
		45	44.956187	163 d
		46	45.953693	*0. 0035%*
		47	46.954546	4.54 d
		48	47.952534	*0.187%*
		49	48.955674	8.72 m
Sc	21	43	42.961151	3.89 h
		44	43.959403	3.97 h
		45	44.955912	*100%*
		46	45.955172	83.8 d
		47	46.952408	3.35 d
		48	47.952231	43.7 h
Ti	22	44	43.959690	60 y
		45	44.958126	3.08 h
		46	45.952632	*8.25%*
		47	46.951763	*7.44%*
		48	47.947946	*73.72%*
		49	48.947870	*5.41%*
		50	49.944791	*5.18%*
		51	50.946615	5.76 m
		52	51.946897	1.7 m
V	23	48	47.952254	16.0 d
		49	48.948516	329 d
		50	49.947158	*0.250%*
		51	50.943960	*99.750%*
		52	51.944775	3.74 m
		53	52.944338	1.60 m
Cr	24	48	47.954032	21.6 h
		49	48.951336	42.3 m
		50	49.946044	*4.35%*
		51	50.944767	27.7 d
		52	51.940507	*83.79%*
		53	52.940649	*9.50%*
		54	53.938880	*2.36%*
		55	54.940840	3.50 m
		56	55.940653	5.94 m
Mn	25	52	51.945565	5.59 d
		53	52.941290	3.7 My
		54	53.940359	312 d
		55	54.938045	*100%*
		56	55.938905	2.58 h
		57	56.938285	85.4 s
Fe	26	52	51.948114	8.27 h
		53	52.945308	8.51 m
		54	53.939611	*5.85%*
		55	54.938293	2.74 y
		56	55.934937	*91.75%*
		57	56.935394	*2.12%*
		58	57.933276	*0.28%*
		59	58.934875	44.5 d
		60	59.934072	1.5 My
		61	60.936745	6.0 m
Co	27	57	56.936291	272 d
		58	57.935753	70.8 d
		59	58.933195	*100%*
		60	59.933817	5.27 y
		61	60.932476	1.65 h
Ni	28	56	55.942132	6.08 d
		57	56.939794	35.6 h
		58	57.935343	*68.08%*
		59	58.934347	0.076 My
		60	59.930786	*26.22%*
		61	60.931056	*1.14%*
		62	61.928345	*3.63%*
		63	62.929669	100 y
		64	63.927966	*0.93%*
		65	64.930084	2.52 h
Cu	29	61	60.933458	3.33 h
		62	61.932584	9.67 m
		63	62.929597	*69.17%*
		64	63.929764	12.7 h
		65	64.927789	*30.83%*
		66	65.928869	5.12 m
		67	66.927730	61.8 h

	Z	*A*	Atomic mass (u)	*Abundance* or Half-life
Zn	30	62	61.934330	9.19 h
		63	62.933212	38.5 m
		64	63.929142	*48.6%*
		65	64.929241	244 d
		66	65.926033	*27.9%*
		67	66.927127	*4.1%*
		68	67.924844	*18.8%*
		69	68.926550	56 m
		70	69.925319	*0.62%*
		71	70.927722	2.45 m
Ga	31	67	66.928202	3.26 d
		68	67.927980	67.7 m
		69	68.925574	*60.11%*
		70	69.926022	21.1 m
		71	70.924701	*39.89%*
		72	71.926366	14.1 h
		73	72.925175	4.86 h
Ge	32	68	67.928094	271 d
		69	68.927965	39.0 h
		70	69.924247	*20.4%*
		71	70.924951	11.4 d
		72	71.922076	*27.3%*
		73	72.923459	*7.8%*
		74	73.921178	*36.7%*
		75	74.922859	82.8 m
		76	75.921403	*7.8%*
		77	76.923549	11.3 h
As	33	73	72.923825	80.3 d
		74	73.923929	17.8 d
		75	74.921596	*100%*
		76	75.922394	26.3 h
		77	76.920647	38.8 h
Se	34	72	71.927112	8.4 d
		73	72.926765	7.1 h
		74	73.922476	*0.89%*
		75	74.922523	120 d
		76	75.919214	*9.4%*
		77	76.919914	*7.6%*
		78	77.917309	*23.8%*
		79	78.918499	0.30 My
		80	79.916521	*49.6%*
		81	80.917992	18.5 m
		82	81.916699	*8.7%*
		83	82.919118	22.3 m
Br	35	77	76.921379	57.0 h
		78	77.921146	6.46 m
		79	78.918337	*50.69%*
		80	79.918529	17.7 m
		81	80.916291	*49.31%*
		82	81.916804	35.3 h
		83	82.915180	2.40 h
Kr	36	76	75.925910	14.8 h
		77	76.924670	74.4 m
		78	77.920365	*0.35%*
		79	78.920082	35.0 h
		80	79.916379	*2.28%*
		81	80.916592	0.229 My
		82	81.913484	*11.58%*
		83	82.914136	*11.49%*
		84	83.911507	*57.00%*
		85	84.912527	10.8 y
		86	85.910611	*17.30%*
		87	86.913355	76.3 m
Rb	37	83	82.915110	86.2 d
		84	83.914385	33.1 d
		85	84.911790	*72.17%*
		86	85.911167	18.6 d
		87	86.909181	*27.83%*
		88	87.911316	17.8 m
Sr	38	82	81.918402	25.6 d
		83	82.917557	32.4 h
		84	83.913425	*0.56%*
		85	84.912933	64.8 d
		86	85.909260	*9.86%*
		87	86.908877	*7.00%*
		88	87.905612	*82.58%*
		89	88.907451	50.6 d
		90	89.907738	28.9 y
Y	39	87	86.910876	79.8 h
		88	87.909501	106.6 d
		89	88.905848	*100%*
		90	89.907152	64.1 h
		91	90.907305	58.5 d
Zr	40	88	87.910227	83.4 d
		89	88.908890	78.4 h
		90	89.904704	*51.45%*
		91	90.905646	*11.22%*
		92	91.905041	*17.15%*
		93	92.906476	1.53 My
		94	93.906315	*17.38%*
		95	94.908043	64.0 d
		96	95.908273	*2.80%*
		97	96.910953	16.7 h

	Z	*A*	Atomic mass (u)	*Abundance* or Half-life
Nb	41	91	90.906996	680 y
		92	91.907194	35 My
		93	92.906378	*100%*
		94	93.907284	20,300 y
		95	94.906836	35.0 d
Mo	42	90	89.913937	5.56 h
		91	90.911750	15.5 m
		92	91.906811	*14.8%*
		93	92.906813	4000 y
		94	93.905088	*9.3%*
		95	94.905842	*15.9%*
		96	95.904679	*16.7%*
		97	96.906021	*9.6%*
		98	97.905408	*24.1%*
		99	98.907712	65.9 h
		100	99.907477	*9.6%*
		101	100.910347	14.6 m
Tc	43	95	94.907657	20.0 h
		96	95.907871	4.3 d
		97	96.906365	4.2 My
		98	97.907216	4.2 My
		99	98.906255	0.211 My
		100	99.907658	15.8 s
Ru	44	94	93.911360	51.8 m
		95	94.910413	1.64 h
		96	95.907598	*5.5%*
		97	96.907555	2.79 d
		98	97.905287	*1.86%*
		99	98.905939	*12.8%*
		100	99.904219	*12.6%*
		101	100.905582	*17.1%*
		102	101.904349	*31.6%*
		103	102.906324	39.3 d
		104	103.905433	*18.6%*
		105	104.907753	4.44 h
Rh	45	101	100.906164	3.3 y
		102	101.906843	207 d
		103	102.905504	*100%*
		104	103.906656	42.3 s
		105	104.905694	35.4 h

	Z	*A*	Atomic mass (u)	*Abundance* or Half-life
Pd	46	100	99.908506	3.63 d
		101	100.908289	8.47 h
		102	101.905609	*1.02%*
		103	102.906087	17.0 d
		104	103.904036	*11.14%*
		105	104.905085	*22.33%*
		106	105.903486	*27.33%*
		107	106.905133	6.5 My
		108	107.903892	*26.46%*
		109	108.905950	13.7 h
		110	109.905153	*11.72%*
		111	110.907671	23.4 m
Ag	47	105	104.906529	41.3 d
		106	105.906669	24.0 m
		107	106.905097	*51.84%*
		108	107.905956	2.37 m
		109	108.904752	*48.16%*
		110	109.906107	24.6 s
Cd	48	104	103.909849	57.7 m
		105	104.909468	55.5 m
		106	105.906459	*1.25%*
		107	106.906618	6.50 h
		108	107.904184	*0.89%*
		109	108.904982	461 d
		110	109.903002	*12.5%*
		111	110.904178	*12.8%*
		112	111.902758	*24.1%*
		113	112.904402	*12.2%*
		114	113.903359	*28.7%*
		115	114.905431	53.5 h
		116	115.904756	*7.5%*
		117	116.907219	2.49 h
In	49	111	110.905103	2.80 d
		112	111.905532	15.0 m
		113	112.904058	*4.29%*
		114	113.904914	71.9 s
		115	114.903878	*95.71%*
		116	115.905260	14.1 s

	Z	*A*	Atomic mass (u)	*Abundance* or Half-life
Sn	50	110	109.907843	4.11 h
		111	110.907734	35.3 m
		112	111.904818	*0.97%*
		113	112.905171	115.1 d
		114	113.902779	*0.66%*
		115	114.903342	*0.34%*
		116	115.901741	*14.54%*
		117	116.902952	*7.68%*
		118	117.901603	*24.22%*
		119	118.903308	*8.59%*
		120	119.902195	*32.58%*
		121	120.904235	27.0 h
		122	121.903439	*4.63%*
		123	122.905721	129 d
		124	123.905274	*5.79%*
		125	124.907784	9.64 d
		126	125.907653	0.23 My
Sb	51	119	118.903942	38.2 h
		120	119.905072	15.9 m
		121	120.903816	*57.21%*
		122	121.905174	2.72 d
		123	122.904214	*42.79%*
		124	123.905936	60.1 d
		125	124.905254	2.76 y
Te	52	118	117.905828	6.00 d
		119	118.906404	16.1 h
		120	119.904020	*0.09%*
		121	120.904936	19.2 d
		122	121.903044	*2.55%*
		123	122.904270	*0.89%*
		124	123.902818	*4.74%*
		125	124.904431	*7.07%*
		126	125.903312	*18.84%*
		127	126.905226	9.35 h
		128	127.904463	*31.74%*
		129	128.906598	69.6 m
		130	129.906224	*34.08%*
		131	130.908524	25.0 m
I	53	125	124.904630	59.4 d
		126	125.905624	12.9 d
		127	126.904473	*100%*
		128	127.905809	25.0 m
		129	128.904988	15.7 My
		130	129.906674	12.4 h
Xe	54	122	121.908368	20.1 h
		123	122.908482	2.08 h
		124	123.905893	*0.095%*
		125	124.906395	16.9 h
		126	125.904274	*0.089%*
		127	126.905184	36.4 d
		128	127.903531	*1.91%*
		129	128.904779	*26.40%*
		130	129.903508	*4.07%*
		131	130.905082	*21.23%*
		132	131.904153	*26.91%*
		133	132.905911	5.24 d
		134	133.905394	*10.44%*
		135	134.907227	9.14 h
		136	135.907219	*8.86%*
		137	136.911562	3.82 m
Cs	55	131	130.905464	9.69 d
		132	131.906434	6.48 d
		133	132.905452	*100%*
		134	133.906718	2.06 y
		135	134.905977	2.3 My
		136	135.907312	13.0 d
Ba	56	128	127.908318	2.43 d
		129	128.908679	2.23 h
		130	129.906321	*0.106%*
		131	130.906941	11.5 d
		132	131.905061	*0.101%*
		133	132.906007	10.5 y
		134	133.904508	*2.42%*
		135	134.905689	*6.59%*
		136	135.904576	*7.85%*
		137	136.905827	*11.23%*
		138	137.905247	*71.70%*
		139	138.908841	83.1 m
La	57	136	135.907636	9.87 m
		137	136.906494	60,000 y
		138	137.907112	*0.090%*
		139	138.906353	*99.910%*
		140	139.909478	1.68 d
		141	140.910962	3.92 h

	Z	*A*	Atomic mass (u)	*Abundance* or Half-life
Ce	58	134	133.908925	76 h
		135	134.909151	17.7 h
		136	135.907172	*0.185%*
		137	136.907806	9.0 h
		138	137.905991	*0.251%*
		139	138.906653	137.6 d
		140	139.905439	*88.45%*
		141	140.908276	32.5 d
		142	141.909244	*11.11%*
		143	142.912386	33.0 h
		144	143.913647	285 d
Pr	59	139	138.908938	4.41 h
		140	139.909076	3.39 m
		141	140.907653	*100%*
		142	141.910045	19.1 h
		143	142.910817	13.6 d
Nd	60	140	139.909552	3.37 d
		141	140.909610	2.49 h
		142	141.907723	*27.2%*
		143	142.909814	*12.2%*
		144	143.910087	*23.8%*
		145	144.912574	*8.3%*
		146	145.913117	*17.2%*
		147	146.916100	11.0 d
		148	147.916893	*5.7%*
		149	148.920149	1.73 h
		150	149.920891	*5.6%*
		151	150.923829	12.4 m
Pm	61	143	142.910933	265 d
		144	143.912591	363 d
		145	144.912749	17.7 y
		146	145.914696	5.53 y
		147	146.915139	2.62 y
		148	147.917475	5.37 d
		149	148.918334	53.1 h
Sm	62	142	141.915198	72.5 m
		143	142.914628	8.75 m
		144	143.911999	*3.1%*
		145	144.913410	340 d
		146	145.913041	103 My
		147	146.914898	*15.0%*
		148	147.914823	*11.2%*
		149	148.917185	*13.8%*
		150	149.917276	*7.4%*
		151	150.919932	90 y
		152	151.919732	*26.7%*
		153	152.922097	46.3 h
		154	153.922209	*22.7%*
		155	154.924640	22.3 m

	Z	*A*	Atomic mass (u)	*Abundance* or Half-life
Eu	63	149	148.917931	93.1 d
		150	149.919702	36.9 y
		151	150.919850	*47.81%*
		152	151.921745	13.5 y
		153	152.921230	*52.19%*
		154	153.922979	8.59 y
		155	154.922893	4.75 y
		156	155.924752	15.2 d
Gd	64	150	149.918659	1.79 My
		151	150.920348	124 d
		152	151.919791	*0.20%*
		153	152.921750	240 d
		154	153.920866	*2.18%*
		155	154.922622	*14.80%*
		156	155.922123	*20.47%*
		157	156.923960	*15.65%*
		158	157.924104	*24.84%*
		159	158.926389	18.5 h
		160	159.927054	*21.9%*
		161	160.929669	3.66 m
Tb	65	157	156.924025	71 y
		158	157.925413	180 y
		159	158.925347	*100%*
		160	159.927168	72.3 d
		161	160.927570	6.91 d
Dy	66	154	153.924424	3.0 My
		155	154.925754	9.9 h
		156	155.924283	*0.06%*
		157	156.925466	8.1 h
		158	157.924409	*0.10%*
		159	158.925739	144.4 d
		160	159.925198	*2.3%*
		161	160.926933	*18.9%*
		162	161.926798	*25.5%*
		163	162.928731	*24.9%*
		164	163.929175	*28.2%*
		165	164.931703	2.33 h
Ho	67	163	162.928734	4570 y
		164	163.930234	29 m
		165	164.930322	*100%*
		166	165.932284	26.8 h
		167	166.933133	3.0 h

	Z	*A*	Atomic mass (u)	*Abundance* or Half-life
Er	68	160	159.929083	28.6 h
		161	160.929995	3.21 h
		162	161.928778	*0.14%*
		163	162.930033	75.0 m
		164	163.929200	*1.60%*
		165	164.930726	10.4 h
		166	165.930293	*33.50%*
		167	166.932048	*22.87%*
		168	167.932370	*26.98%*
		169	168.934590	9.39 d
		170	169.935464	*14.91%*
		171	170.938030	7.52 h
Tm	69	167	166.932852	9.25 d
		168	167.934173	93.1 d
		169	168.934213	*100%*
		170	169.935801	128.6 d
		171	170.936429	1.92 y
Yb	70	166	165.933882	56.7 h
		167	166.934950	17.5 m
		168	167.933897	*0.13%*
		169	168.935190	32.0 d
		170	169.934762	*3.0%*
		171	170.936326	*14.3%*
		172	171.936381	*21.8%*
		173	172.938211	*16.1%*
		174	173.938862	*31.8%*
		175	174.941276	4.19 d
		176	175.942572	*12.8%*
		177	176.945261	1.9 h
Lu	71	173	172.938931	1.37 y
		174	173.940337	3.3 y
		175	174.940772	*97.41%*
		176	175.942686	*2.59%*
		177	176.943758	6.65 d
Hf	72	172	171.939448	1.87 y
		173	172.940513	23.6 h
		174	173.940046	*0.16%*
		175	174.941509	70 d
		176	175.941409	*5.26%*
		177	176.943221	*18.60%*
		178	177.943699	*27.28%*
		179	178.945816	*13.62%*
		180	179.946550	*35.08%*
		181	180.949101	42.4 d
Ta	73	179	178.945930	1.82 y
		180	179.947465	*0.012%*
		181	180.947996	*99.988%*
		182	181.950152	114 d
W	74	178	177.945876	21.6 d
		179	178.947070	37.0 m
		180	179.946704	*0.12%*
		181	180.948197	121 d
		182	181.948204	*26.5%*
		183	182.950223	*14.3%*
		184	183.950931	*30.6%*
		185	184.953419	75.1 d
		186	185.954364	*28.4%*
		187	186.957160	23.7 h
Re	75	183	182.950820	70.0 d
		184	183.952521	38.0 d
		185	184.952955	*37.40%*
		186	185.954986	3.72 d
		187	186.955753	*62.60%*
		188	187.958114	17.0 h
Os	76	182	181.952110	22.1 h
		183	182.953126	13.0 h
		184	183.952489	*0.02%*
		185	184.954042	93.6 d
		186	185.953838	*1.6%*
		187	186.955750	*1.6%*
		188	187.955838	*13.3%*
		189	188.958147	*16.2%*
		190	189.958447	*26.4%*
		191	190.960930	15.4 d
		192	191.961481	*40.9%*
		193	192.964152	30.1 h
Ir	77	189	188.958719	13.2 d
		190	189.960546	11.8 d
		191	190.960594	*37.3%*
		192	191.962605	73.8 d
		193	192.962926	*62.7%*
		194	193.965078	19.3 h
Pt	78	188	187.959395	10.2 d
		189	188.960834	10.9 h
		190	189.959932	*0.014%*
		191	190.961677	2.86 d
		192	191.961038	*0.78%*
		193	192.962987	50 y
		194	193.962680	*32.97%*
		195	194.964791	*33.83%*
		196	195.964952	*25.24%*
		197	196.967340	19.9 h
		198	197.967893	*7.16%*
		199	198.970593	30.8 m

	Z	*A*	Atomic mass (u)	*Abundance* or Half-life
Au	79	195	194.965035	186 d
		196	195.966570	6.17 d
		197	196.966569	*100%*
		198	197.968242	2.696 d
		199	198.968765	3.14 d
Hg	80	194	193.965439	444 y
		195	194.966720	10.5 h
		196	195.965833	*0.15%*
		197	196.967213	64.1 h
		198	197.966769	*10.0%*
		199	198.968280	*16.9%*
		200	199.968326	*23.1%*
		201	200.970302	*13.2%*
		202	201.970643	*29.9%*
		203	202.972872	46.6 d
		204	203.973494	*6.9%*
		205	204.976073	5.1 m
Tl	81	201	200.970819	72.9 h
		202	201.972106	12.2 d
		203	202.972344	*29.52%*
		204	203.973864	3.78 y
		205	204.974428	*70.48%*
		206	205.976110	4.20 m
Pb	82	202	201.972159	53,000 y
		203	202.973391	51.9 h
		204	203.973044	*1.4%*
		205	204.974482	17.3 My
		206	205.974465	*24.1%*
		207	206.975897	*22.1%*
		208	207.976652	*52.4%*
		209	208.981090	3.25 h
Bi	83	207	206.978471	32.9 y
		208	207.979742	0.368 My
		209	208.980399	*100%*
		210	209.984120	5.01 d
		211	210.987269	2.14 m
Po	84	207	206.981593	5.80 h
		208	207.981246	2.90 y
		209	208.982430	102 y
		210	209.982874	138.4 d
At	85	209	208.986173	5.41 h
		210	209.987148	8.1 h
		211	210.987496	7.21 h
Rn	86	211	210.990601	14.6 h
		222	222.017578	3.82 d
Fr	87	212	211.996202	20.0 m
		223	223.019736	22.0 m
Ra	88	223	223.018502	11.43 d
		224	224.020212	3.63 d
		225	225.023612	14.9 d
		226	226.025410	1600 y
Ac	89	225	225.023230	10.0 d
		226	226.026098	29.4 h
		227	227.027752	21.77 y
Th	90	228	228.028741	1.91 y
		229	229.031762	7340 y
		230	230.033134	75,400 y
		231	231.036304	25.52 h
		232	232.038055	*100%*
		233	233.041582	21.8 m
Pa	91	230	230.034541	17.4 d
		231	231.035884	32,800 y
		232	232.038592	1.31 d
		234	234.043308	6.70 h
U	92	233	233.039635	0.1592 My
		234	234.040952	0.2455 My
		235	235.043930	*0.720%*
		236	236.045568	23.42 My
		237	237.048730	6.75 d
		238	238.050788	*99.274%*
		239	239.054293	23.5 m
Np	93	236	236.046570	0.154 My
		237	237.048173	2.14 My
		238	238.050946	2.117 d
Pu	94	238	238.049560	87.74 y
		239	239.052163	24,100 y
		240	240.053814	6561 y
		241	241.056851	14.3 y
		242	242.058743	0.375 My
Am	95	241	241.056829	432 y
		242	242.059549	16.0 h
		243	243.061381	7370 y
Cm	96	246	246.067224	4760 y
		247	247.070354	15.6 My
		248	248.072349	0.348 My
Bk	97	247	247.070307	1380 y
Cf	98	251	251.079587	898 y
		254	254.087323	60.5 d

	Z	*A*	Atomic mass (u)	*Abundance* or Half-life
Es	99	252	252.082979	472 d
Fm	100	257	257.095105	100.5 d
Md	101	258	258.098431	51.5 d
No	102	259	259.101031	58 m
Lr	103	260	260.105504	3.0 m
Rf	104	261	261.108767	65 s
Db	105	262	262.114084	35 s
Sg	106	261	261.116117	0.23 s
Bh	107	262	262.122892	0.10 s
Hs	108	264	264.128395	0.8 ms
Mt	109	266	266.137299	1.7 ms
Ds	110	270	270.144720	0.5 ms
Rg	111	272	272.153615	4 ms

ANSWERS TO ODD-NUMBERED PROBLEMS

Chapter 1

1. 4.527×10^6 m/s
3. (*a*) -7.79×10^5 m/s
   (*b*) 1.008×10^{-13} J, 3.995×10^{-13} J
5. (*a*) 2.13×10^6 m/s
   (*b*) 1.28×10^6 m/s
7. 4.34×10^{-5}
9. $6.1 \times 10^{-6} N$
11. $35.3^\circ, v/\sqrt{2}, v/\sqrt{6}$
13. 2.47×10^6 m/s, -0.508×10^6 m/s
15. (*a*) 0.0104 eV (*b*) 2550 m
17. 4.61×10^{12} rad/s

Chapter 2

1. 101 km/h at 62° east of south
3. 7×10^4 m/s
5. 2.6×10^8 m/s
7. (*a*) 357.1 ns (*b*) 103 m (*c*) 28.8 m
11. $0.402c$
13. 5.0×10^7 m/s
17. $+0.937c, -0.572c$
19. (*a*) $+0.508\mu$s (*b*) -81.5 m
21. (*a*) 2:00 P.M. (*b*) 3:00 P.M.
    (*c*) 1:00 P.M. and 3:00 P.M.
23. 8 y
25. (*a*) $K_i' = K_f' = 0.512mc^2$
    (*b*) $K_i = K_f = 0.458mc^2$
27. $0.958c$
29. $v < 0.115c$
33. (*a*) 773 MeV/c^2 (*b*) 1227 MeV
35. 4.4×10^{-16} kg
37. $p_e = 10.5$ MeV/c, $K_e = 10.0$ MeV
    $p_p = 137.4$ MeV/c, $K_p = 10.0$ MeV
39. (*a*) 1268.1 MeV (*b*) 298.8 MeV/c
    (*c*) 1232 MeV
41. $0.981c$
43. 64.38 μs
45. (*a*) $0.99875c$ (*b*) 400.5 y
47. 2.34 km, 1.07 μs
49. (*a*) 0.648 μs (*b*) 335 m
51. (*a*) $E' = mc^2/\sqrt{(1-u^2/c^2)(1-v^2/c^2)}$

$$p' = \frac{m\sqrt{u^2+v^2-u^2v^2/c^2}}{\sqrt{(1-u^2/c^2)(1-v^2/c^2)}}$$

    (*b*) m^2c^4
53. (*a*) 3.1 MeV (*b*) 7.8 MeV
55. $0.508c$
57. 267.0 MeV, 28.9 MeV

Chapter 3

1. 1.32 mm
3. (*a*) 0.388 nm (*b*) 7.2°
5. (*a*) 1.00×10^7 eV/c, 5.33×10^{-21} kg·m/s
   (*b*) 2.5×10^4 eV/c, 1.3×10^{-23} kg·m/s
   (*c*) 1.2 eV/c, 6.6×10^{-28} kg·m/s
   (*d*) 6.2×10^{-7} eV/c, 3.3×10^{-34} kg·m/s
7. (*a*) 0.124 nm (*b*) 1.24×10^{-3} nm
   (*c*) 1.8 eV to 3.5 eV
9. 0.964 V
11. (*a*) 4.88 eV
19. 1.1 mm, 1.1×10^{-3} eV
21. 0.33 W
23. (*a*) 1.9×10^5 W/m^2 (*b*) 0.26%
25. (*a*) 10.33 keV (*b*) 0.06 keV
29. 3.9×10^{-4} eV
31. 1.17 eV
33. 2.28 eV, 4.10×10^{-15} eV/s
35. (*a*) 2.52 μm (*b*) 0.405
37. 2.724 K
39. (*a*) 5.79×10^{-10} W/m^2, 1.91×10^{-11} W/m^2
    (*b*) 1.81×10^8/s, 2.97×10^7/s
41. 4.1 m/s

Chapter 4

1. (*a*) 13 fm (*b*) 0.025 fm (*c*) 0.73 nm
3. (*a*) $0.143c$ (*b*) -9.72 MV
5. (*a*) $+0.010$ V (*b*) $+100$ V (*c*) $+1.0 \times 10^9$ V
7. (*a*) 88 MeV (*b*) 4.2 MeV (*c*) 1.1 MeV
9. 33 nm
11. $15.2^\circ (n = 1), 31.8^\circ (n = 2), 52.2^\circ (n = 3)$
13. (*a*) 660 m (*b*) 0.33 m
    (*c*) 0.017 mm (*d*) 0.050 Hz
15. 8.4×10^4 Hz
17. 5.8 nm
19. 33 MeV
21. 5.5×10^{-7} eV
23. 0.052 MeV
29. $v_{\text{group}} = 1.5 v_{\text{phase}}$
31. (*b*) 1.50 eV, 6.00 eV, 13.5 eV
33. (*a*) 0.0279 eV (*b*) 3.3 nm (*c*) 2.1 K
35. (*a*) 0.71 MeV (*b*) 0.66 MeV
37. (*a*) 135 MeV (*b*) 4.87×10^{-24} s (*c*) 1.46 fm
39. 3×10^{-9} m

Chapter 5

1. (*b*) $-(B/m)\sqrt{2H/g}, H(1 + B/mg)$
3. 1.1 eV
5. 150 eV, 600 eV, 1350 eV
7. (*a*) $c = a^2 b^2, d = a(b + 1)$
   (*b*) $w = a(2b + 1)$
9. $U(x) = -\hbar^2 b/mx, E = -\hbar^2 b^2/2m$
11. 10.1 eV, 18.9 eV
15. (*a*) 2.63×10^{-5} (*b*) 0.0106 (*c*) 5.42×10^{-3}
17. $5.00E_0, 10.00E_0$
19. $3E_0, 6E_0, 9E_0, 11E_0, 12E_0, \ldots$
21. (*b*) $\sqrt{3\hbar\omega_0/k}, \sqrt{5\hbar\omega_0/k}$
23. (*a*) 0 (*b*) $\hbar\omega_0 m/2$
25. $A^2 dx, 0.368A^2 dx$
27. $B = D = -A\sqrt{E/(U_0 - E)}$
31. (*a*) 2160 eV (*b*) 4.70×10^4 eV/c
    (*c*) 4.2×10^{-3} nm
35. (*b*) $\hbar^2 n^2/4L^2$
37. 0.157

Chapter 6

3. (*a*) 6.57×10^{15} Hz, 45.7 nm
   (*b*) 3.48×10^{15} Hz, 86.2 nm
5. (*a*) 22.8 fm (*b*) 55.0 fm
   (*c*) 4.14 MeV, 0.86 MeV
7. 14 fm
9. (*a*) 8.4 MeV (*b*) 1.61 fm
   (*c*) 6.00 fm (*d*) 8.3×10^{-6}
11. 0.63 MeV
13. 28.2 fm, 19.9 fm, 38.9°
15. 121.51 nm, 102.52 nm, 97.21 nm
17. 2279 nm
19. 91.13 nm, 820.1 nm
21. $\Delta E = 0.306$ eV, 0.97 eV, 2.86 eV, 13.1 eV
23. 7.4 eV
27. -54.40 eV, -13.60 eV, -6.04 eV, -3.40 eV
31. 2.10 eV
33. (*a*) 6.58×10^{12} Hz, 7.72×10^{12} Hz
    (*b*) 6.58×10^9 Hz, 6.68×10^9 Hz
35. (*a*) 15 (*b*) 5 (*c*) 1
37. 7×10^{-8} eV
39. 48.23 nm
41. (*a*) 0.440 nm (*b*) 11.3%

Chapter 7

1. $-me^4/32\pi^2\varepsilon_0^2\hbar^2$
3. 0.0108
5. $35^\circ, 66^\circ, 90^\circ, 114^\circ, 145^\circ$
7. (*a*) 0, 1, 2, 3, 4, 5 (*b*) +6 to −6 in integer steps
   (*c*) 5 (*d*) 4
11. (*a*) 0, 0 (*b*) $0, 3.2 \times 10^{-11}$
    (*c*) $0, 3.2 \times 10^{-11}$
    (*d*) $1.1 \times 10^{-11}, 2.2 \times 10^{-11}$
13. $(3 \pm \sqrt{5})a_0$
15. 0.0054
17. Minima: $55^\circ, 125^\circ$ Maxima: $0^\circ, 90^\circ, 180^\circ$
21. $3s, 2s, 1s, 3d$
23. (*a*) $7s, 7p, 7d, 7f, 7g, 7h, 7i$
    (*b*) $6p, 6f, 5p, 5f, 4p, 4f, 3p, 2p$
25. (*a*) 656.112 nm, 656.182 nm, 656.042 nm
27. $1.89 \text{ eV} \pm 2.55 \times 10^{-5}$ eV,
    $1.89 \text{ eV} \pm 1.95 \times 10^{-5}$ eV
29. 0.651, 0.440
31. $6a_0, 5a_0$
33. 3.3 mm

Chapter 8

1. (*a*) $(2, 1, +1, +1/2), (2, 1, +1, -1/2), \ldots$
   (*b*) 36 (*c*) 30 (*d*) 36
3. (*a*) 14 (*b*) +3/2 (*c*) +8
   (*d*) +2 (*e*) +10
5. (*a*) N, P, As, Sb, Bi
   (*b*) Co, Rh, Ir, Mt
7. (*a*) $[\text{Ar}]4s^2 3d^6$ (*b*) +2
   (*c*) +2 (*d*) +3, +1
9. -1.51 eV, —0.85 eV

11. (*a*) 0.045 eV (*b*) 3.374 eV, 4.373 eV, 4.750 eV (*c*) 3.54 eV, 2.02 eV
13. 3.68 eV, 15.5 eV, 63.7 eV
15. (*a*) 5, 1 (*b*) 2, 4 (*c*) 2, 1
17. 0, 1, 2, 3, 4; 0,1
19. (*a*) 1.12×10^{16} photons/s (*b*) 763 V/m
21. (*a*) 1.84 (*b*) 1.00
23. $1.40\,\text{eV}^{1/2}$, 6.4
25. (*a*) 670.8 nm (*b*) 58.4 nm (*c*) 230 nm, 50.6 nm

Chapter 9

1. 15.4 eV
3. (*a*) 4.25 eV/molecule (*c*) 9.80 eV/molecule
5. (*a*) Li_2 (*c*) CO
7. 5.11 eV
9. (*a*) $30.9 \times 10^{-30}\ \text{C}\cdot\text{m}$ (*b*) 88%
11. 42.7%
13. $4.689 \times 10^3\ \text{eV/nm}^2$
15. (*a*) 0.2626 eV (*b*) 0.2579 eV
17. 23.1 mm, 11.6 mm, 7.71 mm
19. 2.00×10^{-6} eV
23. $hf - 2B(L+1), hf + 2BL$
31. (*a*) 0.27 eV, 0.23 eV, 0.19 eV (*b*) 4.56 eV, 4.60 eV
33. (*a*) 0.317 eV (*b*) $2.37 \times 10^{21}\ \text{eV/m}^2$ (*c*) 2.1×10^{-3} eV
35. (*a*) 8.2×10^{-2} (*b*) 6.8×10^{-3}
37. (*a*) 2.99, 4.97, 6.91 (*b*) 2.94, 4.70, 6.18
39. (*a*) 194.4 μeV

Chapter 10

1. (*a*) 3 (*b*) 3, 6, 1 (*c*) 20%, 40%
3. (*a*) 6 (*b*) 2 (*c*) 4, 2
7. (*a*) +3 (1), +2 (2), +1 (3), 0 (4), . . . (*b*) 3 (7), 2 (5), 1 (3), 0 (1) (*c*) +3 (1), +2 (1), +1 (2), 0 (2), . . .
9. $2\pi(2s+1)m/\hbar^2$
11. $2.7 \times 10^{23}\ \text{m}^{-3}$
13. 0.65, 0.29, 0.06
15. (*a*) 0.0379 eV (*b*) 2.78×10^{21}
17. (*a*) 554 μeV (*b*) 0.066 μeV
19. (*a*) 10^3 atm (*b*) 2.9 K
21. (*a*) $1.84 \times 10^7\ \text{eV/m}^3$ (*b*) 0.035 (*c*) 2.3×10^{-17}
23. 7.04 eV, 4.22 eV
25. (*a*) $4.37 \times 10^{-36}\ \text{m}^{-3}$ (*b*) $6.00 \times 10^{-6}\ \text{m}^{-3}$
27. (*b*) 8.6 km (*c*) $2.2 \times 10^{18}\ \text{kg/m}^3$
29. 0.078 J/K
31. (*a*) $e^{-E/kT}$ (*b*) $E/(e^{E/kT}+1)$ (*c*) $NE/(e^{E/kT}+1)$ (*d*) $R(E/kT)^2 e^{E/kT}/(e^{E/kT}+1)^2$
33. (*a*) 0.3295, 0.3333, 0.3372
35. 0.12 eV
37. 17.1 MeV, 22.9 MeV
39. (*a*) 2.83×10^{-3} nm (*b*) 1.39×10^{-3} nm
41. (*a*) 2.78 ± 0.06 K (*b*) 0.0137 ± 0.0017

Chapter 11

1. (*a*) 1/8 (*b*) $a = 2r$ (*c*) 0.5236
5. (*a*) 6.82 eV (*b*) 6.45 eV (*c*) 3.27 eV
7. −8.96 eV, 1.00 eV
9. 0.255 nm
11. 3.23 K
13. 91.1 K
15. (*a*) 7.09 eV (*b*) 0.11 eV
17. $2.3 \times 10^{24}\ \text{m}^{-3}$
19. 7080 K
21. $426\ \text{W/K}\cdot\text{m}$
23. 790
25. (*a*) 0.20 MeV (*b*) 6.3 mm
27. 603 MHz
29. (*a*) $1.9 \times 10^{-28}, 3.5 \times 10^{-10}$
31. (*a*) −0.094 eV (*b*) −0.040 eV
33. 4.2×10^{-6}
35. 6.8×10^{-5} mA
37. (*a*) 57% and 43% (*b*) 89% and 11%
39. (*a*) 0.4997, 0.5003 (*b*) 0.480, 0.520
41. (*a*) 10.8×10^{-6} (*b*) -45.3×10^{-6}
49. (*a*) 135 K (*b*) 165 K, $1.40m_e$
51. (*a*) 1.00×10^6 (*b*) $1.00 \times 10^3, 1.00 \times 10^{-3}$ (*c*) 0.662 keV

Chapter 12

1. (*a*) $^{19}_{9}\text{F}_{10}$ (*b*) $^{199}_{79}\text{Au}_{120}$ (*c*) $^{107}_{47}\text{Ag}_{60}$
3. (*a*) 15 MeV (*b*) 824 MeV
5. (*a*) 1636.4 MeV, 7.868 MeV (*b*) 1118.5 MeV, 8.410 MeV
7. 7.718 MeV, 8.482 MeV
9. (*a*) 19.814 MeV (*b*) 15.958 MeV
11. 2.5×10^{-3} fm
13. ^{160}Dy: yes, ^{164}Dy: no
15. (*a*) 35 min (*b*) $0.020\ \text{min}^{-1}$ (*c*) $46\ \text{s}^{-1}$
17. 0.0598
19. (*a*) 0.85 μCi (*b*) 0.13%
21. (*a*) Yes (*b*) No (*c*) Yes

25. 0.864 MeV
27. 0.412 MeV, 1.088 MeV, 0.676 MeV
29. 100.1 keV, 300.9 keV, 200.8 keV, ...
31. (*a*) 6 (*b*) 4 (*c*) 42.659 MeV (*d*) 27.8 μW
33. 12.6 fm
35. 37.5 μCi
39. 1.93 mW
41. $1.04 \times 10^{-20}\ s^{-1}, 9.0 \times 10^{8}\ s^{-1}$
43. (*a*) 7.52×10^{-4} MeV (*b*) 3.26×10^{-4} MeV
45. (*a*) 4.67×10^{-9} eV (*b*) 1.95×10^{-3} eV (*c*) 0.097 mm/s

Chapter 13

1. (*a*) ${}_{1}^{1}H_{0}$ (*c*) ${}_{15}^{30}P_{15}$
3. 98 b
5. 8.6×10^{-4} b
7. (*a*) 0.5 (*b*) 0.75 (*c*) 0.9325
11. 1.58 μCi
13. (*a*) −10.313 MeV (*b*) 2.314 MeV
15. 12.201 MeV, 11.152 MeV or 22.706 MeV, 0.647 MeV
17. (*a*) 235.3 MeV (*b*) 202.0 MeV
19. (*a*) 6.546 MeV (*b*) 4.807 MeV
21. (*a*) 1.943 MeV, 1.199 MeV, 7.551 MeV, ...
23. 14.1 MeV
25. 7.274 MeV
31. (*a*) 5.594 MeV (*b*) 0.56 W
33. 4.49 b, 2.20 b
35. 8.662 MeV
37. 9.043 MeV
39. (*a*) 3.2×10^{8} J (*b*) 6.8×10^{8} J

Chapter 14

1. (*a*) Strong (*b*) Electromagnetic (*c*) Weak
7. (*a*) L_e (*b*) S
11. (*a*) 1.29 keV (*b*) 0.21 MeV
13. 179.4 MeV
15. (*a*) 34 MeV (*b*) 218 MeV
17. (*a*) 43 MeV, 19 MeV (*b*) 30 MeV, 4 MeV
19. 387 MeV, 34.9°
21. (*a*) 181 MeV (*b*) −605 MeV
23. (*a*) 2205 MeV (*b*) 903 MeV
25. (*a*) $u\bar{u}$ annihilation, creation of 2 $s\bar{s}$ pairs
27. (*a*) $s \rightarrow u + W^{-}$ and $W^{-} \rightarrow d + \bar{u}$
29. $c\bar{u}$, etc.
31. 0.999635c, 40.2 GeV
33. (*a*) 0.360c (*b*) 0.637c (*c*) 279 MeV
35. 47 MeV

Chapter 15

1. (*a*) 590.0 nm (*b*) 637.1 nm
3. (*b*) 6.64×10^{-4} eV
5. 0.089 nm
7. 1.6×10^{-2} Hz
11. (*b*) 128 rev/s
15. (*a*) 5.8×10^{12} K (*b*) 6.7×10^{-6} s
17. (*a*) 1.0×10^{9} K (*b*) 225 s (*c*) 6600 K, 1.6×10^{5} y
19. $0.27\ m^{-3}$
21. 3.0 eV
23. (*a*) 2.9×10^{5} y (*b*) 1.17 eV (*c*) 1.24
25. (*a*) 9.79 km (*b*) 3.01×10^{39} J (*c*) 6.02×10^{30} J (*d*) 6.98×10^{25} W (*e*) 6.21×10^{-14} W

PHOTO CREDITS

Chapter 1
Opener: Cassini Interplanetary Trajectory illustration. Courtesy of NASA.

Chapter 2
Opener: Statue of Albert Einstein at NAS in Washington, D.C. ROGER L. WOLLENBERG/UPI/Newscom. Page 29: © SSPL/The Image Works. Page 31: Time, Inc. UPI Photo Service/NewsCom. Figure 2.7: GIPhotoStock/Photo Researchers, Inc.

Chapter 3
Opener: Heat radiation from a building using Thermography. Ted Kinsman/Getty Images. Page 79: © Mary Evans Picture Library/The Image Works. Page 85: © SSPL/Science Museum/The Image Works. Page 88: Weber Collection/AIP/Photo Researchers. Figure 3.2: GIPhotoStock/Photo Researchers, Inc. Figure 3.7b: Omikron/Photo Researchers, Inc. Figure 3.7c: Educational Images Ltd./Custom Medical Stock Photo, Inc. Figure 3.8: Omikron/Photo Researchers, Inc.

Chapter 4
Opener: Scanning tunnelling micrograph (STM) showing interactions between cobalt and silver atoms and a copper surface. DRS A. YAZDANI & D. J. HORNBAKER/SCIENCE PHOTO LIBRARY/Photo Researchers, Inc. Page 102: Meggers Gallery/AIP/Photo Researchers, Inc. Page 114: Bettmann/Corbis Images. Figure 4.1 (top): GIPhotoStock/Photo Researchers, Inc. Figure 4.0 bottom (Courtesy C. Joensson, Institut Für Angewandte Physik der Universitat Tubingen.) Figure 4.2: Courtesy Sumio Iijima, Arizona State University. Figure 4.3: Omikron/Photo Researchers, Inc. Figure 4.16: SCIMAT/SCIENCE PHOTO LIBRARY/Photo Researchers, Inc. Figure 4.27: Reprinted with permission from Akira Tonomura, Hitachi, Ltd., T. Matsuda, and T. Kawasaki, Advanced Research Laboratory. From *American Journal of Physics* 57,117. (Copyright 1989). American Association of Physics Teachers.

Chapter 5
Opener: Schrödinger's cat. MEHAU KULYK/SCIENCE PHOTO LIBRARY/Photo Researchers, Inc. Page 140: AIP/Photo Researchers, Inc. Figure 5.18: Image originally created by IBM corporation.

Chapter 6
Opener: Structure of an atom. Michael Dunning/Photo Researchers, Inc. Page 172: © SSPL/The Image Works. Page 184: The Granger Collection, New York.

Chapter 7
Opener: Distribution drawing representing the probability to locate the electron in the $n = 8$ state of hydrogen for angular momentum quantum number $l = 2$ (top) and $l = 6$. © John Wiley & Sons, Inc. Page 219: Photo from Wikipedia: http://commons.wikimedia.org/wiki/File:ZeemanEffect.GIF.

Chapter 8
Opener: Structure of an atom of neon. KENNETH EWARD/BIOGRAFX/SCIENCE PHOTO LIBRARY/Photo Researchers, Inc. Page 226: © Mary Evans Picture Library/Alamy. Page 243: Science Source/Photo Researchers, Inc.

Chapter 9
Opener: A Buckminsterfullerene molecule. PASIEKA/SCIENCE PHOTO LIBRARY/Photo Researchers, Inc. Page 273: Time & Life Pictures/Getty Images. Figure 9.17: Dr. Francesco Moresco FU Berlin now TU Dresden. Figure 9.19: CHRISTIAN DARKIN/SCIENCE PHOTO LIBRARY/Photo Researchers, Inc.

Chapter 10
Opener: Fractal Geometry. GREGORY SAMS/SCIENCE PHOTO LIBRARY/Photo Researchers, Inc. Figure 10.20: Photo from Wikipedia: http://commons.wikimedia.org/wiki/File:Liquid_helium_Rollin_film.jpg. Figure 10.21: Image from Wikipedia: http://en.wikipedia.org/wiki/File:Bose_Einstein_condensate.png.

Chapter 11
Opener: Scanning electron micrograph (SEM) of tungsten crystals. OWER AND SYRED/SCIENCE PHOTO LIBRARY/Photo Researchers, Inc.

Chapter 12
Opener: Gamma scan of a patient with prostate cancer. GJLP/CNRI/SCIENCE PHOTO LIBRARY/Photo Researchers, Inc. Page 370: Bettmann Corbis Images. Page 384: Science Source/Photo Researchers, Inc.

Chapter 13
Opener: Nuclear reactor core of Advanced Test Reactor (ATR) at the Idaho National Engineering and Environmental Lab. Science Source/Photo Researchers, Inc. Page 416: © Photo Researchers, Inc./Alamy. Page 434: Dave Pickoff/AP/Wide World Photos. Figure 13.1b: Courtesy Argonne National Laboratory. Figure 13.2b: Courtesy Purdue University. Figure 13.15: Dietmar Krause/Princeton Plasma Physics Laboratory. Figure 13.18: LLNL/Jacqueline McBride. Figure 13.23: Courtesy D. Bruce Sodee, MD. Figure 13.24: Courtesy Dr. Steve Petersen.

Chapter 14
Opener: Particle tracks from lead ion collisions seen by ALICE (a large ion collider experiment) in CERN. CERN/SCIENCE PHOTO LIBRARY/Photo Researchers, Inc. Page 449: Pictorial Parade/Getty Images, Inc. Page 453: PHYSICS TODAY COLLECTION/AMERICAN INSTITUTE OF PHYSICS/SCIENCE PHOTO LIBRARY/Photo Researchers, Inc. Figure 14.1: FermiLAB. Figure 14.3: Photo Courtesy Lawrence Berkeley National Laboratory. Figure 14.4: FermiLAB. Figure 14.5: FermiLAB. Figure 14.19: Kamioka Observatory, ICCR (Institute for Cosmic Ray Research), The University of Tokyo.

Chapter 15
Opener: Starry Night by Vincent van Gogh, oil on canvas. SuperStock/Getty Images, Inc. Page 480: EMILIO SEGRE VISUAL ARCHIVES/AMERICAN INSTITUTE OF PHYSICS/SCIENCE PHOTO LIBRARY/Photo Researchers, Inc. Page 482: Carl Iwasaki/Time Life Pictures/Getty Images, Inc. Page 486: Richard T. Nowit/Photo Researchers, Inc. Figure 15.1: Data courtesy Hale Observatories. Figure 15.7: Courtesy of The Observatories of the Carnegie Institute of Washington. Figure 15.26: Courtesy of NASA. Figure 15.27: Courtesy Hale Observatories, California Institute of Technology.

INDEX

INDEX TO TABLES

SOME MILESTONES IN THE HISTORY OF MODERN PHYSICS

1887	Albert A. Michelson and Edward W. Morley fail to detect ether.
1896	Henri Becquerel discovers radioactivity.
1900	Max Planck introduces quantum theory to explain thermal radiation.
1905	Albert Einstein proposes the special theory of relativity.
1905	Albert Einstein introduces the concept of the photon to explain the photoelectric effect.
1911	Heike Kamerlingh-Onnes discovers superconductivity.
1911	Ernest Rutherford proposes the nuclear atom, based on experiments of Hans Geiger and Ernest Marsden.
1913	Niels Bohr introduces theory of atomic structure.
1913	William H. Bragg and William L. Bragg (father and son) study X-ray diffraction from crystals.
1914	James Franck and Gustav Hertz show evidence for quantized energy states of atoms.
1914	Henry G. J. Moseley shows relationship between X-ray frequency and atomic number.
1915	Albert Einstein proposes the general theory of relativity.
1916	Robert A. Millikan measures photoelectric effect to confirm Einstein's photon theory.
1919	Ernest Rutherford produces first nuclear reaction that transmutes one element into another.
1919	Sir Arthur Eddington and other British astronomers measure gravitational deflection of starlight and confirm predictions of Einstein's general theory of relativity.
1921	Otto Stern and Walter Gerlach demonstrate spatial quantization and show necessity to introduce intrinsic magnetic moment of electron.
1923	Arthur H. Compton demonstrates change in X-ray wavelength following scattering from electrons.
1924	Louis de Broglie postulates wave behavior of particles.
1925	Wolfgang Pauli proposes the exclusion principle.
1925	Samuel Goudsmit and George Uhlenbeck introduce the concept of intrinsic angular momentum (spin).
1926	Erwin Schrödinger introduces wave mechanics (quantum mechanics).
1926	Max Born establishes statistical, probabilistic interpretation of Schrodinger's wave functions.
1927	Werner Heisenberg develops principle of uncertainty.
1927	Clinton Davisson and Lester Germer demonstrate wave behavior of electrons; G. P. Thomson independently does the same.
1928	Paul A. M. Dirac proposes a relativistic quantum theory.
1929	Edwin Hubble reports evidence for the expansion of the universe.
1931	Carl Anderson discovers the positron (antielectron).
1931	Wolfgang Pauli suggests existence of neutral particle (neutrino) emitted in beta decay.

1932	James Chadwick discovers the neutron.
1932	John Cockcroft and Ernest Walton produce the first nuclear reaction using a high-voltage accelerator.
1932	Ernest Lawrence produces first cyclotron for studying nuclear reactions.
1934	Irène and Frédéric Joliot-Curie discover artificially induced radioactivity.
1935	Hideki Yukawa proposes existence of medium-mass particles (mesons).
1938	Otto Hahn, Fritz Strassmann, Lise Meitner, and Otto Frisch discover nuclear fission.
1938	Hans Bethe proposes thermonuclear fusion reactions as the source of energy in stars.
1940	Edwin McMillan, Glenn Seaborg, and colleagues produce first synthetic transuranic elements.
1942	Enrico Fermi and colleagues build first nuclear fission reactor.
1945	Detonation of first fission bomb in New Mexico desert.
1946	George Gamow proposes big-bang cosmology.
1948	John Bardeen, Walter Brattain, and William Shockley demonstrate first transistor.
1952	Detonation of first thermonuclear fusion bomb at Eniwetok atoll.
1956	Frederick Reines and Clyde Cowan demonstrate experimental evidence for existence of neutrino.
1958	Rudolf L. Mössbauer demonstrates recoilless emission of gamma rays.
1960	Theodore Maiman constructs first ruby laser; Ali Javan constructs first helium-neon laser.
1964	Allan R. Sandage discovers first quasar.
1964	Murray Gell-Mann and George Zweig independently introduce three-quark model of elementary particles.
1965	Arno Penzias and Robert Wilson discover cosmic microwave background radiation.
1967	Jocelyn Bell and Anthony Hewish discover first pulsar.
1967	Steven Weinberg and Abdus Salam independently propose a unified theory linking the weak and electromagnetic interactions.
1974	Burton Richter and Samuel Ting and co-workers independently discover first evidence of fourth quark (charm).
1974	Joseph Taylor and Russell Hulse discover first binary pulsar.
1977	Leon Lederman and colleagues discover new particle showing evidence for fifth quark (bottom).
1981	Gerd Binnig and Heinrich Rohrer invent scanning-tunneling electron microscope.
1983	Carlo Rubbia and co-workers at CERN discover W and Z particles.
1986	J. Georg Bednorz and Karl Alex Müller produce first high-temperature superconductors.
1994	Investigators at Fermilab discover evidence for sixth quark (top).
1995	Eric Cornell and Carl Wieman produce first Bose-Einstein condensation.
1998	Discovery of neutrino oscillations shows that neutrinos have small but nonzero mass.
2003	WMAP satellite data reveal age and composition of universe.

Units

Unit	Abbreviation	Quantity Measured	Unit	Abbreviation	Quantity Measured
gram	g	mass	coulomb	C	electric charge
meter	m	length	ampere	A	electric current
second	s	time	volt	V	electric potential
newton	N	force	ohm	Ω	electric resistance
joule	J	energy	tesla	T	magnetic field
watt	W	power	atomic mass unit	u	mass
electron-volt	eV	energy	curie	Ci	activity
hertz	Hz	frequency	barn	b	cross section
kelvin	K	temperature			

Prefixes of Units

Prefix	Abbreviation	Value	Prefix	Abbreviation	Value
atto	a	10^{-18}	centi	c	10^{-2}
femto	f	10^{-15}	kilo	K	10^{3}
pico	p	10^{-12}	mega	M	10^{6}
nano	n	10^{-9}	giga	G	10^{9}
micro	μ	10^{-6}	tera	T	10^{12}
milli	m	10^{-3}	peta	P	10^{15}

Some Commonly Used Constants and Conversion Factors

(see Appendix A for a more complete list)

Speed of light	$c = 2.998 \times 10^{8}\,\text{m/s}$
Electronic charge	$e = 1.602 \times 10^{-19}\,\text{C}$
Boltzmann constant	$k = 1.381 \times 10^{-23}\,\text{J/K} = 8.617 \times 10^{-5}\,\text{eV/K}$
Planck's constant	$h = 6.626 \times 10^{-34}\,\text{J}\cdot\text{s} = 4.136 \times 10^{-15}\,\text{eV}\cdot\text{s}$
Avogadro's constant	$N_{\text{A}} = 6.022 \times 10^{23}\ \text{mole}^{-1}$
Electron mass	$m_{\text{e}} = 5.49 \times 10^{-4}\,\text{u} = 0.511\,\text{MeV}/c^2$
Proton mass	$m_{\text{p}} = 1.007276\,\text{u} = 938.3\,\text{MeV}/c^2$
Neutron mass	$m_{\text{n}} = 1.008665\,\text{u} = 939.6\,\text{MeV}/c^2$
Bohr radius	$a_0 = 0.0529\,\text{nm}$
Hydrogen ionization energy	$13.6\,\text{eV}$
Thermal energy	$kT = 0.02525\,\text{eV} \cong \frac{1}{40}\,\text{eV}\ (T = 293\,\text{K})$
$hc = 1240\ \text{eV}\cdot\text{nm}\ (\text{MeV}\cdot\text{fm})$	$\hbar c = 197\,\text{eV}\cdot\text{nm}\ (\text{MeV}\cdot\text{fm})$
$\dfrac{e^2}{4\pi\varepsilon_0} = 1.440\,\text{eV}\cdot\text{nm}\ (\text{MeV}\cdot\text{fm})$	$1\,\text{u} = 931.5\,\text{MeV}/c^2$ $1\,\text{eV} = 1.602 \times 10^{-19}\,\text{J}$

Periodic Table of the Elements

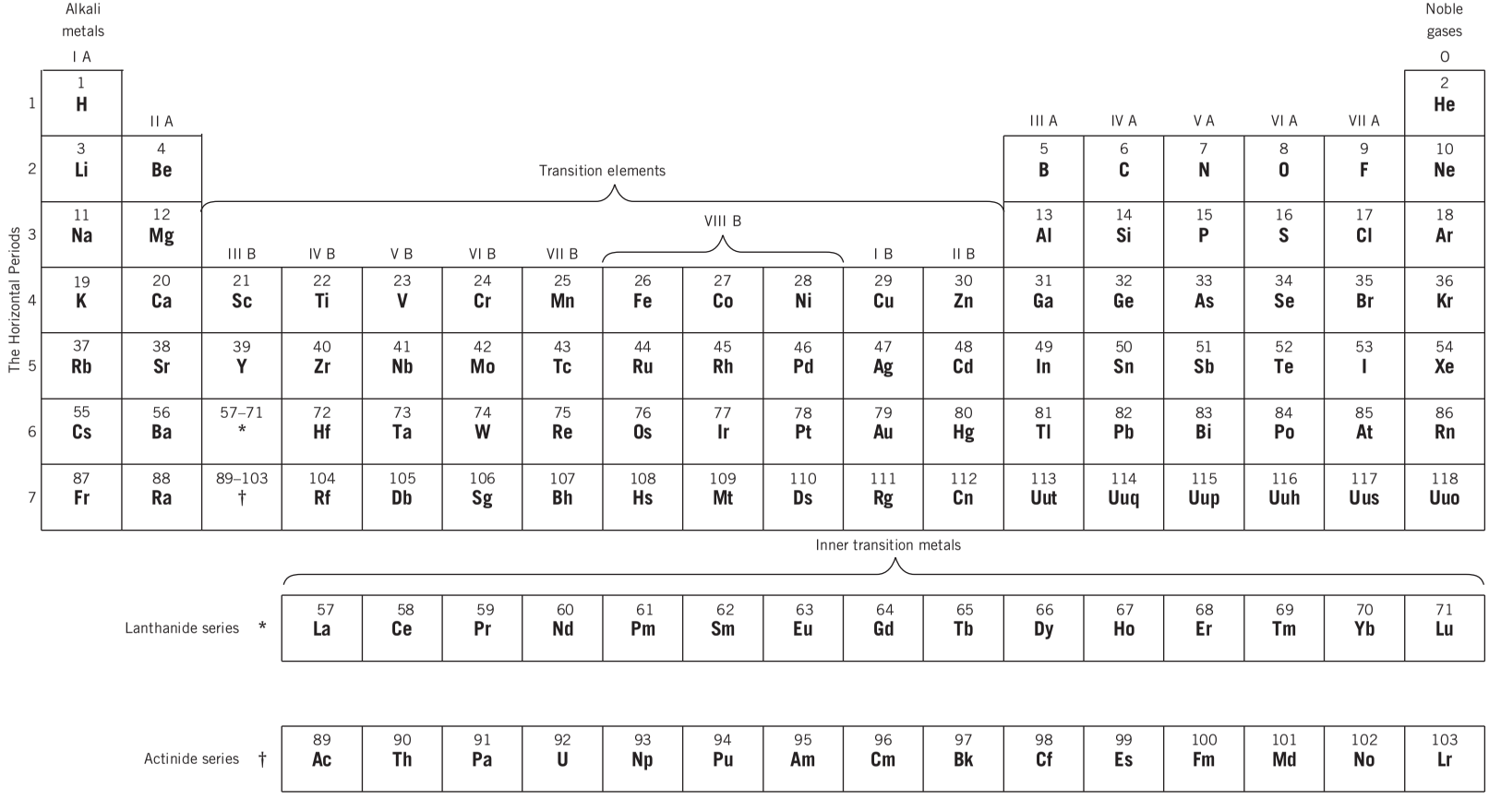

Evidence for the discovery of elements 113–118 has been reported but the results have not yet been confirmed and only temporary names for these elements have been assigned.